Investigating new mycobacterial models to decipher the evolutionary success and the antibiotic resistance of Mycobacterium tuberculosis, the etiological agent of tuberculosis

Camille Sous

Université Paris Cité

École doctorale Bio Sorbonne Paris Cité (ED 562)

Institut Pasteur — Département Microbiologie
Unité de Pathogénomique Mycobactérienne Intégrée

Investigating new mycobacterial models to decipher the evolutionary success and the antibiotic resistance of *Mycobacterium tuberculosis*, the etiological agent of tuberculosis

Par

Camille SOUS

Thèse de doctorat de **Microbiologie**

Dirigée par **Pr. Roland BROSCH**

Présentée et soutenue publiquement le 27/11/2023 devant un jury composé de :

Dr. Priscille BRODIN, Dr, Institut Pasteur de Lille	Examinatrice
Pr. Oana DUMITRESCU, MCU-PH, Ecole Normale Supérieure de Lyon	Rapportrice
Pr. Stephen GORDON, Pr, University College Dublin	Rapporteur
Dr. Christophe GUILHOT, Dr, IPBS	Examinateur
Pr. Isabelle MARTIN-VERSTRAETE, PU, Université Paris Cité	Examinatrice
Pr. Roland BROSCH, Pr, Institut Pasteur, Paris	Directeur de thèse

Université Paris Cité

École doctorale Bio Sorbonne Paris Cité (ED 562)

Institut Pasteur — Department of Microbiology
Unit for Integrated Mycobacterial Pathogenomics

Investigating new mycobacterial models to decipher the evolutionary success and the antibiotic resistance of *Mycobacterium tuberculosis*, the etiological agent of tuberculosis

By

Camille SOUS

PhD thesis in **Microbiology**

Supervised by **Pr. Roland BROSCH**

Public defense on Monday 27th November 2023 in front of the jury composed of:

Dr. Priscille BRODIN, Dr, Institut Pasteur de Lille	Reviewer
Pr. Oana DUMITRESCU, MCU-PH, Ecole Normale Supérieure de Lyon	Reviewer
Pr. Stephen GORDON, Pr, University College Dublin	Reviewer
Dr. Christophe GUILHOT, Dr, IPBS	Reviewer
Pr. Isabelle MARTIN-VERSTRAETE, PU, Université Paris Cité	Reviewer
Pr. Roland BROSCH, Pr, Institut Pasteur, Paris	Thesis director

Titre : Étude de nouveaux modèles mycobactériens pour mieux comprendre le succès évolutif et la résistance aux antibiotiques de *Mycobacterium tuberculosis*, l'agent étiologique de la tuberculose

Résumé : La tuberculose (TB), causée par *Mycobacterium tuberculosis* (*Mtb*), reste l'une des maladies infectieuses humaines les plus meurtrières. *Mtb*, un organisme de niveau de biosécurité 3 (NBS-3), fait l'objet d'études approfondies au niveau biologique et génomique depuis des années, mais certains aspects de son évolution sont encore mal compris, notamment le gain exceptionnel de virulence par rapport à d'autres mycobactéries. Ces dernières années, de nouvelles espèces mycobactériennes opportunistes appartenant aux organismes de NBS-1 ou 2 et nommées *Mycobacterium decipiens*, *Mycobacterium lacus*, *Mycobacterium riyadhense* et *Mycobacterium shinjukuense* ont été isolées d'échantillons cliniques. Une étude préliminaire a révélé un degré de similarité génomique plus élevé avec *Mtb* qu'avec les espèces utilisées comme modèles, telles que les pathogènes occasionnels *Mycobacterium kansasii* ou *Mycobacterium marinum* (NBS-2). Certaines caractéristiques de ces quatre espèces pourraient donc constituer un chainon manquant de l'évolution de *Mtb*. Mon projet de thèse vise à étudier ces quatre espèces par des comparaison phénotypiques, génomiques, et infectieuses afin d'acquérir de nouvelles connaissances sur l'évolution de *Mtb* et de déterminer si l'une de ces espèces pourrait être utilisées comme modèles d'étude de certains aspectes de *Mtb* ou d'autres mycobactéries pathogènes. Afin de déterminer la possibilité d'utiliser une de ces espèces comme modèle de TB, nous avons étudié la capacité de multiplication intracellulaire des espèces dans des modèles *in vitro* et *in vivo*. Nous avons ensuite obtenu leurs séquences génomiques par séquençage long-read et comparé certaines régions génomiques liées à la capacité infectieuse de *Mtb*, comme la sécrétion de la protéine de virulence ESAT-6 par le locus ESX-1 appartenant aux systèmes de sécrétion de type VII, la production de lipides tels que les phthiocérole dimycocérosate (PDIM) et les glycolipides phénoliques. Pour finir, nous avons également étudier la production des lipides oligosaccharides (LOS) lié à la morphologie des colonies chez certaines espèces de mycobactérie comme chez *Mtb* qui a un morphotype rugueux et ne produit pas de LOS. Les études de ce projet nous ont permis de déterminer que *M. decipiens* a une température de croissance optimale de 32-35°C et non 37°C comme les autres espèces étudiées, et que la bactérie présentait des résistances à certains antituberculeux également observées *M. lacus* et *M. riyadhense*. Nous avons également déterminé que *M. riyadhense* était, parmi les quatre espèces, la bactérie la plus virulente, capable de proliférer dans des modèles cellulaires et murins même à faible dose. *M. decipiens* a également montré un profil infectieux intéressant à 35°C dans les cellules mais qui semble atténué à 37°C. Les comparaisons génomiques et analyses moléculaires associées nous ont permis de montrer que le locus *espACD*, indispensable pour la sécrétion de ESAT-6 chez *Mtb*, était présent seulement chez *M. decipiens* qui était capable de sécréter ESAT-6 et sa protéine chaperonne CFP-10, cette sécrétion n'est pas retrouvée chez les autres espèces, excepté *M. lacus* qui est capable de sécréter CFP-10 seule ce qui en fait un modèle d'étude intéressant. L'analyse de certains lipides n'a pas révélé de similitudes importantes pour l'interprétation de l'évolution de *Mtb*. D'après ces données, ces espèces pourraient représenter des modèles intéressant pour l'évolution de *Mtb*, et l'étude de nouveaux antituberculeux dans des conditions de NBS-1 et-2. *M. decipiens* et *M. riyadhense* pourraient être des modèles prometteurs pour l'étude de la TB.

Mots-clés : *Mycobacterium tuberculosis*, évolution, modèle d'étude, facteur de virulence, mycobactérie non-tuberculeuse, *Mycobacterium decipiens*, *Mycobacterium lacus*, *Mycobacterium riyadhense*, *Mycobacterium shinjukuense*

Title: Investigating new mycobacterial models to decipher the evolutionary success and the antibiotic resistance of *Mycobacterium tuberculosis*, the etiological agent of tuberculosis.

Abstract: Tuberculosis (TB), caused by *Mycobacterium tuberculosis* (*Mtb*), remains one of the deadliest human infectious diseases. *Mtb*, a biosafety level 3 (BSL-3) organism, has been the subject of extensive biological and genomic studies for many years, but certain aspects of its evolution are still poorly understood, notably its exceptional gain in virulence compared with other mycobacteria. In recent years, some new opportunistic mycobacterial species belonging to BSL-1 or -2 organisms and named *Mycobacterium decipiens*, *Mycobacterium lacus*, *Mycobacterium riyadhense* and *Mycobacterium shinjukuense* were isolated from clinical samples. A preliminary study revealed a higher degree of genomic similarities with *Mtb* than shown by other species used as models, such as the occasional pathogens *Mycobacterium kansasii* or *Mycobacterium marinum* (BSL-2). Certain characteristics of these four species could therefore constitute a missing link in the evolution of *Mtb*. My thesis project aims to study these four species by phenotypic, genomic, and infectious comparisons in order to gain new insights into the evolution of *Mtb* and to determine whether any of these species could be used as models for studying certain aspects of *Mtb* and other pathogenic mycobacteria. To determine whether one of these species could be used as a TB model, we studied the intracellular multiplication capacity of the species in *in vitro* and *in vivo* models. We then obtained their genomic sequences by long read sequencing and compared certain genomic regions linked to the infectious capacity of *Mtb*, such as secretion of the virulence protein ESAT-6 by the ESX-1 locus belonging to the type VII secretion system, production of lipids such as phthiocerol dimycocerosate (PDIM) and phenolic glycolipids. Finally, we also studied the production of lipooligosaccharides (LOS) linked to colony morphology in certain mycobacterial species such as *Mtb*, which has a rough morphotype and does not produce LOS. The studies in this project enabled us to determine that *M. decipiens* has an optimal growth temperature of 32-35°C and not 37°C like the other species studied, and that the bacterium showed resistance to certain anti-TB drugs, like this was also the case for some of the drugs for *M. lacus* and *M. riyadhense*. We also determined that *M. riyadhense* was the most virulent of the four species, capable of proliferating in cell and mouse models even at lower doses. *M. decipiens* also showed an interesting cellular infectious profile at 35°C but was impaired in its virulence at 37°C. Genomic comparisons and associated molecular analyses enabled us to show that the *espACD* locus, essential for the secretion of ESAT-6 in *Mtb*, was present only in *M. decipiens*, which was able to secrete ESAT-6 and its chaperone protein CFP-10. Secretion of ESAT-6 and CFP-10 was not found in the other species, with the exception of *M. lacus*, which was able to secrete CFP-10 alone, a finding that makes *M. lacus* an interesting study model for studying ESX-1 type VII secretion in greater details. Analysis of selected virulence lipids showed no substantial insights for the interpretation of the evolution of *Mtb*, except that the PDIM locus was found conserved in all four species. While *M. decipiens* or *M. riyadhense* might represent promising TB study models, the fact that the four species show varying sensibilities to anti-tuberculosis drugs makes them interesting models for the study of new anti-tuberculosis molecules that are being developed in various collaborative projects, which can be applied under level one or two biosafety conditions.

Key words: *Mycobacterium tuberculosis*, evolution, study model, virulence factor, non-tuberculous mycobacteria, *Mycobacterium decipiens*, *Mycobacterium lacus*, *Mycobacterium riyadhense*, *Mycobacterium shinjukuense*

INDEX

ABBREVIATIONS

AM: Alveolar macrophage

AMK: Amikacin

ANI: Average nucleotide identity

BCG: Bacille Calmette-Guérin

BDQ: Bedaquiline

BSL: Biosafety level

CFP-10: 10-kDA culture filtrate protein

cGAS: Cyclic GMP-AMP synthase

CLRs: C-type lectin receptors

COVID-19: Coronavirus disease 2019

DCT: Distributive conjugal transfer

ESAT-6: 6 kDa early secretory antigenic target

ESX: ESAT-6 secretion system

ETH: Ethambutol

GPL: Glycopeptidolipid

HGT: Horizontal gene transfer

HIV: Human immunodeficiency virus

IFN: Interferon

IGRA: Interferon gamma release assay

IL: Interleukin

IM Interstitial macrophages

INH: Isoniazid

ITS: Internal transcribed spacer

KO: Knock-out

LAMP: loop-mediated isothermal amplification

LOS: Lipooligosacharide

LPA: Line probe assay

LTBI: Latent tuberculosis infection

MDR-TB: Multi-drug resistant tuberculosis

MIC: Minimal inhibitory concentration

Mtb: *Mycobacterium tuberculosis*

MTBAP: *Mycobacterium tuberculosis* associated phylotype

MTBC: *Mycobacterium tuberculosis* complex

NETs: Neutrophil extracellular traps

NFκB: Nuclear factor-κ B

NK: Natural killer

NLR: NOD-like receptor

NLRP3: NOD-like receptor family, pyrin domain containing 3

NO: Nitric oxide

NOS: Nitrogen reactive species

NTM: Non-tuberculous mycobacteria

OD: Optical density

ORF: Open reading frame

PAMPs: Pathogen-associated molecular pattern

PDIM: Phthiocerol dimycocerosate

PGL: Phenoglycolipid

PPD: Purified protein derivative

Pre-XDR-TB: Pre-extensively resistant tuberculosis

PRR: Pattern recognition receptor

PZA: Pyrazinamide

RD: Region of Difference

RGM: Rapid-growing mycobacteria

RIF: Rifampicin

RNS: Reactive nitrogen species

ROS: Reactive oxygen species

RR-TB: Rifampicin-resistant tuberculosis

SarsCoV-2: severe acute respiratory syndrome coronavirus 2

SG-NTM: Slow-growing non-tuberculous mycobacteria

SGM: Slow-growing mycobacteria

SL: Sulpholipid

SNP: Single nuclear polymorphism

STB: Smooth tubercule bacilli

STING: Stimulator of interferon genes

T7SS: Type VII secretion system

TAT: Twin-arginine translocation

TB: Tuberculosis

TLR: Toll like receptor

TNF: Tumor necrosis factor

TNT: Tumor necrotizing toxin

TST: Tuberculin skin test

WHO: World Health Organization

XDR-TB: Extensively resistant tuberculosis

LIST OF FIGURES

LIST OF TABLES

INTRODUCTION

A. General Information

I. Tuberculosis: definition

Tuberculosis (TB) is an infectious disease caused by *Mycobacterium tuberculosis* (*Mtb*). The most widely observed form of the disease affects the lungs and is named pulmonary TB causing severe symptoms such as cough, often associated with hemoptysis, fever, fatigue, and weight loss. But *Mtb* can also cause extrapulmonary infection in different parts of the body (Pai et al., 2016). According to the World Health Organization (WHO), TB was the primary cause of death caused by a single infectious agent, before being overtaken temporarily by the SARS-CoV-2 infection. In 2019, TB was the 13th cause of death worldwide (World Health Organization, 2022). TB is an old disease and is known since antiquity, whereby its infectious nature has been demonstrated at the end of the 19th century. TB disease is hard to treat due to the requirement of at least 6 months of treatment for drug-sensitive strains, and even longer for drug resistant strains. Despite the existence of many national and international TB programs in most high burden countries, in some situations the accessibility to the treatment is also difficult due to its cost, and it is clear that without appropriate treatment a high mortality rate prevails (Rahlwes et al., 2023).

II. Epidemiology

TB is a very complex disease, and it is important to distinguish between the different forms of the infection with *Mtb*, which can range from a simple infection that is controlled by the immune system of the host to severe cases of TB disease. It is estimated that a quarter of the world's population has been infected with the bacilli, including people who did not report the disease or those whose immune system can control the infection or have successfully eliminated the pathogen (World Health Organization, 2022). Indeed, two main types of infection progression are described for TB, depending on the immune response of the infected host. In the first case, a person is infected by *Mtb*, and its immune system is able to control the infection avoiding the development of the disease. This is called a latent TB infection (LTBI). Conversely, if the infected person develops symptoms, this corresponds to an active TB case. People can develop active TB directly after infection or control the infection

Figure 1: Estimated TB incidence in 2021, for countries with at least 100,000 incident cases. The majority of deaths were reported in the African and South-East Asian region, with 82% of TB deaths, while India alone accounted for 36% of deaths. Picture from (World Health Organization, 2022)**.**

via LTBI and develop the disease later. Among exposed people, around a quarter will be infected by the bacilli while 5 to 10% of these people will develop active TB over the next 5 years, and 10% of the remaining 90% will declare the disease during their lifetime (Goletti & Martineau, 2021; Migliori et al., 2021).

According to the WHO global TB report 2022, cases of untreated TB had increased since the coronavirus disease 2019 (COVID-19) pandemic due to less effective case detection and reduced treatment access. In 2021, 10.6 million new infection cases were estimated with 1.6 million of deaths including 187 000 of HIV-positive patients. More than the two third of new TB disease cases are localized in the southern half of the African continent and Southeast Asia. In 2021, 82% of TB deaths were recorded in African and South-East Asia regions, whereby India alone accounted for 36% of these deaths (Figure 1) (World Health Organization, 2022). This situation can only be improved by implementation of effective anti-TB programs. For example, the WHO milestones aim for TB incidence rate reduction by 90% for 2035. Unfortunately, recent numbers are higher than estimations of 2019, reversing the curve of the TB pandemic, which has been declining since 2005 (World Health Organization, 2022). TB thus remains a global emergency that needs continued attention.

III. Diagnostic of tuberculosis

1. Types of infection

TB transmission primarily occurs via the aerosol route leading to an infection with *Mtb* within the lungs. As introduced earlier, the host can control the infection resulting in a latent *Mtb* infection. This is made possible by the formation of organized structures of immune cells, named granulomas, containing macrophages infected by *Mtb*. The infection is controlled as long as granulomas do not rupture, but under certain conditions the pathogen can continue to multiple within them, although this process is complex, and many exceptions might exist. If the immune system is weakened or the number of bacteria inside granulomas becomes too large, the granulomas may rupture leading to the dissemination of the pathogen. This may occur in the lungs, resulting in active pulmonary TB, or the bacteria may spread to the rest of the body, resulting in extra-pulmonary TB (Pai et al., 2016; Rahlwes et al., 2023).

If *Mtb* is mainly known for causing pulmonary infections, around 15% of cases can lead to extrapulmonary TB with different types (Moule & Cirillo, 2020):

- Lymphadenitis, most often involving the cervical lymph nodes. This type of infection is the most common form of extra-pulmonary TB.
- Pleural tuberculosis, the second form of extra-pulmonary TB, infects the membranes lining the lungs, such as the pleura.
- Musco-skeletal tuberculosis, with different types of infection:
    - Spinal tuberculosis, which causes abscesses between the vertebrae and can lead to paralysis, is the most common type of infection.
    - Bone tuberculosis, which can target bones or joints.
- Infection of the central nervous system, which is rarer but very dangerous. It is characterized by tuberculous meningitis, encephalitis, or abscesses.
- Systemic infection is the most serious form of extra-pulmonary TB, also called miliary TB. It occurs when the pathogen enters the bloodstream. This causes the bacteria to spread throughout the body, resulting in lesions, mainly in highly vascularized organs such as the liver, spleen, or kidneys.

The risk of developing extrapulmonary TB is dependent on various factors such as age, gender, alcohol consumption. A recent study of extrapulmonary and pulmonary TB in the USA revealed that under the age of 14, the risk for children to develop extrapulmonary TB is more than twice as high as that for pulmonary TB. Similar observations were made for alcohol consumers (Banta et al., 2020)

2. Risk factors

Mtb is a highly virulent pathogen causing a high mortality rate if the disease is not treated (Rahlwes et al., 2023). The development of the pathogen after infection or the activation of LTBI into active TB can be enhanced by various risk factors, which add difficulties for the eradication of the disease. Two types of risk factors are identified: exogenous factors such as the bacterial dose, proximity to infected people, individual behavior (smoking, alcohol consumption, pollution) which are mainly linked to the risk of the infection after exposure;

and endogenous factors representing the risk of disease development after infection such as co-infection with HIV, diabetes, malnutrition, poverty (Narasimhan et al., 2013; World Health Organization, 2022). External factors such as specific medical treatments that might perturb existing granulomatous structures, such as TNF blockers, can also lead to activation of LTBI (Ernst, 2012). Homelessness, incarceration, and high alcohol consumption are among the risk factors enhancing extrapulmonary TB (Moule & Cirillo, 2020).

Individual behavior: in general, excessive consumption of various products is harmful to health (fatty, sweet, or salty foods, alcohol, drugs, smoking). Some of these have been shown to increase the risk of infection after exposure to *Mtb* and the development of TB. Alcohol and drugs abuse are notably shown to have an impact on the development of active TB and LTBI, respectively (Deiss et al., 2009). Cigarettes also play a key role in pathogenesis of TB as smoking was shown to impact the immune response of macrophages by affecting the production of TNF-α implicated in the recruitment of immune cells for granuloma formation (Berg et al., 2016; D. R. Silva et al., 2018).

Immunosuppressive conditions (HIV): immunosuppressive diseases are generally risk factors for TB. Among them, immunosuppression caused by the infection with human immunodeficiency virus (HIV) is among the most widespread causes for the development of active TB from LTBI (Narasimhan et al., 2013). The risk of developing TB for HIV-positive patients rises from 2- to 5-fold with early HIV infection to more than 20-fold with advanced HIV infection compared to HIV-negative people (Bell & Noursadeghi, 2018; Tornheim & Dooley, 2018). In general, men have a significantly higher risk of death from co-infection with HIV and TB than women and children under the age of 15 (51%, 28%, and 11% respectively) (World Health Organization, 2022). The two diseases interact via macrophages and immune cells. HIV infects T lymphocytes (CD4+), which play a key role in adapted immunity to defend the body against the development of TB disease. Reduced T-cell mediated immune activation may lead to more rapid multiplication of the pathogen and higher mycobacterial burden (Bell & Noursadeghi, 2018).

Diabetes: diabetes increases the risk of pulmonary TB, and more precisely the risk of LTBI activation, relapse, or death from TB. The risk of relapse for a type-2 diabetic is estimated to

be 4-times higher than for a non-diabetic person (Restrepo, 2016). The reasons for the enhanced susceptibility to TB in type-2 diabetic patients remain uncertain but may be caused by direct effects related to hyperglycemia and indirect effects related to macrophage and lymphocyte functions, resulting in a defect in immunity with a lower proportion of activated alveolar macrophages and altered cytokines level (IL-10 or IFN-γ) (D. R. Silva et al., 2018; Sun et al., 2012).

COVID-19: in 2020, the worldwide pandemic caused by infections with severe acute respiratory syndrome coronavirus 2 (SARS-CoV-2) pushed TB disease temporarily from the leading to the second leading cause of death caused by a single infectious agent (World Health Organization, 2022). As well as having an impact on the delivery of TB treatments during lockdowns, COVID-19 could have had a direct impact on the development of TB infections (Sanduzzi Zamparelli et al., 2022). As both pathogens primarily affect the respiratory system, a co-infection increasing the prevalence of one or both diseases have been considered. According to a study, up to 4% of SARS-CoV-2 infected patients may also be infected with *Mtb* (Ojo et al., 2023). Even if the transformation of latent to active TB was reported in a few cases after COVID-19 episodes, the role of SARS-CoV-2 in the development of TB in the case of co-infection has not yet been recognized or demonstrated. Various hypotheses are being explored for the cause of transformation of latent to active TB, such as for example the use of corticosteroids, depletion of T lymphocytes, or a decrease of cytokine production (Al-kayali et al., 2023; Khayat et al., 2021; Sanduzzi Zamparelli et al., 2022), the results are still limited, and further studies are needed (Sanduzzi Zamparelli et al., 2022; Visca et al., 2020).

Young age and gender: According to meta-analyses, the incidence of TB prevalence is higher in men than in women. These results are even more marked in low- and middle-income countries (Horton et al., 2016). In 2021, 56.5% of detected TB cases were among men, compared with 32.5% among women. The remaining 11% concerned children under the age of 15. Relatively similar percentages are observed for TB-deaths (World Health Organization, 2022). In addition to age, the risk of TB infection in children may be higher depending on household conditions, such as air quality (smoking indoors), food quality and quantity (malnutrition), social contacts (exposure to TB-infected people) (Siddalingaiah et al., 2023).

Treatment of co-infections: Cases of comorbidity can lead to the use of medication designed to target one of the diseases that may also impact the other disease. In some cases, molecules needed to cure a disease may interfere with anti-TB drugs, or vice-versa, or the molecules may alter the host immune responses, leading to increase TB disease (Bell & Noursadeghi, 2018). Particular care is also required when taking treatments for TB and HIV, as drug-drug interactions can be harmful to the patient (Cerrone et al., 2020). Other treatments such as those for transplanted patients (Aguado et al., 2016), or for patients with immune-mediated inflammatory disorders (IMID) involving anti-TNF-α treatment have been reported to be associated with the progressions of LTBI to active TB and to increase the risk of extrapulmonary TB (Harris & Keane, 2010; Petruccioli et al., 2021) and similar observations have also been made for glucocorticoids (Ernst, 2012).

Microbiologic characteristics: The potency of *Mtb* to cause infection can be defined by several microbiological properties related to the pathogen, such as pathogenicity, virulence, bacterial dose, transmission rate, and mortality rate (Tram et al., 2018). Generally speaking, the various strains are categorized according to their infectious properties and geographical area and grouped by lineages. For example, one lineage that is prevalent in Asia (lineage 2, East Asia/Beijing) has been associated with high virulence and global spread. Along with lineage 4, the Euro-American lineage, L2 strains belong to the most widespread strains, while strains from other lineages (e.g. *M. africanum* lineages L5 and L6) are confined to the African continent (Brites & Gagneux, 2015; Gagneux, 2018). Finally, pathogenesis and virulence are also linked to the bacterial dose, given that even a few bacilli are able of causing an infection (Bansal et al., 2018).

3. Diagnostic tests

The COVID-19 pandemic has caused a drop in the number of diagnosed TB cases. Early diagnosis is a very important element in the fight against TB disease and spread of *Mtb* to other people. For the estimated 10.6 million of new TB cases in 2021, only 6.4 million of people were diagnosed. This represents around 60% of new cases, whereas before COVID-19 in 2019, slightly more than 70% of TB cases were detected (World Health Organization, 2020, 2022).

a. Latent tuberculosis infection

During a latent infection, the bacteria are encapsulated in structures formed by the host's immune system. To detect such an infection, two tests are possible (Rahlwes et al., 2023).

The tuberculin skin test (TST) consists of an intradermal injection of a tuberculin purified protein derivative (PPD), obtained from purified, heat inactivated *Mtb* culture supernatant. After a few days, the onset of the cellular immune response is evaluated by measuring the size of the immune reaction in the skin. A person with a LTBI will show moderate cell-mediated immunity to the injected protein site leading to a moderate hypersensitivity reaction, while TB patients with active TB will show stronger responses. The diameter of the induration reaction is measured within 48 to 72 hours to determine whether the test is positive. The diameter also depends on existing risk factors such as a weaker immune response in the case of HIV infection or malnutrition. Without risk factors, an induration reaction larger than 15mm is considered positive for active TB, while the presence of risk factors reduces this width (Kestler & Tyler, 2022; Pai et al., 2016). False-positive results may be detected if the patient has been vaccinated with Bacille Calmette-Guérin (BCG vaccine against TB) after infancy or has received several doses of BCG, or if the patient was exposed with non-tuberculous mycobacteria (Farhat et al., 2006).

Interferon gamma release assay (IGRA) is the second test that can detect LTBI. Like for TST, this test evaluates whether immune cells of the tested person can specifically recognize *Mtb* proteins, but in contrast to the TST, the interaction between the immune cells of the host and *Mtb* antigens is happening in a test tube, which is coated with *Mtb* antigens, and into which whole blood of the tested person is added and incubated. In case of specific cell-mediated immune recognition of *Mtb* proteins, interferon gamma is released and measured by ELISA. There are IGRA tests that use PPD as antigen mix, but there also exist more specific ones, which target virulence proteins of *Mtb* that are absent from BCG, thereby strongly reducing putative false positive results of TST. Nevertheless, also this test can show false positive results in case of exposure to some non-tuberculous mycobacteria that may express and secrete mycobacterial proteins similar to the *Mtb* virulence proteins, used for this test (Kestler & Tyler, 2022; Pai et al., 2016). Blood from patients with TB infection (latent or active) will show

induction of cell-mediated immunity after contact with the antigens that can be measured by the IGRA by specific T-cells (Pai et al., 2014).

Other tests are needed to determine whether it is active or latent TB, as TST and IGRA do not necessarily allow this distinction, even if recent studies described new possibilities to discriminate LTBI and active TB with the use of some other antigens (Meier et al., 2018).

b. Active tuberculosis

In contrast to LTBI, bacilli are no longer confined to granulomas in active TB leading to the development of symptoms. When TB is suspected, different tests can be performed to confirm the diagnosis.

One efficient test to detect TB consists of the analysis of the sputum by liquid and solid culture, microscopic smear analysis and acid-fast detection by Ziehl-Neelsen and fluorochrome stains, but this technique can have a weak sensitivity and it is not always possible to obtain sputum from young children. Other fluids also need to be sampled and analyzed in case of extrapulmonary TB (Acharya et al., 2020; Ba & Rieder, 1999; Shingadia, 2012). Moreover, these technics require a high number of bacteria, rendering the detection sometimes complicated (Furin et al., 2019). Another rapid and not expensive technique, named the loop-mediated isothermal amplification (LAMP) can replace the smear microscopic observation and show a sensitivity of higher than 15% (World Health Organization - Geneva, 2016).

Chest X-ray is a useful tool to detect pulmonary disease in general such as non-tuberculous mycobacterial infection, airflow obstruction diseases, neoplasms, or bronchiectasis. This technique is often used as screening technique in case of pulmonary TB suspicion or to complement positive results from sputum smear analysis (Pai et al., 2016). Chest radiology allows to differentiate between primary and secondary TB depending on the types and place of lesions observed (Acharya et al., 2020).

For HIV-positive patients, T-cell-based technics presented above often have weak sensitivity leading to many false negative results for TB detection (Méndez-Samperio, 2017).

The development of a tool by Helb et al. that was validated by the WHO in 2010, represents a truly significant advance, which does not only facilitate and improve the detection of active TB in HIV-positive and -negative patients, but also enables the detection of rifampin-resistant cases (Helb et al., 2010; World Health Organization, 2011). The technology, named Xpert® MTB/RIF, is based on miniaturized cartridges that are loaded with patient sputum samples, in which the presence of *Mtb* DNA is determined by real-time PCR, including from *Mtb* strains containing mutations causing rifampicin resistance (Furin et al., 2019). Development of new versions of this technology such as Xpert® MTB/RIF Ultra allows now the detection of *Mtb* DNA with higher sensitivity, whereas new models like Xpert® MTB/XDR or MDR/MTB ELITe MGB® are able to detect more mutations in samples that could cause resistance to different anti-TB drugs (Georghiou et al., 2021; Hodille et al., 2019, 2021; Ok et al., 2021).
Another rapid and not expensive method to detect resistance of active TB is the line probe assay (LPA) or nucleic acid amplification test. Different probes were approved by the WHO over the years, including those with a better sensitivity and more resistance mutations (World Health Organization - Geneva, 2013). Mutations allowing resistance against rifampicin, isoniazid, ethambutol, fluoroquinolone, aminoglycosides, capreomycin and streptomycin can be detected with the Genotype MTBDRs/® test approved by the WHO in 2012 for example. Generally, these types of tests are used after a positive result in sputum smear analyses (Acharya et al., 2020; Heemskerk et al., 2015).

For HIV-positive patients, tests that are based on the detection of lipoarabinomannan in urine samples exist. This sensitive test seeks for the detection of lipoarabinomannan, which is part of the mycobacterial cell envelope and gets excreted by *Mtb* during multiplication. Use of other tests, like sputum smear analysis is less efficient for HIV-infected people, mainly because of the detection limit of the test (Furin et al., 2019; Lawn, 2012).

IV. Host-pathogen interaction

Before *Mtb* can efficiently infect the host, the bacteria must withstand several types of host-defenses, mounted by the respiratory system and the host immune system. The respiratory system is made up of several body parts: the nose, sinuses, mouth, pharynx, larynx, trachea, and lungs (bronchi, bronchioles, alveoli) (Torrelles & Schlesinger, 2017).

Figure 2: Infection cycle of *Mtb*. The pathogen is transmitted via the aerosol route by a carrier host, the droplets containing bacilli reach the alveoli and are phagocytized by innate immune cells like AMs and dendritic cells. The innate immune cells form vascularized aggregates to control the infection. Adaptive immune cells like T and B lymphocytes, activated by dendritic cells via antigen presentation in lymph nodes, are recruited in the infection site to reinforce the structure aggregates and form granulomas. Granulomas can clear the bacteria and become calcified granulomas; mycobacteria can enter in dormancy; or replicate within the granulomas. Reactivation of TB occurs when the immune system of the host is deregulated, and bacteria can be transmitted again. Picture from (Chandra et al., 2022).

Several defense systems are present in the various parts, including the ciliated epithelial cells of the trachea and bronchi, which secrete antibodies and antimicrobial peptides in a mucus toxic to pathogens, including *Mtb* (Chai et al., 2018; Y. Li et al., 2012). When droplets containing bacilli are transmitted to a host, they pass through the respiratory system to reach the pulmonary alveoli. For effective transmission, droplets must be very fine (< 5 µm) and contain only few bacilli to reach the pulmonary alveoli. Larger droplets, containing more bacteria, are retained by the upper parts of the respiratory system (Cambier et al., 2014; Chai et al., 2018). Once in the pulmonary alveoli, bacteria encounter type-I and type-II alveolar epithelial cells covered with pulmonary surfactant. This surfactant is composed, among other things, of proteins and hydrolases that have an impact on the bacterial cell wall, altering its capacity for intracellular replication (Arcos et al., 2011). It also contains innate immune cells such as alveolar macrophages and dendritic cells (Chai et al., 2018; Torrelles & Schlesinger, 2017).

1. First lines of immune system defense

Alveolar macrophages (AMs) are the first line of defense in *Mtb* infection and are the first cells to phagocytose bacteria (Figure 2) (Srivastava et al., 2014). Bacteria will be detected by AMs via microbial motifs conserved on their cell wall called pathogen-activated molecular pattern (PAMPs). These motifs are recognized by macrophage pattern-recognition receptors (PRRs), several types of which are involved in *Mtb* recognition: Toll-like receptors (TLRs), nucleotide-binding domain and leucine-rich repeat-containing receptors (NLRs), C-type lectin receptors (CLRs), NOD-like receptors (NLR) and cyclic GMP-AMP synthase (cGAS)/stimulator of interferon genes (STING) (Chandra et al., 2022; Guirado et al., 2013). In the case of *Mtb*, PAMPs are recognized mainly by TLR2 (membrane receptor recognizing lipid motifs) and TLR9 (cytosolic receptor), which helps the bacterium to enter the macrophage and the phagosome (Queval et al., 2017).

A recent study by Cohen et al showed that interstitial macrophages (IMs) also play a role in the immune defense against *Mtb*, as mycobacteria-infected AMs bring the pathogen into contact with IMs following relocalization in the interstitium, where IMs reside (S. B. Cohen et al., 2018). *Mtb*-containing macrophages will then, via cytokine secretion, recruit other

immune cells such as macrophage-derived monocytes, neutrophils, and natural killer cells (NK) (Figure 2) (Liu et al., 2017).

During an immune response, neutrophils play a bactericidal role through the production of reactive oxygen species (ROS) and a death system called NETose. Here, DNA filaments combined with histones and antimicrobial proteins are released outside the cell and form traps called neutrophile extracellular traps (NETs) (Braian et al., 2013; García-Bengoa et al., 2023). Upon *Mtb* infection, NETs have been described as important in containing infection and helping to recruit other immune cells, but do not appear capable of killing mycobacteria (Braian et al., 2013). Some studies have even shown that NETs form favorable niches for bacterial persistence and replication (Chandra et al., 2022). This creates a cycle in which bacteria, released from dying neutrophils after having caused neutrophil necrosis, are phagocytized by macrophages, enabling their potential replication and the recruitment of more neutrophils (Chandra et al., 2022).
NK cells have been shown to be involved in immune defense by secreting cytotoxic granular proteins (perforin, granzyme and granulysin), and triggering apoptosis in infected macrophages (Allen et al., 2015).

Infected cells and recruited immune cells then form a vascularized multicellular structure to contain the bacteria (Figure 2) (Chandra et al., 2022).

2. Granulomas

During the innate immune response, dendritic cells present in pulmonary surfactant phagocytose bacteria and migrate to lymphatic organs to initiate the adaptive immune response. This enables the recruitment of CD4+ and CD8+ T and B lymphocytes (Chai et al., 2018). Thanks to the vascularization of the structure, adaptive immune cells reinforce the multicellular structure formed by innate immune cells and mycobacteria (Chandra et al., 2022; Pagán & Ramakrishnan, 2015). Other cells are also recruited, such as fibroblasts and epithelioid macrophages, to reinforce this structure. This results in the formation of a complex organization of cells known as a granuloma (Figure 2) (Ramakrishnan, 2012; Russell, 2007).

Initially, granulomas were thought to be only a defense mechanism to control infection and limit inflammation (Saunders & Cooper, 2000). But after numerous studies, with zebrafish and non-human primates as models, granulomas have also been shown to be beneficial for the bacteria, since these structures offer them a favorable environment to replication and dissemination (Cadena et al., 2017; Ramakrishnan, 2012).

Once the granuloma is formed, the center becomes devascularized and necrotic, resulting in conditions of hypoxia and nutrient deprivation, and several types of evolution are possible (Chandra et al., 2022). In the first condition, the granuloma's immune cells succeed in completely eliminating the bacilli, causing the immune cells and tissues to degrade and harden. The granuloma thus becomes a calcified granuloma (Lenaerts et al., 2015). In the second condition, the immune cells are unable to eliminate the pathogens, which persist and may even replicate. The necrotic center of the granuloma can drive the bacteria into a state of dormancy or persistence (Chandra et al., 2022; Galagan et al., 2013). This granuloma can remain in the lungs for a lifetime. But in some cases, impairment of the immune system linked to various risk factors as described above, can lead to a disturbance in cell equilibrium, resulting in liquefaction of the caseous center and creating permissive conditions for bacterial replication (M. Kim et al., 2010). These structures eventually break down, releasing the bacteria and triggering the activation of the disease known as active TB. The host then becomes carrier of the disease, and the transmission cycle is initiated by coughing up droplets containing the bacilli (Figure 2). It is then also possible for the released bacilli, especially in large quantities, to spread in the blood or lymphatic system, causing lesions in various organs. In this case, the patient declares extra-pulmonary TB (Rahlwes et al., 2023).

3. Macrophage mechanisms against *Mycobacterium tuberculosis* infection

a. Signaling pathways to control inflammation

Several cytokines are involved in the response to *Mtb* infection within immune cells, such as nuclear factor-kappa B (NFκB), type I interferon (IFN-α and -β), interferon γ (IFN-γ), anti-tumor necrosis factor (TNF-α), interleukin-6 (IL-6), IL-1β and IL-18. These are up regulated by AMs during infection (Chai et al., 2020).

Within the macrophages, recognition of *Mtb* via PRRs leads to different types of receptor-dependents signaling cascades. For example, TLR2, shown to be one of the main receptors enabling pathogen phagocytosis (Maphasa et al., 2021), and CLRs recognize PAMPS which activate NFκB, resulting in the production of various cytokines such as TNF-α, pro-IL-1β and pro-IL-18 (Chandra et al., 2022). Recognition of a 19 kDa lipoprotein by TLR2 also leads to IL-12 production, initiating the recruitment of CD8+ T cells (Cavalcanti et al., 2012; Nigou et al., 2001). The TLR2 signaling cascade also leads, via activation of NFκB, to an increase in the level of the non-activated cytokines pro-IL-1β and pro-IL-18. These cytokines are then activated in their mature form by the NLRP3 inflammasome following cleavage by caspase-1 (S. B. Cohen et al., 2018; Nigou et al., 2001; Simeone et al., 2021).

Mtb recognition by cGAS-STING is made possible by the presence of double-stranded DNA in the cytosol. The presence of this DNA, which is likely mycobacterial DNA released from the *Mtb*-containing phagosome, is mainly due to action of a 6 kDa protein (named ESAT-6) secreted by *Mtb* via the type VII secretion system and having been recognized as a virulence factor. As described in more detail in a separate paragraph further below, ESAT-6 was shown to have membranolytic activity, which is involved in phagosomal rupture, allowing the bacteria or bacterial DNA to translocate into the cytosol (Majlessi & Brosch, 2015). Activation of the cGAS-STING signaling pathway results in the production and release of type I IFN, and in stimulating autophagy, enabling the cell to fight infection (Chai et al., 2018; Majlessi & Brosch, 2015; Watson et al., 2015).

NK cells also secrete the cytokines IFN-γ and TNF-α, enabling the activation of other immune cells such as macrophages. These two cytokines are also produced by CD8+ T cells, as they are the two most important cytokines involved in stabilizing the granuloma structure. If one of these two cytokines is missing, the structure of the granuloma may be affected and rupture, releasing the bacilli (Cavalcanti et al., 2012).

The production of these cytokines not only recruits immune cells, but also triggers the defense mechanisms described below.

b. Phagosome

The first line of defense upon detection of *Mtb* by AMs is the internalization of the bacterium following recognition of the PAMPs, called phagocytosis, into an intracellular vacuole bounded by a bilayer membrane called the phagosome (Tjelle et al., 2000). The phagosome then undergoes various stages of maturation through fusions with endosomes, which in most cases eliminates the phagocytized pathogen if the process is carried out correctly (Uribe-Querol & Rosales, 2017). The proteins involved in phagosome maturation are mainly from the Rab GTPase family (Gutierrez, 2013).

The phagosome having internalized the bacterium recruits an early endosome by reducing the intracellular Ca^{2+} concentration and fuses with it through the recruitment of the Rab5 GTPase protein, which enables the pH decrease to initiate, a key element in combating the pathogen (Poirier & Av-Gay, 2015). This fusion enables the phagosome to acquire the Rab7 small GTPase marker, leading to the fusion of the so-called early phagosome with a late endosome, resulting in the formation of a phagosome called the late phagosome, also containing Golgi proteins (Kinchen & Ravichandran, 2008; Mottola, 2014). Finally, the late phagosome fuses with a lysosome to become a phagolysosome with a very acidic pH allowing the enzymes present to act and using hydrolysis and oxidative stress to effectively kill the pathogen (Nguyen & Yates, 2021).

c. Inflammasome

The inflammasome is a protein synthesized by the activation of NFκB, after assembly of a sensor (nucleotide-binding oligomerization domain (NOD)-like receptor (NLR)) with an effector (pro caspase-1) and an adaptor (apoptosis-associated speck-like protein containing a CARD (ASC)). In the case of a response to *Mtb*, the sensor synthesized is NLR pyrin domain containing 3 (NLRP3) which, thanks to ASC, is connected to pro-caspase-1, which then becomes activated (Bauernfeind et al., 2009; Christgen et al., 2020). The protein complex is assembled following activation of specific PRRs, such as by the presence of *Mtb* DNA in the cytosol due to the action of secreted ESAT-6 (Simeone et al., 2021).

Once the complex is activated, caspase-1 cleaves the pro-inflammatory precursors pro-IL-1β and pro-IL-18 into their mature forms IL-1β and IL-18, which play a central role in the response to infection by stimulating the production of pro-inflammatory cytokines such as IL-6 and TNF-α, enhancing antimicrobial properties during phagocytosis and initiating the adaptive response of CD4+ T lymphocytes (Kelley et al., 2019; van de Veerdonk et al., 2011).

Activation of the NLRP3 inflammasome also activates gasdermin D cleavage by caspase-1, resulting in membrane pore formation causing cell death. This signaling pathway is called pyroptosis and helps to limit bacterial replication by releasing them into the extracellular environment for clearance by other immune cells (Beckwith et al., 2020; He et al., 2015).

d. Autophagy

Autophagy is a cellular defense mechanism used to maintain cellular homeostasis or eliminate pathogens (Maphasa et al., 2021). The process is called xenophagy when it is used against an intracellular pathogen (Rahlwes et al., 2023). Xenophagy involves the recognition of intracellular pathogens and the formation of an autophagosome by the elongation of a double membrane around the pathogen. Once formed, the autophagosome will fuse with a lysosome to form an autophagolysosome and eliminate the pathogen similar to the phagosome-lysosome linkage seen previously (Mintern & Villadangos, 2012).

The process by which homeostasis is regulated is called macroautophagy and, for example, regulates the production of various proteins such as cytokines. When excessive IL-1β or IL-18 production is detected, cytokines are internalized and eliminated by autophagy (Gutierrez et al., 2004; Mintern & Villadangos, 2012).

If defective cell elements or pathogens cannot be eliminated by phagocytosis or autophagy, a cell death pathway may be established.

e. Cellular death pathways

When infected macrophages are unable to complete the process of phagocytosis of the pathogen, or autophagy has not been activated, two cellular death pathways can be used: apoptosis or cell necrosis.

Apoptosis is a programmed cell death, while necrosis is characterized by a disruption of membrane integrity caused by irreversible and uncontrolled damages (Lam et al., 2017). Different signaling pathways are involved in the regulation of programmed and unprogrammed cell death. These pathways are directed by several caspase family proteins (Kesavardhana et al., 2020).

Apoptosis protects the organism from intracellular pathogens such as *Mtb* by forming small vesicles, known as apoptotic bodies, from the plasma membrane, and containing cellular debris and pathogens for phagocytic uptake by neighboring immune cells (Elmore, 2007). It is activated when cell death receptors are activated by external signals and activates caspase family proteins (Kesavardhana et al., 2020). Two different pathways can induce apoptosis: extrinsic apoptosis induced by the binding of TNF-α or Fas ligand to their receptor, activating caspases 8 and 7 (Behar et al., 2011); and intrinsic apoptosis induced by intracellular stress signals such as oxidative stress, DNA damage or nutrient deprivation, leading to permeabilization of the mitochondrial membrane and assembly of a protein complex, called the apoptosome, which induces activation of caspase 9 (S. W. G. Tait & Green, 2010).

Necrosis is induced by the bacterium via the production of TNF-α causing ROS production by the mitochondria (Roca et al., 2019). Necrosis is triggered by a cell death receptor-induced signaling cascade involving protein kinases of the RIPK and MLKL family mainly (Kesavardhana et al., 2020; Pasparakis & Vandenabeele, 2015). Pyroptosis triggered by the NLRP3 inflammasome is a form of inflammatory necrosis (Behar et al., 2010; Pasparakis & Vandenabeele, 2015).

f. Stress-induced defense

To fight the bacteria, macrophages use various regulatory properties. When the pathogen is internalized, within the phagosome, defense mechanisms are initiated, such as the production of radicals causing bacterial stress or metal ions regulation (Niederweis et al., 2015).

To defend against intracellular pathogens like *Mtb*, macrophages can form radicals that can limit bacterial growth when internalized in a phagosome and bring the phagosome to maturation. The cell can use nitric oxide (NO) reactive species and its derivatives reactive nitrogen species (RNS). These are produced by nitric oxide synthase (NOS) and can be converted into other radicals such as nitrogen dioxide (NO_2), nitrous trioxide (N_20_3) or the oxidant peroxynitrile ($OONO^-$), which can have an effect on the bacteria or cellular pathways (Weiss & Schaible, 2015; Wink et al., 2011).
Another form of radical derived from oxygen molecules is also known to have an effect on bacteria. ROS are involved in cellular processes and have antimicrobial activity on intracellular bacteria. Several types of ROS are found in cells, including superoxide anion ($O_2^{\bullet-}$), hydroxyl ($HO^{\bullet}$) and hydrogen peroxide (H_2O_2). These species are mainly formed by NADPH oxidase in the phagosome, or in mitochondria by the mitochondrial respiratory electron transport chain (Nathan & Cunningham-Bussel, 2013; Weiss & Schaible, 2015).

The regulation of metal ions is also a source of defense for macrophages. Depending on the ions, their quantity can be produced excessively if they are toxic to the bacteria, or sequestered if the bacteria use them as a nutrient. Macrophages are capable of sequestering or releasing metal ions, depending on the situation. This mechanism is known as "nutritional immunity" (Niederweis et al., 2015).
Within the phagosome, the exclusion of metals such as iron and manganese is described as an antibacterial mechanism used by the macrophage as such metals are used by the bacteria for survival and replication (Botella et al., 2012). Conversely, the accumulation of metals can become toxic as this can lead to the formation of oxygen and nitrogen radicals (Weiss & Schaible, 2015). For example, the macrophage regulates metals within the phagosome by eliminating iron and manganese favorable to bacterial growth and accumulating zinc and copper, which are toxic in excessive quantities (Neyrolles et al., 2013).

4. *Mycobacterium tuberculosis* defense mechanisms against macrophages

During its evolution, *Mtb* has developed defense mechanisms against the different actions of macrophages and the immune system.

For example, *Mtb* has been shown to secrete numerous apoptosis-inhibiting proteins (Behar et al., 2011; Lerner et al., 2017). This inhibition would allow the induction of cell necrosis, which would give the pathogen an advantage for replication (Lerner et al., 2017). Necrosis is induced by several *Mtb* mechanisms. Firstly, via the NLRP3 inflammasome which, following detection of microbial DNA in the cytosol linked to ESAT-6 action, triggers cell death by pyroptosis. Like necrosis, this cell death system involves the release of bacilli into the extracellular environment before they are phagocytosed again (Mishra et al., 2010). Secondly, secretion of the ESAT-6 protein also promotes necrosis by preventing cell membrane repair, which normally enables the cell to induce apoptosis (Divangahi et al., 2009). This induction of necrosis and inhibition of apoptosis is not found in non-pathogenic mycobacterial species (Behar et al., 2011). The bacterium can also induce necrosis in infected neutrophils through the action of the ESAT-6 protein and the production of ROS by the bacterium (Dallenga et al., 2017).

Mtb is able to block phagosome-lysosome fusion via different signaling pathways. Inhibiting phagosome maturation enables the bacterium to control pH acidity for its survival (Queval et al., 2017). The bacterium is also able to impact inflammasome activity. The inflammasome is linked to ESAT-6 protein secretion by *Mtb*. But *Mtb* can inhibit inflammasome formation in an ESAT-6-independent manner. This inhibition has been shown to be mediated by a phosphokinase protein (PknF) involved in lipid production (Rastogi et al., 2021). It has also been shown that *Mtb* can block autophagolysosome formation by blocking the NADPH oxidase involved in autophagy biogenesis (Chandra et al., 2022).

Metal ion regulation of macrophages can also be countered by *Mtb* through the use of metal efflux and detoxification systems (Niederweis et al., 2015), and the presence of proteins such as Ctp that have been shown to help the bacterium resist zinc accumulation. The MctB and

MymT proteins have also been described as participating in *Mtb* resistance to high concentrations of copper (Botella et al., 2012). *Mtb* is also able to recover iron despite deprivation by the cell thanks to the production of siderophores with a high affinity for iron (Patel et al., 2018).

The pathogen is also able to mask PAMPs with lipids present in the cell wall, allowing it not to induce microbicidal macrophage recruitment but macrophages more permissive to its survival and replication (Pagán & Ramakrishnan, 2015). The bacterium also has a defense mechanism that delays the establishment of the adaptive immune response. When the bacteria reach the alveoli, they are ingested by dendritic cells, which normally migrate rapidly to the lymph nodes. But the bacterium can delay this migration, allowing it to replicate in permissive macrophages before T-cells intervention (Ramakrishnan, 2012).

Finally, *Mtb* is able to enter a state of dormancy when conditions for its survival are unfavorable, such as in the hypoxic conditions of granulomas. This is made possible by the DosRST regulator produced by the mycobacterial genome (Gengenbacher & Kaufmann, 2012).

These survival mechanisms are a non-exhaustive list of all that *Mtb* can do to survive and multiply within immune cells.

V. Prevention and Treatment

Two main types of intervention exist for TB. Preventive intervention to avoid infection or enable the host to better defend itself against development of disease (vaccination). Or curative treatment once the disease has been declared, generally consisting of a 6-month multidrug regimen.

1. Preventive intervention with vaccines

Prevention is an essential element in the fight against TB. Currently, Bacille Calmette-Guerin (BCG) is the only licensed vaccine used at large scale in the prevention of TB infection or TB disease. It was first introduced to be used in humans in 1921 and is used in many high burden

TB countries to protect children from severe extra-pulmonary TB forms (Reuter et al., 2019; World Health Organization, 2022). Children, and in particular those under the age of 2, have a higher risk of developing extra-pulmonary TB, such as tuberculous meningitis, which is among the most dangerous (Moule & Cirillo, 2020; World Health Organization module 5, 2022). Following the COVID-19 pandemic, the number of children vaccinated with BCG fell in 2020 (3.6 million in 2019 vs. 3.2 million in 2020) and has since risen again, with 3.5 million children vaccinated in 2021 (World Health Organization, 2022).

BCG, developed by Albert Calmette and Camille Guerin, is based on an attenuated strain of *Mycobacterium bovis*, a member of the MTBC that causes TB in cattle. The BCG strain has been attenuated by repeated passaging on ox-bile containing potato medium at the beginning of the 20th century, and vaccination with BCG triggers innate and adaptive immune responses in the immune-competent hosts without causing disease. The attenuation of BCG is caused in part by the genomic deletion of region of difference RD1 within the ESX-1 locus, which is encoding a highly immunogenic small protein, named 6 kDa early secreted antigenic target (ESAT-6), that was later also described as being involved in phagosomal rupture during host cell infection (Brosch et al., 2007; Simeone et al., 2012). As BCG was already generated more than hundred years ago and has since been distributed to many laboratories in the world and cultured there, BCG is not a well-defined genetic entity, but rather a cluster of attenuated strains that may show some genetic differences. There are several BCG variants that show additional deletions and/or single nucleotide polymorphisms (SNPs), as well as certain duplications in their bacterial genomes, but they all have in common the deletion of the RD1 region, which occurred before the first BCG culture was used for human vaccination (Brosch et al., 2007).

Even though BCG protects children efficiently from developing severe forms of TB, large scale BCG vaccination in many countries of the world was not able to stop the TB pandemic. One of the reasons is that vaccination at very young age provides protection for the child, which however wanes until the age of adolescence and adulthood. Unfortunately, the protection provided by childhood BCG vaccination against pulmonary TB in later stages of life is not very efficient and for this reason, the international research community is since years searching for new or improved vaccines that might also protect adolescence and adults in high TB burden settings to develop pulmonary TB (Ahmed et al., 2021).

The current outcome of the different research projects can be seen in list of potential vaccine candidates that are in preclinical or clinical evaluation. At the end of 2022, 16 vaccine candidates were in clinical trials: four in phase I, eight in phase II and four in phase III (World Health Organization, 2022).

One of the most promising candidates among these is the MTBVAC vaccine, which corresponds to a live attenuated strain of *Mtb* developed by Biofabri and funded by the TBVI (TuBerculosis Vaccine initiative) consortium. This vaccine has been in phase III of clinical trial in newborns since the end of 2022 (*Efficacy, Safety and Immunogenicity Evaluation of MTBVAC in Newborns in Sub-Saharan Africa (MTBVACN3)*, 2022). The attenuation of the vaccine strain is assured by independent deletions of two genes (*phoP* and *fadD26*) that are both encoding proteins involved in bacterial virulence (*phoP*, virulence regulator, also controlling secretion of the virulence protein ESAT-6, and *fadD26* encoding enzymes that are involved in the production of cell envelope virulence lipids (PDIM) (Hatherill et al., 2020; Martín et al., 2021). MTBVAC is supposed to be more immunogenic and more protective than BCG due to the presence of a much larger number of T-cell epitopes, which are absent from BCG due to the deletion of RD1 and other genomic regions.

Another candidate vaccine in phase III clinical trials is VPM1002 which is being developed by the Serum Institute of India (SSI) and the Vakzine Projekt Management (VPM) (*VPM1002 Tuberculosis Vaccine*, 2023). This vaccine is a recombinant BCG strain in which the *ureC* gene, encoding for urease C and involved in the inhibition of phagosome maturation, has been replaced by the *hylA* from *Listeria monocytogenes*, which is encoding a hemolysis that is suggested to perforate the phagosomal membrane during infection, facilitating the maturation (Nieuwenhuizen et al., 2017).

The MIP/Immuvac developed by Cadila Pharmaceuticals and supported by the Stop TB Partnership entity of the United Nations office is in a phase III of clinical trial and targets adolescents and adults against primary *Mtb* infections (*Immuvac (MIP)*, 2022). The vaccine is composed of a heat-inactivated non-tuberculous mycobacterium *M. indicus parnii*. This vaccine has already been approved by the FDA to treat patients with multibacillary leprosy

and prevent this disease in people in contact with it (J. Li et al., 2020), but its efficacy against tuberculosis is still under debate, requiring further study (Steigler et al., 2022).

In 2023, another vaccine in development entered phase III. The M72/AS01E vaccine candidate developed by GSK (GlaxoSmithKline) and supported by the Bill & Melinda Gates Foundation showed promising results (Lilly Tozer, 2023; World Health Organization, 2022). The vaccine contains recombinant antigenic proteins and an adjuvant to potentiate the immune response (D. R. Tait et al., 2019). The particularity of this vaccine was that it was given to people that had already been infected by *Mtb* but showed a latent infection. The purpose of using the vaccine was thus to prevent development of active TB disease. In a first large phase 2b clinical trial a protection of up to 54 % in prevention of TB disease was observed in the group of vaccinated people compared to the placebo group. (D. R. Tait et al., 2019).

These vaccines are developed as a preventive measure against TB. Research is also underway into vaccines designed to improve the treatment of patients suffering from TB (therapeutic vaccines). Studies show that these vaccines, such as the RUTI vaccine containing purified *Mtb* fragments, stimulate immune systems of patient, thereby potentially reducing the duration of treatment (Prabowo et al., 2019).

Vaccination research is of great interest, as a vaccine with a better protective efficacy than BCG would have a large impact on preventing TB cases, and in addition would also have a strong impact on prevention of transmission of *Mtb*. This research is therefore an important part of the fight against this disease, and forms part of the Essential Immunization Program of the WHO. In addition to the described vaccine projects in advanced clinical trials, a large number of preclinical vaccine research is ongoing in numerous research laboratories of the world, which will however not be further described as such descriptions are beyond the scope of this thesis.

2. Treatment of drug sensitive tuberculosis: first-line anti-tuberculosis drugs

As explained in the first part of the introduction, treatment against TB disease is complex and long. The first line treatment approved since 1980s is composed of four antibiotics for a

minimum of six month: two months with rifampicin, ethambutol, isoniazid, and pyrazinamide followed by four months with rifampicin and isoniazid (World Health Organization, 2022). The parallel use of four anti-TB drugs in the first two months of treatment is necessary to reduce the very high bacterial burden that may exist during active TB to a much lower bacterial count, before the reduction to only two drugs can start for the remaining four months. This complexity is also due to the intracellular growth of the bacteria coupled with is highly hydrophobic cell wall that is hard to penetrate and cross (Bansal et al., 2018). To do so, the four anti-TB agents used as first-line antibiotics have specific roles:

- **Rifampicin** (RIF) is a molecule that interferes with mRNA transcription and elongation by binding the ß-subunit of RNA polymerase complex (Telenti et al., 1993).
- **Isoniazid** or isonicotinic acid hydrazide (INH) is a pro-drug that needs activation inside *Mtb*. INH inhibits the mycolic acid synthesis through inhibition of the carrier protein reductase InhA (Palomino & Martin, 2014), and is only active on replicating bacilli. In classical conditions, InhA used NADH as cofactor to act on mycolic acid synthesis. When INH is used, the molecule needs to be activated by KatG and its active form interact with NAD+ leading to the formation of isonicotinoyl-NAD+ complex which bind to the NADH-binding site of *inhA* with higher affinity than NADH and prevent it action on mycolic acid synthesis (Dokrungkoon et al., 2023).
- **Pyrazinamide** (PZA) is a molecule used principally for latent and semi-dormant bacilli found in granulomas (N. Y. Kim et al., 2023). The mechanism of action of PZA is still under debate (Peterson et al., 2015), the most widely accepted hypothesis being that acidification of the cytoplasmic compartment leads to an imbalance in cellular metabolism. This action is enabled by the passive diffusion of PZA into the cell, followed by transformation into its active form (pyrasinoic acid (POA)) by the PZAse PncA of *Mtb* and return into the extracellular medium. Then, when the environment becomes acidic, the molecule will transport protons inside the cell causing damages in the bacterium (Zhang et al., 2013).
- **Ethambutol** (ETH) is a bacteriostatic molecule and, like INH, has an action on replicating bacilli. The drug blocks the synthesis of arabinogalactan affecting the mycobacterial cell wall (Belanger et al., 1996; Palomino & Martin, 2014). Recently, it was also shown that the molecule affects another component of the cell wall by

targeting the glutamate reductase MurI. This enzyme is crucial for *Mtb* for the biosynthesis of peptidoglycan (Pawar et al., 2019).

3. Treatment of drug resistant tuberculosis: second- & third-line anti-tuberculosis drugs

Drug resistance is one of the main causes of TB treatment failure. Resistance can occur naturally within the bacteria, but it can also be caused by improper use of antibiotics or incorrect intake of treatment by the patient, allowing the bacteria to adapt (Pai et al., 2016). Several degrees of resistance exist for this pathogen. Firstly, monoresistance to rifampicin (RR-TB) or isoniazid, or resistance to both antibiotics known as multidrug resistance (MDR-TB). MDR-TB cases are estimated to represent 3.6% of new cases reported in 2021 and are mainly detected in India (26% of cases), Russia (8.9% of cases), and Pakistan (7.9% of cases) (World Health Organization, 2022).

Other types of resistance have also emerged. The WHO recognizes the terms pre-extensively resistant TB (pre-XDR-TB), which refers to strains that are resistant to rifampicin, isoniazid and all fluoroquinolones, and extensively resistant TB (XDR-TB), which refers to strains that are resistant to bedaquiline or linezolid or both in addition to the previous resistances already mentioned (WHO module 4, 2022).

To fight MDR resistant *Mtb* strains, new molecules called second- or third-line anti-TB drugs have been developed:

- **Fluoroquinolones**, which mainly include levofloxacin and moxifloxacin. These broad-spectrum antibiotics have a bactericidal action by preventing the activity of gyrase or topoisomerase VI, leading to disruption of DNA replication (J. Sarathy et al., 2019).
- **Aminoglycoside** family, such as amikacin, kanamycin, and streptomycin, are injectable molecules. These molecules act on protein synthesis by binding to the bacterial 16S rRNA (Krause et al., 2016).
- **Carbapenems** are molecules belonging to the ß-lactam family, such as meropenem, ertapenem and imipenem, and inhibit the synthesis of peptidoglycans required for the solidity of the bacterial cell wall (van Rijn et al., 2019).

- **Ethionamide** which shares the same target than isoniazid (inhibition of mycolic acid synthesis) (Palomino & Martin, 2014).
- **Bedaquiline** (BDQ) inhibits bacterial ATP synthase, a key enzyme in bacterial respiration. This anti-TB drug is a powerful bactericidal molecule (J. P. Sarathy et al., 2019). The addition of bedaquiline to the treatment of resistant TB has reduced the duration of treatment by several months and also reduced mortality by 3-fold in patients suffering from RR/MDR-TB (Mallick et al., 2022).
- **Linezolid** inhibits protein synthesis by binding to the bacterial ribosome and mitochondria (Singh et al., 2019).

The three anti-TB drugs approved by drug agencies after more than 40 years are bedaquiline and delamanid, approved in 2014 by the European Medicine Agency (EMA) (in 2012 for bedaquiline by the Food Drug Administration (FDA)), and pretomanid, approved in 2020 by the EMA (in 2019 by the FDA) (Perrin et al., 2022). Delamanid and pretomanid have a similar mode of action, inhibiting mycolic acid synthesis and altering the bacterial cell wall (Mudde et al., 2022).

Typically, today MDR- TB is treated with a 6-month regimen of bedaquiline, pretomanid, linezolid and moxifloxacin. If the strain is found to be resistant to fluoroquinolone, treatment is continued without moxifloxacin. Treatment is adapted according to strain resistance and patient conditions such as age, possible side effects, previous use of antibiotics (Vanino et al., 2023; WHO module 4, 2022).

4. New drug development

In 2022, 22 clinical development trials were underway. These trials include either research on new molecules, or research using molecules already in use for TB with new combinations to reduce the duration of therapy (World Health Organization, 2022).

Different goals are being pursued for the use of these molecules. Firstly, the study of new molecules capable of acting on the bacterium itself, thereby combating resistance, such as pretomanid (the latest molecule to be validated by the WHO). In addition to these approved

molecules, there are also several compounds with new modes of action in preclinical and clinical development, to mention just a few of the most promising ones: benzothiazinones which kill *Mtb* by blocking arabinan synthesis (Makarov et al., 2009)**;** SQ109, a new ethylene diamine that targets the essential MmpL3 mycolic acid transporter (Tahlan et al., 2012; Zheng et al., 2018) or the imidazopyridine amide telacebec (Q203) targeting the mycobacterial respiratory cytochrome bc1 complex (Pethe et al., 2013)**.**

Secondly, existing anti-TB molecules in different combinations or doses may be more effective against the pathogen, such as the RIFASHORT project, which is testing higher doses of rifamycins (rifampicin, rifampin or rifapentine) to reduce the duration of therapy from 6 to 4 months (Jindani et al., 2023).

It should also be mentioned that there exist several research consortia that look for developing new drugs. One of them is the ERA4TB (European regimen accelerator for tuberculosis) project (*ERA4TB - The Project*, n.d.), whose main objective is to create a European open platform to accelerate the development of new regimens for the treatment of TB.

Finally, research is being carried out to potentiate molecules using host-directed strategies. These treatments consist of using a molecule to improve the response of the immune system, either by potentiating the effect of a molecule during treatment, such as by increasing the uptake of the molecule by macrophages, as in the case of Verapamil, a drug used to treat hypertension, which inhibits the *Mtb* efflux pump, thus increasing the concentration of anti-TB agents in the bacterium, and potentiates several anti-TB agents in resistant or non-resistant TB (C. Chen et al., 2018), or by boosting immune cell responses to improve their ability to defend themselves against infection, for example by potentiating macrophage defense mechanisms such as phagocytosis and autophagy (Kolloli & Subbian, 2017)

B. Evolution of mycobacteria

I. Fast and slow growers

In the tree of life, the genus *Mycobacterium* belongs to the phylum *Actinobacteria*, and the family *Mycobacteriaceae* (Hug et al., 2016)**.** Bacteria belonging to this genus were first described as *Mycobacterium* in 1896 by Lehmann and Neumann due to their characteristic cell wall composed of mycolic acid lipids, the cell shape, and the aerobic growth (Lehmann & Neumann, 1896; Meehan et al., 2021). Mycobacteria are considered as rod-shaped and acid-fast high G+C Gram-positive bacteria (Cook et al., 2009). The genus contains almost 200 classified species, most of them representing harmless, environmental species, and some that can cause infections in humans and animals. The species can be divided into different groups regarding the type of infection they can cause. Three groups are described in the general classification: mycobacteria causing tuberculosis, containing mainly the members of the *Mycobacterium tuberculosis* complex; mycobacteria causing leprosy (*Mycobacterium leprae*); and non-tuberculous mycobacteria (NTM), also called atypical mycobacteria, corresponding to environmental and opportunist mycobacteria (Astier et al., 2017; Meehan et al., 2021; Van Ingen, 2013).

In a more general way, mycobacterial species can also be distinguished by their growth rate. Mycobacteria with colonies appearing on agar plates in less than 7 days are named rapid-growing mycobacteria (RGM), while the ones that need more than 7 days to form colonies are the slow-growing mycobacteria (SGM) (Forbes et al., 2018). RGM represent around half of the *Mycobacterium* genus species. Among them, six groups can be classified: *Mycobacterium fortiutum* group; *M. chelonae*/*M. abscessus* complex; *M. smegmatis* group; *M. mucogenicum* group*; M. mageritense*/*M. wolinskyi*; and mycobacteria with pigmentation. The other half corresponds to the SGM group (Brown-Elliott & Philley, 2017). Pathogens and opportunist mycobacteria are mainly found in the SGM group, even if some pathogens may also be found among the RGM, such as the well-known opportunistic pathogen *Mycobacterium abscessus* (Bachmann et al., 2020).

During the evolution of the *Mycobacterium* genus, SGM are thought to have evolved from RGM. One of the most common markers used to differentiate RGM and SGM is the insertion

of 12 to 14 nucleotides in the majority of 16S rRNA sequences of the SGM (Tortoli et al., 2017). This evolution is marked by characteristic genomic differences such as the suppression of the *livFGMH* operon involving in the transport of some amino acids used for bacterial growth; the *shaACDEFG* operon helping in the pH regulation during extreme conditions; two ABC transporters representing one of the most common ATP transporters in bacteria; and the multiplication of *mce1* operons in pathogenic mycobacteria and more precisely in SGM. *mce1* operons were acquired in RGM but their multiplication in SGM is supposed to facilitate entry into the macrophage, enhancing the intracellular, pathogenic lifestyle (Bachmann et al., 2020).

Identification of mycobacterial species is generally based on the analysis of sequences such as the 16S rRNA, and 16S-23S spacer sequences; and housekeeping genes including *hsp65*, *rpoB*, and *gyrA* (Forbes et al., 2018; Gupta et al., 2018). However, a phylogenetic cohesion, particularly among RGM, is difficult to describe because of the existence of a huge genomic diversity among the species. To bypass these difficulties, Gupta and colleagues recently proposed a new classification of the genus *Mycobacterium* by splitting the genus into five new genera (*Mycolicibacterium*, *Mycolicibacter*, *Mycolicibacillus*, *Mycobacteroides* and an emended *Mycobacterium*). These changes were proposed according to selected genomic differences observed between the mycobacterial species:

- *Mycobacterium* (*Tuberculosis-Simiae* clade): contains the SGM, including members of the *Mycobacterium tuberculosis* complex, slow-growing (SG-) NTM, and *M. leprae*, with an exception for the *M. terrae* complex, whose members represent slow and intermediate growing species. Genomic comparison revealed the presence of the same amino acid deletion in an unknown protein for each species of the clade.
- *Mycobacteroides* (*Abscessus-Chelonae* clade): contains the members of *M. chelonae*/*M. abscessus* complex and forms a deep branching in the phylogeny of the *Mycobacterium* genus.
- *Mycolicibacter* (*Terrae* clade): contains the *M. terrae* complex mycobacteria. They have the particularity of having a 14-nucleotide insertion in their 16S rRNA sequence, which has long been considered a feature of SGM in general.
- *Mycolicibacterium* (*Fortuitum-Vaccae* clade): contains the majority of the RGM, mostly considered non-pathogenic to humans, even if a few infection cases were reported.

- *Mycolicibacillus* (*Triviale* clade): contains three SGM species (*M. trivialis*, *M. koreensis*, and *M. parakoreensis*) with the particularity of not having the nucleotide insertion in their 16S rRNA sequence described for the *Mycolicibacter* clade.

The reclassification, which was also taken into consideration by certain strain collections, is strongly contested in the scientific community and suggestions were made by a consortium of specialist in mycobacterial taxonomy to ignore the new names (Tortoli et al., 2019). Despite some putative simplifications for the classification of mycobacteria, it is important to remember that any renaming of species should not cause confusion in clinical treatment, which would likely be the case for the proposed changes. Moreover, by combining multiple approaches for defining genus boundaries (16S rRNA gene similarity, amino acid identity index, average nucleotide identity, alignment fraction and percentage of conserved proteins) Meehan and coworkers have shown that the original Mycobacterium genus definition was strongly supported by their analysis over the proposed split of the genus in five new genera. (Armstrong & Parrish, 2021; Meehan et al., 2021). For all these reasons, in this thesis the traditional mycobacterial nomenclature will be used, as the "old" names remain validly published and anyone is free to continue to use them.

II. Mycobacterium causing tuberculosis

One of the most important pathogens of the *Mycobacterium* genus is *Mtb*. During the evolution of this obligate pathogen, genomic changes occurred in the genome of the progenitor bacteria that likely allowed adaptation to an intracellular lifestyle (Sapriel & Brosch, 2019). The host adaptation further resulted in the differentiation of selected tubercle bacilli into distinct lineages that were able to infect humans and/or animals. All these bacteria now form the *Mycobacterium tuberculosis* complex, whereby different members have undergone several host adaptation processes and show distinct host preferences.

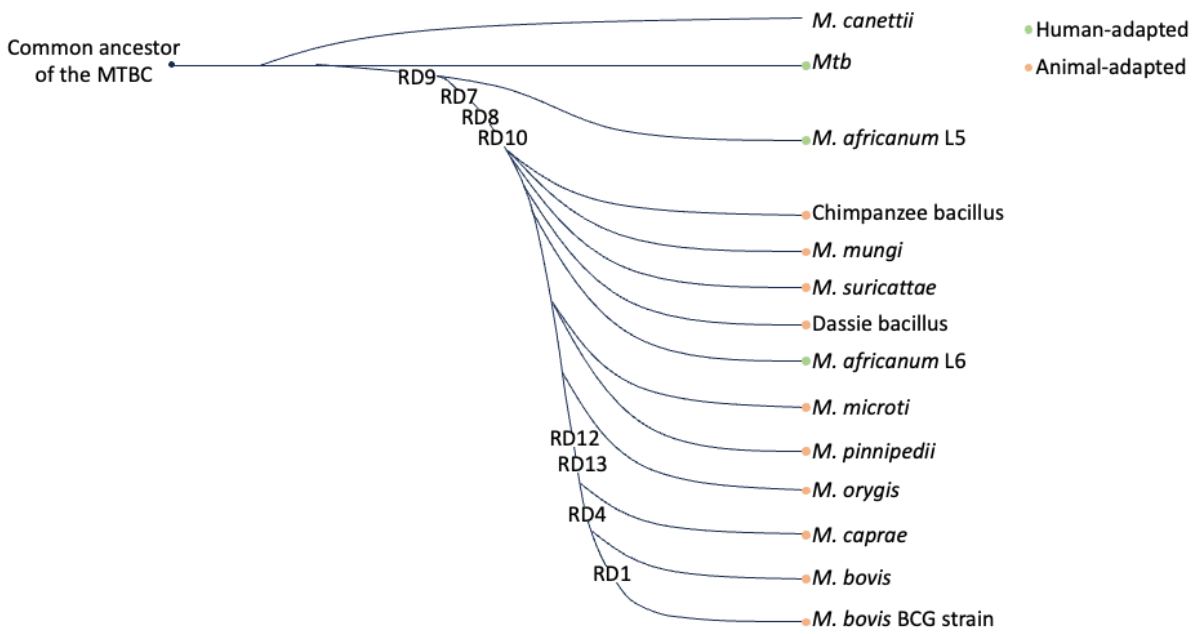

Figure 3: Schematic diagram illustrating the evolution of the *Mycobacterium tuberculosis* complex members and the closely related species *M. canettii*. The depicted regions of difference (RDs) represent genomic deletions that occurred in selected lineages at the branching points.

1. *Mycobacterium tuberculosis* complex

The *Mycobacterium tuberculosis* complex (MTBC) includes mycobacterial species able to cause TB disease in humans and/or animals (Gagneux, 2018). The complex is composed of 12 groups sharing more than 99.9% of genome sequence identity: *M. tuberculosis*, *M. africanumm*, *M. bovis*, "chimpanzee bacillus", "dassie bacillus", *M. capreae*, *M. microti*, *M. mungi*, *M. orygis*, *M. pinnipedii*, *M. suricattae*, and *M. bovis* BCG strains (Bespiatykh et al., 2021; Gagneux, 2018). Another group of closely related tubercle bacilli, named *M. canettii* also share a very high nucleotide identity but these strains can be considered outside the MTBC as these strains show clear traces of recent horizontal gene transfer (HGT) events and a recombinogenic population structure compared to the clonal and monomorphic MTBC (Boritsch et al., 2014; Brites et al., 2018)**.** *M. canettii* strains are thus considered as an outgroup, which can be found primarily in the geographic region around the horn of African, and whose ancestors might have been constituted a pool of genetically rather diverse tubercle bacilli, from which the MTBC has evolved by clonal evolution and adaptation to the mammalian host. As regards the host spectrum, *Mtb* and *M. africanum* show a host preference for humans while all other members of the MTBC represent animal-adapted species. Throughout MTBC evolution, it is likely that genomic changes happened, allowing bacterial adaptation to selected hosts. These differences are represented by the presence or absence of certain regions of difference (RD) in the size range of 2 to 13 kb (Figure 3) (Guimaraes & Zimpel, 2020), as well as numerous SNPs and small indels. The distribution of the various RD regions in the MTBC, has allowed a solid phylogenetic model to be developed for the MTBC, in which an *M. canettii*-like ancestor strain has diverged into different lineages of the MTBC by clonal expansion. In the figure 3, branching points are characterized by the absence of selected RD regions, which can serve as markers for phylogenic tree construction. Indeed, region RD9 is absent from *M. africanum* to *M. bovis* lineages, followed by the deletion of three other RDs (RD7, RD8, RD10) that are present in L5 strains of *M. africanum*, but are missing from *M. africanum* L6 strains and animal-adapted MTBC members. Finally, two additional RDs (RD12 and RD13) are deleted from *M. caprae* strains followed by the additional deletion of RD4 from all *M. bovis* and *M. bovis* BCG strains (Figure 3) (Brosch et al., 2002; Tientcheu et al., 2017).

In the early days of molecular typing of MTBC members, *Mtb* was thought to have evolved from *M. bovis* (Bottai et al., 2013; Stead et al., 1995), but sequencing of *Mtb* (Cole et al., 1998) and *M. bovis* (Garnier et al., 2003) genomes revealed a smaller genome size for *M. bovis* than for *Mtb*. Together with the results from the analysis of the distribution of above-described RDs, a revised evolutionary scenario was described, in which *M. bovis* and other animal-adapted strains represent a lineage of tubercle bacilli that has branched off from *Mtb*-like strains (Brosch et al., 2002). Further studies then revealed that the last common ancestor of the MTBC, most likely resembled *M. canettii* strains, which are rare tuberculosis-causing mycobacteria (Figure 3) (Garnier et al., 2003; Supply et al., 2013).

The best-known reservoir of MTBC members is the mammalian host, associated primarily with airborne transmission (Ehrt et al., 2018). However, it remains possible that under certain conditions MTBC members might also be accounted in the environment. For example, different studies have shown that *Mtb* can survive for many days in river water and can even infect rodents by drinking it (Gao et al., 2018; Martinez et al., 2019). Similar studies were performed with soil for *Mtb*, *M. canettii*, and *M. bovis*. The three strains were able to infect mice by the oral route after 12-month of incubation in soil, although an earlier study revealed that *Mtb* found in soil was sensitive to sunlight exposure (Ghodbane et al., 2014; Martinez et al., 2019). Recently, a putative environmental reservoir of *M. bovis* and *Mtb* was suggested by a study undertaken in Tanzania, where qPCR screening using specific primers for RD4 and RD9 genomic regions, generated positive hits for the presence of *M. bovis* and *Mtb* DNA in various environmental samples, including cattle and goat faeces, soil, water, and household dust (Emma Travis et al., 2019).

Each MTBC member is primarily specific to their mammalian host reservoirs: human for *M. africanum* and *Mtb*; cattle for *M. bovis*; chimpanzee for the “chimpanzee bacillus”; rock hyrax for the “dassie bacillus”; rodents for *M. microti*; mongoose for *M. mungi*; seals for *M. pinnipedii*; antelope for *M. orygis*; meerkats for *M. surricattae*; and goats for *M. caprae* (Brites et al., 2018; Tientcheu et al., 2017). Interspecies transmission is hard to determine due to the strong similarity between MTBC species. However, zoonosis was already demonstrated, mostly between human and cattle or goat.

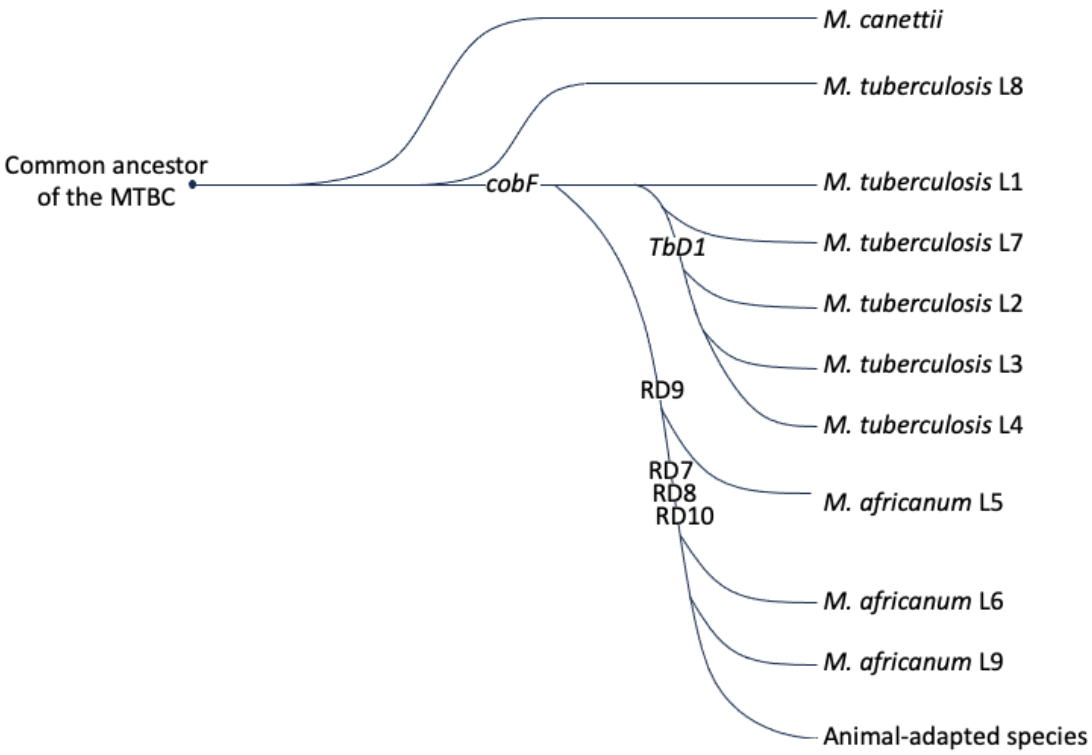

Figure 4: Schematic diagram illustrating the different lineages of human-adapted MTBC members. The cited regions of difference (RDs) or genomic regions or genes are absent in all strains after the branching.

It was shown that *M. bovis* and *M. caprae* are responsible of 1 to 3% of human TB worldwide (Gagneux, 2018). Generally, pathogens are transmitted to human through human-animal contact or by the consumption of food products such as milk (Guimaraes & Zimpel, 2020). Zoonosis between animal-adapted species have also been found. For example, infection by *M. bovis* and *M. caprae* were reported in cattle, goats, sheep, pigs and more, while *M. orygis* was found in antelopes, Indian cattle, as well as in humans in India and Africa (van Ingen et al., 2012). Interspecies transmissions are rarely described for other MTBC members (*M. microti*, *M. mungi*, *M. pinnipedii*, and *M. surricattae*) (Guimaraes & Zimpel, 2020; Kock et al., 2021), although they may exist, as shown by some rare human infections caused by *M. microti* (Orgeur et al., 2021)**.**

Conversely, infection of animals by human pathogens (reverse zoonosis) have already been described with cases of *Mtb* or *M. africanum* infections in cattle and goats in different part of the world (Kock et al., 2021), although some caution must be taken for the interpretation of such results, as *Mtb* strains were repeatedly demonstrated to be attenuated in cattle in experimental infection trials (Villarreal-Ramos et al., 2018; Whelan et al., 2010).

2. Tuberculosis in human: lineages 1 to 9

During evolution, several lineages evolved from the putative ancestor of *Mtb* due to a few genomic changes. The human-adapted pathogens from the MTBC were previously described as being composed of seven lineages with five lineages representing *Mtb sensu stricto* and two others *M. africanum* strains (Gagneux, 2018). In 2020, a new lineage of *Mtb sensu stricto* was described by Ngabonziza et al. representing the eighth lineage and, since 2021 a study of Coscolla and colleagues described a new lineage associated to *M. africanum* species, raising the total number of lineages to 9. Lineages 1 to 4, 7 and 8 correspond to *Mtb sensu stricto* strains, while lineages 5, 6, and 9 are associated with *M. africanum* (Coscolla et al., 2021; Gagneux, 2018; Ngabonziza et al., 2020).

Various genomic differences, including SNPs, presence or absence of small indels and RDs are found among the 9 lineages (Figure 4). For the human adapted strains, one of the first discovered markers was the TbD1 region, which is deleted in *Mtb sensu stricto* lineages L2, L3 and L4, and is present in lineages L1, L7, and L8, which can classify the *Mtb* strains in two

categories: ancestral *Mtb* (intact TbD1 with L1, L7, and L8) and modern *Mtb* (truncated TbD1 with L2 to L4). This deletion was shown to increase virulence of the bacteria in certain experimental infection models, such as the guinea pig model and was suggested to enhance the epidemic spread of the TbD1-deleted lineages (Bottai et al., 2020). The two strains described for lineage L8 have the particularity to have the complete sequence of the cobF genomic region, which is hypothesized to be involved in cobalamin and vitamin B12 synthesis. The *cobF* gene is commonly present in *M. canettii* strains and some NTM, while all known members of the MTBC (except L8 strains) have lost this region during evolution (Ngabonziza et al., 2020; Supply et al., 2013). *Mtb* strains of lineage L8 thus are very interesting isolates that are localized in the phylogenetic tree at the branching point between *M. canettii* strains and the MTBC members (Figure 4).

The other human-adapted strains of the MTBC are the *M. africanum* strains, which are localized in a different branch of the phylogenetic tree of the MTBC. The strains of the two best-studied lineages of *M. africanum* (L5 and L6) have different deletions in their genome. The first one is the deletion of the RD9 region in both lineages, while L6 strains also lack regions RD7, RD8 and RD10. These deletions are shared with the animal-adapted MTBC members (Figure 3 and 4) (Brites & Gagneux, 2015; Brosch et al., 2002). *M. africanum* L9 was described by Coscolla et al., but only few isolates were categorized into L9. Phylogenetic markers used to describe the new lineage were based on a combination of specific SNPs, and no important deletion was found compared to other lineages (Coscolla et al., 2021; Shitikov & Bespiatykh, 2023).

As explained in the previous part, MTBC members speciated from *Mtb* precursor species and not from *M. bovis* (Brosch et al., 2002). Researchers focused on the different *Mtb* lineages to determine where tuberculosis-causing bacteria have first emerged. To do so, they studied the dissemination of selected lineages around the world. L2 and L4 were described as the two most widespread lineages in the world (Gagneux, 2018). L5 and L6 are the two lineages predominant in West Africa and cause more than 50% of TB cases there (de Jong et al., 2010; M. L. Silva et al., 2022), while L7, L8 and L9 are restricted to East Africa (Coscolla et al., 2021; de Jong et al., 2010), and the highest percentage of *M. canettii* infection is also related to East Africa (Gagneux, 2018; Supply et al., 2013). Based on these observations, the hypothesis that

Figure 5: Composition of the mycobacterial cell envelope. The different layers of the cell envelope are represented on the left of the figure with a picture of cryo-electron microscopy of vitreous section of *M. smegmatis.* Image adapted from (Le Chevalier et al., 2014).

tuberculosis-causing mycobacteria emerged in East Africa is the most plausible (Blouin et al., 2012; Boritsch et al., 2014; Comas et al., 2013; Coscolla et al., 2021; Gagneux, 2018; Ngabonziza et al., 2020).

3. Characteristics of mycobacteria

As explained earlier, mycobacteria are complex organisms due to the composition of their cell envelope (Cook et al., 2009). While they are considered as High G+C Gram-positive bacteria, the mycobacterial cell envelope is very different to the cell envelope of the commonly known Gram-positive bacterial species regrouped in the phylum Firmicutes. As complex organisms within the phylum *Actinobacteria*, mycobacteria have supplemental layers rendering them unique. The cell envelope is composed of different lipids layers, representing around 40% of the cell dry weight, and other structures: the inner membrane; a layer of peptidoglycan; a layer of arabinogalactan; the outer membrane, composed of different types of lipids responsible for the highly hydrophobic properties of the mycobacteria such as mycolic acids; and finally the capsule, mostly made up of polysaccharides and proteins (Figure 5) (Garcia-Vilanova et al., 2019; Jackson, 2014). The lipid composition of the cell envelope of the mycobacteria can influence the morphology of the colony, resulting in rough morphotypes for MTBC members, which differ from the genomically closely related *M. canettii* clade, which usually show a smooth morphotype. The change in colony morphology has been suggested to be an evolutionary event that might have increased the virulence of tuberculosis-causing mycobacteria developing towards the clonal population of MTBC members (Boritsch et al., 2016).

The mycobacterial characteristics are also due to their high G+C content (65% for *Mtb*) (Cole et al., 1998). Among the *Mycobacterium* genus, species are characterized by different genome sizes, ranging from 3.2 Mb for *M. leprae* to 8.1 Mb for *M. dioxanotrophicus* with an average of 5.7 Mb (Behra et al., 2022). The speciation of *Mtb* is marked by a genome size reduction compared to closely related mycobacteria. Genome sizes of MTBC members are around 4.3 to 4.4 Mb (Sapriel & Brosch, 2019). This particularity was suggested to result in host adaptation, with the deletion of genes that were originally needed for survival in the

environment and the insertion of new genomic regions by HGT or multiplication of genes dedicated to the pathogenic lifestyle (Bachmann et al., 2020).

III. *Mycobacterium canettii*

As previously evocated, *M. canettii* is a clade of tuberculosis-causing mycobacteria that are closely related to the MTBC. As shown in figure 3 and 4, *M. canettii* was suggested to resemble in many characteristics the putative progenitor of the MTBC (Supply et al., 2013; Tientcheu et al., 2017). Unlike MTBC members, which share 99.9% of sequence identity (Gagneux, 2018), *M. canettii* strains show a somehow greater genomic variability with many traces of inter-strain recombination events. There are only a few strains known for *M. canetti*, which have been regrouped into eight clusters named STB-A, STB-D, STB-E, STB-G, STB-H, STB-I, STB-J, and STB-K (Boritsch et al., 2016; Supply & Brosch, 2017). *M. canettii* strains are also known for their particular colony morphology, as they commonly present smooth and glossy colonies, a feature which is also reflected in the name of Smooth tubercule bacilli (STB), which was used sometimes to described them (Supply & Brosch, 2017).

For *M. canettii*, only few cases of human infection have been reported. As mentioned before, the majority of cases are linked to the geographical region of the Horn of Africa, reinforcing the hypothesis of the emergence of tuberculosis-causing mycobacteria in East Africa (Boritsch et al., 2014; Ngabonziza et al., 2020). Genomic analysis showed that *M. canettii* strains share many genomic characteristics of the MTBC (GC content, overall gene content, gene deletions, gene multiplication and insertion by HGT), whereby somewhat larger genome sizes have been observed (Supply & Brosch, 2017). While *M. canettii strains* can cause human infections, no human-to-human transmission was observed (Blouin et al., 2014), and thus *M. canettii* is hypothesized to have an environmental reservoir. For now, the hypothesis is not confirmed, as all of the known *M. canettii* strains were isolated from patients and no isolation of *M. canettii* from environmental sources was achieved (Gagneux, 2018; Supply & Brosch, 2017). However, the characteristics observed in *M. canettii* strains that have been genomically and phenotypically characterized make a putative environmental origin still very likely. For example, the finding that *M. canettii* strains show numerous traces of -likely recent- horizontal transfer, brings up the question where such transfer could occur (Supply & Brosch, 2017). It is

clear that *M. canettii* strains are different from the strict pathogens from the MTBC (Astier et al., 2017; Boritsch et al., 2016). All these characteristics render *M. canettii* strains of great interest to better understand the evolutionary steps, such as the gain in virulence in certain hosts and the transformation to a strict pathogen, that were helping tuberculosis-causing mycobacteria to evolve towards the key pathogen *Mtb* that we know today (Supply & Brosch, 2017).

Figure 6: Phylogenetic tree of the genus *Mycobacterium*. A majority of mycobacterial species are represented on the phylogenetical tree with RGM on the half and SGM on the left half of the tree. Picture from (Tortoli et al., 2017).

C. Non-tuberculous mycobacteria

I. Presentation of non-tuberculous mycobacteria

1. Non-tuberculous mycobacteria: definition

As mentioned before, non-tuberculous mycobacteria (NTM) are defined as bacterial species belonging to the genus *Mycobacterium* that are not part of the tubercle or leprosy bacilli (Cowman et al., 2019; "Diagnosis and Treatment of Disease Caused by Nontuberculous Mycobacteria," 1997) the latter, causing TB and leprosy, respectively. For now, more than 170 species are classified as NTM and described as ubiquitous environmental mycobacteria with different sources such as soil, water, domestic and wild animal (Figure 5)(Dos Anjos et al., 2020; Porvaznik et al., 2016). The majority of NTM (around 95 %) are non-pathogenic for humans or animals (Johansen et al., 2020), while the remaining NTM can cause infection diseases in humans, livestock, and wildlife (Nishiuchi et al., 2017).

Belonging to the *Mycobacterium* genus, NTM are characterized by showing a highly lipid rich outer membrane that give them hydrophobic properties, allowing them to form biofilms and attach to rough surfaces (Sharma & Upadhyay, 2020). This property provides them with many benefits such as a strong resistance to different disinfectants, and high persistence. They are also capable of multiplication in low oxygen conditions, allowing their development in various environments such as stagnant water (Falkinham, 2018; Ratnatunga et al., 2020).

2. Phylogeny of non-tuberculous mycobacteria

As explained in the previous section, NTM belong to the Mycobacterium genus and are classified in the third category according to the type of infection (mycobacteria that do not cause tuberculosis or leprosy) (Lehmann & Neumann, 1896; Meehan et al., 2021; Van Ingen, 2013).

The group of NTM includes a large variety of mycobacterial species, thus further classification inside this group should be done to facilitate their identification. The first classification of NTM was made by Runyon in 1959 and was based on their growth rate and their pigment

production. Types I to III are slow growing species, represented by photochromogen mycobacteria for type I; scotochromogen mycobacteria for type II; and non-chromogen mycobacteria for type III, meaning that type I NTM produce yellow pigments after light exposure, type II NTM produce pigment without light exposure and type III NTM produce no pigments, respectively. The last group (Type III) included the fast-growing mycobacteria without distinction of pigment production (Bastos Nogueira et al., 2021; Runyon, 1959).
Unfortunately, the Runyon classification was not sufficient for easy identification of patient isolates and application of appropriate treatment. Later, new classification methods of NTM were introduced, such as a classification that was based on the type of disease NTM can cause, distinguishing four main groups: pulmonary disease, lymphadenitis, cutaneous disease, and disseminated disease, even though some species can cause more than one type of disease (British Thoracic Society, 2000; Koh et al., 2002). Recent advances in research now allow to rapidly identify NTM with molecular biology methods, leading to improved patient care (Koh et al., 2002).

3. Epidemiology of non-tuberculous mycobacteria

Infections caused by NTM were rare and not well known before the end of the 20th century. During the 21st century, an increase in NTM infection cases was observed due to different factors. First, the number of NTM infections is likely on the rise, as the populations in industrialized countries increasingly show medical conditions that make individuals more susceptible to opportunistic mycobacteria. Secondly, the detection technics were improved, and specially equipped laboratories became increasingly capable of appropriately identifying mycobacteria (Nishiuchi et al., 2017). Unfortunately, progress in the refinement of the equipment is often not possible in all countries or laboratory, so that mis-identification or no-identification of mycobacteria is still prevalent in many settings. (Sharma & Upadhyay, 2020).

NTM usually are opportunistic pathogens and cause infections principally in immunocompromised patients (AIDS or HIV+ patients with low CD4+ cell counts, for example) or patients with chronic pulmonary disease, but NTM infections can also happen in immunocompetent individuals. They can cause different types of infections such as pulmonary disease, skin and soft tissue infections, musculoskeletal infection, and lymphadenitis, but

pulmonary diseases are the most common infections caused by NTM (Akram & Rawla, 2023; Griffith et al., 2007). Studies showed that the risk of NTM infection increases with age, whereby most of them occurred in patients over 60 years old, with a predominance in women (Gopalaswamy et al., 2020).

Prevalence of NTM was studied in different countries over time, which allowed to highlight the increase of infection cases. As an example, the prevalence of pulmonary diseases caused by NTM in the USA increased from 1.4/100,000 to 6.6/100,000 between 1994-1996 and 2004-2006, respectively (Prevots et al., 2010). In the UK, the rates of infections raised from 5.6/100,000 to 7.6/100,000 between 2007 and 2012 for individuals with positive cultures (Shah et al., 2016), while in Germany, the increase of pulmonary disease was from 2.3/100,000 to 3.3/100,000 between 2009 and 2014 (Ringshausen et al., 2016).

II. The "old" ones

Apart from causing disease as opportunistic pathogens, certain NTM species received also broad attention as model organisms for the study of selected features of other mycobacterial diseases, including TB. As such, the two major NTM used to study mycobacterial virulence mechanisms were *Mycobacterium kansasii* and *Mycobacteruim marinum,* as they were long considered as the phylogenetically closest mycobacteria of the MTBC (Berg & Ramakrishnan, 2012; J. Wang et al., 2015). Importantly, they were also easier to manipulate, given their status as biosafety level (BSL)-2 organisms, in contrast to *Mtb*, which is a BSL-3 pathogen.

1. *Mycobacterium kansasii*

Mycobacterium kansasii was first isolated in 1953 from two patients in Kansas City and described by Bulher and Pollak. Cultures revealed an acid-fast bacterium which became yellow after light exposure. This particularity made it belong to NTM group I (photochromogen) and it was called the yellow bacillus (Johnston et al., 2017; J. Wang et al., 2015).

Genomic and molecular analyses of *M. kansasii* isolates revealed the existence of five subtypes of the bacteria due to molecular differences and polymorphisms (principally on the 16S-23S rRNA and *hsp65* gene). Subtype-I appears to be responsible for most human infections (Johnston et al., 2017; Picardeau et al., 1997). Recently, a new classification of the

five sub-species was proposed by the team of Jagielski et al., who have suggested that the previously defined subtypes were too different from each other, and who proposed to rename the subtypes II to VI as *Mycobacterium persicum* (type-II); *Mycobacterium pseudokansasii* (type-III); *Mycobacterium ostraviense* (type-IV); *Mycobacterium innocens* (type-V); and *Mycobacterium attenuatum* (type-VI) leading to the creation of the *Mycobacterium kansasii* complex (Jagielski et al., 2020; Mussi et al., 2021).

Bacteria from *M. kansasii* complex have an optimal growth temperature of 37°C and as a SGM, colonies appear in 2 to 3 weeks with smooth to rough morphology (J. Wang et al., 2015).
The major reservoir known for *M. kansasii* is tap water and opportunistic infections may occur via the aerosol route (Johnston et al., 2017). Human-to-human transmission has never been formally established, except for one potential case described by Ricketts et al. in 2014, where a wife and husband showed *M. kansasii* infections with indistinguishable genetic fingerprints. Overall, *M. kansasii* infections are not common and mainly occur in immunocompromised patients or patients with existing pulmonary disease. Pulmonary infections caused by *M. kansasii* lead often to similar symptoms as *Mtb* infections, such as chest pain, productive cough, weight loss, but *M. kansasii* is also able to cause other types of infections, such as skin and soft tissue infections, musculoskeletal infection, and lymphadenitis (Akram & Rawla, 2023).

2. *Mycobacterium marinum*

Mycobacterium marinum was first described in 1926 by Aronson. It was initially isolated from a dead seawater fish from the Philadelphia Aquarium and thus often considered to infect only marine fish (Aubry et al., 2017). However, it is also possible that the first case of human infection with *M. marinum* was already described in 1886 by Riehl and Paltauf, when they described a form of skin TB observed principally on hands and arms of a patient and had named this infection *tuberculosis cutis verrucosa*, although the causative mycobacterium was not further identified then (Collins et al., 1985).

Different strains of *M. marinum* were isolated in the following years but described as other species, such as *M. balnei*, *M. platypoecilus*, and *M. anabantid*, but they were finally

considered as belonging to a same species (Aubry et al., 2017; Gauthier & Rhodes, 2009). With two other species, *M. marinum* is considered as one of the most common bacteria responsible of mycobacteriosis in fish and causing several types of symptoms such as alteration of coordination, abdominal swelling, loss of weight or granuloma formation in different organs (Hashish et al., 2018; Novotny et al., 2004). As for human infection, apart from the unidentified cases reported above, new insights were made during an outbreak of granuloma skin formation in users of a public swimming pool in Sweden in 1939, which was attributed in 1954 to infection with *M. marinum* (Aubry et al., 2017; Linell & Norden, 1954). Indeed*, M. marinum* is a water-borne infectious agent that is now known as the origin of the fish tank granuloma disease. As a fish pathogen, its optimal growth temperature is around 30-32°C and shows a growth failure at 37°C, specifically in primary cultures. It belongs to the group I of Runyon classification because it is photochromogen (colonies produce yellow pigment after light exposure) (Stephen & Gluckman, 1995). Due to its restricted growth temperature, *M. marinum* in general is not able to cause pulmonary infection in humans but can lead to infections with granuloma formation in cooler parts of the body, such as in the extremities (Franco-Paredes et al., 2018).

Nowadays, infections via public swimming pools have drastically decreased due to chlorination disinfection processes. The most common infection pathway is for people manipulating aquaria or having activities in natural water environment (Aubry et al., 2017).

M. marinum is also an often-used model for investigating mycobacterial pathogenicity mechanisms, as it shares orthologs of many virulence genes of *Mtb* (Stinear et al., 2008), and induces a TB-like disease in fish. Both of these features contribute to the popularity that *M. marinum* has gained for infection experiments in zebrafish and zebrafish larvae (Berg & Ramakrishnan, 2012). However, while the *M. marinum* model is a popular model for studying cell biological questions in infection biology, the restricted temperature range of *M. marinum* makes this species less attractive for experiments in mammalian infection models, asking for alternative new model mycobacterial species that correspond to BSL-1 or BSL-2 safety classifications and show high similarity with *Mtb* at the genomic level, but support higher growth temperatures. A few examples of mycobacteria that might meet these criteria are described in the next paragraph.

III. The "new" ones

At the beginning of the 21st century, four new mycobacterial species that seem closely related to the tubercle bacilli were isolated from clinical samples in different parts of the world. They were named *Mycobacterium decipiens*, *Mycobacterium lacus*, *Mycobacterium riyadhense*, and *Mycobacterium shinjukuense*, respectively. These species are also included in the phylogenetic tree shown in Figure 5, from where it is obvious that they are close relatives of *Mtb*. The following part will present the isolation of these four mycobacterial species with description of the first cases, and the initial genetic analyses which classified them as new species (comparison with other mycobacterial species of mycolic cell-wall profile; *hsp65* and *rpoB* genes; 16S RNA sequence; and 16S-23S rRNA internal transcribed spacer (ITS) sequence).

1. Presentation of the species and infection cases

***Mycobacterium decipiens*:**

M. decipiens was first isolated in 2012 and then in 2016 from a woman of 58-year-old and a girl of 5-year-old, and it is described by two articles in the literature (Brown-Elliott et al., 2018; Simner et al., 2014). Both patients acquired their symptoms after holidays in a tropical area (US Virgin Islands and the Republic of Maldives) and declared having small injuries at one of their body extremities. Both patients declared swelling, pain at the thumb and wrist for the first case, and at the abdomen for the young girl with fever.

Both strains revealed positive results for MTBC-specific probes from Hologic AccuProbe but the GenoType CM test identified them as non-specified *Mycobacterium*. The profile of mycolic acids by HPLC analysis was close to the one of *Mtb*.

Analysis of gene sequences revealed that the 16S rRNA sequence have 99.4% of similarity with members of MTBC. The *hsp65* gene has the highest degree of similarity with *M. intracellulare* (95.3%) followed by *Mtb* with a similarity between 94-95%. The closest resemblance of the *rpoB* gene sequence is also noticed with *Mtb* with almost 90%.

The average nucleotide identity (ANI) value between the two strains and members of MTBC was below 98%, showing they are not belonging to the MTBC.

Mycobacterium lacus:

Isolation of *M. lacus* dates from 2000 and was from a bursitis of the elbow of a 68-year-old woman, described by Turenne et al. in 2002. The infection pathway was supposed to be during a bump of her elbow on a stone in a lake in Canada, even though there was no wound. Her elbow became painful and swollen so a medical intervention was made to excise the bursitis. After 6 months, the bursitis was still there. Mycobacteriological tests were performed and revealed the presence of acid-fast bacteria with negative results for Gen-Probe AMPLIFIED *Mycobacterium Tuberculosis* test and Gen-Probe AccuProbe for MTBC, *M. avium* complex and *M. kansasii*. Analysis of the *hsp65* gene, 16S rRNA gene and 16S-23S spacer region sequences and HPLC results revealed an unknown mycobacterium.

Molecular analysis of this strains revealed that it had similarities with *M. gastri* for mycolic acid composition. The 16S rRNA sequence shared a similarity of 99% with *M. malmoense* and *M. marinum*. Comparison of 16s-23S rRNA ITS sequence revealed a high similarity with *M. gastri*, *M. marinum, M. ulcerans* and *M. kansasii* with respectively 88.2%, 88%, 87.4%, and 87.3% of similarity.

For now, only one case of infection was described in the literature (Turenne et al., 2002).

Mycobacterium riyadhense:

M. riyadhense was first isolated from a 19-year-old patient in 2009 in Saudi Arabia and described by van Ingen et al. The patient suffered from swelling and pain on his eye after a blunt trauma. Medical analysis revealed a tumor in its maxillary sinus. Bacterial analysis was performed from sinus lavage and presence of mycobacteria was tested. Due to identification of mycobacterial species, the patient was declared to have a bone tuberculosis and treated consequently.

To identify the species of the mycobacterium, three commercial line-probe assays were used: Hain GenoType MTBC, GenoType AS/CM, and INNO-LiPA MYCOBACTERIA v2. Two of the three tests have detected species belonging to the MTBC and one showed non-specific results. Tuberculin skin test reaction also give positive results (Godreuil et al., 2012).

Sequence comparison of the 16S rRNA gene revealed a higher degree of similarity with *M. malmoense* and *M. szulgai* (99%). The *hsp65* gene sequence had 95% of similarity with

M. genavense, *M. bohemicum*, and *M. malmoense*, whereas the *rpoB* gene was closest to *M. avium* (93%), *M. paraturberculosis* (93%), and *Mtb* (91%). Finally, the 16S-23S rRNA ITS sequence shared 91% of similarity with *M. szulgai*, *M. kansasii*, and *M. marinum* (van Ingen et al., 2009).

24 cases were described since the characterization of the first isolation. From what it is known in the literature, different types of infection are described (pulmonary, bone, spine, brain, and lymph node infections) (Alenazi et al., 2019; Choi et al., 2012; Godreuil et al., 2012; Saad et al., 2015; van Ingen et al., 2009; Varghese et al., 2017). All cases were cured with treatments from 2 to 12 months with two exceptions reported, one case of relapse before recovery and one death.

Mycobacterium shinjukuense:

Between 2004 and 2006, seven cases of pulmonary infections were detected in Japan and *M. shinjukuense* was identified. The seven cases were detected in immunocompetent patients between 57- and 89-year-old. Cases were reported in literature by Saito et al. in 2011.

Commercial TB identification tests gave false positive results for Gen-Probe AMPLIFIED Mycobacterium Tuberculosis test and TRC Rapid MTB assay and negative results with Gen-Probe AccuProbe for MTBC, COBAS AMPLICOR Mycobacterium Tuberculosis and COBAS TaqMan Mycobacterium Tuberculosis test.

Mycolic acid analysis of the first strain case revealed some similarities with *M. malmoense*. Analysis of specific genomic sequences revealed highest similarity with *M. marinum* (91.9%) and *M. ulcerans* (91.7%) for the *hsp65* gene, with *M. kansasii* (95.0%) for the *rpoB* gene, and the ITS sequence is closest to the one of *M. gordonae* but with a lower percentage of similarity of 81.1%. Finally, the sequence of the 16S rRNA revealed 97.8% similarity with MTBC or 98.6% with *Mtb* (H37Rv strain), which might explain the false positive reaction of the TB test based on the 16S rRNA sequence (Saito et al., 2011; Takeda et al., 2016).

Since 2004, more than ten cases of *M. shinjukuense* lung infections were described in the literature (Taoka et al., 2020). Some patients had previous pulmonary infection history, other had comorbidities, but some had no particular infection history and were immunocompetent.

No death was reported, and all patients recovered. Due to the cross reaction of the *Mtb* identification tests, it is hypothesized that several infections with *M. shinjukuense* were misidentified as *Mtb* infections (Moon et al., 2015; Oshima et al., 2015; Takeda et al., 2016; Taoka et al., 2020; Watanabe et al., 2013), emphasizing that the number of *M. shinjukuense* infections might have been underestimated.

2. The close relatives of the *Mycobacterium tuberculosis* complex

The speciation of MTBC is hypothesized to be the event where pathogens of this group became adapted to specific hosts. *M. kansasii* is considered as one of the closest mycobacteria related to *Mtb,* as it can cause human infection with TB-like symptoms and shares genomic characteristics with *Mtb* that were interpreted as a possibility that *M. kansasii* could represent the environmental ancestor of *Mtb* (Guan et al., 2020; J. Wang et al., 2015). *M. marinum* is also closely related to the members of MTBC sharing key orthologous genes for virulence (Stinear et al., 2008). Even though both share many genomic characteristics with MTBC, it was shown that the genomes of MTBC members must have undergone major changes after branching from these species during their evolution towards becoming a major pathogen.

These changes included large genome size reductions, with loss of core genes as well as of accessory genes, such as the genes encoding the proteins involved in synthesis of pigments that are still present in *M. marinum* (Tobin & Ramakrishnan, 2008) and *M. kansasii* (J. Wang et al., 2015) but absent from the MTBC members (Boritsch et al., 2014). In parallel, other genetic events must have also happened, such as for example the acquisition of toxin-antitoxin genes supposedly acquired by HGT, which are present in high numbers in tubercle bacilli, but which have only few genes in *M. marinum* or *M. kansasii*. Looking at these numerous differences between *M. kansasii* and *M. marinum* on the one hand and members of the MTBC on the other hand, the existence of a missing link in the evolution of the highly

Figure 7: Phylogenetic tree of mycobacterial species based on more than 100 universally conserved bacterial genes and their associated proteins. The new clade named MTBAP is represented in red close to *Mtb*, meaning that it shares more characteristics with *Mtb* than the *M. marinum* and *M. kansasii* species found further down the tree. Picture from (Sapriel & Brosch, 2019).

virulent pathogens belonging to the MTBC and the mainly environmental isolates of *M. kansasii* and *M. marinum* was often evoked (Sapriel & Brosch, 2019; J. Wang et al., 2015).

In their recent study, G. Sapriel and R. Brosch compared the four recently discovered mycobacterial species *M. decipiens*, *M. lacus*, *M. riyadhense*, and *M. shinjukuense,* with the two comparator species *M. kansasii* and *M. marinum* and with *Mtb*, respectively*,* using different phylogenomic approaches. The obtained results were leading them to describe a new clade that was shared between MTBC and the four mycobacterial species. This clade was named *Mtb*-associated phylotype (MTBAP). Genomic comparisons performed in this study revealed that the four mycobacterial species shared a higher ANI with *Mtb* than the two previous comparator species (79.5 to 84% with the four mycobacteria against 77 and 78% for *M. marinum* and *M. kansasii* respectively). This study also compared the genomic resemblance with phylogeny analysis, based on more than 100 universally conserved bacterial genes, which also showed the close relationship of the four mycobacterial species with the MTBC and the existence of the common clade (Figure 6).

Finally, in this study the presence of genes encoding selected virulence factors that were known to have been acquired by HGT during *Mtb* speciation were analyzed. The results showed that 35 genes reported to be implicated during *Mtb* infection for bacterial survival were shared in the strains of the MTBAP, revealing that some virulence characteristics of the MTBC members that were previously considered as being exclusively present in the MTBC, had likely been acquired before the speciation of the MTBC by a common ancestor shared with the four mycobacterial species *M. decipiens*, *M. lacus*, *M. riyadhense*, and *M. shinjukuense*.

With all comparison studies on genomic characteristics of the two comparator species, the four mycobacteria and *Mtb*, the new lineage named MTBAP shares unique genomic evolution characteristics with *Mtb*.

« élément sous droit, diffusion non autorisée »

« copyright material, unauthorized distribution »

Figure 8: Secretion systems present in *Mtb* genome. Picture from (Pal et al., 2022)**.**

D. RESEARCH AXES

I. Virulence factors

A large number of virulence factors were discovered in *Mtb* and in the *Mtb* genome over the years, even though a lack of detailed knowledge about many of them still exists.
One of the most efficient and unbiased ways to identify potential virulence factors in *Mtb* is linked to the use of high-density transposon insertion libraries, which allowed - for example - the identification of more than 200 genes that were required for optimal *in vivo* growth of *Mtb* during mouse infection experiments (Sassetti & Rubin, 2003). Among these potential virulence genes, several were linked to bacterial secretion systems. Indeed, different secretion systems are present in *Mtb* to ensure the transport and secretion of bacterial proteins through the complex cell envelope of *Mtb*. As shown in Figure 8, some of the systems present in *Mtb* are commonly found also in many other bacteria, such as the SecA1-mediated general secretory pathway or the SecA2-operated pathway that is present in several other Gram-positive bacteria, like *Listeria monocytogenes*, *Bacillus subtilis* or *Clostridium difficile*. Moreover, *Mtb* also carries a twin-arginine translocation (TAT) system, which can be found in many Gram-negative bacterial species, like for example in *Pseudomonas aeruginosa* or *Legionella pneumophila* (Green & Mecsas, 2016). Finally, *Mtb* also carries several type seven secretion systems (T7SS) which are less common in other bacteria, although some more distantly related versions of the T7SS, named T7bSS can also be found in *L. monocytogenes*, *B. anthracis* and *Staphylococcus aureus* (Gröschel et al., 2016). In mycobacteria, T7SS allow to secrete selected proteins across the highly hydrophobic cell envelope (Bottai et al., 2017; Green & Mecsas, 2016). The cell envelope composition of *Mtb* is also a source of virulence factors by itself, as revealed by the presence of selected lipids such as the mycolic acid lipids and phthiocerol dimycocerosates (DIM/PDIM) lipids (Madacki et al., 2019), which do play an important role during infection (Augenstreich et al., 2017).

Another large group of proteins that was revealed by transposon-mediated screens to be involved in the virulence of *Mtb* is the PE/PPE protein family, which are named after the characteristic N-terminal Pro-Glu (PE) or Pro-Pro-Glu (PPE) amino acid motifs. Selected members of these protein families were found to play a role in host pathogen interaction and

« élément sous droit, diffusion non autorisée »

« copyright material, unauthorized distribution »

Figure 9: Genetic organization of the ESX systems from T7SS in *Mtb* H37Rv. The five ESX systems of *Mtb* are represented with the ortholog genes within the same color. Genes from *espACD* operon located outside the ESX-1 locus are represented as they are paralogues of *espEFH* genes from ESX-1 system. Picture from (Bitter et al., 2009).

« élément sous droit, diffusion non autorisée »

« copyright material, unauthorized distribution »

Figure 10: Structural cryo-electron microscopy representation of an ESX system inner-membrane complex (ESX-5) from the T7SS of *Mtb*. The different components of the system are represented by color in comparison with the ESX-5 locus represented in (a). Globally, structures of ESX systems are similar within the five ESX systems from the T7SS of *Mtb*. The components inner (dark green) and outer (light green) EccB5, EccC5 (blue), inner (beige) and outer (orange) EccD5, MycP5 (red), and EccE5 (purple) form a pore structure allowing the secretion of effector proteins such as ESAT-6 like proteins. Picture from (Bunduc et al., 2021).

in immune evasion (Ates, 2020), however, due to a large redundance of proteins, their exact function often remains unclear. Some of them also show orthologs between MTBC and NTM species, but the majority of such proteins are assumed to be species-specific and would have been acquired or evolved during *Mtb* speciation (Sapriel & Brosch, 2019).

From this short, non-exhaustive summary above, it can be seen that the virulence factors of *Mtb* are quite diverse and may belong to different functional categories. Hence, in the chapter below, a selection of some major virulence factors of *Mtb* that have been described to be involved in *Mtb* pathogenicity will be detailed.

1. Type VII Secretion Systems

The first elements of the type VII secretion systems of *Mtb* were discovered through the analysis of the *Mtb* genome sequence (Cole et al., 1998), when particular gene clusters encoding a type III ATPase and showing similarity in gene content and gene organization were noticed (Tekaia et al., 1999). These clusters were later shown to encode bacterial secretion systems involved in the secretion of small, highly immunogenic mycobacterial virulence proteins (Pym, Brodin, et al., 2002; Stanley et al., 2003; Young, 2003) and were named Type VII secretion systems (T7SS) (Abdallah et al., 2007). Over the years, studies on T7SS highlighted the existence of five systems in *Mtb*, named ESX-1 to ESX-5 (Brodin et al., 2004), for which a specific nomenclature was elaborated (Bitter et al., 2009). As shown in Figure 7 and 8, the five genomic loci are composed of a set of core genes that were named ESX-conserved components (*ecc*) which form the secretion apparatus responsible of the secretion of the various Esx proteins, which are also encoded within the loci. Moreover, the systems also contain specific PE and PPE genes and certain genes encoding accessory proteins that were named ESX-secretion associated Proteins (Esp) (Fortune et al., 2005).

a. The five ESX systems: evolutionary considerations

The ESX systems likely evolved from plasmid-based genomic loci, which might have then been exchanged between actinobacterial strains and have developed into loci that are now situated in the bacterial chromosome (Dumas et al., 2016; Newton-Foot et al., 2016).

For mycobacteria, the ESX-4 locus is considered as the ancestor locus of all ESX clusters as it contains the simplest genomic organization and is most widely spread among mycobacterial species, whereby the four others are supposed to have evolved from ESX-4 through insertion and duplication of genes. In contrast, the ESX-5 and ESX-2 loci are likely the most recently evolved systems, as they are only found in SGM and not in RGM (Bottai et al., 2017; Dumas et al., 2016; Gey Van Pittius et al., 2001; Vaziri & Brosch, 2019).

ESX-3 is present in almost all mycobacterial species, suggesting that ESX-3 might correspond to the first ESX duplication in the mycobacterial genome with following adaptations (Newton-Foot et al., 2016). ESX-3 was shown to be an essential system for *Mtb* under laboratory growth conditions (Sassetti & Rubin, 2003) and is involved in iron uptake via the mycobactin pathway (Siegrist, Unnikrishnan, McConnell, et al., 2009).

ESX-1 is present in RGM and SGM but has been deleted during evolution from several SGM, such as members of the *M. avium complex* and *M. ulcerans/M. xenopi* strains. Moreover, partial deletions of ESX-1 have also been observed in several members of the MTBC, such as *M. bovis* BCG, *M. microti*, the "dassi bacillus" and *M. mungii* (Gröschel et al., 2016). ESX-1 is involved in the virulence of several SGM, including *Mtb* (Brodin et al., 2004; Gröschel et al., 2016). Besides its function as a virulence factor, ESX-1 was also described as being implicated in HGT via distributive conjugal transfer (DCT) in *M. smegmatis* together with ESX-4 (Gray et al., 2016). In contrast, in tubercle bacilli of the *M. canettii* clade that are very closely related to *Mtb* and also show HGT events of the DCT type, ESX-1 was not required for DCT (Madacki et al., 2021).

b. The five ESX systems: functional considerations

As mentioned above, ESX-4 is likely the most ancestral ESX system but only few functions have recently been described for *Mtb*. For example, ESX-4 was described to be essential for the export of the CpnT protein, containing the tuberculosis necrotizing toxin (TNT), which is the only toxin known for *Mtb* and which is leading to necrotic cell death of host cells (Pajuelo et al., 2021). Another, recent study suggested the importance of the ESX-4 system for heme acquisition in *Mtb* (Sankey et al., 2023). It was also observed that the ESX-4 system of *Mtb* and

many other mycobacteria lack EccE4, representing one of the conserved components of the ESX secretion machine (Bitter et al., 2009). Interestingly, *M. abscessus* encodes an ESX-4 system that also harbors the EccE4 protein (Dumas et al., 2016). Using a high-density transposon insertion screen Laencina et al. identified the ESX-4 system as a key virulence factor of *M. abscessus* (Laencina et al., 2018). It thus seems that the ESX-4 system might have a different function in *M. abscessus* and *Mtb*.

The most well-described role of ESX-5 is the export and secretion of PE and PPE proteins, which may also be involved in *Mtb* virulence (Bottai et al., 2012; Houben et al., 2012). ESX-5 and PPE proteins also play an important role for outer membrane permeability of pathogenic mycobacteria and nutrient transport across the mycomembrane of *Mtb* (Ates et al., 2015; Q. Wang et al., 2020).

Similar to the ESX-5 system, ESX-2 is found only in some SGM, but little is known about its function (Vaziri & Brosch, 2019). A recent publication suggested that it might be involved in the permeabilization of the phagosomal membrane together with ESX-1 and ESX-4 (Pajuelo et al., 2021), but more work is needed to clearly define its function.

As mentioned above, the ESX-3 system was shown to be involved in the iron and zinc homeostasis in standard and low iron culture conditions in SGM, whereas in RGM such as *M. smegmatis,* ESX-3 is not essential for growth except during starvation conditions (Serafini et al., 2013; Siegrist, Unnikrishnan, Mcconnell, et al., 2009).

ESX-1 was the first system discovered and is likely the most well studied due to its secreted, highly immunogenic proteins. In *Mtb*, ESX-1 plays a role in the intracellular growth of the pathogen and stimulates the innate and adaptive immune response of the host cell (Gröschel et al., 2016), allowing the bacterium to rupture the phagosomal membrane. This access to the cytosol is managed by the secretion of the two ESX-1 proteins named ESAT-6 and CFP-10 (Simeone et al., 2012), that will be described in more detail in the following part.

c. ESAT-6 and CFP-10 proteins from the ESX-1 locus

The 6-kDa early secreted antigenic target known as ESAT-6 or EsxA was discovered in 1995 (Sørensen et al., 1995) and was the first substrate of the T7SS described. It was followed by the 10-kDA culture filtrate protein called CFP-10 or EsxB identified in 1998 (Berthet et al., 1998), which is encoded just upstream of esxA in the ESX-1 locus (Figure 7). Over the years, ESAT-6 was classified as one of the major virulence factors of *Mtb* (Guinn et al., 2004; Renshaw et al., 2002, Pym et al., 2002) while CFP-10 was suggested to have rather a protective and transport role for ESAT-6 (De Jonge et al., 2007). Structural biology approaches showed that ESAT-6 and CFP-10 form a tight 1:1 complex in form of a four-helical-bundle structure (De Jonge et al., 2007; Renshaw et al., 2002) and are likely also secreted as such a complex in most cases, as suggested by equal amounts of ESAT-6 and CFP-10 in the supernatant of *Mtb* cultures (Brodin et al., 2006). Interestingly, later research revealed that certain *Mtb* mutant strains were able to secrete CFP-10, but not ESAT-6 (Aguilo et al., 2017), a finding which argues that ESAT-6 and CFP-10 might not always be secreted as a 1:1 complex.

As regards functional insights, many studies found that ESAT-6 and/or CFP-10 were involved in virulence of *Mtb* and related mycobacteria (Gröschel et al., 2016). One of these effects is linked to the contribution of ESAT-6 in the induction of phagosomal damage by *Mtb* in the host cell. Indeed, ESX-1-proficient strains of *Mtb* can rupture the phagosome and get access to the cytosol, whereas strains which do not secrete ESAT-6 cannot (Simeone et al., 2012; van der Wel et al., 2007). Similarly, *M. bovis* BCG strains which represent natural ESX-1 deletion mutants remain inside the phagosome, an effect that can be reversed by the integration of the *Mtb* ESX-1 locus into the genome of *M. bovis* BCG (Simeone et al., 2012). This highlights the important role of ESX-1 and ESAT-6 for the infection process. Many studies with purified ESAT-6 protein tried to define the precise role of ESAT-6 but quite some open questions still remain. The ESAT-6 protein was suggested to be pH sensitive which could lead to a conformational change during infection depending on phagosomal pH (De Jonge et al., 2007; De Leon et al., 2012). It was also hypothesized that ESAT-6 might form pores in the phagosome membrane and cause membrane leakage (Ma et al., 2015). However, the term “pore-forming” might be somehow misleading, as this activity is usually restricted to classical hemolysins, such as those of *S. aureus* or *Clostridium perfringens*, which require the necessary organization to

form well-defined membrane pores in host cells, which is not the case for ESAT-6 (Conrad et al., 2017).

Many studies have shown that the virulence of *Mtb* was correlated with the level of ESAT-6 secretion. For example, the amount of ESAT-6 secretion is higher in clinical *Mtb* strains than in H37Rv strain defined as the reference laboratory strain (Anes et al., 2023), a phenomenon which is likely linked to the regulation of the ESX-1 locus by *whiB6*. Indeed, reference strain H37Rv carries a nucleotide insertion in the promoter region of gene *whiB6*, located right upstream of the ESX-1 locus that disables the regulatory function of the WhiB6 regulator in strain H37Rv and lowers the secretion of ESAT-6 to baseline level (Solans et al., 2014), which is however sufficient for causing average virulence of H37Rv in mouse models of many research laboratories. These examples show that many aspects about ESAT-6/CFP-10 secretion mechanisms and the ESX-1 secretion machinery are still not always well understood. Moreover, it is known that the secretion of ESAT-6/CFP-10 is also dependent on genes outside the ESX-1 locus, such has the *espACD* cluster or the *phoPR* locus (Ates & Brosch, 2017), which will be described in more detail below.

d. Downstream regulation of ESAT-6/CFP-10 secretion

The secretion of ESAT-6/CFP-10 is a complex mechanism. Over the years, several research teams worked on the regulation pathway of ESX-1 proteins and highlight a complex regulation cascade involving operons, genes and two component systems outside the ESX-1 locus and separated by more than 200kb such as *phoP/R* and *mprA/B* two component systems, *espR* gene or the *espACD* cluster (Figure 9).

The *espACD* operon is restricted to pathogenic SGM and supposed to have been acquired independently during species evolution as the genomic locations are different between pathogenic species such as *M. leprae*, *M. marinum*, or *Mtb* (Ates & Brosch, 2017; Majlessi et al., 2015).

The *espACD* locus shares homology with genes in the ESX-1 locus named *espEFH* (Bitter et al., 2009; Tiwari et al., 2019). (Figure 7, 9). Research was performed to determine the role of the three genes and confirmed the essential role they have for ESAT-6/CFP-10 secretion.

Figure 11: Representation of the regulation of ESAT-6 and CFP-10 secretion. Secretion of both protein is controlled by the two component systems phoP/R and mprA/B, espR gene and they are co-secreted with EspA and EspC from *espACD* operon. Picture from (Ates & Brosch, 2017).

Indeed, EspA was found to be secreted in a co-dependent manner with ESAT-6 and CFP-10 (Fortune et al., 2005; Garces et al., 2010), similar to EspC that is encoded downstream of *espA* in an operon together with *espA* and *espD* and is also secreted in codependency with ESAT-6 and CFP-10 (Gröschel et al., 2016; MacGurn et al., 2005). Both EspA/C are effectors of ESX-1 despite being encoded elsewhere in the genome (Figure 9) (DiGiuseppe Champion et al., 2009; Fortune et al., 2005; Tiwari et al., 2019). In depth studies of EspC revealed that the protein formed high-molecular weight polymerization complexes with filamentous structure, suggesting a possible implication in the formation of a hypothetic ESX-1 secretion needle (Ates & Brosch, 2017; Lou et al., 2017) . Moreover, EspC was shown to be a highly immunogenic protein (Millington et al., 2011; Sayes et al., 2016) that is involved in the survival of *Mtb* in macrophages through the induction of endoplasmic reticulum stress by activating apoptosis signaling pathways (Guo et al., 2021). EspD is a cytosolic chaperone (Fortune et al., 2005) and can be secreted in ESX-1 independent manner but has a role for ESAT-6/CFP-10 secretion as it stabilized EspA and EspC (J. M. Chen et al., 2012; Tiwari et al., 2019). Finally, EspA requires the secretion of EspC and EspD. An *espC* knock-out (KO) mutant led to a defect in the secretion of EspA and other ESX-1 components (J. M. Chen et al., 2012).
The *espACD* operon is thus of great importance for ESAT-6/CFP-10 secretion, which adds an additional level of complexity for the regulation of ESAT-6/CFP-10 secretion. As shown in Figure 9, the expression of the *espACD* operon depends on several major regulators of *Mtb*, such as PhoPR and MprAB.

The *phoPR* operon is a two-component system constituted by a sensor histidine kinase PhoR and the response regulator PhoP, which controls more than 80 genes in the *Mtb* genome (Majlessi et al., 2015; Malaga et al., 2023; Walters et al., 2006). This major regulatory system was described to have a strong impact on *Mtb* virulence during infection (Pérez et al., 2001), in part through the influence on ESAT-6 secretion (Frigui et al., 2008), as it controls the *espACD* operon via regulation of the DNA binding protein EspR (ESX-1 secreted protein regulator) (Blasco et al., 2012; Majlessi et al., 2015; Raghavan et al., 2008).

Another two-component system was shown to regulate *espACD* operon and more precisely EspA: the *mprAB* operon (X. Pang et al., 2013). This system is activated under environmental

stress conditions such as surface stress and allows the bacteria to better survive under difficult conditions (Manganelli et al., 2023; X. Pang et al., 2013).

As mentioned above, secretion of EspA is dependent on EspR which was shown to be linked to disease severity (Genestet et al., 2022). Interestingly, binding sites for EspR and MprA/B are found in the region of difference 8 (RD8), which is located just upstream of the EspACD operon. RD8 is a genomic region that is present in *Mtb* strains, but which is deleted from *M. africanum* lineages 6 and 9 strains and all animal adapted lineages of the MTBC (Brosch et al., 2002)**.** This deletion leads to an absence of the EspR- and MprA/B-binding sites upstream of the EspACD operon and thereby changes the expression of EspACD with consequences on secretion of ESAT-6 in *M. bovis* strains (Gonzalo-Asensio et al., 2014).

2. Lipids

Lipids are a very important part of the mycobacterial cell envelope as they represent around 40% of its dry weight (Ghazaei, 2018). Analysis of the genome sequence of *Mtb* has revealed that a large portion of the coding capacity of *Mtb* is devoted to the production of enzymes involved in lipid metabolism (lipogenesis and lipolysis) (Cole et al., 1998). Despite some similarities in lipid profiles within mycobacteria, numerous differences exist between non-pathogenic RGM, such as *M. smegmatis* and pathogenic SGM species such as *Mtb*, *M. kansasii*, and *M. marinum*. Hereafter, some details about specific lipids known to be implicated in *Mtb* virulence will be discuss.

a. Phtiocerol dimycocerosates

Phthiocerol dimycocerosates are known in mycobacterial research for years and have been abbreviated PDM (Brennan & Nikaido, 1995), DIM (Augenstreich et al., 2017) or PDIM (Quigley et al., 2017). They are non-covalently bound lipids in the mycobacterial outer membrane. The enzymes that encode the synthesis of PDIM are encoded in a ≈ 50 kb-spanning genomic region (Cole et al., 1998). Transposon mutation screens identified several of these genes as essential for *Mtb* virulence (Camacho et al., 1999; Cox et al., 1999). PDIM were known to have a role in cell envelop solidity and new roles were recently discovered, such as their implication in

detergent resistance acting on permeability of the envelope or their implication in facilitating bacterial multiplication during infection, as they act to counter the acidification of phagosomes and reduce macrophage viability (Augenstreich et al., 2017; Passemar et al., 2014). Their role in reducing cell wall permeability has an impact on antibiotic resistance and tolerance as loss of PDIM leads to an increase of rifampicin susceptibility and a higher susceptibility to antibiotic combinations (Block et al., 2023).

PDIM are also implicated in the phagosomal rupture as they work in synergy with ESAT-6. However, it is important to note that a defect in PDIM production does not affect the secretion of ESAT-6. For now, the mechanism of PDIM and ESAT-6 cooperation remains unclear (Augenstreich et al., 2020; Quigley et al., 2017).

Similar to the presence of the *espACD* operon in only few selected mycobacteria, PDIM synthesis was found to be specific to a few pathogenic, SGM species that are containing the *ppsABCDE*, *mas*, and *mmpl7* genes in their genomes (Augenstreich et al., 2017; Brennan & Nikaido, 1995). All these characteristics, together with the finding that *Mtb* strains used in the laboratory may spontaneously lose the ability for PDIM synthesis (Domenech & Reed, 2009) make these lipids one of the key virulence factors during *Mtb* infection.

b. Phenolic glycolipid & Sulfolipid

Apart from PDIM, in some mycobacteria like *M. leprae*, *M. kansasii*, *M. bovis*, and some strains of *Mtb* (Forrellad et al., 2013), other types of lipids, named phenolic glycolipids (PGL), are produced and the enzymes involved in the synthesis of these lipids are encoded in a locus directly downstream of the PDIM locus (Augenstreich et al., 2020; Gordon et al., 2009; Guilhot et al., 2014). PGL are known to have several roles in mycobacteria such as contributing to cell wall impermeability, phagocytosis, nitrosative and oxidative stress defense and formation of biofilms (Ramos et al., 2020). Two genes of this locus were detected to be particularly important: *pks1/pks15* which may exist as a functional single open reading frame (ORF) or as non-functional split ORF, depending on the phylogenetic position of the *Mtb* strain. The single ORF encodes for a polyketide synthase that plays a critical role in PGL biosynthesis. This particularity is observed in *M. bovis*, *M. leprae*, and hypervirulent *Mtb* strains whereas in

other strains like *Mtb* H37Rv or Erdmann (laboratory strains), a mutation causes a frameshift separating the ORF into *pks1* and *pks15*, leading to a non-functional gene and defect in PGL production (Constant et al., 2002; Ramos et al., 2020). The knockout of the single *pks15/1* gene in a PGL-producer strain did not affect the capacity of multiplication of the *Mtb* strain but the strain lost its hypervirulent phenotype (Forrellad et al., 2013). It was also shown that the frameshift in the pks15/1 will not affect PDIM production, whereas knocking out of *mas* or *mmpl7* present in the neighboring PDIM locus will affect PGL and PDIM production (Augenstreich et al., 2020).

Another abundant type of lipids is represented by the sulfolipids (SL) and more precisely the sulfolipid-1 (SL-1). They were found to be involved in *Mtb* virulence with different implications such as the inhibition of mitochondrial oxidative phosphorylation, and stimulation; and the suppression of cytokine and ROS production in host leukocytes (Seeliger et al., 2012). It was finally demonstrated that despite previous knowledge, SL-1 are not implicated in the alteration of phagosome-lysosome fusion (Augenstreich et al., 2017). Moreover, this locus is under the control of PhoPR system with two important genes for the SL-1 synthesis and secretion, named *pks2* and *mmpL8*. Interestingly, mutants for each gene led to a defect in SL-1 secretion but only the mutation of *mmpL8* caused a decrease of bacterial enumeration in mice (Converse et al., 2003; Forrellad et al., 2013).

II. Morphology

Classification of mycobacteria species are made through several characteristics such as the doubling time, the Runyon classification, the pathogenicity, and the morphology. In this chapter, the differences observed in colony morphology of mycobacterial species and the impact of the morphology on the mycobacterial virulence will be exposed.

1. Two types of morphology

Among strains and species of the *Mycobacterium* genus, two colony morphologies can usually be distinguished. They can have a smooth or a rough morphotype, although the interpretation of the individual morphotypes is not always easy.

One of the most studied mycobacterial species, having both morphotypes, is *M. abscessus*, a RGM responsible mainly for pulmonary infections in susceptible hosts (Johansen et al., 2020). This mycobacterium shows different morphotypes depending on the variant, which also cause differences in virulence. The morphology of the *M. abscessus* variant is determined by the presence of a glycolipid, named glycopeptidolipid (GPL). A variant with GPL production will have a smooth morphotype and will be cleared in mouse lungs, whereas a GPL-deficient variant with rough morphology will persist in the lungs (Rüger et al., 2014). The transition from a smooth to a rough morphotype is usually caused by loss of function mutations that occur in genes from the GPL locus, which encode for proteins involved in the synthesis or transport of GPLs (Pawlik et al., 2013).

In SGM, species with different morphotype variants are observed for *M. avium*, a NTM that can cause pulmonary infection in susceptible, mostly immune-compromised humans (Daley, 2017). Variants can have a smooth opaque, smooth transparent or rough colony morphology. These differences were also shown to impact the virulence of the bacteria with avirulent strains for smooth opaque colony, virulent for smooth transparent variant and variable virulence for rough morphotype which can be more virulent than the smooth transparent variants (Torrelles et al., 2002). The smooth opaque morphotype is supposed to be derived from mice infected with smooth transparent variants. Like for *M. abscessus*, apparition of rough morphotypes is associated with the deletion of GPL surface antigens (Torrelles et al., 2002).

Smooth and rough morphotypes were also observed for *M. kansasii*, and the rough colonies were shown to have a higher persistence in mice than smooth morphotypes (Mussi et al., 2021; Picardeau et al., 1997). But for this species and the majority of SGM which produce PDIM and PGL, the morphology is not shaped by the presence of GPL, as they are absent for such species. In this case, the lipids that are responsible for the colony morphology are the lipooligosaccharides (LOS) (Belisle & Brennan, 1989; Johansen et al., 2020).

As introduced earlier, *Mtb* evolved towards a rough morphotype during its evolution, while the closest relative *M. canettii* shows a smooth morphotype (Boritsch et al., 2016).

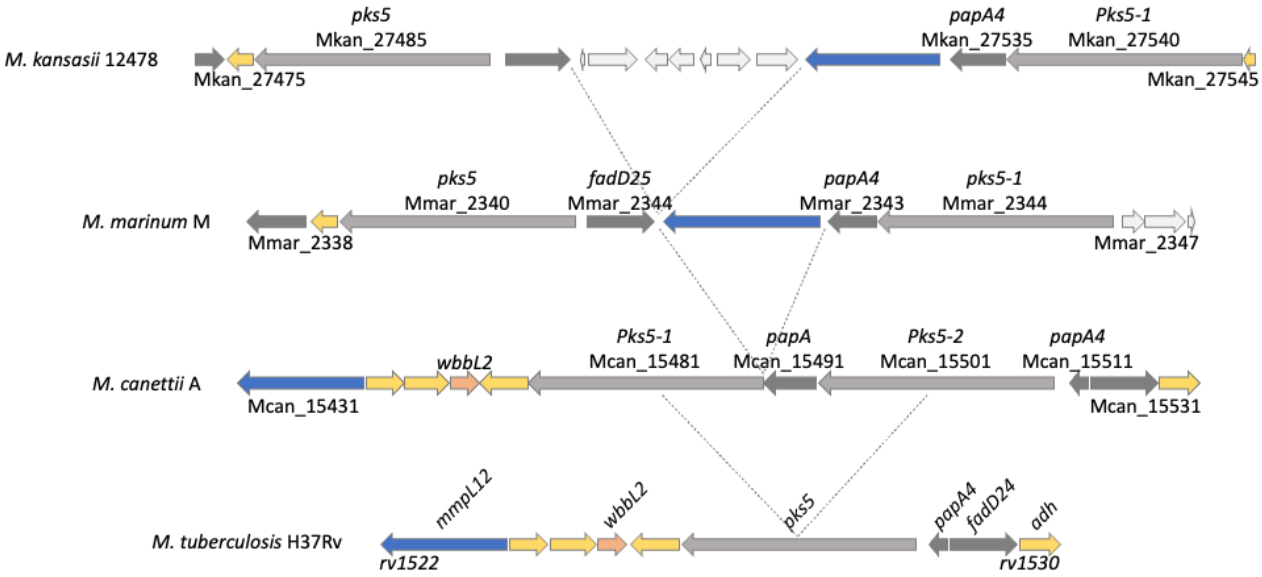

Figure 12: Representation of lipooligosaccharide locus evolution of *M. kansasii* ATCC12478, *M. marinum* M, *M. canettii* STB-A, and *Mtb* H37Rv. The *Mtb* LOS locus is marked by various evolutionary steps in mycobacteria, with gene deletions observed when comparing the genomes of *M. kansasii*, *M. marinum*, *M. canettii* and *Mtb*. These steps enabled *Mtb* to reduce its locus to a single pks5 gene compared with the other three species, leading to a defect in LOS production enhancing its virulence.

This change is due to the loss of LOS production in *Mtb,* a finding that will be detailed in the next chapter.

2. Lipooligosaccharide locus

Morphology of the mycobacterial colonies is controlled by the production of GPL for nonpathogenic and some opportunist mycobacterial species, or by other surface-exposed lipids named lipooligosaccharides (LOS) for other NTM or obligate pathogens among the SGM. Production of LOS was first identified in *M. kansasii* (Hunter et al., 1983) and later in other NTM such as *M. marinum* (Burguière et al., 2005; Ren et al., 2007). For *M. kansasii*, it was found that rough and dry variants lack the 8 types of LOS. LOS-deficient variants (rough morphotype) showed persistent infections in mice compared to smooth colony variants, which were eliminated from the organs of the mice (Belisle & Brennan, 1989). *M. marinum* produces four types of LOS and the loss of their production is assimilated, in this species, to an alteration of the morphology and not a complete change of smooth to rough morphology (Burguière et al., 2005; Szulc-Kielbik et al., 2017).

The LOS locus of LOS-producers is composed of different genes including two encoding for polyketide synthases (*pks5*) that are separated by at least one gene encoding a polyketide synthase-associated acyltransferase (*pap* gene). In *M. marinum* and *M. kansasii*, more genes are found between the two *pks5* genes (Boritsch et al., 2016). Several *pap* genes localized inside the LOS locus are needed for encoding the enzymes involved in LOS secretion, and another gene, named *fadD25* and its gene product FadD25 were shown to be essential for the synthesis of the LOS core structure in *M. marinum* (Figure 10) (Van Der Woude et al., 2012). During the evolution of the tubercle bacilli, the number of genes between the two *pks5* decreased, until the two *pks5* merged to have only one *pks5* in *Mtb* genome (Boritsch et al., 2016) (Figure 10). This characteristic feature increased the hydrophobicity of *Mtb,* and it is suggested to be an advantage for the evolution of *Mtb* as strict pathogen (Garcia-Vilanova et al., 2019; Supply & Brosch, 2017).

Roles of LOS in bacterial morphology are fairly well studied, but their role in bacterial life and pathogenicity has yet to be fully explored. In NTM, LOS were shown to contribute to different

roles such as the formation of biofilm, the bacterial motility, or entering the host macrophages (Burguière et al., 2005; Ren et al., 2007). It was also shown that lack of LOS production in *M. marinum* mutant increased the virulence of the bacteria in zebrafish and macrophages (Alibaud et al., 2014; Van Der Woude et al., 2012). Knowing these characteristics, presence of LOS in the bacterial cell wall suggests that they might lead to decrease bacterial virulence by masking some cell wall-proteins (Alibaud et al., 2014). This speculation might explain why LOS deficient mutants of tubercle bacilli were selected during speciation of the MTBC, whereas a smooth, hydrophilic propriety could be more suitable for the environmental life of NTM (Minnikin et al., 2015). A similar observation was also made for *M. canettii*, when a smooth LOS-producing variant was compared with a LOS-deficient isogenic rough variant during infection experiments in guinea pigs. These experiments showed that both morphotypes were virulent in this very sensitive model, causing disseminated infection and lung damage, albeit the rough variant was even more virulent under the used experimental settings (Boritsch et al., 2016).

III. Infection

NTM can cause different types of infection in humans, usually with a higher percentage of extrapulmonary infection than *Mtb,* like *Mtb* many NTM can also be transmitted by aerosol which is the most efficient spread of infection of bacteria causing pulmonary infections (Giannoni et al., 2023). To evaluate virulence and the pathogenicity of a species, different models can be used for *in vitro* and *in vivo* studies.

1. *In vitro*

As a first step to study pathogenicity (the potential ability to produce disease) and virulence (the quantitative degree of pathogenicity) of mycobacteria is to find appropriate models. As pathogenic mycobacteria grow and survive inside macrophages and induce their death during infection, primary macrophages, and cell lines can be used for initial evaluations (Johnson & Abramovitch, 2015; Mussi et al., 2021). Different types of primary macrophages and cell lines exist, and their use depends on the purpose of the study such as the evaluation of virulence, antimicrobial activity, gene expression, or intracellular host-pathogen interaction markers

(Johnson & Abramovitch, 2015). The four most common types of macrophages used for infection studies are the human monocyte derived macrophage (hMDM) and murine bone marrow derived macrophages (BMDM) for primary cells; or the human THP-1 derived macrophages and the murine J774 macrophages for cell lines (Johnson & Abramovitch, 2015; Mendoza-Coronel & Castañón-Arreola, 2016).

Cell lines have the advantages to be easily cultured with a homogenous genetic background. However, they also present disadvantages such as the acquisition of phenotypic differences compared to primary cells, and a genomic instability. To counter these problems, the use of primary cells is possible as they offer a better physiological model and are more representative of the heterogeneity of donors especially for host-pathogens interaction (Andreu et al., 2017; Mendoza-Coronel & Castañón-Arreola, 2016).

However, involvement of other immune cells during infection and the uptake properties of antibiotics are different between *in vitro* and *in vivo* infections as they are more interactions in animal models due to the complexity of organs and the immune system (Maphasa et al., 2021).

2. *In vivo*

Several animal models exist to study the virulence of tubercle bacilli, such as mouse, guinea pig, rabbit, or non-human primate infection models. The three last models represent very interesting study models as the animals develop necrotic granuloma than closer resemble those of humans, compared to murine models, but these animals are larger, more expensive and more difficult to maintain. For these reasons, the murine model is often used in many research laboratories (Driver et al., 2012). Mice with several genetic backgrounds can be used for TB and TB-like disease study, with two main groups described: resistant and susceptible mice, which show different traits that need to be considered for experiments (age, sex, routes of infection) (Soldevilla et al., 2022).

As explained before, TB affects more men in human population (World Health Organization, 2022), whereas NTM infections are predominantly detected in women over 60-years old (Gopalaswamy et al., 2020). Susceptibility is also different in mice. It was shown to be higher

in male for some NTM such as *M. marinum*, *M. avium* or *M. intracellulare* (Soldevilla et al., 2022; Yamamoto et al., 1991).

In general, NTM are less virulent than *Mtb,* so a higher dose of bacteria needs to be sprayed or injected into mice to avoid rapid clearance and to induce persistence (Mussi et al., 2021; J. Wang et al., 2015). In the environment, NTMs are able to counterbalance this lack of virulence through their ability to form biofilms, which allows them to have a higher bacterial concentration when infecting a host (Mussi et al., 2021).

The question which types of mice to use is also depending on the research question and the type of evaluation that needs to be done, such as the evaluation of virulence, vaccine efficiency etc., as the genetic background of the host has an impact on susceptibility (Driver et al., 2012).
Among the different genetic backgrounds that exist for mice, three of them are generally used for TB studies. First, the C57BL/6 and the BALB/c models are widely used as TB study model, principally for testing drugs against TB. Both are based on immunocompetent mice that are considered as relatively resistant to *Mtb* infection. As explained before, in these models the granulomas obtained due to infection, do not correspond to the typical human granuloma structures with necrotic, hypoxic centers. However, most of classical anti-TB agents do not need to be tested under hypoxic conditions allowing the C57BL/6 and the BALB/c to remain good models for drug testing (Nuermberger, 2017; Soldevilla et al., 2022). They have the particularity to reproduce a latent TB infection due to their slow progression (Soldevilla et al., 2022). The third model is the C3HeB/FeJ mice also called “Kramnik model”. These mice are immunocompetent, but highly susceptible to *Mtb* infection, and they have the capacity to develop active and progressive TB with the formation of hypoxic and encapsulated granulomas with a necrotic center (Driver et al., 2012; Soldevilla et al., 2022). However, some studies revealed a heterogeneity in lung pathology with this mouse lineage, which have to be taken into consideration for certain experiments such as drug testing (Lanoix et al., 2015).

Murine models are the most common *in vivo* model used in TB studies, especially at the beginning of preclinical development, as mice are usually easier to manipulate and to maintain

compared to other animal models, but the type of mice has to be chosen depending on the types of scientific questions and experimental needs.

IV. Antibiotic tolerance/resistance

The role of anti-TB agents used to treat TB are described in the first part of the introduction. Here, the next chapter will focus on the resistance that mycobacteria can acquire, and on the phenomena that lead to these resistances.

1. Acquisition of *Mycobacterium tuberculosis* resistance

a. Resistance to first-line agents

As explained in the first part of the introduction, the most common resistances found for *Mtb* are those for rifampicin and isoniazid (MDR-TB).

Rifampicin resistance is usually linked to mutations of selected codons on the *rpoB* gene, coding for the ß-subunit of the RNA-polymerase. These mutations lead to conformational changes of the RNA polymerase, thereby decreasing the affinity for the rifampicin molecule (Palomino & Martin, 2014). Mutations happen most often in the region named the rifampicin resistance-determining region encoding 27 amino acids, with two main mutations leading to a high resistance level: Ser531Leu and His526Tyr. Structural bumps are created by the mutation of Ser531 into Leu531, while the mutation of His526 to Asp526 creates repulsion of charged residues leading to a decrease of rifampicin and RpoB affinity (Y. Pang et al., 2013; Rostamian et al., 2023).

For isoniazid, mutations most commonly concern the *katG* and *inhA* genes, with changes that lead to the substitution of Ser315 by Thr315 in KatG, or mutations in the promoter region of *inhA*. The KatG Ser315Thr mutant is the product of patient-mediated selection processes as this mutant is associated with clinically significant levels of isoniazid resistance but retains active catalase-peroxidase production and virulence in the mouse model (Pym, Saint-Joanis, et al., 2002). The KatG mutation prevents the formation of the isonicotinoyl-NAD+ complex, causing a high level of resistance, while the mutation on *inhA* promoter leads to an

overexpression of InhA causing a low resistance level as there is more NADH-binding site of *inhA* available than isonicotinoyl-NAD+ complex formed (Dokrungkoon et al., 2023; Marrakchi et al., 2000).

The major mechanism of *Mtb* pyrazinamide resistance is linked to a mutation in the *pncA* gene (or its promoter), which codes for the pyranizamiadase/nicotinamidase activity required to convert pyrazinamide into its active form (Scorpio & Zhang, 1996; Zhang et al., 2013). *M. bovis* is naturally resistant to pyrazinamide due to a mutation in the *pncA* gene that modifies His57 into Asp57 in PncA (Scorpio & Zhang, 1996). However, another major mutation can happen in the *rpsA* gene, whose gene product is implicated in the binding of pyrazinamide. Two main non-synonymous mutations are observed in RpsA, encoded by the *rpsA* gene of *M. canettii,* which is naturally resistant to pyrazinamide (Thr5Ala, Thr210Ala) without *pncA* mutation (Feuerriegel et al., 2013).

The fourth agent of the first-line TB treatment is ethambutol. In almost 75% of cases, the resistance to ethambutol is caused by mutations in the *embB* gene, localized inside the *embCAB* operon of *Mtb* (Brossier et al., 2015). Three *embB* codons are identified to be involved in most of the ethambutol resistant *Mtb* strains (positions 306, 406 and 497), found in the region named ethambutol resistance-determining region (Boni et al., 2023; Bwalya et al., 2022).

b. Resistance to second- and tird-line agents

Resistance to fluoroquinolones, one of the most potent second-line drugs occur in pre-XDR-TB and XDR-TB. Those resistances can be caused by different mutations. Fluoroquinolones act on the DNA topoisomerase II and more particularly by inhibiting the two subunits A and B (encoded by *gyrA* and *gyrB*). Resistance is acquired by the bacteria due to mutations in those subunits. Commonly, mutations of codons 88, 90, 91, and 94 are observed for *gyrA* with a higher prevalence for Asp94Gly and Ala90Val and codons 500 and 538 for *gyrB* (Kabir et al., 2020; Zhang & Yew, 2009). GyrA mutations lead to a higher level of resistance compared to those in GyrB, and generally, two mutations in *gyrA* or one mutation on each gene are observed, leading to high level resistance (Zhang & Yew, 2009). Resistance to the different

fluoroquinolones depends on the types of mutations. For example, bacteria with an Ala90Val mutation in GyrA will be resistant to levofloxacin but can be treated with higher doses of moxifloxacin. The Asp94Gly mutation provides resistance to both levofloxacin and moxifloxacin, while an Asp94Ala mutation results only in resistance to levofloxacin (Kabir et al., 2020).

Bedaquiline is one of the latest approved anti-TB agents and is highly efficient against TB. However, resistances start to be observed in some *Mtb* strains with mutations in genes implicated in MmpS5-MmpL5 regulation. Upregulation of MmpS5-MmpL5 commonly involve mutations in gene *rv0678,* encoding a transcriptional inhibitor of the two proteins, leading to a low-level of resistance. More rarely, mutations may also occur in the *atpE* gene, which encodes the C subunit of the ATP synthase, the main target of bedaquiline, causing high resistance level of *Mtb* (Andres et al., 2020; Mallick et al., 2022; Sonnenkalb et al., 2023).

2. Differences in drug resistance between *Mycobacterium tuberculosis* and non-tuberculous mycobacteria

NTM are rarely treated with the classical TB treatment as they commonly have less sensitivity for some of the anti-TB agents, and the difference is more marked between RGM and SGM.

The rapid grower *M. abscessus,* for example, is naturally resistant to the classical anti-TB drugs and most of the other available antibiotics. Its treatment generally involves a macrolide molecule such as clarithromycin or azithromycin, amikacin, and ß-lactams (Alcaraz et al., 2022). Interestingly, resistances to anti-TB agents in *M. abscessus* are not caused by the same common resistance mechanisms that are usually acquired by *Mtb*.

Rifampicin resistance in RGM such as *M. abscessus* and *M. smegmatis* is not due to the major *rpoB* mutations found in *Mtb* (Alcaraz et al., 2022; Nessar et al., 2012), but it is due to the naturally occurring ribosylation of rifampicin by ADP-ribosytransferase, encoded by the *arr* gene that is not present in *Mtb* (Rominski et al., 2017). Similar observations were made for INH resistance in *M. abscessus*, which is mainly due to the inability of KatG of *M. abscessus* to transform the molecule into its active form in the bacterium (Gagliardi et al., 2020). *M. abscessus* can also acquire high level of resistance to aminoglycosides like amikacin or streptomycin, by a mutation of the 16S rRNA in the *rrs* gene (codons 1406, 1408, 1409, and 1491) (Giannoni et al., 2023; Nessar et al., 2011; Van Ingen et al., 2012).

For SGM, NTM antibiotic treatment commonly consists of rifampicin, ethambutol, and a macrolide molecule with addition of amikacin or streptomycin, if needed. But different mutations exist on those species, such as those causing resistance to macrolides like for clarithromycin, due to a mutation of the 23S rRNA preventing the binding of the macrolide molecules to the ribosome. The mutation was found in the *rrl* gene (positions 2058 or 2059) in strains of the *M. avium* complex or the fast-growing *M. abscessus* (Brown-Elliott & Woods, 2019; Van Ingen et al., 2012). Moreover, mutations in the *rrl* gene were also shown to have an impact on the efficacy of linezolid in *M. smegmatis*.

The current treatment for *M. kansasii* infection is composed of rifampicin, ethambutol, and isoniazid (Brown-Elliott & Woods, 2019). However, rifampicin resistance can be caused in *M. kansasii* by the same mutations as in *Mtb* (Van Ingen et al., 2012), while other factors are likely involved in *M. avium* rifampicin resistance (Obata et al., 2006; Wu et al., 2018).

Finally, low level of bedaquiline resistance is also observed in NTM, such as in *M. intracellulare,* caused by a mutation in the *mmpT5* gene leading to a downregulation of Mmps5-MmpL5 expression (Wu et al., 2018).

Taken together, this means that acquisition of resistance in NTM is dependent on the species, and some antibiotics are difficult to test under *in vitro* conditions, as their actions may depend on different properties, such as the pH level or medium compositions (Van Ingen et al., 2012).

THESIS OBJECTIVES

The *Mycobacterium* genus belongs to the phylum *Actinobacteria* and comprises a large number of species known as mycobacteria. This genus can be divided into two groups, according to the growth rate (fast- and slow-growing) of the different species. While most of the species are harmless environmental bacteria, some species of the *Mycobacterium* genus are opportunistic or obligate pathogens in humans and/or animals (Forbes et al., 2018). The *Mycobacterium* genus can also be divided into three categories: mycobacteria causing tuberculosis, mainly belonging to the members of the MTBC, mycobacteria causing leprosy (*M. leprae*), and non-tuberculous mycobacteria classified as potentially opportunistic pathogens or non-pathogenic mycobacteria (Meehan et al., 2021). Commonly, opportunistic or pathogenic species belong to the SGM, with a few exceptions such as *M. abscessus* (Bachmann et al., 2020), which in recent years has become a major pathogen for cystic fibrosis patients.

The MTBC groups together pathogenic species that are genetically close (>99% genome sequence identity) and cause TB in humans and/or animals (Gagneux, 2018). The members of this complex are thought to have evolved clonally from a common ancestor, of which *M. canettii*, a presumed environmental TB-causing mycobacterium might be the closest representative (Supply & Brosch, 2017). *Mtb* and *M. africanum* are the human-adapted species of the MTBC, while *M. bovis* represents likely the best-known animal-adapted member of the MTBC (Gagneux, 2018).

TB is the major leading cause of human death due to a single pathogen. *Mtb* is extremely well adapted to humans, having acquired numerous virulence factors during its early evolution as well as having lost certain factors that were not anymore adapted to its emerging pathogenic lifestyle. Despite the many studies carried out on this pathogen, many stages of its evolution remain still poorly understood, such as the acquisition of certain virulence factors that are specific to the MTBC species and found in no other species of the *Mycobacterium* genus, although this comparison also depends largely on comparator species used for these analyses. Many hypotheses are based on HGT, which would have allowed the ancestor of TB causing bacteria and/or the MTBC to acquire such particularities. Other genomic modifications have also been noted that are thought to have happened during the evolution of the MTBC, such

as a reduction in genome size, including the loss of certain core genes compared with other mycobacteria (Bachmann et al., 2020; Sapriel & Brosch, 2019; J. Wang et al., 2015).

As *Mtb* is a highly pathogenic organism, a BSL-3 laboratory is required for its handling. To facilitate research, NTM are often used as study models to investigate certain common mechanisms shared with *Mtb*, or in contrast are used for distinguishing *Mtb* from other mycobacteria. Two slow-growing opportunistic NTM are often used as models: *M. marinum* and *M. kansasii*, as they were long considered as the most closely related species to *Mtb* and to its ancestor (Berg & Ramakrishnan, 2012; J. Wang et al., 2015). But even though these two species share many common features with *Mtb*, some evolutionary steps of *Mtb* are not found in these two species, sometimes rendering the accuracy of the models and the knowledge gained for *Mtb* -related questions obsolete (Sapriel & Brosch, 2019).

A recent study by Sapriel and Brosch showed that four NTM isolated from patients in the 2000s share more evolutionary traits with *Mtb* than the two previously used comparators. These species, named *M. decipiens*, *M. lacus*, *M. riyadhense*, and *M. shinjukuense* were suggested to share a common ancestor with MTBC members, based on an analysis that revealed that these species were sharing some unique evolutionary features with MTBC members (Sapriel & Brosch, 2019).

My PhD project aims to characterize these four species in order to establish new insight into *Mtb* evolution and investigate the possibility of using one or more of them as models for mycobacterial studies mimicking *Mtb* functions, while being considered as BSL-1 or -2 organisms, which makes safety containment easier than by working directly with *Mtb* strains.

For this purpose, the objectives of my thesis were the following:

- Characterize the four species at bacteriological level.
- Determine the genomic similarities shared by these species and *Mtb*.
- Determine the infectious capacity of the species in models used for mycobacteria.
- Determine the possibility of using one or more of these species as a model for studying TB.

MATERIALS AND METHODS

Bacterial strain

M. decipiens (ATCC TSD-117), M. lacus (DSM 44577), M. riyadhense (DSM 45176), and M. shinjukuense (DSM 45663) were purchased from the ATCC or the German Collection of Microorganisms and Cell Cultures, respectively. Laboratory mycobacterial strains used in this study include M. kansasii (ATCC 12478), M. bovis BCG Pasteur 1173P2 and M. tuberculosis H37Rv. M. decipiens ATCC TSD-117 was isolated from thumb and wrist of an 58-year-old woman and corresponds to a BSL-2 organism; M. lacus DSM 44577 was isolated from the elbow of a 68-year-old woman and corresponds to a BSL-1 organism; M. riyadhense DSM 45176 was isolated from a tumor in the maxillary sinus of a 19-year-old man and corresponds to a BSL-1 organism; and M. shinjukuense DSM 45663 was isolated from sputum and bronchial lavage fluid samples of elderly patients and corresponds to a BSL-2 organism.
All strains were grown in Middlebrook 7H9 medium (Becton-Dickinson) supplemented with 10% of albumin dextrose catalase (ADC, Difco Laboratories) and 0.05% Tween 80. *M. lacus*, *M. riyadhense*, *M. shinjukuense*, *M. kansasii*, *M. bovis* BCG Pasteur and *M. tuberculosis* H37Rv were incubated at 37°C and *M. decipiens* cultures were incubated at 35°C. Solid cultures were carried out on Middlebrook 7H11 agar medium supplemented with 10% of oleic acid albumin dextrose catalase (OADC, Difco Laboratories) incubated at 37°C or 35°C for *M. decipiens* for 17 to 25 days depending on the strains.

Extraction of genomic DNA

Pellets of cultures in exponential phase were recovered and 5mL of solution I (saccharose 25%, EDTA 50mM pH8, Tris-HCl 50mM pH8, Thiourea 50mM, H_20) with 250µL of lysozyme 10mg/mL were added. Solutions were mixed and incubated 4h at 37°C. 5mL of solution II (SDS 1%, Tris-HCl 100mM pH8, Proteinase K 0.4mg/mL, H_20) were added and mixed. Solutions were transferred into 10mL Nalgene bottles (Fisher Scientific) with 2.5mL of zirconium beads, shaken 3 times at 30Hz for 3 min, and incubated over night at 65°C. Solutions were transferred without the beads and NaCl solution was added at a final concentration of 0.625M, and mixed by inversion. The aqueous phases were transferred into new tubes after centrifugation at 5000g for 10 min. 5mL of Phenol/Chloroform/Isoamyl alcohol were added to the aqueous phases, mixed and centrifuged at 5000g for 10 min. The resulting new aqueous phases were

transferred into new tubes and 2 volumes of ice-cold ethanol 99% were added and mixed by inversion before being incubated at -20°C for at least 2h. The tubes were then centrifuged at 10,000g for 30 min at 4°C, and supernatants were discarded. Pellets were washed once with 5mL of cold ethanol 70% by adding the ethanol onto the pellets followed by centrifugation at 10,000g for 10 min at 4°C. Supernatants were discarded again, and pellets were dried and resuspended in 1X TE buffer.
The quality and concentration of each DNA sample was then analyzed using the Qbit dsDNA quantification assay (Invitrogen).

Sequencing of genomic DNA

Genomic DNAs were used to construct libraries for long reads using the Pacific BioScience (PacBio) thanks to a collaboration with Laurence Ma and Thomas Cokelaer from the Biomics platform of the Institut Pasteur Paris. Reads were assembled into contigs by the DryLab from Institut Pasteur Paris. Annotation of the genomes were performed with the software Prokka (Seemann, 2014). The obtained genome sequences were imported into the MicroScope platform (Vallenet et al., 2017).

Genomic comparisons

Genomic comparisons of various loci were performed using the software offered by the MicroScope platefrom, BLASTn and BLASTp (Altschul et al., 1990) comparisons and Artemis Comparison Tool software (Carver et al., 2005). The percentages of amino acid identity were obtained for selected predicted gene products and reported in different genomic maps. The genomes of the four species *M. decipiens, M. lacus*, *M. riyadhense*, and *M. shinjukuense* were compared to those of *Mtb* H37Rv and *M. kansasii* 12478.

PCR primer design

Specific PCR primers were designed for *M. decipiens, M. lacus*, *M. riyadhense*, *M. shinjukuense*, and *M. kansasii*. Unique genomic regions for each species were determined by BLAST comparisons and by using the MicroScope platform from the Genoscope and the

Primer name	Primer sequence	Application
Mdec_1F	TGGTGTCGAAGTGTATGTGCTTA	*M. decipiens* detection (unique region)
Mdec_1R	ATCTTCAGCGATCTCGACTTCTC	
Mlac_1F	TAACCATTACCGTGACCAGGAAG	*M. lacus* detection (unique region)
Mlac_1R	TTAGCGAGATTGTCTCCATCTGG	
Mriy_1 F	ATCAAAAGCAAGCCGACTTTCTC	*M. riyadhense* detection (unique region)
Mriy_1R	TGAACATGTCAACGGCATATTGG	
Mshi_1F	GCTCTCACGCTATGTATTTCACC	*M. shinjukuense* detection (unique region)
Mshi_1R	TATGGATGAGGTCGTCAATCACC	
Mkan_1F	ATCTGAATCAGGTCGATACGCAA	*M. kansasii* detection (unique region)
Mkan_1R	CGATTGGTCTTTCAGCCAGTTTT	
Mdec_2F	ATAACTTGCTGGAGATCGTGGTT	*M. decipiens* ESX-2 locus downstream Mdec_14907
Mdec_2R	TACGAAAGTTACTTCACCGACGA	
Mdec_3F	GAGATATTCACGCCGTTGCAAAT	*M. decipiens* ESX-2 locus upstream Mdec_10038
Mdec_3R	GCATTGGAGATCTCGATCGGATA	
Mdec_4F	TGCCGGACTGACCAGCTATA	*M. decipiens* ESX-2 locus downstream Mdec_10042
Mdec_4R	CCGGCAATATCTACGTCAGTGA	
Mriy_2F	CACTCAAATACTGGTTGGCGATC	*M. riyadhense* ESX-2 locus downstream Mriy_14414
Mriy_2R	ACTCCGGAAAGCTTCTTCACC	
Mriy_3F	GAGATATTCACGCCGTTGCAAAT	*M. riyadhense* ESX-2 locus upstream Mriy_14486
Mriy_3R	GATCAAGACCAAGGTTGAACGTC	
Mriy_4F	CCTATGCAGTTGGTGTCCAGT	*M. riyadhense* ESX-2 locus downstream Mriy_14489
Mriy_4R	ATTTCTTTAGCCAGTCCGCCAT	
Mdec_2F	CAAAACGCATGATGACCGGATG	Verification of additional contig in *M. decipiens* PacBio sequence
Mdec_2R	TCCATCGCTATCTCACGTTCAC	
Mdec_3F	CGAATTCTTGATGTCGTCGAGC	Verification of additional contig in *M. decipiens* PacBio sequence
Mdec_3R	CGAATTCTTGATGTCGTCGAGC	
Mdec_3F’	CAAGCATTTTCAGACGTACCGAAC	
Mdec_4F	GAACAAATCGTTGAGGTTGAACTCG	Verification of additional contig in *M. decipiens* PacBio sequence
Mdec_4R	CGGTGTAGTCAGCCAATTGTTG	

Table 1: Primers designed for this study.

Artemis Comparison Tool software (Carver et al., 2005). Primers for each species were designed with Primer3plus software. The specificity of the selected primers for each species was confirmed by PCR arrays and these primers were then used for controlling the authenticity of the mycobacterial cultures used in phenotypic characterization experiments. The absence of cross-contaminations between cultures was verified before each experiment by subjecting an aliquot of the culture to PCR tests with an annealing temperature of 60°C. Primers designed and used for this study are detailed in table 1.

Lipid extraction

Crude lipid extracts from different strains were obtained from 50ml culture each, grown in 7H9 ADC up to an optical density (OD_{600nm}) of 1. Bacteria were recovered by centrifugation at 4000 rpm for 10 min and frozen. In step 1, each pellet was thawed and resuspended in 3mL of Chloroform/Methanol ($CHCl_3$/CH_3OH) (1:2, vol/vol), transferred into a first glass tube, and vortexed before being incubated for 2h at 55-60°C, vortexed again and centrifuged at 1600 rpm for 5 min. In step 2, the supernatant (organic phase) was recovered and transferred into a second glass tube (lipid recovery tube), which was allowed to evaporate, accelerated by addition of nitrogen gas. In step 3, to increase the quantity of extracted lipids, the pellet remaining in the first glass tube was resuspended in 3mL of $CHCl_3$/CH_3OH (2:1, vol/vol), and the same procedure of vortexing, incubation and centrifugation as used in step 1 was applied, after which the supernatant was transferred into the lipid recovery tube and allowed to evaporate to dryness, using nitrogen. To further increase the lipid quantity, in step 4 all procedures of step 3 were repeated one more time. Finally, 3mL of $CHCl_3$/CH_3OH/H_2O (4:2:1, vol/vol/vol) were added to the lipid recovery tube, vortexed and centrifuged at 1600 rpm for 5 min. The organic phase was recovered into a new glass tube and dried under nitrogen.

Thin layer chromatography

Extracted lipids were resuspended in $CHCl_3$/CH_3OH (2:1, vol/vol) and deposited on glass silica gel G60 F_{254} plates (Merck) for detection of lipooligosaccharides (LOS) and on aluminum silica gel G60 F_{254} plates (Merck) for detection of phtiocerol dimycosersates (PDIM). Lipids were then separated on plates using following solvents and visualization methods:

- LOS with $CHCl_3/CH_3OH/H_2O$ (30:12:1, vol/vol/vol) as solvent and a visualization by spraying 0.2% anthrone solution (wt/vol) in concentrated H_2SO_4 followed by heating for 10 min at 110°C.
- PDIM with C_6H_{14} 40-60°C/$(C_2H_5)_2O$ (9:1 vol/vol) as solvent and a detection with 10% $CuSO_4$ in 8% H_3PO_4 followed by charring.

Culture of cell line

The human monocyte cell line THP-1 (ATCC-TIB-202) was used. This cell line was originally generated from peripheral blood from an acute monocytic leukemia patient and is a widely used tool in cell biology. THP-1 cells were cultured with complete medium composed of RPMI-1640 GlutaMax (Gibco) and 10% of inactivated Fetal Bovine Serum (FBS, Dutscher) at 37°C 5% CO_2. The medium was renewed every 48 hours until confluency was reach without exceeding five passages. Cells were then differentiated into macrophages by adding PMA (phorbol-12-myristate-13-acetate) at 10 ng/mL in RPMI-1640 GlutaMax – FBS 5% for 48 hours, after which they were ready to be used in infection experiments.

***In vitro* experiments**

Mycobacterial cultures in exponential phase were prepared by several washing steps with phosphate-buffered saline (PBS) and aggregates were broken by passing the culture through 10µm-filters (Pluristrainer). Concentrations of bacteria were then determined by measuring the OD of the cultures using previously determined equivalences:

- *M. decipiens*: $OD_{600nm} = 1 \Leftrightarrow 5.5 \times 10^7$ bacteria/mL
- *M. lacus*: $OD_{600nm} = 1 \Leftrightarrow 1.5 \times 10^8$ bacteria/mL
- *M. riyadhense*: $OD_{600nm} = 1 \Leftrightarrow 3.0 \times 10^8$ bacteria/mL
- *M. shinjukuense*: $OD_{600nm} = 1 \Leftrightarrow 1.5 \times 10^8$ bacteria/mL
- *M. kansasii*: $OD_{600nm} = 1 \Leftrightarrow 8.0 \times 10^7$ bacteria/mL
- *M. bovis* BCG Pasteur: $OD_{600nm} = 1 \Leftrightarrow 5.5 \times 10^8$ bacteria/mL
- *M. tuberculosis* H37Rv: $OD_{600nm} = 1 \Leftrightarrow 1.0 \times 10^8$ bacteria/mL

Differentiated THP-1 cells were infected with mycobacteria at a multiplicity of infection (MOI) of 1:20 (1 bacterium for 20 THP-1 cells) for 3 hours. A treatment with amikacin 0.1mg/mL was performed for 1 hour to eliminated extracellular mycobacteria.
The capacity of infection of the strains was determined by counting the bacterial load at time intervals from day 0 to day 7 (days 0, 3, 5 and 7). For determination of the bacterial counts macrophages were lysed with PBS 0.1% Triton X-100 and 5-fold serial dilutions were prepared, which were deposited on 7H11 10% OADC plates and incubated for 17 to 25 days at 35°C or 37°C after which colony forming units (CFUs) were counted.

***In vivo* experiments**

Studies were performed in agreement with the European and French guidelines (EC Directive 2010/63/UE and French Law 2013-118 issued on 1 February 2013). These experiments were approved by the Institut Pasteur safety committee (protocol 11.245) and by the relevant Ethics Committee (Comités d'éthique en experimentation animale 89) and by the French Ministry for Higher Education and Research (nos da180023 2018060717283847 v1 and dap220021 2022042811231522_v1). Bacterial solutions were prepared similarly to those used for THP-1 infections, resulting in a 5mL final solution of 2.5 x 10^6 CFUs/mL. Seven weeks-old female C57BL/6J mice (Charles River Laboratories) and seven weeks-old male C3HeB/FeJ mice (Jackson laboratory) were infected by aerosol using a custom-made aerosolization system. The inhaled bacterial load was determined by CFU counting of bacilli per lung at day 0 or 1 post infection in selected mice, while the *in vivo* growth capacity of the different strains was determined on lung and spleen samples by CFU counting at different time points post infection (from 4 to 14 weeks). CFUs determined from lungs were deposited on 7H11 plates supplemented with 10% OADC and 10% PANTA (Becton Dickinson) antibiotic mixture.

Western Blotting

Bacterial cultures in exponential growth phase were washed and resuspended in 7H9 0.2% dextrose and 0.05% Tween 80 for 48 hours. Supernatants and pellets were then collected and treated with protease inhibitor cocktails (cOmplete EDTA-free protease inhibitor, Sigma). Cellular membranes were broken by shaking the suspension with zirconium beads and

TissueLyser II (Qiagen) before treatment with protease. Both supernatants and cell lysates were filtered through a 0.22µm-PVDF membrane. Protein concentrations were measured using Nanodrop (1mg/mL).

50 µg of total proteins were loaded on a NuPage 4–12% Bis-Tris polyacrylamide gel (ThermoFisher) and separated by SDS-PAGE at 200 V during 30 minutes. Proteins were then transferred onto a nitrocellulose membrane using an iBlot dry blotting system (Invitrogen) and membranes were incubated for 1 hour at RT in TBS 0.1% Tween 20 (TBS-T) and 5% non-fat dry milk. The membranes were washed with TBS-T and polyclonal primary antibodies α-ESAT-6 (lab stock (Brodin et al., 2005)), α-CFP-10 (a kind gift from I. Rosenkrands, Statens Serum Institut, Copenhagen, Denmark), α-SigA (a kind gift from I. Rosenkrands, Statens Serum Institut, Copenhagen, Denmark) and a commercial polyclonal α-Ag85B (Abcam, ab43019) were incubated in TBS-T 3% BSA with red phenol at room temperature for 2h. The secondary α-rabbit antibodies were incubated, after washing membranes at room temperature, for 1 hour in TBS-T 3% BSA with red phenol. Finally, membranes were washed a last time before protein revelation using the SuperSignal West Femto Maximum Sensitivity Substrate (Thermo Fisher).

Resazurin assay and determination of antibiotic resistance

Mycobacterial cultures in exponential phase were prepared by several washing steps with PBS and aggregates were eliminated by filtrating cultures through a 10 µm-filter (Pluristrainer). Bacterial suspensions were prepared in 7H9 10% ADC broth at a final concentration of 0.005 OD_{600nm} and 100µL were disposed in 96-well plates. Antibiotics were prepared and filtered, and added to the first well to obtain a specific concentration, then serial dilutions were performed to obtain antibiotic ranges as follow:

- Bedaquiline: 3.2 – 1.6 – 0.8 – 0.4 - 0.2 – 0.1 – 0.05 – 0.025 – 0.0125 – 0.00625 – 0.00313 – 0.00156 – 0.00078 – 0.00039 µg/mL
- Isoniazid: 32 – 16 – 8 – 4 – 2 – 1 – 0.5 – 0.25 – 0.125 – 0.0625 – 0.0313 – 0.0156 – 0.0078 µg/mL
- ethambutol: 60 – 30 – 15 – 7.5 – 3.75 – 1.88 – 0.94 – 0.47 – 0.23 – 0.12 µg/mL
- rifampicin: 4 – 2 – 1 – 0.5 – 0.25 – 0.125 – 0.0625 – 0.0313 – 0.0156 – 0.0078 – 0.0039 – 0.002 µg/mL

Plates were incubated at 37°C for 9 days for *M. lacus*, 10 days for *M. riyadhense*, 12 days for *M. shinjukuense*, 6 days for *M. kansasii and Mtb* and for 8 days at 35°C for *M. decipiens*. After the incubation period, 30µL of 0.01% resazurin solution (resazurin sodium salt, Sigma) were added and incubated over night at the same temperature than previously used. Plates were read with an excitation wavelength of 570nm and emission of 590nm, and results were recorded

RESULTS

In the interests of facilitating presentation and understanding, this section will be divided into several chapters, grouping together the different results as follows:

- A section dealing with the phenotypic characterization of the four species, which enabled us to optimize their growth in order to obtain optimal quantities for the various experiments, and to determine the resistance of the species to selected anti-TB drugs.
- A section dealing with the infectious capacity of the four species in order to determine whether some of them might be used as new models for TB research.
- A genomic comparison section, supported by selected molecular biology analyses to further characterize these yet understudied species and to further evaluate their potential use as a study model.

For most experiments we use *M. kansasii*, one of the two most widely used comparator model for TB research and *Mtb* H37Rv as a control.

Selected results presented here are also part of a scientific article under preparation for submission to a scientific journal, the draft of which can be found in the appendix.

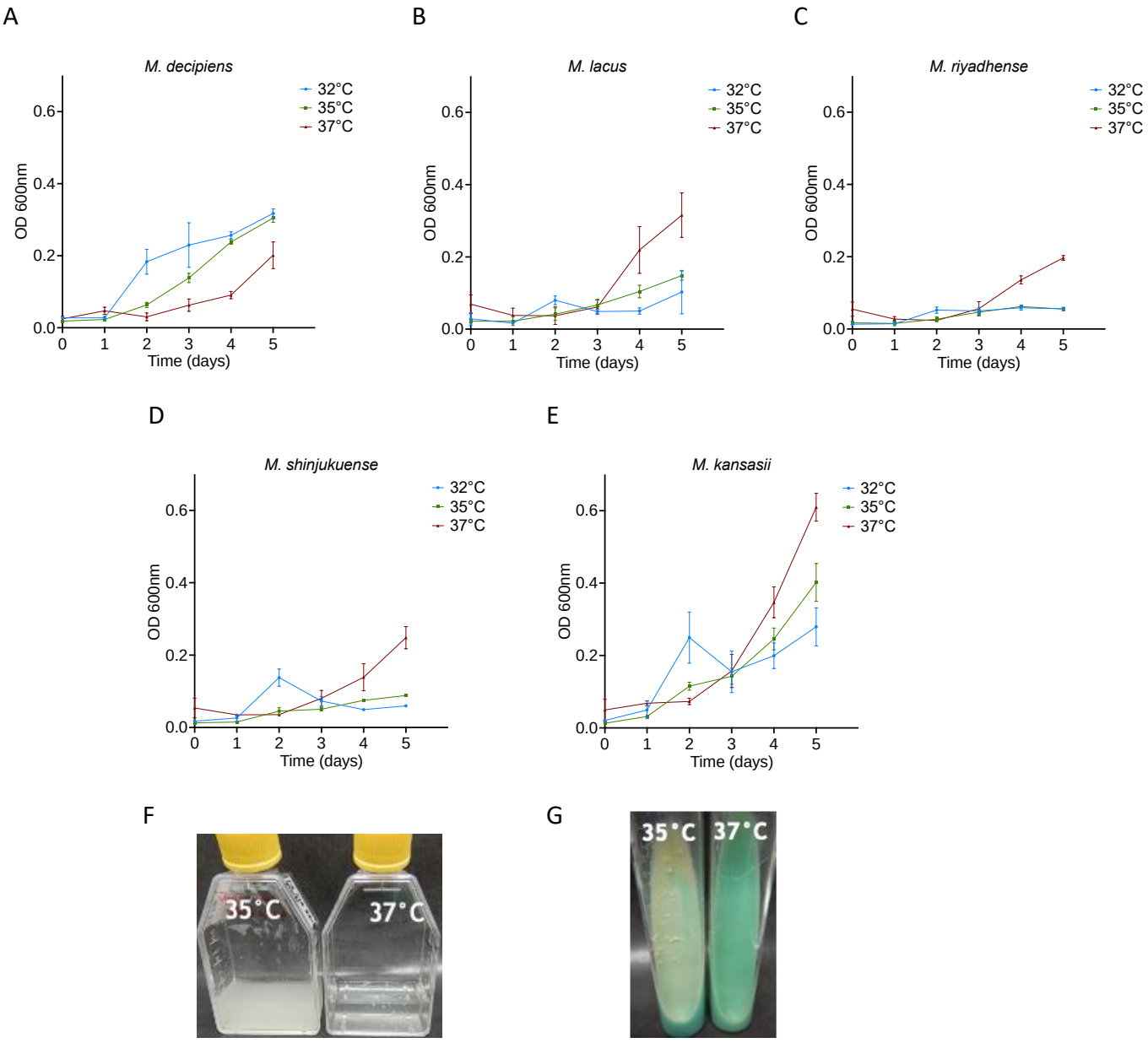

Figure 13: Growth comparison for *M. decipiens*, *M. lacus*, *M. riyadhense*, *M. shinjukuense*, and *M. kansasii*. Growth measurement over time at an OD of 600nm for *M. decipiens* (A), *M. lacus* (B), *M. riyadhense* (C), *M. shinjukuense* (D), and *M. kansasii* (E). Growth was measured at 32°C, 35°C, and 37°C for each strain once a day for 5 days. Results of two independent experiments under classic culture conditions. Picture of *M. decipiens* growth at 35°C and 37°C in 7H9 ADC liquid cultures (F), and on LJ tubes (G) were taken after 10 days of incubation. Comparable quantities of bacteria were used for both temperatures.

I. Phenotypic characterization of the four species

Growth optimization

For the practical work of my thesis, reference strains of the mycobacterial species *M. decipiens*, *M. lacus*, *M. riyadhense* and *M. shinjukuense* were purchased from DSM or ATCC strain culture collections, and as these species had not yet been cultured before in the host laboratory, the first part of the work was therefore dedicated to phenotypically characterize them in order to optimize their growth and be able to study them in the best possible way in later experiments, involving genome sequencing, molecular biology, and experimental infection studies.

The first step was hence to culture the four species of SGM, following the recommendations indicated by the suppliers, which involved incubation at 37°C in Middlebrook 7H9 medium supplemented with 10% ADC for liquid cultures, and/or on plates of Middlebrook 7H11 medium supplemented with 10% OADC or on slants of Lowenstein-Jensen (LJ) medium for cultures on solid media. However, after several long-lasting attempts of growing *M. decipiens* under the indicated conditions, we repeatedly noticed a growth defect for this reference strain, which even after two months of incubation had a very low culture yield on both liquid and solid media. After testing several variations in growth media without much effect, we also investigated different temperatures by comparing the growth of the four strains and *M. kansasii* by measuring ODs at 600nm at 32°C, 35°C and 37°C over a period of 5 days. While *M. lacus*, *M. riyadhense*, *M. shinjukuense* and *M. kansasii* clearly grew better at 37°C than at 32°C or 35°C (Figure 13B-E), *M. decipiens* grew better at 32°C and 35°C (Figure 13A). Furthermore, a visual comparison between liquid cultures of 7H9 ADC and solid cultures on LJ medium at 35°C and 37°C clearly reflects the growth failure of *M. decipiens* at 37°C (Figure 13F-G). These experiments enabled us to conclude that *M. decipiens* behaved differently to information and recommendations given by the culture collection from which the strain had been obtained. It seems that this difference in growth is more pronounced during primary cultures, starting directly from the lyophilized stock or from stock cultures stored at -80°C and can be partly compensated after several passages in liquid cultures.

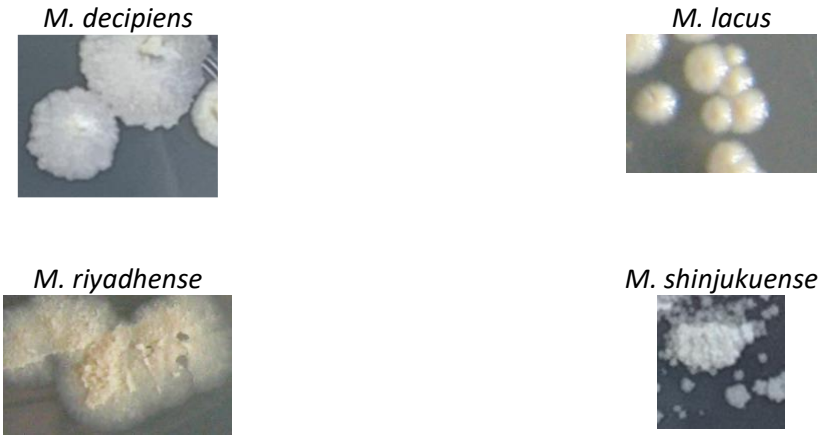

Figure 14: Pictures of colony of *M. decipiens*, *M. lacus*, *M. riyadhense*, and *M. shinjukuense*. Cultures were grown on 7H11 OADC medium for 14 to 25 days of incubation at 35°C for *M. decipiens* and 37°C for others.

	M. decipiens	*M. lacus*	*M. riyadhense*	*M. shinjukuense*
Bedaquiline	0.0125 – 0.025	0.0125 – 0.025	0.05 – 0.1	0.00625 – 0.0125
Ethambutol	10 – 11	7 – 8	7 – 8	4 – 8
Isoniazid	1 – 2	4 – 8	5 – 8	0.5 – 1
Rifampicin	0.9 – 1	0.15 – 0.25	0.06 – 0.125	0.015 – 0.03

Table 2: Determination of MIC range by resazurin assay. Concentrations are in µg/mL. Experiments were carried out in four biological replicates with technical duplicates for each experiment.

	M. decipiens	*M. lacus*	*M. riyadhense*	*M. shinjukuense*
Bedaquiline	S	S	S	S
Ethambutol	R	R	R	S
Isoniazid	I	R	R	S
Rifampicin	I	S	S	S

Table 3: Determination of resistance or susceptibility of *M. decipiens*, *M. lacus*, *M. riyadhense*, and *M. shinjukuense* to anti-TB drugs. The capacity of resistance of the species were based on *Mtb* and *M. kansasii* MIC values from (Degiacomi et al., 2020; Woods et al., 2011). I: intermediate; R: resistant; S: susceptible**.**

For further experiments, we decided to grow *M. decipiens* at 35°C rather than 32°C or 37°C in order to promote its growth without deviating too much from the growth temperature of the other used reference strains. It should also be noted that *M. riyadhense* and *M. shinjukuense* seem to grow more slowly than the other species at their optimum temperature, and appear to be unable to grow, or at least to grow much more slowly, at 32°C and 35°C (Figure 13C-D).

Determination of the colony morphotypes

Once the growth temperatures of the strains had been determined, the bacteria were plated on 7H11 OADC medium to determine their colony morphology.
We found that both smooth and rough morphologies were present within the species and all colonies were unpigmented. Following incubation of the species, we determined that under our conditions used, *M. decipiens*, *M. riyadhense* and *M. shinjukuense* showed a rough phenotype, while *M. lacus* exhibited a smooth morphotype (Figure 14). These results are in line with descriptions found in the literature, except for *M. shinjukuense,* which is described as having a smooth phenotype in the study describing the bacterium (Saito et al., 2011).

Antibiotic Resistance

To further characterize the four species, we sought to get insights into the antibiotic resistance profiles of the strains. This knowledge is an important element in the phenotypic characterization of strains and bacterial species in general, as well as for the evaluation of their potential use as models of TB infection.

To this end, we selected four anti-TB drugs. Three first-line agents (Isoniazid, Rifampicin and Ethambutol), and one new-generation third-line agent (Bedaquiline) which has been used for a decade in the treatment of resistant TB (Mallick et al., 2022).
These anti-TB agents were tested at different concentrations on *M. decipiens*, *M. lacus*, *M. riyadhense* and *M. shinjukuense*, and compared with tests on *M. kansasii* and *Mtb*. The concentrations evaluated were chosen on the basis of known resistance profiles of *Mtb* and determined according to minimal inhibitory concentration (MIC) against *Mtb* and/or *M. kansasii* (Degiacomi et al., 2020; Woods et al., 2011). With this in mind, we were able to

obtain the MICs of the strains (Table 2) using colorimetric resazurin tests (photos of the plates in appendix) and spectrophotometer measurements.

Based on the literature, we were then able to determine whether the strains were sensitive, resistant, or intermediate to the anti-TB drugs tested. According to the MICs, three of the four species showed intermediate or complete resistance to ethambutol and isoniazid, *M. shinjukuense* being the exception with full sensitivity. In addition, *M. decipiens* showed intermediate resistance to rifampicin, while the other three species were fully susceptible to this first-line TB drug. Finally, all four mycobacterial species under study were sensitive to bedaquiline (Table 3).

The low activity of isoniazid and ethambutol against *M. decipiens*, *M. lacus* and *M. riyadhense* prompted us to examine this question in greater detail. It is true that *Mtb* is particularly sensitive to isoniazid, compared with other mycobacteria such as *Mycobacterium smegmatis*, because isoniazid is a prodrug which must be converted inside the bacterium into an active molecule. In *Mtb*, this activation process is carried out by KatG, an enzyme with catalase and peroxidase activity, whereby the active molecule acts on InhA (Dokrungkoon et al., 2023; Palomino & Martin, 2014). We therefore analyzed the genomic sequences of the three strains for the presence of *katG* and *inhA* orthologs. The KatG mutation most commonly causing *Mtb* resistance is the mutation of Ser315 to Thr315 (Pym, Saint-Joanis, et al., 2002). This mutation is not found in any of the three species, but we can observe that numerous other mutations are present in the KatG protein sequence of all three species, some of which are similar.

The action of ethambutol blocks the synthesis of key cell wall structural elements in *Mtb*. The gene mainly affected by mutations causing resistance is *embB*, which harbors three major resistance mutations (Boni et al., 2023; Brossier et al., 2015). Of these three most common mutations, only *M. lacus* shows a mutation from Gly406 to Pro406 in its EmbB protein. But this is not the common mutation found in *Mtb* (Gly406Ala). However, the 597bp sized ethambutol resistance determining region in *Mtb* shows several mutations in all three strains, but none of which appears to be shared among the three species (Bwalya et al., 2022).

Finally, given the intermediate resistance of *M. decipiens* to rifampicin, we also studied the sequence of *rpoB*, coding for the beta subunit of RNA polymerase, which represents the target of rifampicin (Telenti et al., 1993). Analysis of RpoB has shown that the known *Mtb* mutations causing rifampicin resistance are not found in the *M. decipiens* RpoB sequence (Palomino & Martin, 2014).

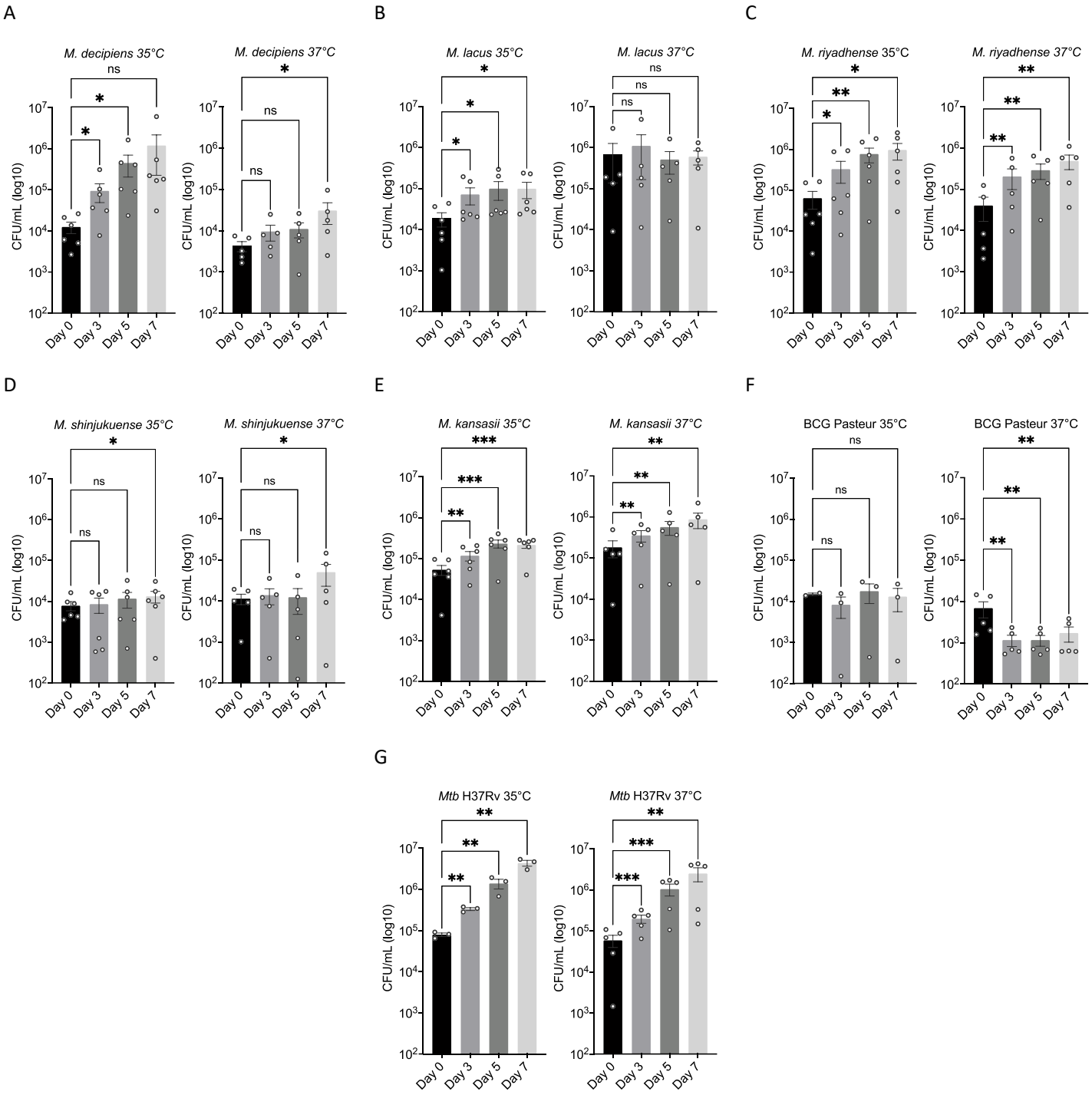

Figure 15: Determination of the intracellular multiplication capacity of *M. decipiens*, *M. lacus*, *M. riyadhense*, *M. shinjukuense*, *M. kansasii, M. bovis* BCG Pasteur strain, and *Mtb* in THP-1 cellular model. Infection of THP-1 derived macrophages determined by CFU counting at 0, 3, 5 and 7 days after infection. Results represent between 3 and 6 independent experiments at 35°C and 37°C for *M. decipiens* (A), *M. lacus* (B), *M. riyadhense* (C), *M. shinjukuense* (D), *M. kansasii* (E), *M. bovis* BCG Pasteur strain (F), and *Mtb* H37Rv (G). Data are represented as means and SEM of 3 to 6 biological experiments, each experiments containing 3 technical replicates. Statistical differences in CFUs were determined by a two-way ANOVA test with Dunnett's multiple comparisons test (*P < 0.033; **P < 0.002; ***P < 0.001; ns: non-significant).

II. Infection experiments

In vitro experiments: THP-1 infection

To determine whether the four species could represent an interesting model for TB research, we compared their ability to multiply in a cellular infection model, using cells from a THP-1 cell line differentiated into macrophages. To best match the optimal growth temperature of *M. decipiens*, infections were carried out both at 35°C and 37°C for 7 days, first removing extracellular bacteria. The capacity for intracellular growth was determined by counting CFUs after 0, 3, 5 and 7 days. For comparison with *Mtb*, the quantity of bacteria used to infect the cells was based on the concentration of *Mtb* enabling the cells to survive for 7 days, corresponding to an MOI of 1 bacterium per 20 macrophages (1:20). In order to have a negative control, corresponding to a strain that does not multiply in host cells, the attenuated *M. bovis* BCG Pasteur vaccine strain was also included in the experiments.

Our results confirmed that *Mtb* multiplies in THP-1 based host cells at 37°C and 35°C, in both cases with a 2-log increase of the bacterial load over 7 days (Figure 15G). The results also showed that *M. kansasii* is able to multiply in THP-1 cells but at a lower rate than *Mtb*, showing less than one log increase of CFU counts in seven days (Figure 15E), while the BCG Pasteur strain shows a decreasing concentration in THP-1 cells, consistent with its virulence attenuation (Figure 15F).

In the case of *M. lacus* and *M. shinjukuense*, there was very little, if any, increase in bacterial load, but no decrease. This can be assimilated to a state of persistence, although it is not yet clear if the bacteria were able to persist, or if the cells were killing the bacteria at the same rate as they multiplied (Figure 15B, 15D). However, it appears that *M. lacus* can weakly replicate at 35°C, which was not the case for the infection at 37°C (Figure 15B). One possible explanation for this might be that, since this temperature is not the optimal temperature for the bacterium nor the THP-1 cells, it could trigger stress signaling pathways that might provide an advantage for the bacterial cell.

M. decipiens and *M. riyadhense* show a capacity to multiply at both temperatures, but the increase is smaller at 37°C than at 35°C for *M. decipiens*, which can be explained by its above-described growth defect at the higher temperature (Figure 15A).

A

	C3HeB/FeJ		C57BL/6L	
	Titration (CFU/mL)	Day 1 CFU	Titration (CFU/mL)	Day 1 CFU
M. decipiens	1,66E+06	37.5	1,66E+06	20,6
M. lacus	1,88E+05	322.5	3,50E+05	271,9
M. riyadhense	8,75E+05	540	1,50E+05	15
M. shinjukuense	1,41E+06	5	4,25E+05	16,9
M. kansasii	1,20E+06	22.5	7,00E+05	39,4
BCG Pasteur	2,46E+06	22.5	1,79E+06	18,7
Mtb H37Rv	2,55E+06	7.5	5,38E+05	9,4

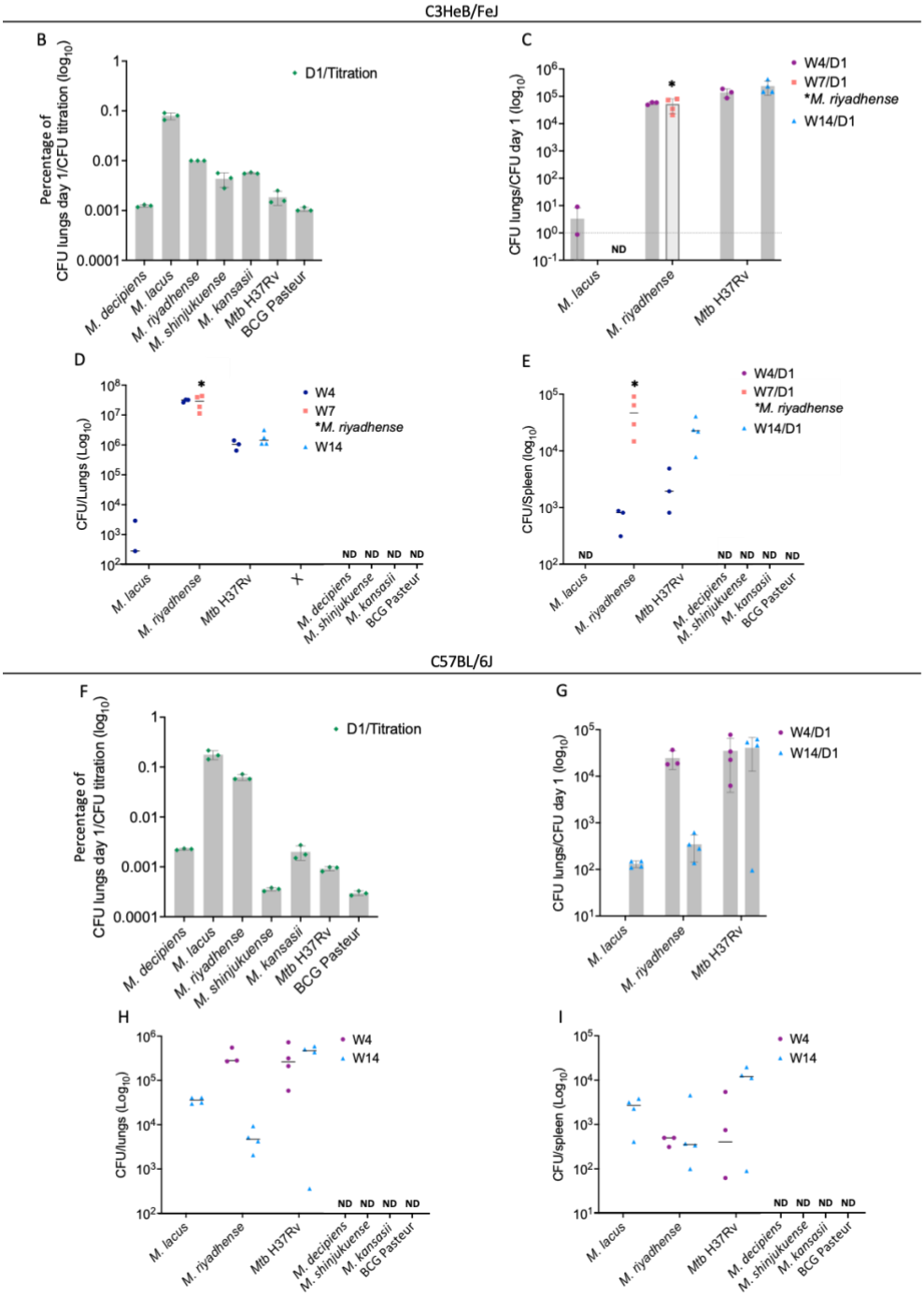

Figure 16: Determination of the infection and *in vivo* growth capacity of *M. decipiens*, *M. lacus*, *M. riyadhense*, *M. shinjukuense*, *M. kansasii*, *M. bovis* BCG Pasteur strain, and *Mtb* H37Rv in two murine models. Dose of infection at day 1 and titration of aerosolized culture of both infections are indicated (A). Results from C3HeB/FeJ infection are represented by the ratios of the CFUs D1/CFUs Titration (B), and ratios of different time points versus the Day 1 (C). Ratios were calculated after the determination of the *in vivo* growth characteristics of the different species by CFU counting at 4-, 7- and 14-weeks post-infection in lungs (D) and spleens (E). Same results are presented for the C57BL/6J infection with ratios of CFUs D1/CFUs titration (F), CFUs W4/CFUs D1 and CFUs W14/ CFUs D1 (G); and the raw data of the CFUs counting after 4- and 14-weeks post-infection in lungs (H) and spleens (I). Each experiment was performed once, the represented values correspond to the number of mice at each time point.

The multiplication capacity of *M. decipiens* at 35°C is quite impressive, with an increase of almost 2-log compared with barely 1 log at 37°C on day 7. Conversely, *M. riyadhense* shows a similar increase between the two temperatures, with a multiplicity of 1 to 1.5 log in 7 days (Figure 15C).

***In vivo* experiments: mouse infection**

To study the ability of the bacteria to multiply intracellularly, the THP-1 cell infection is an accurate model. However, such *in vitro* infection experiments might only partially reflect the ability of bacteria to multiply in a more complex host. In order to determine the ability of bacteria to multiply inside the host in presence of defense mechanisms of the innate and adaptive immune systems, *in vivo* models are needed. We thus set up pilot *in vivo* infection experiments using two different mouse models. Here, female C57BL/6J and male C3HeB/FeJ mice were subjected to aerosolized suspensions of *M. decipiens*, *M. lacus*, *M. riyadhense*, *M. shinjukuense*, *M. kansasii*, *M. bovis* BCG Pasteur and *Mtb* H37Rv. For these initial experiments, solutions with a target concentration at 2.5 x 10^6 CFUs/mL were prepared and 5ml of solution of each strain were loaded into the devices used for generating the aerosol to which groups of mice were exposed in a custom-made aerosolization apparatus inside the BSL3 animal facility. From previous experiments it is known that in the case of infection with *Mtb*, the use of such a concentration generates a low-dose infection of approximately 10 to 100 CFUs per lungs in mice. The final doses administered to the groups of mice were assessed by CFU quantification in lung homogenates obtained from control mice at day 1 post-infection, in addition to plating dilutions of the solutions right after the aerosol challenge. The *in vivo* growth capacities of each strain were determined by CFU counts, obtained from homogenized mouse lungs and spleens at 4-, and 14-weeks post-infection.

Analyses of the CFU counts obtained from plating the solutions used for infection and results from day 1 infection control mice showed a certain heterogenicity in the counts among the different species, which might have been caused by different colony morphologies and other bacterial surface differences, likely impacting on OD measurements, clumping and physical behavior during aerosolization. For this reason, ratios of bacterial lung infections are shown in figures 16B and 16F, using the bacterial concentrations of the aerosolized solutions and the obtained CFU counts at day 1 post-infection for C3HeB/FeJ and C57BL/6J mice, respectively,

whereby it should be noted that *M. lacus* which depicts a smooth colony morphology type, and *M. riyadhense* which depicts a mixed smooth-rough colony morphology type, showed higher counts than the other species, which show rough morphotypes. It is likely that this higher numbers have influenced to some extend their relative *in vivo* growth characteristics compared to the other tested species.

We noted that *M. decipiens*, *M. shinjukuense*, *M. kansasii* and the BCG Pasteur strain were not detected at weeks 4 and 14 post-infection in organs of C3HeB/FeJ and C57BL/6J mice (Figure 16D-E, 16H-I), although bacteria were detected on day 1 in the lungs (Figure 16A-B, F). We conclude from these results that these bacterial species are eliminated by the mice's immune system. It is not surprising that *M. kansasii* is also eliminated by the host, as the initial infectious doses were targeted to compare well with that for *Mtb* infection. Our results show that this opportunistic NTM species has a lower level of virulence than *Mtb* in both types of mice, confirming previously described results (J. Wang et al., 2015).

For *M. decipiens*, infection of THP-1 cells showed that this bacterium had a lower multiplication capacity at 37°C (Figure 15A), probably due to a growth defect at this temperature (Figure 13A, 13F-G). This may be one of the reasons why this bacterium is also rapidly eliminated by the murine host.

Finally, *M. shinjukuense* showed no ability to multiply in THP-1 macrophages (Figure 15D) and the BCG strain showed a decrease in bacterial numbers over time in THP-1 macrophages (Figure 15F), which is consistent with their elimination by the mice's immune system.

M. lacus was detected in both mouse infection models, but in different ways. In C57BL/6J mice, the bacterium was detected in the lungs and spleens at 14 weeks post-infection, but not at 4 weeks (Figure 16H-I), whereas in C3HeB/FeJ mice, it was only detected at 4 weeks post-infection and seems to have been eliminated afterwards (Figure 16D-E). We also note that during aerosol infection, the number of bacteria reaching the lungs was higher than for other strains, likely due to a higher dose used (Figure 16B, F), which might be linked to differences in the colony morphology for this strain. As with *M. kansasii*, the dose for this bacterium may need to be higher to avoid clearance inside the mouse lungs. However, the quantity of bacteria reaching the lungs was greater than for *M. kansasii* (Figure 16A-B), which may explain the detection of *M. lacus* compared with *M. kansasii*. Furthermore, considering the CFU-D1/CFU-titration ratios for this strain obtained in C3HeB/FeJ mice, the ability of the bacteria to multiply

in the lung at week 4 post-infection is almost zero (Figure 16C), which is consistent with the THP-1 infection results which tended towards a persistent state of the bacteria (Figure 15B). Surprisingly, the bacteria were not detected in C57BL/6J mice at week 4 post-infection, whereas bacteria were present in the lungs and spleen at week 14 (Figure 16H-I), for which we have presently no clear explanation. In any case, the detected CFU levels of *M. lacus* remain low for all the conditions in which *M. lacus* was detected. Given the higher infection doses found in the mouse lungs at day 1 for both mouse models, the 4 and 14 weeks results still point to an overall very low virulence level of this species, that is much lower than that of *Mtb*.

M. riyadhense presented a surprising profile during these infection experiments, with a higher *in vivo* growth capacity and anticipated virulence than other NTM. Indeed, the percentage of bacteria reaching the lungs during aerosolization was rather high compared to other bacteria (just after *M. lacus*) (Figure 16A-B, F). Upon infection of C3HeB/FeJ mice, animals infected with this strain began to lose considerable weight. According to the rules of the ethical protocol, we had to cull them at half of the targeted time, i.e., at 7 weeks post-infection instead of 14 weeks (Figure 16C-E). It has to be mentioned that the CFU counts for day 1 controls were found to be much higher (≈ 500 CFUs) than for other species used (except for M. lacus). For example, the initial dose of *M. riyadhense* was 50 times higher than the one of *Mtb* (500 vs. 10 CFUs, respectively), which certainly also contributed the pronounced virulence effects seen for this species, which even disseminated to the spleen, like *Mtb* (Figure 16D-E), but it remained unclear how infection dynamics between *M. riyadhense* and *Mtb* might compare when similar initial bacterial doses were deposited in the lungs of mice.

As such, the dose of CFU contained in the aerosolized solution was reduced for the C57BL/6J mouse infection experiment. This enabled us to obtain comparable day 1 CFU counts between *M. riyadhense* and *Mtb* (≈ 10 CFU for both species) (Figure 16A). Data analysis showed that at an equivalent loading dose on day 1, *M. riyadhense* has similar infection capacity than *Mtb* up to 4 weeks post-infection in the lungs and spleens of C57BL/6J mice, but that the mice were able to better control the infection afterwards, resulting in a reduced number of CFUs of *M. riyadhense* in the lungs of these mice compared to *Mtb* (Figure 16G-I). Relative to all the NTM species tested in this work, the *M. riyadhense* reference strain seems to be clearly the

most virulent one, and also might be the best adapted non-BSL-3 strain for establishing a new mycobacterial virulence model mimicking *Mtb* infection characteristic in mice.

III. Genomic study

Genome sequencing

Once the strains had been cultured, we extracted the genomic DNA of the four species for genome sequencing. Whereas sequence information for the four species that was generated by Illumina-based short read sequencing techniques was available in NCBI public databases, mostly in form of assembled contigs, we were interested to obtain complete genome sequences and for this purpose, a Pacific Biosciences-based sequence technique generating long sequence reads was used. The genome sequences of the strains were obtained following library construction and sequencing, carried out by the Biomics platform of the Institut Pasteur, and the processing of the reads, followed by the assembly of the contigs was performed in collaboration with the Dry Lab of the Institut Pasteur.

With the exception of *M. lacus*, which showed some contamination issues in the DNA preparation, we were able to obtain the complete genome sequences for all the remaining three strains. Assembly of the *M. riyadhense* genome showed the presence of three contigs, which is consistent with existing knowledge for this bacterium, as two of the contigs correspond to plasmids (Guan et al., 2021). We were therefore able to obtain the sequence of the whole chromosome, measuring 6,155,284 bp (Table 4), and those of the plasmids, together representing 479,926 bp. Sequencing of *M. shinjukuense* revealed a smaller chromosome length than the other two species, with a genome of 4,489,120 bp without plasmids (Table 4). Sequencing of *M. decipiens* revealed the presence of two contigs, one large one (5.3 Mb) and one small one (17 kb), whereby the smaller one showed a large sequence overlap with the large contig. PCR amplification experiments using selected primers then showed that the smaller contig did not correspond to a plasmid or extrachromosomal sequence but was well part of the chromosome. The reason why the assembly program generated an extra contig was likely due to a small region of difference of 2 kb inside this part of the genome that was apparently deleted in the genomes of a subfraction of the bacteria used to prepare the genomic DNA from. Further PCR tests on fresh cultures of *M. decipiens* revealed that the deletion was no longer found in these more recent cultures. *M. decipiens* thus contains a single chromosome with a length of 5,301,783 bp and no plasmid. The genome

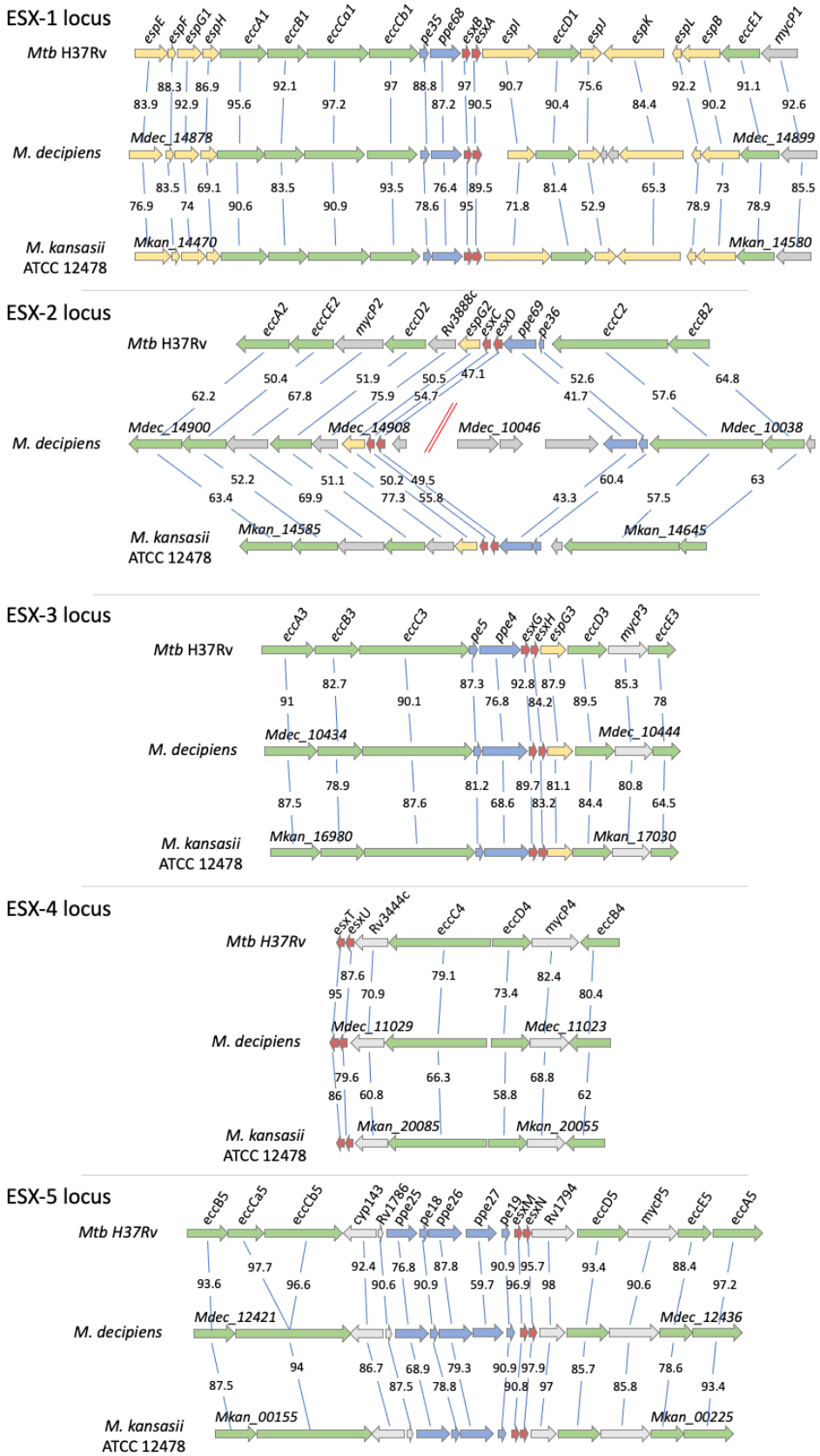

% of amino acid identity (ESX-1)	*Mtb*	*M. kansasii*
M. kansasii	79.8	-
M. decipiens	90.2	79.5
M. lacus	81.1	84.4
M. riyadhense	78.8	83.7
M. shinjukuense	80.5	84

% of amino acid identity (ESX-2)	Mtb	M. kansasii
M. kansasii	87.7	-
M. decipiens	56.4	57.8
M. lacus	90.2	89.1
M. riyadhense	56.2	57.3
M. shinjukuense	90.2	86.7

% of amino acid identity (ESX-3)	*Mtb*	*M. kansasii*
M. kansasii	80.9	-
M. decipiens	86.0	80.7
M. lacus	81.7	81.9
M. riyadhense	82.8	82.4
M. shinjukuense	81.3	82.0

% of amino acid identity (ESX-4)	*Mtb*	*M. kansasii*
M. kansasii	68.8	-
M. decipiens	81.3	68.9
M. lacus	71.2	67.7
M. riyadhense	71.6	69.1
M. shinjukuense	72.4	68.9

% of amino acid identity (ESX-5)	*Mtb*	*M. kansasii*
M. kansasii	86.5	-
M. decipiens	90.4	86.9
M. lacus	86.8	87.2
M. riyadhense	85.9	84.6
M. shinjukuense	87.0	87.8

Figure 17: Genomic comparisons of ESX loci of *M. decipiens* with *Mtb* and *M. kansasii*. Comparisons were performed using Artemis Comparison Tool (Carver et al., 2005), and the MicroScope (Vallenet et al., 2017) database from the Genoscope. Associated tables represented the average of amino acid identity of the locus for the four strains compared to *Mtb* and *M. kansasii*. Percentages were determined using Mage software from the Genoscope.

sequences were then deposited in the Microbial Genome Annotation and Analysis platform "MicroScope" (Vallenet et al., 2017) and further analyzed.

Genomic comparison of the type VII secretion systems

By obtaining the genomic sequences of *M. decipiens*, *M. riyadhense*, and *M. shinjukuense* and by using the sequences available on NCBI for *M. lacus*, *M. kansasii*, and *Mtb*, we were able to undertake genomic comparisons of selected genomic loci between the four species and the comparator species *M. kansasii* and *Mtb,* in order to determine whether the selected regions of the strains were closer related to *Mtb* than to *M. kansasii* or vice versa. We decided to compare well-known *Mtb* virulence factors, and at first selected the genes encoding the five ESX type VII secretion systems of *Mtb*. The available tools of the MicroScope database (Vallenet et al., 2017), including the Artemis Comparison Tool (ACT) (Carver et al., 2005) were used to draw different gene maps and obtain the percentages of amino acid identities among predicted homologous proteins of the different species.

Figure 17 shows an example of the comparisons made for the 5 ESX loci of *M. decipiens* compared with those of *Mtb* and *M. kansasii*. These comparisons were made for each locus of the four strains and are available in the appendix. Tables including average locus similarity were also produced to determine whether the strains were more similar to *M. kansasii* or *Mtb* (Figure 17).

From this analysis we can conclude that with the exception of the ESX-2 locus, the predicted proteins of the various ESX loci of *M. decipiens* share the highest amino acid identity percentages with those from *Mtb*, compared to those of the other three species. In contrast, the ESX-2 locus of *M. decipiens* was found in two distinct parts of the *M. decipiens* genome (Figure 17), a separation which was verified with PCR amplification experiments using specific primers. Moreover, the amino acid identity percentages of the predicted ESX-2 proteins with those of *Mtb* as well as with *M. kansasii* are only around 56.4% and 57.8%, respectively. Surprisingly, the ESX-2 locus of *M. riyadhense* shows the same separation as observed in *M. decipiens* and also shows quite low protein similarities with ESX-2 loci from the other tested mycobacterial species (Supplementary Figure in Appendix 3). Based on these results

we hypothesize that the split ESX-2 loci seen in *M. decipiens* and *M. riyadhense* might have a common phylogenetic origin that is different to the ESX-2 loci of the other tested mycobacterial species and might result from previous HGT events. Little is currently known about the biological role of the ESX-2 secretion system in mycobacteria (Vaziri & Brosch, 2019); however, it is clear that ESX-2 systems belong to the evolutionary youngest ESX systems as they are only present in selected SGM (Dumas et al., 2016). Our results now add a new perspective for future experimental work to decipher the origin and function of the mycobacterial ESX-2 system.

Detection of the ESAT-6 virulence factor

As explained in the introduction, one of the most well-known virulence factors of *Mtb* is the secretion of the ESAT-6 protein and its chaperone CFP-10 (Gröschel et al., 2016). This protein has been shown in several studies to be involved in phagosomal disruption during *Mtb* infection (Simeone et al., 2012; van der Wel et al., 2007). Furthermore, the attenuated *M. bovis* BCG vaccine strain harbors a deleted ESX-1 locus and therefore does not produce and secrete these two proteins, resulting in the inability of the bacterium to exit from phagosomes in immune cells during infection (Simeone et al., 2012). We therefore wanted to check whether the four species investigated in our study were capable of secreting these two proteins, with particular focus on those species that showed abilities to multiply in the different virulence models studied previously (THP-1 and mice), such as *M. decipiens*, which was able to multiply in THP-1 cells (Figure 15A), or *M. riyadhense*, which in addition to be able to multiply in macrophages (Figure 15C), also showed a relatively high virulence in C3HeB/FeJ and C57BL/6J mice, even when using lower infection doses (Figure 16).

We performed Western blotting experiments on cell lysate fractions and culture supernatants from exponentially grown cultures of the four species investigated in our study, The *M. decipiens* culture was carried out at its optimal growth temperature of 35°C (Figure 13A, F-G), as this was the temperature at which the bacterium grew best in THP-1 (Figure 15A), whereas the cultures of the other species were grown at 37°C. The experiment also included *Mtb* as a control, which as previously explained, produces and secretes the two targeted ESX-1 proteins.

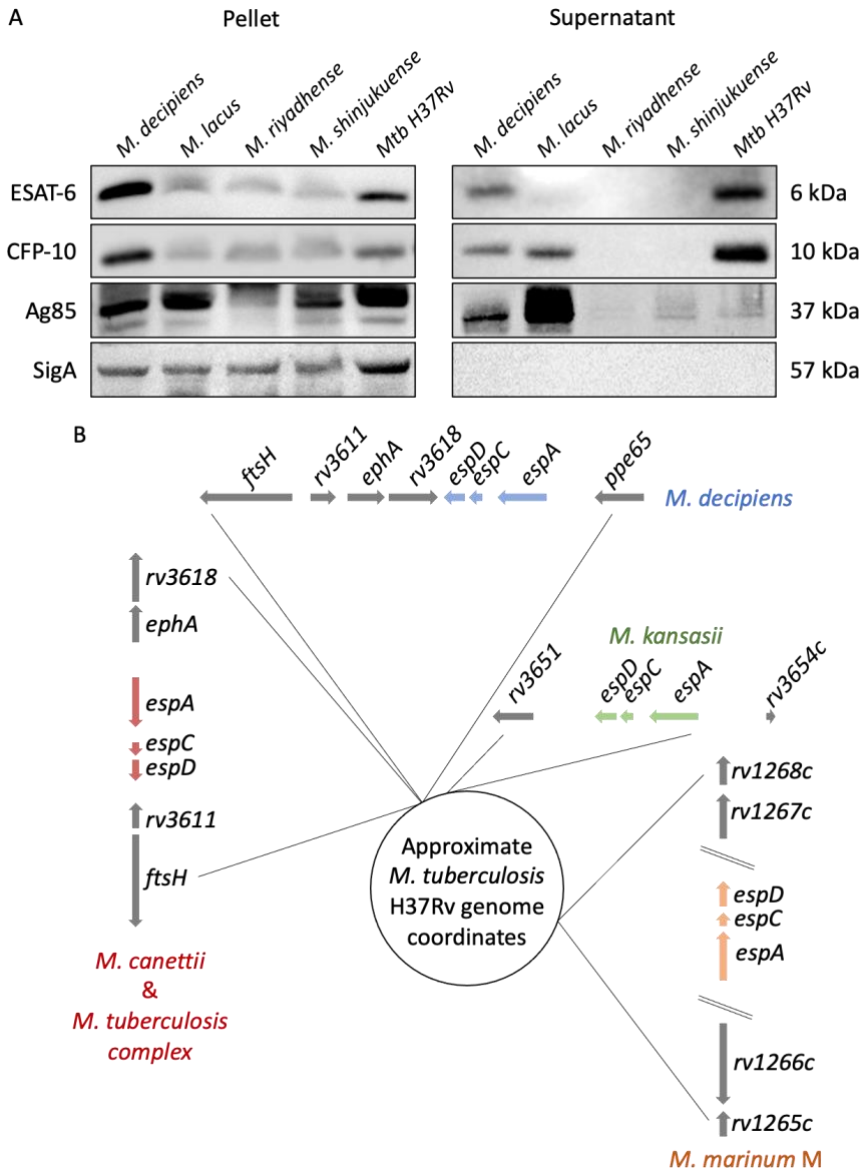

Figure 18: Detection of ESAT-6 and CFP-10 secretion in *M. decipiens*, *M. lacus*, *M. riyadhense*, *M. shinjukuense*, and *Mtb*. 50µg of proteins were migrated on SDS-PAGE for 30 min at 200V and transferred on nitrocellulose membrane for 7 min at 110 V (A). Genomic position of the orthologous genes of the *espACD* cluster that is present in the genome of *M. decipiens*, compared to the genomic locations of the *espACD* clusters in *Mtb*, *M. kansasii*, and *M. marinum*. (B). Note that the orthologous flanking genes of the *espACD* cluster identified in the various species, refer to the *M. tuberculosis* H37Rv gene nomenclature and genomic localization.

For specific protein detection, we used polyclonal antibodies to anti-ESAT-6 and anti-CFP-10, as well as anti-SigA antibodies that were allowing us to exclude the possibility of cell lysis in the cultures. Moreover, commercial anti-Ag85b antibodies were used for evaluation of the presence of proteins in the supernatant. The absence of SigA in the supernatant fractions shown in Figure 18A validate the absence of cell lysis in the preparation of the culture supernatants. The results obtained with the anti-Ag85b antibody shows the presence of this protein in the supernatant, even if for certain strains (*M. riyadhense*, *M. shinjukuense*, and *Mtb*) the amounts appear very weak. Antigen 85b is considered to be exported via the twin arginine translocation (TAT) system and the amounts present in the supernatant may vary. This is also shown by the results obtained for *Mtb*, which shows very little Ag85b but large amounts of ESAT-6 and CFP-10. The use of the anti-Ag85 antibody as putative control for the presence of secreted proteins might thus not have been the best choice for this purpose and the use of another antibody is recommended for future experiments and to fully validate the results obtained for *M. riyadhense* and *M. shinjukuense*.

As regards ESAT-6 and CFP-10, both proteins were shown to be produced by the four strains, and *M. decipiens* seems to be able to produce more than *M. lacus*, *M. riyadhense* and *M. shinjukuense* (Figure 18A). However, only *M. decipiens* was shown to be able to secrete ESAT-6, while CFP-10 is secreted by *M. decipiens* and *M. lacus*. The result for *M. lacus* is rather surprising, as the two proteins usually are secreted in a 1:1 complex-dependent manner (De Jonge et al., 2007; Renshaw et al., 2002). However, as previously discussed, a study recently showed that certain *Mtb* mutants, such as the attenuated MTBVAC vaccine strain, are capable of independently secreting the CFP-10 protein (Aguilo et al., 2017). Such situation might also be the case for *M. lacus*.

It therefore seems that among the four tested species, only *M. decipiens* is capable of secreting the ESAT-6 virulence protein and its CFP-10 chaperone protein. As explained in the introduction, the secretion of ESAT-6 and CFP-10 is a complex mechanism dependent on genes inside the ESX-1 locus as well as genes localized outside the ESX-1 locus (Ates & Brosch, 2017). Indeed, although the mechanisms of secretion through the complex mycobacterial cell envelope are still not fully understood, it has been demonstrated that this secretion is under the control of at least two two-component systems such as the *phoPR* or the *mprAB* regulatory

systems which among many other functions also control the expression of the *espACD* operon, either directly or indirectly. The EspACD operon itself is directly linked to the secretion of ESAT-6 and CFP-10 by a yet unexplained co-dependence of secretion seen between ESAT-6 / CFP-10, and EspA / EspC (J. M. Chen et al., 2012; Fortune et al., 2005; MacGurn et al., 2005). Indeed, the *espACD* operon is a special feature of certain SGM species, including *Mtb*, *M. kansasii*, *M. marinum*, *M. liflandii*, *M. haemophilium*, *M. lepromatosis* and *M. leprae*. It is thought that this *espACD* operon was independently acquired during the evolution of SGM in several selected species, where it was mostly integrated into the genomes at different genomic sites (Ates & Brosch, 2017; Majlessi et al., 2015).

We therefore investigated whether the results obtained by Western blotting were consistent with this information. We thus looked for the presence of the *espACD* cluster in the genomes of the four species under study, and to our surprise it was only found in *M. decipiens*, and not in the other three species tested. Next, we compared the position of the orthologous *espACD* cluster in relation to the *Mtb* genome because, as it was acquired independently by HGT, its position may be different for each mycobacterial species (Ates & Brosch, 2017). Intriguingly, the *espACD* cluster of *M. decipiens* is localized in a similar genomic region as that of *Mtb*, but with a two-gene shift in the operon insertion point (Figure 18B).

When looking at the ESAT-6 and CFP-10 secretion profile obtained by Western blotting, it is clear that *M. decipiens* was the only one among the four species that was able to secrete ESAT-6 and CFP-10 into the culture supernatant. Importantly, *M. decipiens* was also the only one which harbors an *espACD* operon in its genome, and this finding further confirms the previously identified link between ESAT-6 /CFP-10 secretion with secretion of EspA and EspC from the EspACD locus.

However, it should also be noted that CFP-10 secretion is possible without the presence of the EspACD cluster in the genome, as shown by the results obtained for *M. lacus*. This example suggests that CFP-10 may still be secreted without the impact of the EspACD cluster, similar to the situation previously reported for the MTBVAC strain, which is a PhoP deletion strain that hence shows a downregulated EspACD cluster, which is associated with a lack of ESAT-6 secretion (Frigui et al., 2008), despite CFP-10 secretion (Aguilo et al., 2017). With a similar secretion phenotype, *M. lacus* thus represents an interesting new reference strain for the study of this intriguing scientific question in more detail, while *M. decipiens* represents an

A

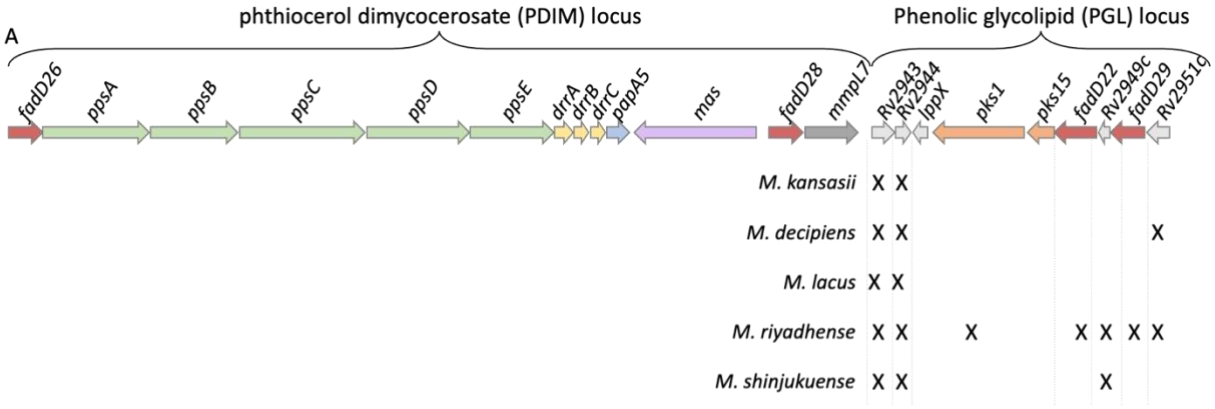

B

% of amino acid identity with *Mtb*	*fadD26*	*ppsA*	*ppsB*	*ppsC*	*ppsD*	*ppsE*	*drrA*	*drrB*	*drrC*	*papA5*	*mas*	*fadD28*	*mmpL7*
M. decipiens	87.3	84.0	81.3	87.3	84.5	84.9	89.1	75.8	87.9	86.6	91.5	80.9	68.7
M. lacus	84.9	78.1	80.5	86.1	83.6	85.2	86.2	70	76.7	81.5	82.6	81.3	63.7
M. riyadhense	58.6	57.5	75.3	68.0	67.7	79.7	81.3	66.6	66.3	62.8	82.1	78.2	59.5
M. shinjukuense	85.4	78.8	77.2	80.2	79.3	82.6	83.4	74.3	70.3	68.5	80.7	79.7	62
M. kansasii	84.0	79.5	79.8	84.4	81.9	83.8	86.4	71.2	85.9	83.2	84.8	79.3	62.0

C

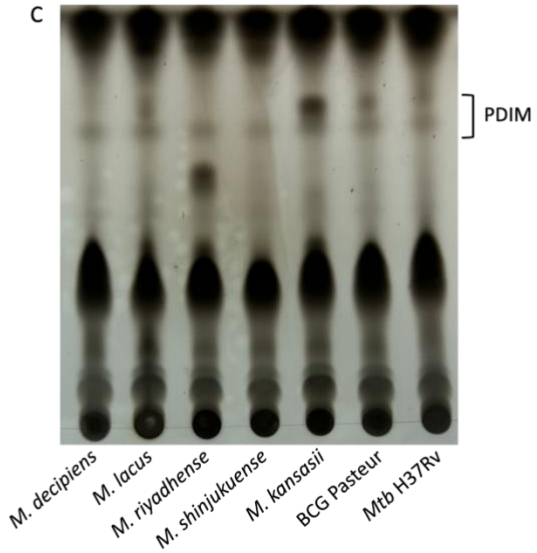

Figure 19: Analysis of PDIM lipids in *M. decipiens*, *M. lacus*, *M. riyadhense*, *M. shinjukuense*, and *M. kansasii* compared to *Mtb* and BCG Pasteur. Genomic comparisons of the PDIM locus and the downstream PGL locus were performed using Artemis Comparison Tool, and Microscope database from the Genoscope. Each gene of the PDIM locus was present within the four species under study, whereas various differences were found for those in the PGL locus. Genes absent from the PGL locus are annotated with an X (A), percentages of amino acid identity of the PDIM locus compared to *Mtb* are reported in the table (B), and the production of PDIM was detected by TLC using Petroleum ether (40:60)/diethyl ether (9:1) and revealed with 10% $CuSO_4$ in 8% H_3PO_4 before charring (C).

interesting new strain for the study of the ESAT-6/CFP-10 — EspA/EspC co-secretion dependance. Together, both species thus provide powerful new models for getting deeper mechanistic insights into this important ESX-1-linked biological phenomenon. As an additional advantage we note that both models do not require the use of a BSL-3 containment, making the studies much easier to organize.

Analysis of the phthiocerol dimycocerosate (PDIM) lipids

Another type of well-known virulence factors of *Mtb* are the PDIM lipids that are present in the outer layer of the bacterial cell wall, and which play an important role during infection. Comparison of the genomic locus that harbors the genes encoding the enzymes which are synthesizing or transporting these lipids showed that the locus was conserved within the four species under study and within *M. kansasii*. However, a comparison of the protein similarities with orthologous proteins of *Mtb* showed a big difference for some strains, with sometimes less than 60% amino acid identity for certain enzymes (Figure 19B). *M. riyadhense* appears to be the strain with the highest differences for this locus, given the low similarities displayed with orthologous proteins of the other members of the clade, while *M. decipiens* again shows the highest similarities with *Mtb* proteins (Figure 19B). The key difference between *M. riyadhense* and *Mtb* can also be seen in the genomic locus located just downstream of the PDIM locus, which is containing the genes encoding proteins involved in the synthesis of phenolic glycolipids (PGL). Interestingly, the PGL locus is also known to be involved in *Mtb* virulence, but in a different way than the PDIMs. Indeed, it was shown that loss of function mutations in genes of the PGL locus decrease rather than prevent *Mtb* virulence and can cause a loss of hypervirulent phenotypes (Forrellad et al., 2013). This locus is in fact not present in *M. riyadhense*, whereas only certain genes are absent in the three other species under study (Figure 19A).

Despite the higher similarity observed between *M. decipiens* and *Mtb* enzymes involved in PDIM synthesis, as compared with the other species, experimental PDIM analysis did not show a similar profile between the two species. When the lipid extractions of the different species were subjected to thin-layer chromatography, using petroleum ether (40:60)/diethyl ether (9:1, vol/vol) as solvent, followed by revelation with 10% copper in 8% phosphoric acid and

heating, we observed that among the four species under study only *M. lacus* appears to have a similar profile as *Mtb* in PDIM migration. *M. kansasii* also shows similarities in the profile but produces higher amounts than the *Mtb* and BCG control strains (Figure 19C). These initial results suggest that the amounts of PDIM produced in *M. decipiens*, *M. riyadhense* and *M. shinjukuense* are below detection level of our experimental setup. These results also open new questions on the impact of PDIM on virulence of NTM species. While for *Mtb* strains a clear correlation was shown between absence of PDIM and attenuation (Domenech & Reed, 2009), this seems to be less clear for NTM species, as many of them do not produce PDIM and still retain certain virulence capacities, as we also show here for *M. riyadhense*. Further in-depth studies of the lipid profiles of this species are needed to get deeper insights into potential links of lipid and virulence profiles.

Analysis of the lipooligosaccharide (LOS) locus

As discussed in the introduction, morphology has repeatedly been described as having a potential impact on the virulence of mycobacteria. *M. abscessus*, for example, has both types of morphology (smooth and rough) which, depending on the variants, do not present the same virulence, and similar observations have been described for the SGM *Mycobacterium avium* (Torrelles et al., 2002). A study has also shown that *M. canettii*, the MTBC progenitor-like mycobacterium with smooth colony morphology, can display increased virulence in animal models for variants with a rough phenotype. This study also showed that smooth colony morphology in *M. canettii* was due to the production of lipooligosaccharides (LOS), which are synthetisized by enzymes encoded in the genomic LOS locus (Boritsch et al., 2016). These findings led to the hypothesis that, during speciation, *Mtb* might have lost selected genes in the LOS locus associated with the smooth morphotype and thereby acquired the rough phenotype that enhanced its virulence (Boritsch et al., 2016).

Interestingly, LOS are also produced by *M. kansasii,* which has a smooth colony morphology and also acquires a higher virulence when their production is interrupted (Belisle & Brennan, 1989). As mentioned above, the production of these lipids is dependent on the LOS locus, and more specifically on one or two polyketide synthases known as Pks5 and a Pks5-associated protein named Pap. The presence of two homologs of *pks5* and an associated *pap* gene is a

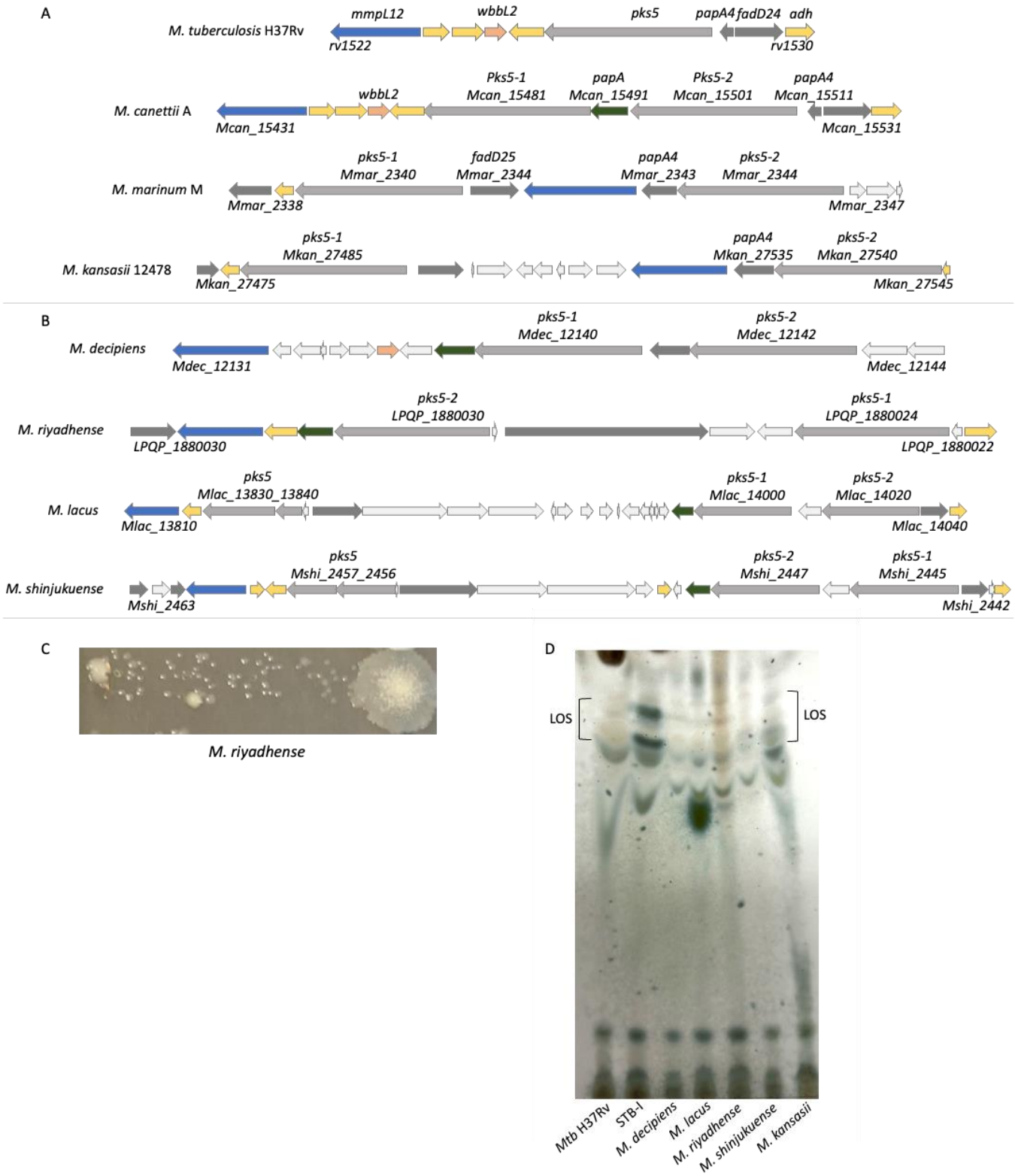

Figure 20: Analysis of LOS locus. Genomic organization of the LOS locus of *Mtb*, *M. canettii*, *M. marinum*, *M. kansasii* (A), *M. decipiens*, *M. lacus*, *M. riyadhense*, and *M. shinjukuense* (B) were represented using Artemis Comparison Tool and Mage software from the Genoscope. The different morphologies of *M. riyadhense* are represented in the picture (C). LOS profiles of the strains were represented on TLC using $CHCl_3/CH_3OH/HO_2$ (30:12:1, vol/vol/vol) and revealed by spraying 0.2% anthrone solution in concentrated H_2S0_4 before heating (D). Public sequence of *M. riyadhense* was used for this comparison as our PacBio derived sequence slightly differed in the *pks5*-2 gene length and the publicly available sequences seemed more appropriate for this analysis.

prerequisite for LOS production, as in *M. canettii*, *M. kansasii* and *M. marinum*, whereas a single *pks5* gene and no associated *pap* gene is present in *Mtb*, resulting in the inactivation of the LOS production machinery (Figure 20A).

The four species studied here have different morphologies: rough for *M. decipiens*, *M. riyadhense* and *M. shinjukuense*, and smooth for *M. lacus* (Figure 14). But the feature that caught our attention was the appearance of several morphotypes for *M. riyadhense* after infection experiments, particularly those from mouse models. Indeed, after infecting mice, *M. riyadhense* colonies showed three different morphotypes: rough colonies, opaque smooth colonies, and translucent smooth colonies (Figure 20C). Moreover, the smooth morphotype seemed to be the predominant one after infection, with some variation in proportions.

Following these observations, we studied the LOS locus of the strains to determine the number of *pks5* gene copies in relation to morphology.
By comparing the four strains (Figure 20B) with the groups represented by *M. canettii*/*Mtb* and *M. marinum*/*M. kansasii* (Figure 20A), quite different organization variants of the loci are observed. While the locus in *M. decipiens* with two full length *pks5* copies and an intervening *pap* gene resembles the locus in *M. canetti*, the organization of the *pks5* gene section is different in the other species. *M. riyadhense* also harbors two full length *pks5* genes and a *pap* gene as well some other genes inbetween them in the LOS locus, whereas *M. lacus* and *M. shinjukuense* do not have the same organization as the other species. Both loci show however a similar organization among each other, with certain *pks5* sequences appearing truncated and thus in larger numbers, and several genes having mostly no homology with genes from the LOS loci in the other species (Figure 20A-B).

To further investigate these organizational differences, we performed thin-layer chromatography to visualize the LOS. Lipids were migrated in $CHCl_3$/CH_3OH/H_20 (30:12:1, vol/vol/vol) solvent and revealed by spraying a 0.2% anthrone solution in concentrated sulfuric acid, followed by heating for 10 min at 110°C. Chromatography showed differences in LOS production between strains (Figure 20D). In order to have a more robust control, we used, in addition to *M. kansasii* shown to produce LOS, a strain of *M. canettii* (STB-I) that was described as a strong LOS-producer (Boritsch et al., 2016). By looking at the TLC

results, it seems that the *M. canettii* strain used definitely produces a large amount of LOS, whereas *M. kansasii* shows already less LOS (Figure 20D). As for the four species under study, we only could see very little, if any LOS on the TLCs, even for the species that show a genomic organization of their LOS loci that would predict production of these lipids. However, as the synthesis of LOS not only depends on enzymes encoded in the core region of the LOS locus, but also on glycosyltransferases and methyltransferases encoded by genes adjacent to the locus (Boritsch et al., 2016; Nataraj et al., 2015) it is difficult to make predictions and correlations between the genomic organization and the phenotypic evaluation of lipid content. In fact, we initially were hoping to find a clear-cut correlation between the genomic organization of the LOS biosynthesis loci, the amounts of LOS produced and the observed colony morphologies, but found that the situation involving different species with different genetic backgrounds was rich in nuances and much more complex than originally thought, a finding that might be further complicated by the presence of several different colony morphology types in the same culture, as seen for *M. riyadhense*.

DISCUSSION

The main aim of this thesis was to explore the genomes, the evolution and selected phenotypes of four NTM species that are thought to share common evolutionary features with *Mtb*, the etiological agent of human TB, and to investigate the possibility of using one or more of these NTM species as a model for the study of TB due to their easier handling.

Mtb is a complex organism to study, notably because it is a class 3 pathogen (BSL-3), which implies the need for special equipment for its handling. To facilitate this, scientific research uses study models to investigate the virulence mechanisms of the pathogen through them. For this purpose, the NTM *M. kansasii*, and *M. marinum*, which are class 2 organisms (BSL-2), are widely used and recognized as *Mtb* study models (Berg & Ramakrishnan, 2012; J. Wang et al., 2015). Indeed, both species share many genomic features with MTBC members. *M. kansasii* has been repeatedly designated as possibly representing the environmental ancestor of *Mtb*, which after several modifications of its genome became an obligate pathogen and primarily intracellular bacterium (Guan et al., 2020; J. Wang et al., 2015). *M. marinum* is also a closely related species to the MTBC, sharing key orthologous genes encoding virulence factors of the pathogen (Stinear et al., 2008). In addition, the development of the zebrafish model of infection has added additional knowledge and power to this mycobacterial infection model (Ramakrishnan, 2020).
However, certain steps in the evolution of *Mtb* are not shared by these two species, resulting in gaps in our understanding of the evolution of the pathogen and sometimes rendering comparisons more difficult (Sapriel & Brosch, 2019).

The *Mycobacterium* genus is further complemented by new species isolated over recent years. Among them, four species have been isolated from patients between the early 2000s and today and classified as new species due to their outstanding characteristics (*M. decipiens*, *M. lacus*, *M. riyadhense*, and *M. shinjukuense*) (Brown-Elliott et al., 2018; Saito et al., 2011; Turenne et al., 2002; van Ingen et al., 2009). These four species have been shown to be genomically closer to the MTBC than are *M. kansasii* and *M. marinum*, and to share some features of *Mtb* evolution that were previously considered unique to *Mtb* (Sapriel & Brosch, 2019).

The phylogenetic position of these species as the currently known closest mycobacterial species of the MTBC and the *M. canettii* outgroup prompted us to study them in more detail. To do this, we phenotypically characterized the four species, then studied their infection capacity in typical models for *Mtb* infection, and in parallel, to better understand their action and the characteristics they might share with *Mtb*, we compared selected genomic details with those of *Mtb* and the known comparator species *M. kansasii*.

In their study, G. Sapriel and R. Brosch described *M. decipiens* as the species sharing the most genomic traits with *Mtb*. However, our results from phenotypic characterization of the strains indicate that *M. decipiens* differs in its optimal growth temperature compared to *Mtb*. Indeed, it appears that this species has an optimal growth temperature between 32°C and 35°C, and not 37°C as other species compared in this study and as indicated on the supplier's data sheet or in the literature (Brown-Elliott et al., 2018; Simner et al., 2014). It could therefore be that *M. decipiens* shares some common growth characteristics with *M. marinum*, which has an optimal growth temperature of 30-32°C and is unable to grow at 37°C (Aubry et al., 2017; Hashish et al., 2018). Another important example of a pathogenic mycobacterium with lower temperature optimum is *Mycobacterium leprae*, which is known to preferentially infect peripheral body parts that show a lower overall temperature, such as the skin (Shepard, 1965). Nevertheless, *M. decipiens* subcultures seem to be able to adapt and grow at 37°C thereafter. It is also possible for the bacterium to multiply in host cells, but at a much lower rate than at 35°C.

Beyond the temperature differences, *Mtb*'s evolutionary characteristic of reduced genome size is not found in *M. decipiens*. In fact, during its long-term evolution, the genome size of *Mtb* was reduced to 4.4 Mb, compared with 6.4 Mb and 6.6 Mb for *M. kansasii* and *M. marinum,* respectively (Sapriel & Brosch, 2019). Of the four investigated species, *M. riyadhense* comes closest to the genome size of *M. kansasii* and *M. marinum* with 6.3 Mb, followed by *M. decipiens* (5.2 Mb) and *M. lacus* (5.1 Mb), while *M. shinjukuense* exhibits a 4.4 Mb genome size that is very similar to that of *Mtb*.

As another feature that differentiates the four NTM species under study and *M. marinum* and *M. kansasii* is the feature of pigmentation. Indeed *M. marinum* and *M. kansasii*, as primarily environmental organisms produce a yellow pigment, which protects them from UV radiation

and other environmental sources of damage. This feature of photochromogenicity, which they share with other predominantly environmental opportunistic pathogens, such as *M. avium*, is due to the presence of a *crtEIB* cluster in their genomes, responsible for carotenoid biosynthesis involved in photochromogenicity (Ramakrishnan et al., 1997). Genomic comparisons between *M. marinum*, *M. kansasii*, *Mtb*, and the four species, has shown that the *crtEIB* gene cluster is not present in the genomes of *M. decipiens, M. lacus*, *M. riyadhense, M. shinjukuense* and *Mtb*, explaining the absence of pigmentation in these latter strains, and suggesting a different habitat than *M. marinum* and *M. kansasii*.

M. decipiens, among others, has also shown differences in antibiotic resistance. Although slow growing NTM infections are generally treated with a regimen based on rifampicin, ethambutol, and a macrolide molecule, with the addition of amikacin or streptomycin, if necessary, treatment needs to be adapted according to the species and their resistances (Van Ingen et al., 2012). Pyrazinamide, the fourth first-line anti-TB, was not included in this study because, in addition to its infrequent use in the treatment of NTM, its dependence on acidic pH to become active makes it difficult to test in vitro (Mok et al., 2021; Zhang et al., 2013).
Of the four species, *M. decipiens* showed the most resistance (rifampicin, ethambutol, and isoniazid) to the four anti-TB drugs tested, while *M. shinjukuense* showed sensitivity for these four molecules.
Although we do not know the exact reason why *M. decipiens* shows this intermediate resistance to rifampicin, as analysis of RpoB has shown that the known *Mtb* mutations causing resistance are not found in the *M. decipiens* sequence (Palomino & Martin, 2014). One possibility for resistance of *M. decipiens* to rifampicin is the presence of an *arr* gene encoding a Rifampin ADP-ribosyl transferase in the genome of *M. decipiens* that shows 78.9% amino acid identity with the orthologous enzyme in *M. smegmatis*. Rifampicin ribosylation is an efficient mechanism to cause rifampicin resistance in the RGM species *M. smegmatis* (Quan et al., 1997) and *M. abscessus* (Rominski et al., 2017). Interestingly, *M. decipiens* was the only among the four tested species that encoded a rifampin ADP-ribosyl transferase in its genome, and *arr* orthologs are also absent from most other SGM, including *Mtb*. However, there seems to be another exception, as shown by the presence of *arr* genes in the genomes of the closely related group of *M. marinum*, *M. liflandii* and *M. ulcerans* species. It remains yet unclear if these encoded ADP-ribosyl transferases are biologically active, as *M. marinum* strains were

described as being sensitive to rifampicin (Aubry et al., 2000) and rifampicin is also part of the antibiotic treatment against Buruli ulcer, caused by *M. ulcerans* (O'Brien et al., 2012)**.** It is thus difficult to predict with confidence the mechanism with which *M. decipiens* resists to rifampicin, but the exceptional presence of an *arr* gene in this SGM makes *M. decipiens* an interesting model to study the function of rifampin ADP-ribosyl transferases in SGM.
M. lacus and *M. riyadhense* share with *M. decipiens* resistance to isoniazid and ethambutol. However, the results of *in vitro* tests to isoniazid and ethambutol should be taken with caution, as it is known that in NTM, the reaction of bacteria to molecules can differ for the same strain (Brown-Elliott & Woods, 2019). In addition, some NTM are known to be less sensitive to certain anti-TB drugs than *Mtb*, even though the mutations causing isoniazid resistance in *Mtb* (Pym, Saint-Joanis, et al., 2002) are not found in other species, notably *M. marinum* or *M. avium*, which are both intrinsically resistant to isoniazid (Reingewertz et al., 2020). Ethambutol resistance in *Mtb* is mainly due to a mutation in the EmbB protein sequence (Brossier et al., 2015; Bwalya et al., 2022). However, the most frequently implicated mutations are not found in *M. decipiens* and *M. riyadhense*. *M. lacus* shows a mutation in the *embB* protein sequence (Gly406Pro) which could be the source of its resistance, although in *Mtb* the most frequent mutation is Gly406Ala. In addition, another dozen mutations in the ethambutol resistance determining region have been found in *M. lacus*, whose putative impact on resistance is not known (Boni et al., 2023; Brossier et al., 2015).

To determine whether an NTM can be a good study model for TB, it is important to study its intracellular multiplication capacity. To this end, we compared the infection capacity of the four strains with that of *Mtb* and the known comparator *M. kansasii* in different models (Johnson & Abramovitch, 2015; Soldevilla et al., 2022). For these experiments we used the infection doses corresponding to those commonly used for *Mtb*, which for NTM can lead in some cases to premature bacterial elimination during infection, due to lower virulence, especially in *in vivo* models (Mussi et al., 2021; J. Wang et al., 2015). However, as our primary aim was to compare the virulence of the species under study with that of Mtb, we targeted doses used for *Mtb* infection also for NTM.

For this project, we therefore compared the intracellular multiplication capacity of the four species with that of *M. kansasii* and *Mtb* in THP-1 macrophages. To get a broader picture, we

also added the attenuated *M. bovis* BCG Pasteur strain as an additional comparator and control.

As outlined in the results section, we found that *M. lacus* and *M. shinjukuense* could survive inside THP-1 macrophages over 7 days, but did not increase their number at 37°C, while there was a slight increase observed for *M. lacus* at 35°C. In contrast, *M. decipiens* and *M. riyadhense* multiplied at both temperatures, but the increase was smaller at 37°C than at 35°C for *M. decipiens*, which likely is associated with its optimal growth temperature that was found to be below 37°C for this species. In comparison with *Mtb*, which at both temperatures showed a 1.5-log increase of the bacterial load over 7 days, the intracellular growth of *M. decipiens* and *M. riyadhense* was found to be inferior, which confirms the high virulence of *Mtb.*

From these experiments we can thus rank *M. lacus* and *M. shinjukuense* as the least virulent species, followed by *M. decipiens* and *M. riyadhense.* As regards the suitability to serve as a model for host-pathogenicity studies, *M. decipiens* and *M. riyadhense* thus seem to represent the more appropriate potential models than the other two species.

As regards the experiments for virulence evaluation in mice we have to emphasize that the results obtained represent data from preliminary experiments as only one infection experiment was undertaken for each mouse model. In addition, we had also to face some variation in the infectious doses used, as different colony morphologies impacted the prediction of infectious doses from OD measurements. In the experiments, female C57BL/6J and male C3HeB/FeJ mice were subjected to aerosolized suspensions of *M. decipiens*, *M. lacus*, *M. riyadhense*, *M. shinjukuense*, *M. kansasii*, *M. bovis* BCG Pasteur and *Mtb* H37Rv. For these experiments, solutions with a target concentration at 2.5 x 10^6 CFUs/mL were prepared from which 5ml were aerosolized in the infection chambers inside the BSL-3 animal houses, which in the case of infection with *Mtb* commonly generates a low-dose infection of approximately 10 to 100 CFUs per lungs in mice.

As outlined in the results section, we found that *M. decipiens*, *M. shinjukuense*, *M. kansasii* and the BCG Pasteur strain were not detected at weeks 4 and 14 post-infection in organs of C3HeB/FeJ and C57BL/6J mice (Figure 16C-D, 16H-I), although bacteria were detected on day 1 in the lungs (Figure 16A-B, F). While these results clearly demonstrated that these species were less virulent than *Mtb*, it is difficult to conclude from our results that the bacteria were

completely unable to replicate in mice, given the relatively low dose of infection distributed to mice compared to the dose generally required for NTM (J. Wang et al., 2015). Conversely, our results showed that even at lower doses, *M. riyadhense* was able to infect mice and cause disease, whereas at higher infection doses that are often used for NTM infection, *M. riyadhense* caused too severe infection for the mice within a few weeks (4/6 weeks), requiring us to cull the mice before the end of the foreseen experiment duration.

In conclusion, we found that among the various NTM species tested, *M. riyadhense* showed the strongest virulence in mice, while the infection with the other three species and *M. kansasii* were efficiently controlled in the used mouse infection models. In the case of *M. lacus*, even a very high infectious dose did not result in a longer lasting infection.

In terms of a suitable model for host-pathogen interaction, as for the above-described THP-1 model, *M. riyadhense* might represent the most interesting model, while *M. decipiens* seems to be impacted by the body temperature of mice which is beyond 35°C, its optimal growth temperature.

To complete our virulence studies and search for putative biological explanations for the results obtained in THP-1 cells and mice, we investigated selected virulence factors that are reported to play an important role for *Mtb* pathogenicity in the four species. At first, we concentrated on one very well-known virulence effect of mycobacterial pathogens, which is linked to the synthesis and secretion of the ESAT-6 protein by the ESX-1 type VII secretion (T7S) system (Brodin et al., 2004) that has been described to induce phagosomal rupture and necrosis in selected immune cells (Majlessi & Brosch, 2015; Simeone et al., 2012, 2021). Comparison of genomic organization of the ESX-1 loci in the four species under study showed that *M. decipiens* shares a higher similarity in the ESX-1 proteins with *Mtb* than the other species. Indeed, most *M. decipiens* ESX-1 proteins show up to 90% amino acid identity with the orthologous proteins in *Mtb*, which is about 10% higher than the commonly observed ~ 80% of maximal amino acid identity for ESX-1 proteins of the other species, including *M. kansasii.* This higher similarity between *M. decipiens* and *Mtb* proteins was also true for proteins of three other ESX systems, namely ESX-3, ESX-4 and ESX-5, which correlates with the overall very close genomic relatedness of *M. decipiens* and *Mtb*, which can also be observed in other genomic regions. One exception to the rule was the ESX-2 system. As shown in figure 17 of the results section, the ESX-2 locus of *M. decipiens* is divided into two regions that are

localized in different sections of the genome. In addition, the similarity of ESX-2 proteins of *M. decipiens* with those of *Mtb* is rather low and range between 42-76% amino-acid identity. The most likely reason for this situation is that the ESX-2 system of *M. decipiens* has a different phylogenetic origin than the ESX-2 system of *Mtb* and seems to have been acquired by *M. decipiens* during its evolution via HGT from a more distantly related mycobacterial species. It is noteworthy that *M. riyadhense* harbors an ESX-2 system that closely resembles the genomic organization of ESX-2 in *M. decipiens* and shows low protein similarity of ESX-2 proteins with *Mtb* orthologs. ESX-2 proteins of *M. decipiens* and *M. riyadhense* show a high percentage of amino acid identity among the respective orthologs, ranging between 79.7% for EccE2 to 91.7% for EccA2, and ESX-2 systems with similar genomic organization are also present in certain other slow growing NTM species such as *Mycobacterium szulgai* or *Mycobacterium simiae*. It is also noteworthy that the genome of *M. marinum*, for example, does not harbor any ESX-2 system at all. Thus, in SGM, there are at least three configurations possible, one with no ESX-2 system, one with an *M. decipiens*- and *M. riyadhense*-like ESX-2 system and one with an *Mtb*-like ESX-2 system. It seems that during evolution of slow growing mycobacterial pathogens, different types of ESX-2 systems have been recovered by certain mycobacterial species that are otherwise phylogenetically very closely related, as shown by the example of diverging ESX-2 systems in *M. decipiens* and *Mtb*. It seems also likely that such a situation was created by HGT events, and not by continued vertical evolution. At present, it remains unclear which biological functions the different ESX-2 systems might fulfill as reports on ESX-2 proteins are scare. As one exception, there was a recent report where ESX-2 proteins of *Mtb* were described as being involved together with ESX-4 proteins in the permeabilization of the phagosomal membrane and toxin secretion (Pajuelo et al., 2021). However, further studies will be required to confirm these observations and evaluate which types of ESX-2 systems might fulfill such functions.

Focusing again on ESX-1 systems, our analysis has shown that among the four species studied, *M. riyadhense* is the species characterized by ESX-1 proteins that show the lowest percentages of amino acid identities with ESX-1 proteins of *Mtb*. In addition, in immunoblotting experiments, secretion of ESAT-6 was only demonstrated for *M. decipiens* and not for *M. riyadhense* or the other two remaining species. At present, we do not know why *M. riyadhense* does not secrete ESAT-6 in *in vitro* grown cultures. One possible explanation is

that *M. riyadhense* lacks the presence in its genome of an *espACD* operon, which is one of the components essential for *Mtb* to secrete this protein (Ates & Brosch, 2017). In addition, it is not known whether ESAT-6 and its protein partner CFP-10 are well expressed under *in vitro* growth conditions in this species. In any case, we found that *M. riyadhense* showed the highest virulence of the four tested NTM species in THP-1 and mouse infection models and at the same time the amounts of ESX-1 proteins in Western blots were low. From these observations it seems that the relatively high virulence of *M. riyadhense* is independent of the weakly expressed ESX-1 related functions observed *in vitro* in this species. While for *Mtb* the functionality of the ESX-1 locus and appropriate ESAT-6/CFP-10 secretion is a requirement for full virulence, in other mycobacterial species the impact of ESX-1 functions on virulence may be less crucial. There are numerous examples in the literature where mycobacterial species that are naturally devoid of ESX-1 systems, such as the animal pathogens *Mycobacterium mungi* or *Mycobacterium microti*, the members of the *M. avium* complex, or strains of the emerging pathogen *M. abscessus* may still retain a relatively high virulence potential (Alexander et al., 2018; Johansen et al., 2020; Orgeur et al., 2021).

Looking at the ESAT-6 secretion profiles of the remaining species we observed that *M. lacus* did not secrete ESAT-6 but was able to secrete CFP-10. It should be emphasized that similar to *M. riyadhense* and *M. shinjukuense*, *M. lacus* is lacking an *espACD* cluster in its genome. Secretion of the CFP-10 protein without its protein partner ESAT-6 has recently been described in the *Mtb*-based vaccine strain MTBVAC, which is deleted for the two-component regulator PhoP that also regulates the *espACD* cluster (Aguilo et al., 2017), showing that for certain genetic conditions the ESAT-6/CFP-10 complex may not always be secreted as a 1:1 complex (De Jonge et al., 2007; Renshaw et al., 2002). Further studies are needed to determine whether the other components required for ESAT-6/CFP-10 secretion are functional in *M. lacus*, and whether the addition of the functional *espACD* cluster would be sufficient for the bacterium to secrete the ESAT-6/CFP-10 complex, and thus improve intracellular multiplication capacity. While *M. decipiens* appears to be capable of secreting ESAT-6, and therefore to have all the systems necessary for its secretion functional (*phoPR*, *mprAB*, *espR*, *espACD*), the protein sequence of ESAT-6 does not share 100% identity with the one of *Mtb*, which may have an impact on its action once secreted. Further studies are therefore needed to determine whether the protein secreted by *M. decipiens* enables the

bacterium to relocalize in the cytosol during infection. These studies would also be of interest for *M. riyadhense*, to find out whether the bacterium is able to cause infection in the same way as *Mtb*.

To further investigate selected virulence determinants in the four species, we focused on the production of certain lipids, including phthiocerol dimycocerosate (PDIM) which, in addition to playing a role in bacterial cell wall strength, have also been shown to be important during infection, working in synergy with ESAT-6 to permeabilize the phagosomal membrane (Augenstreich et al., 2017; Passemar et al., 2014). Downstream of the PDIM locus, the PGL locus harbors the genes encoding the enzymes that synthesize phenolic glycolipids (PGL), whose role during infection has also been shown by their involvement in defense mechanisms linked to oxidative and nitrosative stress or cell permeability (Ramos et al., 2020).

Our study of these two loci showed that the PDIM locus was relatively conserved within the four species, but with low percentages of amino acid identity for some of them. In addition, chromatography results show that the migration profile of these lipids is different between the four species, *Mtb* and *M. kansasii*. Genomic comparisons of the PGL locus showed more differences between the strains and *Mtb*. Two genes were found to be absent in *M. lacus*, and an additional gene is also deleted from the sequence of *M. decipiens* and *M. shinjukuense*. However, the two genes absent from *M. lacus* are also absent from the genome of *M. kansasii*, which is capable of producing PGLs (Elsaidi & Lowary, 2015). Further studies are therefore needed to determine whether *M. lacus* is capable of producing PGLs like *M. kansasii*, and whether the third gene deleted in the genomes of *M. decipiens* and *M. shinjukuense* is sufficient to prevent PGL production. On the other hand, it is clear that *M. riyadhense* does not produce PGLs, as no gene from the locus is found in its genome. However, the absence of PGLs in *Mtb* has been shown to attenuate infection as it prevents the bacterium from recruiting monocytes in sufficient numbers during the infectious cycle but does not prevent it to cause disease (Cambier et al., 2017). Furthermore, a change in the PDIM locus in *Mtb* has a more deleterious effect on its ability to infect, especially as a defect in PDIM production linked to one or more mutations in the PDIM locus can lead to a defect in PGL production by altering the expression of the PGL locus (Constant et al., 2002; Ramos et al., 2020).

Clearly, the absence of PGLs and the low percentages of similarity compared with *Mtb* do not prevent *M. riyadhense* from being the most virulent NTM species in our study. It is therefore possible to hypothesize that, during its evolution, the PDIMs and PGLs loci were modified to be more adapted to intracellular life and to increase the capacity of the pathogen to infect host, enabling it, among other things, to facilitate its control over the host immune system.

Finally, we also noted differences in the locus responsible for lipooligosaccharide (LOS) lipid biogenesis. This locus is linked to different colony morphologies in *M. canettii* versus *Mtb*. During speciation, it seems likely that the *Mtb* genome underwent modifications including a *pks5* gene recombination, resulting in suppression of LOS production by the bacterium and a rough morphotype, in contrast to the *M. canettii* species, which has a smooth phenotype with two functional copies of the *pks5* gene and its associated *pap* gene (Boritsch et al., 2016). The composition of the locus of *M. marinum* and *M. kansasii* is also different from that of *M. canettii*, but still two copies of *pks5* are found in the locus that seem to correlate positively with the smooth morphotype observed for these species. According to the colony morphologies observed during strain characterization, we expected to find an organization similar to *Mtb* for *M. decipiens* and *M. shinjukuense*, given their rough phenotype, and vice versa for *M. lacus*, whereas the different morphologies observed after infection raised questions about the *M. riyadhense* locus. As the results of the locus comparison analysis and the analysis of LOS production by the species were inconclusive in relation to the question raised, it is difficult for the time being to conclude which lipids are responsible for the morphology of these four strains, given the wide variability of genes and gene products involved in mycobacterial morphology. Indeed, besides the enzymes synthesizing the lipid core structures, glycosyltransferases and methyltransferases encoded by genes adjacent to the LOS locus (Boritsch et al., 2016; Nataraj et al., 2015) are also necessary to finalize the process.

Bringing together the various results collected during this thesis project, we can conclude that *M. decipiens*, *M. lacus*, *M. riyadhense* and *M. shinjukuense* are highly interesting mycobacterial species that show many genomic and phenotypic traits shared with the key human pathogen *Mtb*, but also show many differences relative to *Mtb*. From analyses of different genomic loci, we can conclude that *M. decipiens* is clearly the NTM species that

shows the highest overall protein similarities with *Mtb*, compared to all other species currently known, including *M. marinum* and *M. kansasii*. However, despite the higher percentages of amino acid identity in proteins between *Mtb* and *M. decipiens* compared with the other three species, *M. riyadhense* was shown to be the most virulent in our study models. It is possible that this difference is due to the growth temperature of *M. decipiens*, which showed a strong decrease in intracellular multiplication capacity at temperatures above 35°C, including at 37°C, the body temperature of humans and many other mammalian hosts, and the optimal growth temperature of *Mtb.* Although further studies are needed to validate our hypotheses, our results suggest that *M. decipiens*, being genomically most closely related to *Mtb*, could be used as powerful *in vitro* study model for investigating important mycobacterial features, such as the mechanisms underlying the co-secretion of ESAT-6/CFP-10 and EspA/EspC, or the biological functions of the ESX-2 system, while *M. riyadhense* could be a useful model for virulence studies in murine infection models, as the bacterium presented remarkable virulence and pathogenicity in both tested mouse models of infection despite being categorized as biosafety class 1 organism (BSL-1). Finally, *M. lacus* and *M. shinjukuense* were found to be completely attenuated in our virulence experiments but could also be used as *in vitro* models for studying mycobacterial genome reduction, as found in *M. shinjukuense*, or as model to investigate the ability to uniquely secrete CFP-10 and not ESAT-6, as seen for *M. lacus*. Genetic manipulation of *M. lacus*, such as the integration of an *espACD* operon from *Mtb* or *M. decipiens* will lead to new insights into the evolutionary framework by which low virulent opportunistic pathogens may emerge towards specialized human pathogens.

BIBLIOGRAPHY

Abdallah, A. M., Gey van Pittius, N. C., DiGiuseppe Champion, P. A., Cox, J., Luirink, J., Vandenbroucke-Grauls, C. M. J. E., Appelmelk, B. J., & Bitter, W. (2007). Type VII secretion — mycobacteria show the way. *Nature Reviews Microbiology*, *5*(11), 883–891. https://doi.org/10.1038/nrmicro1773

Acharya, B., Acharya, A., Gautam, S., Ghimire, S. P., Mishra, G., Parajuli, N., & Sapkota, B. (2020). Advances in diagnosis of Tuberculosis: an update into molecular diagnosis of Mycobacterium tuberculosis. *Molecular Biology Reports*, *47*(5), 4065–4075. https://doi.org/10.1007/s11033-020-05413-7

Aguado, J. M., Silva, J. T., Samanta, P., & Singh, N. (2016). Tuberculosis and Transplantation. *Microbiology Spectrum*, *4*(6). https://doi.org/10.1128/microbiolspec.TNMI7-0005-2016

Aguilo, N., Gonzalo-Asensio, J., Alvarez-Arguedas, S., Marinova, D., Gomez, A. B., Uranga, S., Spallek, R., Singh, M., Audran, R., Spertini, F., & Martin, C. (2017). Reactogenicity to major tuberculosis antigens absent in BCG is linked to improved protection against Mycobacterium tuberculosis. *Nature Communications*, *8*, 16085. https://doi.org/10.1038/ncomms16085

Ahmed, A., Rakshit, S., Adiga, V., Dias, M., Dwarkanath, P., D'Souza, G., & Vyakarnam, A. (2021). A century of BCG: Impact on tuberculosis control and beyond. *Immunological Reviews*, *301*(1), 98–121. https://doi.org/10.1111/imr.12968

Akram, S. M., & Rawla, P. (2023). *Mycobacterium kansasii Infection*. StatPearls. https://www.ncbi.nlm.nih.gov/books/NBK430906/

Alcaraz, M., Roquet-Banères, F., Leon-Icaza, S. A., Abendroth, J., Boudehen, Y. M., Cougoule, C., Edwards, T. E., & Kremer, L. (2022). Efficacy and Mode of Action of a Direct Inhibitor of Mycobacterium abscessus InhA. *ACS Infectious Diseases*, *8*(10), 2171–2186. https://doi.org/10.1021/acsinfecdis.2c00314

Alenazi, T. H., Alanazi, B. S., Alsaedy, A., Khair, A., Solomon, R., & Al Johani, S. M. (2019). Mycobacterium riyadhense as the opportunistic infection that lead to HIV diagnosis: A report of 2 cases and literature review. *Journal of Infection and Public Health*, *12*(2), 285–288. https://doi.org/10.1016/j.jiph.2018.05.006

Alexander, K. A., Laver, P. N., Williams, M. C., Sanderson, C. E., Kanipe, C., & Palmer, M. V. (2018). Pathology of the Emerging Mycobacterium tuberculosis Complex Pathogen, Mycobacterium mungi, in the Banded Mongoose (Mungos mungo). *Veterinary Pathology*, *55*(2), 303–309. https://doi.org/10.1177/0300985817741730

Alibaud, L., Pawelczyk, J., Gannoun-Zaki, L., Singh, V. K., Rombouts, Y., Drancourt, M., Dziadek, J., Guérardel, Y., & Kremer, L. (2014). Increased phagocytosis of Mycobacterium marinum mutants defective in lipooligosaccharide production a structure-activity relationship study. *Journal of Biological Chemistry*, *289*(1), 215–228. https://doi.org/10.1074/jbc.M113.525550

Al-kayali, R. S., Kashkash, M. F., Alhussein Alhajji, A. H., & Khouri, A. (2023). Activation of tuberculosis in recovered COVID-19 patients: a case report. *Annals of Medicine & Surgery*, *85*(2), 280–283. https://doi.org/10.1097/MS9.0000000000000188

Allen, M., Bailey, C., Cahatol, I., Dodge, L., Yim, J., Kassissa, C., Luong, J., Kasko, S., Pandya, S., & Venketaraman, V. (2015). Mechanisms of Control of Mycobacterium tuberculosis by NK Cells: Role of Glutathione. *Frontiers in Immunology*, *6*. https://doi.org/10.3389/fimmu.2015.00508

Altschul, S. F., Gish, W., Miller, W., Myers, E. W., & Lipman, D. J. (1990). Basic local alignment search tool. *Journal of Molecular Biology*, *215*(3), 403–410. https://doi.org/10.1016/S0022-2836(05)80360-2

Andres, S., Merker, M., Heyckendorf, J., Kalsdorf, B., Rumetshofer, R., Indra, A., Hofmann-Thiel, S., Hoffmann, H., Lange, C., Niemann, S., & Maurer, F. P. (2020). Bedaquiline-resistant tuberculosis: Dark clouds on the horizon. *American Journal of Respiratory and Critical Care Medicine*, *201*(2112), 1564–1568. https://doi.org/10.1056/nejmoa2004500

Andreu, N., Phelan, J., De Sessions, P. F., Cliff, J. M., Clark, T. G., & Hibberd, M. L. (2017). Primary macrophages and J774 cells respond differently to infection with Mycobacterium tuberculosis. *Scientific Reports*, *7*. https://doi.org/10.1038/srep42225

Anes, E., Pires, D., Mandal, M., & Azevedo-Pereira, J. M. (2023). ESAT-6 a Major Virulence Factor of Mycobacterium tuberculosis. *Biomolecules*, *13*(6), 968. https://doi.org/10.3390/biom13060968

Arcos, J., Sasindran, S. J., Fujiwara, N., Turner, J., Schlesinger, L. S., & Torrelles, J. B. (2011). Human Lung Hydrolases Delineate *Mycobacterium tuberculosis* –Macrophage Interactions and the Capacity To Control Infection. *The Journal of Immunology*, *187*(1), 372–381. https://doi.org/10.4049/jimmunol.1100823

Armstrong, D. T., & Parrish, N. (2021). Current Updates on Mycobacterial Taxonomy, 2018 to 2019. *Journal of Clinical Microbiology*, *59*(7), e0152820. https://doi.org/10.1128/JCM.01528-20

Aronson, J. D. (1926). Spontaneous Tuberculosis in Salt Water Fish. *The Journal of Infectious Diseases*, *39*, 315–320.

Astier, H., Briquet, A., & Garnotel, E. (2017). Mycobacterium canettii, une mycobactérie du complexe tuberculosis Dossier scientifique. *Revue Francophone Des Laboratoires*, *496*, 47–59.

Ates, L. S. (2020). New insights into the mycobacterial PE and PPE proteins provide a framework for future research. *Molecular Microbiology*, *113*(1), 4–21. https://doi.org/10.1111/mmi.14409

Ates, L. S., & Brosch, R. (2017). Discovery of the type VII ESX-1 secretion needle? *Molecular Microbiology*, *103*(1), 7–12. https://doi.org/10.1111/mmi.13579

Ates, L. S., Ummels, R., Commandeur, S., van der Weerd, R., Sparrius, M., Weerdenburg, E., Alber, M., Kalscheuer, R., Piersma, S. R., Abdallah, A. M., Abd El Ghany, M., Abdel-Haleem, A. M., Pain, A., Jiménez, C. R., Bitter, W., & Houben, E. N. G. (2015). Essential Role of the ESX-5 Secretion System in Outer Membrane Permeability of Pathogenic Mycobacteria. *PLoS Genetics*, *11*(5). https://doi.org/10.1371/journal.pgen.1005190

Aubry, A., Jarlier, V., Escolano, S., Truffot-Pernot, C., & Cambau, E. (2000). Antibiotic susceptibility pattern of Mycobacterium marinum. *Antimicrobial Agents and Chemotherapy*, *44*(11), 3133–3136. https://doi.org/10.1128/AAC.44.11.3133-3136.2000

Aubry, A., Mougari, F., Reibel, F., & Cambau, E. (2017). Mycobacterium marinum. *Microbiology Spectrum*, *5*(2). https://doi.org/10.1128/microbiolspec.tnmi7-0038-2016

Augenstreich, J., Arbues, A., Simeone, R., Haanappel, E., Wegener, A., Fadel Sayes, |, Le Chevalier, F., Chalut, | Christian, Malaga, W., Guilhot, C., Brosch, | Roland, & Astarie-Dequeker, C. (2017). ESX-1 and phthiocerol dimycocerosates of Mycobacterium tuberculosis act in concert to cause phagosomal rupture and host cell apoptosis. *Cellular Microbiology*, *19*(7). https://doi.org/10.1111/cmi.12726

Augenstreich, J., Haanappel, E., Sayes, F., Simeone, R., Guillet, V., Mazeres, S., Chalut, C., Mourey, L., Brosch, R., Guilhot, C., & Astarie-Dequeker, C. (2020). Phthiocerol Dimycocerosates From Mycobacterium tuberculosis Increase the Membrane Activity of Bacterial Effectors and Host Receptors. *Frontiers in Cellular and Infection Microbiology*, *10*. https://doi.org/10.3389/fcimb.2020.00420

Ba, F., & Rieder, H. L. (1999). A comparison of fluorescence microscopy with the Ziehl-Neelsen technique in the examination of sputum for acid-fast bacilli. *The International Journal of Tuberculosis and Lung Disease : The Official Journal of the International Union against Tuberculosis and Lung Disease*, *3*(12), 1101–1105.

Bachmann, N. L., Salamzade, R., Manson, A. L., Whittington, R., Sintchenko, V., Earl, A. M., & Marais, B. J. (2020). Key Transitions in the Evolution of Rapid and Slow Growing Mycobacteria Identified by Comparative Genomics. *Frontiers in Microbiology*, *10*. https://doi.org/10.3389/fmicb.2019.03019

Bansal, R., Sharma, D., & Singh, R. (2018). Tuberculosis and its Treatment: An Overview. *Mini-Reviews in Medicinal Chemistry*, *18*(1). https://doi.org/10.2174/1389557516666160823160010

Banta, J. E., Ani, C., Bvute, K. M., Lloren, J. I. C., & Darnell, T. A. (2020). Pulmonary vs. extra-pulmonary tuberculosis hospitalizations in the US [1998–2014]. *Journal of Infection and Public Health*, *13*(1), 131–139. https://doi.org/10.1016/j.jiph.2019.07.001

Bastos Nogueira, L., Nogueira Garcia, C., Santos Corrêa da Costa, M., Brauner de Moraes, M., Shu Kurizky, P., & Martins Gomes, C. (2021). Non-tuberculous cutaneous mycobacterioses. *Anais Brasileiros de Dermatologia*, *96*(5), 527–538. https://doi.org/10.1016/j.abd.2021.04.005

Bauernfeind, F. G., Horvath, G., Stutz, A., Alnemri, E. S., MacDonald, K., Speert, D., Fernandes-Alnemri, T., Wu, J., Monks, B. G., Fitzgerald, K. A., Hornung, V., & Latz, E. (2009). Cutting Edge: NF-κB Activating Pattern Recognition and Cytokine Receptors License NLRP3 Inflammasome Activation by Regulating NLRP3 Expression. *The Journal of Immunology*, *183*(2), 787–791. https://doi.org/10.4049/jimmunol.0901363

Beckwith, K. S., Beckwith, M. S., Ullmann, S., Sætra, R. S., Kim, H., Marstad, A., Åsberg, S. E., Strand, T. A., Haug, M., Niederweis, M., Stenmark, H. A., & Flo, T. H. (2020). Plasma membrane damage causes NLRP3 activation and pyroptosis during Mycobacterium tuberculosis infection. *Nature Communications*, *11*(1), 2270. https://doi.org/10.1038/s41467-020-16143-6

Behar, S. M., Divangahi, M., & Remold, H. G. (2010). Evasion of innate immunity by Mycobacterium tuberculosis: is death an exit strategy? *Nature Reviews Microbiology*, *8*(9), 668–674. https://doi.org/10.1038/nrmicro2387

Behar, S. M., Martin, C. J., Booty, M. G., Nishimura, T., Zhao, X., Gan, H.-X., Divangahi, M., & Remold, H. G. (2011). Apoptosis is an innate defense function of macrophages against Mycobacterium tuberculosis. *Mucosal Immunology*, *4*(3), 279–287. https://doi.org/10.1038/mi.2011.3

Behra, P. R. K., Pettersson, B. M. F., Ramesh, M., Das, S., Dasgupta, S., & Kirsebom, L. A. (2022). Comparative genome analysis of mycobacteria focusing on tRNA and non-coding RNA. *BMC Genomics*, *23*(1). https://doi.org/10.1186/s12864-022-08927-5

Belanger, A. E., Besra, G. S., Ford, M. E., Mikusová, K., Belisle, J. T., Brennan, P. J., & Inamine, J. M. (1996). The embAB genes of Mycobacterium avium encode an arabinosyl transferase involved in cell wall arabinan biosynthesis that is the target for the antimycobacterial drug ethambutol. *Proceedings of the National Academy of Sciences*, *93*(21), 11919–11924. https://doi.org/10.1073/pnas.93.21.11919

Belisle, J. T., & Brennan, P. J. (1989). Chemical Basis of Rough and Smooth Variation in Mycobacteria. *Journal of Bacteriology*, *171*(6), 3465–3470.

Bell, L. C. K., & Noursadeghi, M. (2018). Pathogenesis of HIV-1 and Mycobacterium tuberculosis co-infection. *Nature Reviews Microbiology*, *16*(2), 80–90. https://doi.org/10.1038/nrmicro.2017.128

Berg, R. D., Levitte, S., O'Sullivan, M. P., O'Leary, S. M., Cambier, C. J., Cameron, J., Takaki, K. K., Moens, C. B., Tobin, D. M., Keane, J., & Ramakrishnan, L. (2016). Lysosomal Disorders Drive Susceptibility to Tuberculosis by Compromising Macrophage Migration. *Cell*, *165*(1), 139–152. https://doi.org/10.1016/j.cell.2016.02.034

Berg, R. D., & Ramakrishnan, L. (2012). Insights into tuberculosis from the zebrafish model. *Trends in Molecular Medicine*, *18*(12), 689–690. https://doi.org/10.1016/j.molmed.2012.10.002

Berthet, F.-X., Birk Rasmussen, P., Rosenkrands, I., Andersen, P., & Gicquel, B. (1998). A Mycobacterium tuberculosis operon encoding ESAT=6 and a novel low-molecular-mass culture filtrate protein (CFP-10). In *Microbiology* (Vol. 144).

Bespiatykh, D., Bespyatykh, J., Mokrousov, I., & Shitikov, E. (2021). A Comprehensive Map of Mycobacterium tuberculosis Complex Regions of Difference. *MSphere*, *6*(4). https://doi.org/10.1128/msphere.00535-21

Bitter, W., Houben, E. N. G., Bottai, D., Brodin, P., Brown, E. J., Cox, J. S., Derbyshire, K., Fortune, S. M., Gao, L. Y., Liu, J., Van Pittius, N. C. G., Pym, A. S., Rubin, E. J., Sherman, D. R., Cole, S. T., & Brosch, R. (2009). Systematic genetic nomenclature for type VII secretion systems. *PLoS Pathogens*, *5*(10). https://doi.org/10.1371/journal.ppat.1000507

Blasco, B., Chen, J. M., Hartkoorn, R., Sala, C., Uplekar, S., Rougemont, J., Pojer, F., & Cole, S. T. (2012). Virulence regulator EspR of Mycobacterium tuberculosis is a nucleoid-associated protein. *PLoS Pathogens*, *8*(3), e1002621. https://doi.org/10.1371/journal.ppat.1002621

Block, A. M., Namugenyi, S. B., Palani, N. P., Brokaw, A. M., Zhang, L., Beckman, K. B., & Tischler, A. D. (2023). Mycobacterium tuberculosis Requires the Outer Membrane Lipid Phthiocerol Dimycocerosate for Starvation-Induced Antibiotic Tolerance. *MSystems*, *8*(1). https://doi.org/10.1128/msystems.00699-22

Blouin, Y., Cazajous, G., Dehan, C., Soler, C., Vong, R., Hassan, M. O., Hauck, Y., Boulais, C., Andriamanantena, D., Martinaud, C., Martin, É., Pourcel, C., & Vergnaud, G. (2014). Progenitor " *Mycobacterium canettii* " Clone Responsible for Lymph Node Tuberculosis Epidemic, Djibouti. *Emerging Infectious Diseases*, *20*(1), 21–28. https://doi.org/10.3201/eid2001.130652

Blouin, Y., Hauck, Y., Soler, C., Fabre, M., Vong, R., Dehan, C., Cazajous, G., Massoure, P.-L., Kraemer, P., Jenkins, A., Garnotel, E., Pourcel, C., & Vergnaud, G. (2012). Significance of the Identification in the Horn of Africa of an Exceptionally Deep Branching Mycobacterium tuberculosis Clade. *PLoS ONE*, *7*(12), e52841. https://doi.org/10.1371/journal.pone.0052841

Boni, F. G., Hamdi, I., Moukendza Koundi, L., Dai, Y., Shrestra, K., Abokadoum, M. A., Ekomi Moure, U. A., Suleiman, I. M., & Xie, J. (2023). The Gene and Regulatory Network Involved in Ethambutol Resistance in Mycobacterium tuberculosis. *Microbial Drug Resistance*, *29*(5), 175–189. https://doi.org/10.1089/mdr.2021.0239

Boritsch, E. C., Frigui, W., Cascioferro, A., Malaga, W., Etienne, G., Laval, F., Pawlik, A., Le Chevalier, F., Orgeur, M., Ma, L., Bouchier, C., Stinear, T. P., Supply, P., Majlessi, L., Daffé, M., Guilhot, C., & Brosch, R. (2016). Pks5-recombination-mediated surface remodelling in Mycobacterium tuberculosis emergence. *Nature Microbiology*, *1*(2). https://doi.org/10.1038/nmicrobiol.2015.19

Boritsch, E. C., Supply, P., Honoré, N., Seeman, T., Stinear, T. P., & Brosch, R. (2014). A glimpse into the past and predictions for the future: The molecular evolution of the tuberculosis agent. *Molecular Microbiology*, *93*(5), 835–852. https://doi.org/10.1111/mmi.12720

Botella, H., Stadthagen, G., Lugo-Villarino, G., de Chastellier, C., & Neyrolles, O. (2012). Metallobiology of host–pathogen interactions: an intoxicating new insight. *Trends in Microbiology*, *20*(3), 106–112. https://doi.org/10.1016/j.tim.2012.01.005

Bottai, D., di Luca, M., Majlessi, L., Frigui, W., Simeone, R., Sayes, F., Bitter, W., Brennan, M. J., Leclerc, C., Batoni, G., Campa, M., Brosch, R., & Esin, S. (2012). Disruption of the ESX-5 system of Mycobacterium tuberculosis causes loss of PPE protein secretion, reduction of cell wall integrity and strong attenuation. *Molecular Microbiology*, *83*(6), 1195–1209. https://doi.org/10.1111/j.1365-2958.2012.08001.x

Bottai, D., Frigui, W., Sayes, F., Di Luca, M., Spadoni, D., Pawlik, A., Zoppo, M., Orgeur, M., Khanna, V., Hardy, D., Mangenot, S., Barbe, V., Medigue, C., Ma, L., Bouchier, C., Tavanti, A., Larrouy-Maumus, G., & Brosch, R. (2020). TbD1 deletion as a driver of the evolutionary success of modern epidemic Mycobacterium tuberculosis lineages. *Nature Communications*, *11*(1). https://doi.org/10.1038/s41467-020-14508-5

Bottai, D., Gröschel, M. I., & Brosch, R. (2017). Type VII secretion systems in gram-positive bacteria. In *Current Topics in Microbiology and Immunology* (Vol. 404, pp. 235–265). Springer Verlag. https://doi.org/10.1007/82_2015_5015

Bottai, D., Stinear, T. P., Supply, P., & Brosch, R. (2013). Mycobacterial Pathogenomics and Evolution. *Microbiology Spectrum*, *2*(1). https://doi.org/10.1128/microbiolspec.MGM2-0025

Braian, C., Hogea, V., & Stendahl, O. (2013). Mycobacterium tuberculosis-Induced Neutrophil Extracellular Traps Activate Human Macrophages. *Journal of Innate Immunity*, *5*(6), 591–602. https://doi.org/10.1159/000348676

Brennan, P. J., & Nikaido, H. (1995). The envelope of mycobacteria. *Annual Review of Biochemistry*, *64*, 29–63. https://doi.org/10.1146/annurev.bi.64.070195.000333

Brites, D., & Gagneux, S. (2015). *Co-evolution of Mycobacterium tuberculosis and Homo sapiens*. www.immunologicalreviews.com

Brites, D., Loiseau, C., Menardo, F., Borrell, S., Boniotti, M. B., Warren, R., Dippenaar, A., Parsons, S. D. C., Beisel, C., Behr, M. A., Fyfe, J. A., Coscolla, M., & Gagneux, S. (2018). A New Phylogenetic Framework for the Animal-Adapted Mycobacterium tuberculosis Complex. *Frontiers in Microbiology*, *9*. https://doi.org/10.3389/fmicb.2018.02820

British Thoracic Society. (2000). Management of opportunistic mycobacterial infections: Joint Tuberculosis Committee guidelines, 1999. *Thorax*, *55*, 210–218.

Brodin, P., De Jonge, M. I., Majlessi, L., Leclerc, C., Nilges, M., Cole, S. T., & Brosch, R. (2005). Functional analysis of early secreted antigenic target-6, the dominant T-cell antigen of Mycobacterium tuberculosis, reveals key residues involved in secretion, complex formation, virulence, and immunogenicity. *Journal of Biological Chemistry*, *280*(40), 33953–33959. https://doi.org/10.1074/jbc.M503515200

Brodin, P., Majlessi, L., Marsollier, L., de Jonge, M. I., Bottai, D., Demangel, C., Hinds, J., Neyrolles, O., Butcher, P. D., Leclerc, C., Cole, S. T., & Brosch, R. (2006). Dissection of ESAT-6 system 1 of Mycobacterium tuberculosis and impact on immunogenicity and virulence. *Infection and Immunity*, *74*(1), 88–98. https://doi.org/10.1128/IAI.74.1.88-98.2006

Brodin, P., Rosenkrands, I., Andersen, P., Cole, S. T., & Brosch, R. (2004). ESAT-6 proteins: protective antigens and virulence factors? *Trends in Microbiology*, *12*(11), 500–508. https://doi.org/10.1016/j.tim.2004.09.007

Brosch, R., Gordon, S. V., Garnier, T., Eiglmeier, K., Frigui, W., Valenti, P., Dos Santos, S., Duthoy, S., Lacroix, C., Garcia-Pelayo, C., Inwald, J. K., Golby, P., Garcia, J. N., Hewinson, R. G., Behr, M. A., Quail, M. A., Churcher, C., Barrell, B. G., Parkhill, J., & Cole, S. T. (2007). Genome plasticity of BCG and impact on vaccine efficacy. *Proceedings of the National Academy of Sciences*, *104*(13), 5596–5601. https://doi.org/10.1073/pnas.0700869104

Brosch, R., Gordon, S. V, Marmiesse, M., Brodin, P., Buchrieser, C., Eiglmeier, K., Garnier, T., Gutierrez, C., Hewinson, G., Kremer, K., Parsons, L. M., Pym, A. S., Samper, S., Van Soolingen, D., & Cole, S. T. (2002). A new evolutionary scenario for the Mycobacterium tuberculosis complex. *PNAS*, *99*(6), 3684–3689. www.pnas.orgcgidoi10.1073pnas.052548299

Brossier, F., Sougakoff, W., Bernard, C., Petrou, M., Adeyema, K., Pham, A., Amy De La Breteque, D., Vallet, M., Jarlier, V., Sola, C., & Veziris, N. (2015). Molecular analysis of the embCAB locus and embR gene involved in ethambutol resistance in clinical isolates of Mycobacterium tuberculosis in France. *Antimicrobial Agents and Chemotherapy*, *59*(8), 4800–4808. https://doi.org/10.1128/AAC.00150-15

Brown-Elliott, B. A., & Philley, J. V. (2017). Rapidly Growing Mycobacteria. *Microbiology Spectrum*, *5*(1). https://doi.org/10.1128/microbiolspec.tnmi7-0027-2016

Brown-Elliott, B. A., Simmer, P. J., Trovato, A., Hyle, E. P., Droz, S., Buckwalter, S. P., Borroni, E., Branda, J. A., Iana, E., Mariottini, A., Nelson, J., Matteelli, A., Toney, N. C., Scarparo, C., de Man, T. J. B., Vasireddy, R., Gandhi, R. T., Wengenack, N. L., Cirillo, D. M., … Tortoli, E. (2018). Mycobacterium decipiens sp. nov., a new species closely related to the Mycobacterium tuberculosis complex. *International Journal of Systematic and Evolutionary Microbiology*, *68*(11), 3557–3562. https://doi.org/10.1099/ijsem.0.003031

Brown-Elliott, B. A., & Woods, G. L. (2019). Antimycobacterial susceptibility testing of nontuberculous mycobacteria. *Journal of Clinical Microbiology*, *57*(10). https://doi.org/10.1128/JCM

Bulher, V. B., & Pollak, A. (1953). Buhler 1953 - Human infection with atypical acid-fast organisms. *Amercian Journal of Clinic Pathology*, *23*, 363-"è'374.

Bunduc, C. M., Fahrenkamp, D., Wald, J., Ummels, R., Bitter, W., Houben, E. N. G., & Marlovits, T. C. (2021). Structure and dynamics of a mycobacterial type VII secretion system. *Nature*, *593*(7859), 445–448. https://doi.org/10.1038/s41586-021-03517-z

Burguière, A., Hitchen, P. G., Dover, L. G., Kremer, L., Ridell, M., Alexander, D. C., Liu, J., Morris, H. R., Minnikin, D. E., Dell, A., & Besra, G. S. (2005). LosA, a key glycosyltransferase involved in the biosynthesis of a novel family of glycosylated acyltrehalose lipooligosaccharides from Mycobacterium marinum. *Journal of Biological Chemistry*, *280*(51), 42124–42133. https://doi.org/10.1074/jbc.M507500200

Bwalya, P., Solo, E. S., Chizimu, J. Y., Shrestha, D., Mbulo, G., Thapa, J., Nakajima, C., & Suzuki, Y. (2022). Characterization of embB mutations involved in ethambutol resistance in multi-drug resistant Mycobacterium tuberculosis isolates in Zambia. *Tuberculosis*, *133*. https://doi.org/10.1016/j.tube.2022.102184

Cadena, A. M., Fortune, S. M., & Flynn, J. L. (2017). Heterogeneity in tuberculosis. *Nature Reviews Immunology*, *17*(11), 691–702. https://doi.org/10.1038/nri.2017.69

Camacho, L. R., Ensergueix, D., Perez, E., Gicquel, B., & Guilhot, C. (1999). Identification of a virulence gene cluster of Mycobacterium tuberculosis by signature-tagged transposon

mutagenesis. *Molecular Microbiology*, *34*(2), 257–267. https://doi.org/10.1046/j.1365-2958.1999.01593.x

Cambier, C. J., Falkow, S., & Ramakrishnan, L. (2014). Host evasion and exploitation schemes of Mycobacterium tuberculosis. *Cell*, *159*(7), 1497–1509. https://doi.org/10.1016/j.cell.2014.11.024

Cambier, C. J., O'Leary, S. M., O'Sullivan, M. P., Keane, J., & Ramakrishnan, L. (2017). Phenolic Glycolipid Facilitates Mycobacterial Escape from Microbicidal Tissue-Resident Macrophages. *Immunity*, *47*(3), 552-565.e4. https://doi.org/10.1016/j.immuni.2017.08.003

Carver, T. J., Rutherford, K. M., Berriman, M., Rajandream, M. A., Barrell, B. G., & Parkhill, J. (2005). ACT: The Artemis comparison tool. *Bioinformatics*, *21*(16), 3422–3423. https://doi.org/10.1093/bioinformatics/bti553

Cavalcanti, Y. V. N., Brelaz, M. C. A., Lemoine Neves, J. K. de A., Ferraz, J. C., & Pereira, V. R. A. (2012). Role of TNF-Alpha, IFN-Gamma, and IL-10 in the Development of Pulmonary Tuberculosis. *Pulmonary Medicine*, *2012*, 1–10. https://doi.org/10.1155/2012/745483

Cerrone, M., Bracchi, M., Wasserman, S., Pozniak, A., Meintjes, G., Cohen, K., & Wilkinson, R. J. (2020). Safety implications of combined antiretroviral and anti-tuberculosis drugs. *Expert Opinion on Drug Safety*, *19*(1), 23–41. https://doi.org/10.1080/14740338.2020.1694901

Chai, Q., Lu, Z., & Liu, C. H. (2020). Host defense mechanisms against Mycobacterium tuberculosis. *Cellular and Molecular Life Sciences*, *77*(10), 1859–1878. https://doi.org/10.1007/s00018-019-03353-5

Chai, Q., Zhang, Y., & Liu, C. H. (2018). Mycobacterium tuberculosis: An adaptable pathogen associated with multiple human diseases. *Frontiers in Cellular and Infection Microbiology*, *8*(MAY). https://doi.org/10.3389/fcimb.2018.00158

Chandra, P., Grigsby, S. J., & Philips, J. A. (2022). Immune evasion and provocation by Mycobacterium tuberculosis. *Nature Reviews Microbiology*, *20*(12), 750–766. https://doi.org/10.1038/s41579-022-00763-4

Chen, C., Gardete, S., Jansen, R. S., Shetty, A., Dick, T., Rhee, K. Y., & Dartois, V. (2018). Verapamil Targets Membrane Energetics in Mycobacterium tuberculosis. *Antimicrobial Agents and Chemotherapy*, *62*(5). https://doi.org/10.1128/AAC.02107-17

Chen, J. M., Boy-Röttger, S., Dhar, N., Sweeney, N., Buxton, R. S., Pojer, F., Rosenkrands, I., & Cole, S. T. (2012). EspD Is Critical for the Virulence-Mediating ESX-1 Secretion System in Mycobacterium tuberculosis. *Journal of Bacteriology*, *194*(4), 884–893. https://doi.org/10.1128/JB.06417-11

Choi, J. I., Lim, J. H., Kim, S. R., Lee, S. H., Park, J. S., Seo, K. W., Jeon, J. B., & Jeong, J. (2012). Lung infection caused by Mycobacterium riyadhense confused with Mycobacterium tuberculosis: The first case in Korea. *Annals of Laboratory Medicine*, *32*(4), 298–303. https://doi.org/10.3343/alm.2012.32.4.298

Christgen, S., Place, D. E., & Kanneganti, T.-D. (2020). Toward targeting inflammasomes: insights into their regulation and activation. *Cell Research*, *30*(4), 315–327. https://doi.org/10.1038/s41422-020-0295-8

Cohen, S. B., Gern, B. H., Delahaye, J. L., Adams, K. N., Plumlee, C. R., Winkler, J. K., Sherman, D. R., Gerner, M. Y., & Urdahl, K. B. (2018). Alveolar Macrophages Provide an Early Mycobacterium tuberculosis Niche and Initiate Dissemination. *Cell Host & Microbe*, *24*(3), 439-446.e4. https://doi.org/10.1016/j.chom.2018.08.001

Cole, S. T., Brosch, R., Parkhill, J., Garnier, T., Churcher, C., Harris, D., Gordon, S. V., Eiglmeier, K., Gas, S., Barry III, C. E., Tekaia, F., Badcock, D., Basham, D., Brown, D., Chiilingworth, T., Connor, R., Davies, R., Devlin, K., Feltwell, T., … Barrel, B. G. (1998). Deciphering the biology of Mycobacterium tuberculosis from the complete genome sequence. *Nature*, *393*, 537–544.

Collins, C. H., Grange, J. M., Noble, W. C., & Yates, M. D. (1985). Mycobacterium marinum infections in man. *Journal of Hygiene*, *94*(2), 135–149. https://doi.org/10.1017/S0022172400061349

Comas, I., Coscolla, M., Luo, T., Borrell, S., Holt, K. E., Kato-Maeda, M., Parkhill, J., Malla, B., Berg, S., Thwaites, G., Yeboah-Manu, D., Bothamley, G., Mei, J., Wei, L., Bentley, S., Harris, S. R., Niemann, S., Diel, R., Aseffa, A., … Gagneux, S. (2013). Out-of-Africa migration and Neolithic coexpansion of Mycobacterium tuberculosis with modern humans. *Nature Genetics*, *45*(10), 1176–1182. https://doi.org/10.1038/ng.2744

Conrad, W. H., Osman, M. M., Shanahan, J. K., Chu, F., Takaki, K. K., Cameron, J., Hopkinson-Woolley, D., Brosch, R., & Ramakrishnan, L. (2017). Mycobacterial ESX-1 secretion system mediates host cell lysis through bacterium contact-dependent gross membrane disruptions. *Proceedings of the National Academy of Sciences of the United States of America*, *114*(6), 1371–1376. https://doi.org/10.1073/pnas.1620133114

Constant, P., Perez, E., Malaga, W., Lanéelle, M. A., Saurel, O., Daffé, M., & Guilhot, C. (2002). Role of the pks15/1 gene in the biosynthesis of phenolglycolipids in the Mycobacterium tuberculosis complex: Evidence that all strains synthesize glycosylated p-hydroxybenzoic methyl esters and that strains devoid of phenolglycolipids harbor a frameshift mutation in the pks15/1 gene. *Journal of Biological Chemistry*, *277*(41), 38148–38158. https://doi.org/10.1074/jbc.M206538200

Converse, S. E., Mougous, J. D., Leavell, M. D., Leary, J. A., Bertozzi, C. R., & Cox, J. S. (2003). MmpL8 is required for sulfolipid-1 biosynthesis and Mycobacterium tuberculosis virulence. *PNAS*, *100*(10), 6121–6126. www.pnas.orgcgidoi10.1073pnas.1030024100

Cook, G. M., Berney, M., Gebhard, S., Heinemann, M., Cox, R. A., Danilchanka, O., & Niederweis, M. (2009). Physiology of Mycobacteria. *Advances in Microbial Physiology*, *55*. https://doi.org/10.1016/S0065-2911(09)05502-7

Coscolla, M., Gagneux, S., Menardo, F., Loiseau, C., Ruiz-Rodriguez, P., Borrell, S., Otchere, I. D., Asante-Poku, A., Asare, P., Sánchez-Busó, L., Gehre, F., Sanoussi, C. N., Antonio, M., Affolabi, D., Fyfe, J., Beckert, P., Niemann, S., Alabi, A. S., Grobusch, M. P., … Brites, D. (2021). Phylogenomics of mycobacterium africanum reveals a new lineage and a complex evolutionary history. *Microbial Genomics*, *7*(2), 1–14. https://doi.org/10.1099/mgen.0.000477

Cowman, S., Van Ingen, J., Griffith, D. E., & Loebinger, M. R. (2019). Non-tuberculous mycobacterial pulmonary disease. *European Respiratory Journal*, *54*(1). https://doi.org/10.1183/13993003.00250-2019

Cox, J. S., Chen, B., McNeil, M., & Jacobs, W. R. (1999). Complex lipid determines tissue-specific replication of Mycobacterium tuberculosis in mice. *Nature*, *402*(6757), 79–83. https://doi.org/10.1038/47042

Daley, C. L. (2017). Mycobacterium avium complex disease. *Microbiology Spectrum*, *5*(2). https://doi.org/10.1128/microbiolspec.tnmi7-0045-2017

Dallenga, T., Repnik, U., Corleis, B., Eich, J., Reimer, R., Griffiths, G. W., & Schaible, U. E. (2017). M. tuberculosis-Induced Necrosis of Infected Neutrophils Promotes Bacterial Growth

Following Phagocytosis by Macrophages. *Cell Host & Microbe*, *22*(4), 519-530.e3. https://doi.org/10.1016/j.chom.2017.09.003

de Jong, B. C., Antonio, M., & Gagneux, S. (2010). Mycobacterium africanum-review of an important cause of human tuberculosis in West Africa. *PLoS Neglected Tropical Diseases*, *4*(9). https://doi.org/10.1371/journal.pntd.0000744

De Jonge, M. I., Pehau-Arnaudet, G., Fretz, M. M., Romain, F., Bottai, D., Brodin, P., Honoré, N., Marchal, G., Jiskoot, W., England, P., Cole, S. T., & Brosch, R. (2007). ESAT-6 from Mycobacterium tuberculosis dissociates from its putative chaperone CFP-10 under acidic conditions and exhibits membrane-lysing activity. *Journal of Bacteriology*, *189*(16), 6028–6034. https://doi.org/10.1128/JB.00469-07

De Leon, J., Jiang, G., Ma, Y., Rubin, E., Fortune, S., & Sun, J. (2012). Mycobacterium tuberculosis ESAT-6 exhibits a unique membrane-interacting activity that is not found in its ortholog from non-pathogenic Mycobacterium smegmatis. *Journal of Biological Chemistry*, *287*(53), 44184–44191. https://doi.org/10.1074/jbc.M112.420869

Degiacomi, G., Sammartino, J. C., Sinigiani, V., Marra, P., Urbani, A., & Pasca, M. R. (2020). In vitro Study of Bedaquiline Resistance in Mycobacterium tuberculosis Multi-Drug Resistant Clinical Isolates. *Frontiers in Microbiology*, *11*. https://doi.org/10.3389/fmicb.2020.559469

Deiss, R. G., Rodwell, T. C., & Garfein, R. S. (2009). Tuberculosis and Illicit Drug Use: Review and Update. *Clinical Infectious Diseases*, *48*(1), 72–82. https://doi.org/10.1086/594126

Diagnosis and Treatment of Disease Caused by Nontuberculous Mycobacteria. (1997). *American Journal of Respiratory and Critical Care Medicine*, *156*(2), S1–S25. https://doi.org/10.1164/ajrccm.156.2.atsstatement

DiGiuseppe Champion, P. A., Champion, M. M., Manzanillo, P., & Cox, J. S. (2009). ESX-1 secreted virulence factors are recognized by multiple cytosolic AAA ATPases in mycobactria. *Molecular Microbiology*, *73*(5), 950–962. https://doi.org/10.1111/j.1365-2958.2009.06821.x

Divangahi, M., Chen, M., Gan, H., Desjardins, D., Hickman, T. T., Lee, D. M., Fortune, S., Behar, S. M., & Remold, H. G. (2009). Mycobacterium tuberculosis evades macrophage defenses by inhibiting plasma membrane repair. *Nature Immunology*, *10*(8), 899–906. https://doi.org/10.1038/ni.1758

Dokrungkoon, T., Tulyaprawat, O., Suwannakarn, K., & Ngamskulrungroj, P. (2023). In vitro modeling of isoniazid resistance mechanisms in Mycobacterium tuberculosis H37Rv. *Frontiers in Microbiology*, *14*. https://doi.org/10.3389/fmicb.2023.1171861

Domenech, P., & Reed, M. B. (2009). Rapid and spontaneous loss of phthiocerol dimycocerosate (PDIM) from Mycobacterium tuberculosis grown in vitro: implications for virulence studies. *Microbiology (Reading, England)*, *155*(Pt 11), 3532–3543. https://doi.org/10.1099/mic.0.029199-0

Dos Anjos, L. R. B., Parreira, P. L., Torres, P. P. T. S., Kipnis, A., Junqueira-Kipnis, A. P., & Rabahi, M. F. (2020). Non-tuberculous mycobacterial lung disease: A brief review focusing on radiological findings. *Revista Da Sociedade Brasileira de Medicina Tropical*, *53*, 1–9. https://doi.org/10.1590/0037-8682-0241-2020

Driver, E. R., Ryan, G. J., Hoff, D. R., Irwin, S. M., Basaraba, R. J., Kramnik, I., & Lenaerts, A. J. (2012). Evaluation of a mouse model of necrotic granuloma formation using C3HeB/FeJ mice for testing of drugs against Mycobacterium tuberculosis. *Antimicrobial Agents and Chemotherapy*, *56*(6), 3181–3195. https://doi.org/10.1128/AAC.00217-12

Dumas, E., Christina Boritsch, E., Vandenbogaert, M., Rodríguez de la Vega, R. C., Thiberge, J.-M., Caro, V., Gaillard, J.-L., Heym, B., Girard-Misguich, F., Brosch, R., & Sapriel, G. (2016). Mycobacterial Pan-Genome Analysis Suggests Important Role of Plasmids in the Radiation of Type VII Secretion Systems. *Genome Biology and Evolution*, *8*(2), 387–402. https://doi.org/10.1093/gbe/evw001

Efficacy, Safety and Immunogenicity Evaluation of MTBVAC in Newborns in Sub-Saharan Africa (MTBVACN3). (2022, October 12). ClinicalTrials.Gov. https://classic.clinicaltrials.gov/ct2/show/NCT04975178?term=NCT04975178&draw=2&rank=1

Ehrt, S., Schnappinger, D., & Rhee, K. Y. (2018). Metabolic principles of persistence and pathogenicity in Mycobacterium tuberculosis. *Nature Reviews Microbiology*, *16*(8), 496–507. https://doi.org/10.1038/s41579-018-0013-4

Elmore, S. (2007). Apoptosis: A Review of Programmed Cell Death. *Toxicologic Pathology*, *35*(4), 495–516. https://doi.org/10.1080/01926230701320337

Elsaidi, H. R. H., & Lowary, T. L. (2015). Effect of phenolic glycolipids from Mycobacterium kansasii on proinflammatory cytokine release. A structure–activity relationship study. *Chemical Science*, *6*(5), 3161–3172. https://doi.org/10.1039/C4SC04004J

Emma Travis, A. R., Hung, Y., Porter, D., Paul, G., James, R., Roug, A., Kato-Maeda, M., Kazwala, R., Smith, W. A., Hopewell, P., Courtenay, O., & Wellington, E. M. (2019). *Environmental Reservoirs of MTBC in Ruaha Environmental reservoirs of Mycobacterium bovis and Mycobacterium tuberculosis in the Ruaha region, Tanzania*. https://doi.org/10.1101/790824

ERA4TB - The project. (n.d.). ERA4TB (European Accelerator of Tuberculosis Regime). Retrieved September 16, 2023, from https://era4tb.org/the-project/

Ernst, J. D. (2012). The immunological life cycle of tuberculosis. *Nature Reviews Immunology*, *12*(8), 581–591. https://doi.org/10.1038/nri3259

Falkinham, J. O. (2018). Challenges of NTM drug development. *Frontiers in Microbiology*, *9*(JUL). https://doi.org/10.3389/fmicb.2018.01613

Farhat, M., Greenaway, C., Pai, M., & Menzies, D. (2006). False-positive tuberculin skin tests: what is the absolute effect of BCG and non-tuberculous mycobacteria? *The International Journal of Tuberculosis and Lung Disease : The Official Journal of the International Union against Tuberculosis and Lung Disease*, *10*(11), 1192–1204.

Feuerriegel, S., Köser, C. U., Richter, E., & Niemann, S. (2013). Mycobacterium canettii is intrinsically resistant to both pyrazinamide and pyrazinoic acid. *Journal of Antimicrobial Chemotherapy*, *68*(6), 1439–1450. https://doi.org/10.1093/jac/dkt042

Forbes, B. A., Hall, G. S., Miller, M. B., Novak, S. M., Rowlinson, M.-C., Salfinger, M., Somoskövi, A., Warshauer, D. M., & Wilson, M. L. (2018). Practice Guidelines for Clinical Microbiology Laboratories: Mycobacteria. *Clinical Microbiology Reviews*, *31*(2). https://doi.org/10.1128/CMR

Forrellad, M. A., Klepp, L. I., Gioffré, A., García, J. S., Morbidoni, H. R., de la Paz Santangelo, M., Cataldi, A. A., & Bigi, F. (2013). Virulence factors of the mycobacterium tuberculosis complex. *Virulence*, *4*(1), 3–66. https://doi.org/10.4161/viru.22329

Fortune, S. M., Jaeger, A., Sarracino, D. A., Chase, M. R., Sassetti, C. M., Sherman, D. R., Bloom, B. R., & Rubin, E. J. (2005). Mutually dependent secretion of proteins required for mycobacterial virulence. *PNAS*, *102*(30), 10676–10681. www.pnas.orgcgidoi10.1073pnas.0504922102

Franco-Paredes, C., Marcos, L. A., Henao-Martínez, A. F., Rodríguez-Morales, A. J., Villamil-Gómez, W. E., Gotuzzo, E., Bonifaz, A., & Heredia, C. (2018). Cutaneous Mycobacterial Infections. *Clinical Microbiology Revue*, *32*(1). https://doi.org/10

Frigui, W., Bottai, D., Majlessi, L., Monot, M., Josselin, E., Brodin, P., Garnier, T., Gicquel, B., Martin, C., Leclerc, C., Cole, S. T., & Brosch, R. (2008). Control of M. tuberculosis ESAT-6 secretion and specific T cell recognition by PhoP. *PLoS Pathogens*, *4*(2). https://doi.org/10.1371/journal.ppat.0040033

Furin, J., Cox, H., & Pai, M. (2019). Tuberculosis. *The Lancet*, *393*(10181), 1642–1656. https://doi.org/10.1016/S0140-6736(19)30308-3

Gagliardi, A., Selchow, P., Luthra, S., Schäfle, D., Schulthess, B., & Sander, P. (2020). KatG as Counterselection Marker for Nontuberculous Mycobacteria. *Antimicrobial Agents and Chemotherapy*, *64*(5), 1–3. https://doi.org/10.1128/AAC

Gagneux, S. (2018). Ecology and evolution of Mycobacterium tuberculosis. *Nature Reviews Microbiology*, *16*(4), 202–213. https://doi.org/10.1038/nrmicro.2018.8

Galagan, J. E., Minch, K., Peterson, M., Lyubetskaya, A., Azizi, E., Sweet, L., Gomes, A., Rustad, T., Dolganov, G., Glotova, I., Abeel, T., Mahwinney, C., Kennedy, A. D., Allard, R., Brabant, W., Krueger, A., Jaini, S., Honda, B., Yu, W.-H., … Schoolnik, G. K. (2013). The Mycobacterium tuberculosis regulatory network and hypoxia. *Nature*, *499*(7457), 178–183. https://doi.org/10.1038/nature12337

Gao, J., Guo, M., Teng, L., Bao, R., Xian, Q., Wang, X., & Ho, W. (2018). Guinea pig infected with mycobacterium tuberculosis via oral consumption. *Journal of Applied Animal Research*, *46*(1), 1323–1328. https://doi.org/10.1080/09712119.2018.1505622

Garces, A., Atmakuri, K., Chase, M. R., Woodworth, J. S., Krastins, B., Rothchild, A. C., Ramsdell, T. L., Lopez, M. F., Behar, S. M., Sarracino, D. A., & Fortune, S. M. (2010). EspA acts as a critical mediator of ESX1-dependent virulence in Mycobacterium tuberculosis by affecting bacterial cell wall integrity. *PLoS Pathogens*, *6*(6). https://doi.org/10.1371/journal.ppat.1000957

García-Bengoa, M., Meurer, M., Goethe, R., Singh, M., Reljic, R., & von Köckritz-Blickwede, M. (2023). Role of phagocyte extracellular traps during Mycobacterium tuberculosis infections and tuberculosis disease processes. *Frontiers in Microbiology*, *14*. https://doi.org/10.3389/fmicb.2023.983299

Garcia-Vilanova, A., Chan, J., & Torrelles, J. B. (2019). Underestimated Manipulative Roles of Mycobacterium tuberculosis Cell Envelope Glycolipids During Infection. *Frontiers in Immunology*, *10*. https://doi.org/10.3389/fimmu.2019.02909

Garnier, T., Eiglmeier, K., Camus, J.-C., Medina, N., Mansoor, H., Pryor, M., Duthoy, S., Grondin, S., Lacroix, C., Monsempe, C., Simon, S., Harris, B., Atkin, R., Doggett, J., Mayes, R., Keating, L., Wheeler, P. R., Parkhill, J., Barrell, B. G., … Hewinson, R. G. (2003). The complete genome sequence of Mycobacterium bovis. *PNAS*, *100*(13), 7877–7882. www.defra.gov.ukanimalh

Gauthier, D. T., & Rhodes, M. W. (2009). Mycobacteriosis in fishes: A review. *Veterinary Journal*, *180*(1), 33–47. https://doi.org/10.1016/j.tvjl.2008.05.012

Genestet, C., Refrégier, G., Hodille, E., Zein-Eddine, R., Le Meur, A., Hak, F., Barbry, A., Westeel, E., Berland, J.-L., Engelmann, A., Verdier, I., Lina, G., Ader, F., Dray, S., Jacob, L., Massol, F., Venner, S., & Dumitrescu, O. (2022). Mycobacterium tuberculosis genetic features associated with pulmonary tuberculosis severity. *International Journal of Infectious Diseases*, *125*, 74–83. https://doi.org/10.1016/j.ijid.2022.10.026

Gengenbacher, M., & Kaufmann, S. H. E. (2012). *Mycobacterium tuberculosis* : success through dormancy. *FEMS Microbiology Reviews*, *36*(3), 514–532. https://doi.org/10.1111/j.1574-6976.2012.00331.x

Georghiou, S. B., Penn-Nicholson, A., de Vos, M., Macé, A., Syrmis, M. W., Jacob, K., Mape, A., Parmar, H., Cao, Y., Coulter, C., Ruhwald, M., Pandey, S. K., Schumacher, S. G., & Denkinger, C. M. (2021). Analytical performance of the Xpert MTB/XDR® assay for tuberculosis and expanded resistance detection. *Diagnostic Microbiology and Infectious Disease*, *101*(1), 115397. https://doi.org/10.1016/j.diagmicrobio.2021.115397

Gey Van Pittius, N. C., Gamieldien, J., Hide, W., Brown, G. D., Siezen, R. J., & Beyers, A. D. (2001). The ESAT-6 gene cluster of Mycobacterium tuberculosis and other high G+C Gram-positive bacteria. *Genome Biology*, *2*(10), RESEARCH0044. https://doi.org/10.1186/gb-2001-2-10-research0044

Ghazaei, C. (2018). Mycobacterium tuberculosis and lipids: Insights into molecular mechanisms from persistence to virulence. *Journal of Research in Medical Sciences*, *23*(1). https://doi.org/10.4103/jrms.JRMS_904_17

Ghodbane, R., Medie, F. M., Lepidi, H., Nappez, C., & Drancourt, M. (2014). Long-term survival of tuberculosis complex mycobacteria in soil. *Microbiology (United Kingdom)*, *160*(PART 3), 496–501. https://doi.org/10.1099/mic.0.073379-0

Giannoni, F., Lanni, A., Iacobino, A., & Fattorini, L. (2023). Epidemiology and drug susceptibility of nontuberculous mycobacteria (NTM) in Italy in 2016-2020 and the Italian Multicentre Study on Nontuberculous Mycobacteria (IMS-NTM). *Ann Ist Super Sanità*, *59*(2), 132–138. https://doi.org/10.4415/ANN_23_03_06

Godreuil, S., Marchandin, H., Michon, A.-L., Ponsada, M., Chyderiotis, G., Brisou, P., Bhat, A., & Panteix, G. (2012). Mycobacterium riyadhense Pulmonary Infection, France and Bahrain. *Emerging Infectious Diseases*, *18*(1), 176–178. https://doi.org/10.3201/eid1801.110751

Goletti, D., & Martineau, A. R. (2021). Pathogenesis and Immunology of Tuberculosis. In *Essential Tuberculosis* (pp. 19–27). Springer International Publishing. https://doi.org/10.1007/978-3-030-66703-0_3

Gonzalo-Asensio, J., Malaga, W., Pawlik, A., Astarie-Dequeker, C., Passemar, C., Moreau, F., Laval, F., Daffé, M., Martin, C., Brosch, R., & Guilhot, C. (2014). Evolutionary history of tuberculosis shaped by conserved mutations in the PhoPR virulence regulator. *Proceedings of the National Academy of Sciences of the United States of America*, *111*(31), 11491–11496. https://doi.org/10.1073/pnas.1406693111

Gopalaswamy, R., Shanmugam, S., Mondal, R., & Subbian, S. (2020). Of tuberculosis and non-tuberculous mycobacterial infections - A comparative analysis of epidemiology, diagnosis and treatment. *Journal of Biomedical Science*, *27*(1). https://doi.org/10.1186/s12929-020-00667-6

Gordon, S. V., Bottai, D., Simeone, R., Stinear, T. P., & Brosch, R. (2009). Pathogenicity in the tubercle bacillus: Molecular and evolutionary determinants. *BioEssays*, *31*(4), 378–388. https://doi.org/10.1002/bies.200800191

Gray, T. A., Clark, R. R., Boucher, N., Lapierre, P., Smith, C., & Derbyshire, K. M. (2016). Intercellular communication and conjugation are mediated by ESX secretion systems in mycobacteria. *Science*, *354*(6310), 347–350. https://doi.org/10.1126/science.aag0828

Green, E. R., & Mecsas, J. (2016). Bacterial Secretion Systems: An Overview. *Microbiology Spectrum*, *4*(1). https://doi.org/10.1128/microbiolspec.vmbf-0012-2015

Griffith, D. E., Aksamit, T., Brown-Elliott, B. A., Catanzaro, A., Daley, C., Gordin, F., Holland, S. M., Horsburgh, R., Huitt, G., Iademarco, M. F., Iseman, M., Olivier, K., Ruoss, S., Von Reyn, C. F., Wallace, R. J., & Winthrop, K. (2007). An official ATS/IDSA statement: Diagnosis, treatment, and prevention of nontuberculous mycobacterial diseases. *American Journal of Respiratory and Critical Care Medicine*, *175*(4), 367–416. https://doi.org/10.1164/rccm.200604-571ST

Gröschel, M. I., Sayes, F., Simeone, R., Majlessi, L., & Brosch, R. (2016). ESX secretion systems: Mycobacterial evolution to counter host immunity. *Nature Reviews Microbiology*, *14*(11), 677–691. https://doi.org/10.1038/nrmicro.2016.131

Guan, Q., Garbati, M., Mfarrej, S., Almutairi, T., Laval, T., Singh, A., Fagbo, S., Smyth, A., Browne, J. A., Urrahman, M. A., Alruwaili, A., Hoosen, A., Meehan, C. J., Nakajima, C., Suzuki, Y., Demangel, C., Bhatt, A., Gordon, S. V., Alasmari, F., & Pain, A. (2021). Insights into the ancestry evolution of the Mycobacterium tuberculosis complex from analysis of Mycobacterium riyadhense. *NAR Genomics and Bioinformatics*, *3*(3). https://doi.org/10.1093/nargab/lqab070

Guan, Q., Ummels, R., Ben-Rached, F., Alzahid, Y., Amini, M. S., Adroub, S. A., van Ingen, J., Bitter, W., Abdallah, A. M., & Pain, A. (2020). Comparative Genomic and Transcriptomic Analyses of Mycobacterium kansasii Subtypes Provide New Insights Into Their Pathogenicity and Taxonomy. *Frontiers in Cellular and Infection Microbiology*, *10*. https://doi.org/10.3389/fcimb.2020.00122

Guilhot, C., Chalut, C., & Daffé, M. (2014). Biosynthesis and Roles of Phenolic Glycolipids and Related Molecules in *Mycobacterium tuberculosis*. In *The Mycobacterial Cell Envelope* (pp. 271–289). ASM Press. https://doi.org/10.1128/9781555815783.ch17

Guimaraes, A. M. S., & Zimpel, C. K. (2020). Mycobacterium bovis: From genotyping to genome sequencing. *Microorganisms*, *8*(5). https://doi.org/10.3390/microorganisms8050667

Guinn, K. M., Hickey, M. J., Mathur, S. K., Zakel, K. L., Grotzke, J. E., Lewinsohn, D. M., Smith, S., & Sherman, D. R. (2004). Individual RD1-region genes are required for export of ESAT-6/ CFP-10 and for virulence of Mycobacterium tuberculosis. *Mol Microbiology*, *51*(2), 359–370.

Guirado, E., Schlesinger, L. S., & Kaplan, G. (2013). Macrophages in tuberculosis: friend or foe. *Seminars in Immunopathology*, *35*(5), 563–583. https://doi.org/10.1007/s00281-013-0388-2

Guo, Q., Bi, J., Wang, H., & Zhang, X. (2021). Mycobacterium tuberculosis ESX-1-secreted substrate protein EspC promotes mycobacterial survival through endoplasmic reticulum stress-mediated apoptosis. *Emerging Microbes and Infections*, *10*(1), 19–36. https://doi.org/10.1080/22221751.2020.1861913

Gupta, R. S., Lo, B., & Son, J. (2018). Phylogenomics and comparative genomic studies robustly support division of the genus Mycobacterium into an emended genus Mycobacterium and four novel genera. *Frontiers in Microbiology*, *9*(FEB). https://doi.org/10.3389/fmicb.2018.00067

Gutierrez, M. G. (2013). Functional role(s) of phagosomal Rab GTPases. *Small GTPases*, *4*(3), 148–158. https://doi.org/10.4161/sgtp.25604

Gutierrez, M. G., Master, S. S., Singh, S. B., Taylor, G. A., Colombo, M. I., & Deretic, V. (2004). Autophagy Is a Defense Mechanism Inhibiting BCG and Mycobacterium tuberculosis Survival in Infected Macrophages. *Cell*, *119*(6), 753–766. https://doi.org/10.1016/j.cell.2004.11.038

Harris, J., & Keane, J. (2010). How tumour necrosis factor blockers interfere with tuberculosis immunity. *Clinical and Experimental Immunology*, *161*(1), 1–9. https://doi.org/10.1111/j.1365-2249.2010.04146.x

Hashish, E., Merwad, A., Elgaml, S., Amer, A., Kamal, H., Elsadek, A., Marei, A., & Sitohy, M. (2018). Mycobacterium marinum infection in fish and man: Epidemiology, pathophysiology and management; a review. *Veterinary Quarterly*, *38*(1), 35–46. https://doi.org/10.1080/01652176.2018.1447171

Hatherill, M., White, R. G., & Hawn, T. R. (2020). Clinical Development of New TB Vaccines: Recent Advances and Next Steps. *Frontiers in Microbiology*, *10*. https://doi.org/10.3389/fmicb.2019.03154

He, W., Wan, H., Hu, L., Chen, P., Wang, X., Huang, Z., Yang, Z.-H., Zhong, C.-Q., & Han, J. (2015). Gasdermin D is an executor of pyroptosis and required for interleukin-1β secretion. *Cell Research*, *25*(12), 1285–1298. https://doi.org/10.1038/cr.2015.139

Heemskerk, D., Caws, M., Marais, B., & Farrar, J. (2015). *Tuberculosis in Adults and Children* (Vol. 2). Springer International Publishing. https://doi.org/10.1007/978-3-319-19132-4

Helb, D., Jones, M., Story, E., Boehme, C., Wallace, E., Ho, K., Kop, J., Owens, M. R., Rodgers, R., Banada, P., Safi, H., Blakemore, R., Lan, N. T. N., Jones-López, E. C., Levi, M., Burday, M., Ayakaka, I., Mugerwa, R. D., McMillan, B., … Alland, D. (2010). Rapid Detection of *Mycobacterium tuberculosis* and Rifampin Resistance by Use of On-Demand, Near-Patient Technology. *Journal of Clinical Microbiology*, *48*(1), 229–237. https://doi.org/10.1128/JCM.01463-09

Hodille, E., Genestet, C., Delque, T., Ruffel, L., Benito, Y., Fredenucci, I., Rasigade, J.-P., Lina, G., & Dumitrescu, O. (2021). The MTB/MDR ELITe MGB® Kit: Performance Assessment for Pulmonary, Extra-Pulmonary, and Resistant Tuberculosis Diagnosis, and Integration in the Laboratory Workflow of a French Center. *Pathogens*, *10*(2), 176. https://doi.org/10.3390/pathogens10020176

Hodille, E., Maisson, A., Charlet, L., Bauduin, C., Genestet, C., Fredenucci, I., Rasigade, J.-P., Lina, G., & Dumitrescu, O. (2019). Evaluation of Xpert MTB/RIF Ultra performance for pulmonary tuberculosis diagnosis on smear-negative respiratory samples in a French centre. *European Journal of Clinical Microbiology & Infectious Diseases*, *38*(3), 601–605. https://doi.org/10.1007/s10096-018-03463-1

Horton, K. C., MacPherson, P., Houben, R. M. G. J., White, R. G., & Corbett, E. L. (2016). Sex Differences in Tuberculosis Burden and Notifications in Low- and Middle-Income Countries: A Systematic Review and Meta-analysis. *PLOS Medicine*, *13*(9), e1002119. https://doi.org/10.1371/journal.pmed.1002119

Houben, E. N. G., Bestebroer, J., Ummels, R., Wilson, L., Piersma, S. R., Jiménez, C. R., Ottenhoff, T. H. M., Luirink, J., & Bitter, W. (2012). Composition of the type VII secretion system membrane complex. *Molecular Microbiology*, *86*(2), 472–484. https://doi.org/10.1111/j.1365-2958.2012.08206.x

Hug, L. A., Baker, B. J., Anantharaman, K., Brown, C. T., Probst, A. J., Castelle, C. J., Butterfield, C. N., Hernsdorf, A. W., Amano, Y., Ise, K., Suzuki, Y., Dudek, N., Relman, D. A., Finstad, K. M., Amundson, R., Thomas, B. C., & Banfield, J. F. (2016). A new view of the tree of life. *Nature Microbiology*, *1*, 16048. https://doi.org/10.1038/nmicrobiol.2016.48

Hunter, S., Murphy, R. C., Clay, K., Gorent, M. B., & Brennan, P. J. (1983). Trehalose-containing Lipooligosaccharides A NEW CLASS OF SPECIES-SPECIFIC ANTIGENS FROM MYCOBACTERIUM*. *The Journal of Biological Chemistry*, *258*(17), 10481–10487.

Immuvac (MIP). (2022, November 1). Stop TB Partnership. https://newtbvaccines.org/vaccine/immuvac/

Jackson, M. (2014). The mycobacterial cell envelope-lipids. *Cold Spring Harbor Perspectives in Medicine*, *4*(10). https://doi.org/10.1101/cshperspect.a021105

Jagielski, T., Borówka, P., Bakuła, Z., Lach, J., Marciniak, B., Brzostek, A., Dziadek, J., Dziurzyński, M., Pennings, L., van Ingen, J., Žolnir-Dovč, M., & Strapagiel, D. (2020). Genomic Insights Into the Mycobacterium kansasii Complex: An Update. *Frontiers in Microbiology*, *10*. https://doi.org/10.3389/fmicb.2019.02918

Jindani, A., Atwine, D., Grint, D., Bah, B., Adams, J., Ticona, E. R., Shrestha, B., Agizew, T., Hamid, S., Jamil, B., Byamukama, A., Kananura, K., Mugisha Taremwa, I., Bonnet, M., Camara, L. M., Bah-Sow, O. Y., Bah, K. S., Bah, N. M., Sow, M., … Harrison, T. S. (2023). Four-Month High-Dose Rifampicin Regimens for Pulmonary Tuberculosis. *NEJM Evidence*, *2*(9). https://doi.org/10.1056/EVIDoa2300054

Johansen, M. D., Herrmann, J. L., & Kremer, L. (2020). Non-tuberculous mycobacteria and the rise of Mycobacterium abscessus. *Nature Reviews Microbiology*, *18*(7), 392–407. https://doi.org/10.1038/s41579-020-0331-1

Johnson, B. K., & Abramovitch, R. B. (2015). Macrophage infection models for Mycobacterium tuberculosis. In *Methods in Molecular Biology* (Vol. 1285, pp. 329–341). http://www.springer.com/series/7651

Johnston, J. C., Chiang, L., & Elwood, K. (2017). Mycobacterium kansasii . *Microbiology Spectrum*, *5*(1). https://doi.org/10.1128/microbiolspec.tnmi7-0011-2016

Kabir, S., Tahir, Z., Mukhtar, N., Sohail, M., Saqalein, M., & Rehman, A. (2020). Fluoroquinolone resistance and mutational profile of gyrA in pulmonary MDR tuberculosis patients. *BMC Pulmonary Medicine*, *20*(1). https://doi.org/10.1186/s12890-020-1172-4

Kelley, N., Jeltema, D., Duan, Y., & He, Y. (2019). The NLRP3 Inflammasome: An Overview of Mechanisms of Activation and Regulation. *International Journal of Molecular Sciences*, *20*(13), 3328. https://doi.org/10.3390/ijms20133328

Kesavardhana, S., Malireddi, R. K. S., & Kanneganti, T.-D. (2020). Caspases in Cell Death, Inflammation, and Pyroptosis. *Annual Review of Immunology*, *38*(1), 567–595. https://doi.org/10.1146/annurev-immunol-073119-095439

Kestler, B., & Tyler, S. K. (2022). Latent tuberculosis testing through the ages: the search for a sleeping killer. *American Journal of Physiology-Lung Cellular and Molecular Physiology*, *322*(3), L412–L419. https://doi.org/10.1152/ajplung.00217.2021

Khayat, M., Fan, H., & Vali, Y. (2021). COVID-19 promoting the development of active tuberculosis in a patient with latent tuberculosis infection: A case report. *Respiratory Medicine Case Reports*, *32*, 101344. https://doi.org/10.1016/j.rmcr.2021.101344

Kim, M., Wainwright, H. C., Locketz, M., Bekker, L., Walther, G. B., Dittrich, C., Visser, A., Wang, W., Hsu, F., Wiehart, U., Tsenova, L., Kaplan, G., & Russell, D. G. (2010). Caseation of human tuberculosis granulomas correlates with elevated host lipid metabolism. *EMBO Molecular Medicine*, *2*(7), 258–274. https://doi.org/10.1002/emmm.201000079

Kim, N. Y., Kim, D. Y., Chu, J., & Jung, S.-H. (2023). *pncA* Large Deletion is the Characteristic of Pyrazinamide-Resistant *Mycobacterium tuberculosis* belonging to the East Asian Lineage. *Infection & Chemotherapy*, *55*(2), 247. https://doi.org/10.3947/ic.2023.0037

Kinchen, J. M., & Ravichandran, K. S. (2008). Phagosome maturation: going through the acid test. *Nature Reviews Molecular Cell Biology*, *9*(10), 781–795. https://doi.org/10.1038/nrm2515

Kock, R., Michel, A. L., Yeboah-Manu, D., Azhar, E. I., Torrelles, J. B., Cadmus, S. I., Brunton, L., Chakaya, J. M., Marais, B., Mboera, L., Rahim, Z., Haider, N., & Zumla, A. (2021). Zoonotic Tuberculosis – The Changing Landscape. *International Journal of Infectious Diseases*, *113*, S68–S72. https://doi.org/10.1016/j.ijid.2021.02.091

Koh, W.-J., Kwon, O. J., & Soo Lee, K. (2002). Nontuberculous Mycobacterial Pulmonary Diseases in Immunocompetent Patients. *Korean J Radiol*, *3*, 145–157.

Kolloli, A., & Subbian, S. (2017). Host-Directed Therapeutic Strategies for Tuberculosis. *Frontiers in Medicine*, *4*. https://doi.org/10.3389/fmed.2017.00171

Krause, K. M., Serio, A. W., Kane, T. R., & Connolly, L. E. (2016). Aminoglycosides: An Overview. *Cold Spring Harbor Perspectives in Medicine*, *6*(6), a027029. https://doi.org/10.1101/cshperspect.a027029

Laencina, L., Dubois, V., Le Moigne, V., Viljoen, A., Majlessi, L., Pritchard, J., Bernut, A., Piel, L., Roux, A.-L., Gaillard, J.-L., Lombard, B., Loew, D., Rubin, E. J., Brosch, R., Kremer, L., Herrmann, J.-L., & Girard-Misguich, F. (2018). Identification of genes required for Mycobacterium abscessus growth in vivo with a prominent role of the ESX-4 locus. *Proceedings of the National Academy of Sciences of the United States of America*, *115*(5), E1002–E1011. https://doi.org/10.1073/pnas.1713195115

Lam, A., Prabhu, R., Gross, C. M., Riesenberg, L. A., Singh, V., & Aggarwal, S. (2017). Role of apoptosis and autophagy in tuberculosis. *American Journal of Physiology-Lung Cellular and Molecular Physiology*, *313*(2), L218–L229. https://doi.org/10.1152/ajplung.00162.2017

Lanoix, J.-P., Lenaerts, A. J., & Nuermberger, E. L. (2015). Heterogeneous disease progression and treatment response in a C3HeB/FeJ mouse model of tuberculosis. *Disease Models & Mechanisms*, *8*, 603–610. https://doi.org/10.1242/dmm.019513

Lawn, S. D. (2012). Point-of-care detection of lipoarabinomannan (LAM) in urine for diagnosis of HIV-associated tuberculosis: a state of the art review. *BMC Infectious Diseases*, *12*(1), 103. https://doi.org/10.1186/1471-2334-12-103

Le Chevalier, F. Le, Cascioferro, A., Majlessi, L., Herrmann, J. L., & Brosch, R. (2014). *Mycobacterium tuberculosis* evolutionary pathogenesis and its putative impact on drug development. *Future Microbiology*, *9*(8), 969–985. https://doi.org/10.2217/fmb.14.70

Lehmann, K. B., & Neumann, R. O. (1896). *Atlas und grundriss der bakteriologie und lehrbuch der speziellen bakteriologischen diagnostik. J.F. Lehmann.*

Lenaerts, A., Barry, C. E., & Dartois, V. (2015). Heterogeneity in tuberculosis pathology, microenvironments and therapeutic responses. *Immunological Reviews*, *264*(1), 288–307. https://doi.org/10.1111/imr.12252

Lerner, T. R., Borel, S., Greenwood, D. J., Repnik, U., Russell, M. R. G., Herbst, S., Jones, M. L., Collinson, L. M., Griffiths, G., & Gutierrez, M. G. (2017). *Mycobacterium tuberculosis* replicates within necrotic human macrophages. *Journal of Cell Biology*, *216*(3), 583–594. https://doi.org/10.1083/jcb.201603040

Li, J., Zhao, A., Tang, J., Wang, G., Shi, Y., Zhan, L., & Qin, C. (2020). Tuberculosis vaccine development: from classic to clinical candidates. *European Journal of Clinical Microbiology & Infectious Diseases*, *39*(8), 1405–1425. https://doi.org/10.1007/s10096-020-03843-6

Li, Y., Wang, Y., & Liu, X. (2012). The Role of Airway Epithelial Cells in Response to Mycobacteria Infection. *Clinical and Developmental Immunology*, *2012*, 1–11. https://doi.org/10.1155/2012/791392

Lilly Tozer. (2023, June 28). Promising tuberculosis vaccine gets US$550-million shot in the arm. *Nature*.

Linell, F., & Norden, A. (1954). Mycobacterium balnei, a new acid-fast bacillus occurring in swimming pools and capable of producing skin lesions in humans. *Acta Tuberculosea Scandinavica. Supplementum*, *33*, 1–84.

Liu, C. H., Liu, H., & Ge, B. (2017). Innate immunity in tuberculosis: host defense vs pathogen evasion. *Cellular & Molecular Immunology*, *14*(12), 963–975. https://doi.org/10.1038/cmi.2017.88

Lou, Y., Rybniker, J., Sala, C., & Cole, S. T. (2017). EspC forms a filamentous structure in the cell envelope of Mycobacterium tuberculosis and impacts ESX-1 secretion. *Molecular Microbiology*, *103*(1), 26–38. https://doi.org/10.1111/mmi.13575

Ma, Y., Keil, V., & Sun, J. (2015). Characterization of Mycobacterium tuberculosis EsxA membrane insertion: Roles of N- and C-terminal flexible arms and central helix-turn-helix motif. *Journal of Biological Chemistry*, *290*(11), 7314–7322. https://doi.org/10.1074/jbc.M114.622076

MacGurn, J. A., Raghavan, S., Stanley, S. A., & Cox, J. S. (2005). A non-RD1 gene cluster is required for Snm secretion in Mycobacterium tuberculosis. *Molecular Microbiology*, *57*(6), 1653–1663. https://doi.org/10.1111/j.1365-2958.2005.04800.x

Madacki, J., Mas Fiol, G., & Brosch, R. (2019). Update on the virulence factors of the obligate pathogen Mycobacterium tuberculosis and related tuberculosis-causing mycobacteria. *Infection, Genetics and Evolution*, *72*, 67–77. https://doi.org/10.1016/j.meegid.2018.12.013

Madacki, J., Orgeur, M., Fiol, G. M., Frigui, W., Ma, L., & Brosch, R. (2021). Esx-1-independent horizontal gene transfer by mycobacterium tuberculosis complex strains. *MBio*, *12*(3). https://doi.org/10.1128/mBio.00965-21

Majlessi, L., & Brosch, R. (2015). Mycobacterium tuberculosis Meets the Cytosol: The Role of cGAS in Anti-mycobacterial Immunity. *Cell Host & Microbe*, *17*(6), 733–735. https://doi.org/10.1016/j.chom.2015.05.017

Majlessi, L., Prados-Rosales, R., Casadevall, A., & Brosch, R. (2015). Release of mycobacterial antigens. *Immunological Reviews*, *264*(1), 25–45. https://doi.org/10.1111/imr.12251

Makarov, V., Manina, G., Mikusova, K., Möllmann, U., Ryabova, O., Saint-Joanis, B., Dhar, N., Pasca, M. R., Buroni, S., Lucarelli, A. P., Milano, A., De Rossi, E., Belanova, M., Bobovska, A., Dianiskova, P., Kordulakova, J., Sala, C., Fullam, E., Schneider, P., … Cole, S. T. (2009). Benzothiazinones kill Mycobacterium tuberculosis by blocking arabinan synthesis. *Science (New York, N.Y.)*, *324*(5928), 801–804. https://doi.org/10.1126/science.1171583

Malaga, W., Payros, D., Meunier, E., Frigui, W., Sayes, F., Pawlik, A., Orgeur, M., Berrone, C., Moreau, F., Mazères, S., Gonzalo-Asensio, J., Rengel, D., Martin, C., Astarie-Dequeker, C., Mourey, L., Brosch, R., & Guilhot, C. (2023). Natural mutations in the sensor kinase of the PhoPR two-component regulatory system modulate virulence of ancestor-like tuberculosis bacilli. *PLoS Pathogens*, *19*(7), e1011437. https://doi.org/10.1371/journal.ppat.1011437

Mallick, J. S., Nair, P., Abbew, E. T., Van Deun, A., & Decroo, T. (2022). Acquired bedaquiline resistance during the treatment of drug-resistant tuberculosis: a systematic review. *JAC-Antimicrobial Resistance*, *4*(2). https://doi.org/10.1093/jacamr/dlac029

Manganelli, R., Cioetto-Mazzabò, L., Segafreddo, G., Boldrin, F., Sorze, D., Conflitti, M., Serafini, A., & Provvedi, R. (2023). SigE: A master regulator of Mycobacterium tuberculosis. *Frontiers in Microbiology*, *14*. https://doi.org/10.3389/fmicb.2023.1075143

Maphasa, R. E., Meyer, M., & Dube, A. (2021). The Macrophage Response to Mycobacterium tuberculosis and Opportunities for Autophagy Inducing Nanomedicines for Tuberculosis Therapy. *Frontiers in Cellular and Infection Microbiology*, *10*. https://doi.org/10.3389/fcimb.2020.618414

Marrakchi, H., Lanéelle, G., & Quémard, A. (2000). InhA, a target of the antituberculous drug isoniazid, is involved in a mycobacterial fatty acid elongation system, FAS-II. *Microbiology*, *146*, 289–296.

Martín, C., Marinova, D., Aguiló, N., & Gonzalo-Asensio, J. (2021). MTBVAC, a live TB vaccine poised to initiate efficacy trials 100 years after BCG. *Vaccine*, *39*(50), 7277–7285. https://doi.org/10.1016/j.vaccine.2021.06.049

Martinez, L., Verma, R., Croda, J., Horsburgh, C. R., Walter, K. S., Degner, N., Middelkoop, K., Koch, A., Hermans, S., Warner, D. F., Wood, R., Cobelens, F., & Andrews, J. R. (2019). Detection, survival and infectious potential of Mycobacterium tuberculosis in the environment: A review of the evidence and epidemiological implications. *European Respiratory Journal*, *53*(6). https://doi.org/10.1183/13993003.02302-2018

Meehan, C. J., Barco, R. A., Loh, Y. H. E., Cogneau, S., & Rigouts, L. (2021). Reconstituting the genus mycobacterium. *International Journal of Systematic and Evolutionary Microbiology*, *71*(9). https://doi.org/10.1099/ijsem.0.004922

Meier, N. R., Jacobsen, M., Ottenhoff, T. H. M., & Ritz, N. (2018). A Systematic Review on Novel Mycobacterium tuberculosis Antigens and Their Discriminatory Potential for the Diagnosis of Latent and Active Tuberculosis. *Frontiers in Immunology*, *9*. https://doi.org/10.3389/fimmu.2018.02476

Méndez-Samperio, P. (2017). Diagnosis of Tuberculosis in HIV Co-infected Individuals: Current Status, Challenges and Opportunities for the Future. *Scandinavian Journal of Immunology*, *86*(2), 76–82. https://doi.org/10.1111/sji.12567

Mendoza-Coronel, E., & Castañón-Arreola, M. (2016). Comparative evaluation of in vitro human macrophage models for mycobacterial infection study. *Pathogens and Disease*, *74*(6). https://doi.org/10.1093/femspd/ftw052

Migliori, G. B., Ong, C. W. M., Petrone, L., D'Ambrosio, L., Centis, R., & Goletti, D. (2021). The definition of tuberculosis infection based on the spectrum of tuberculosis disease. *Breathe*, *17*(3), 210079. https://doi.org/10.1183/20734735.0079-2021

Millington, K. A., Fortune, S. M., Low, J., Garces, A., Hingley-Wilson, S. M., Wickremasinghe, M., Kon, O. M., & Lalvani, A. (2011). Rv3615c is a highly immunodominant RD1 (Region of Difference 1)-dependent secreted antigen specific for Mycobacterium tuberculosis infection. *Proceedings of the National Academy of Sciences of the United States of America*, *108*(14), 5730–5735. https://doi.org/10.1073/pnas.1015153108

Minnikin, D. E., Lee, O. Y. C., Wu, H. H. T., Besra, G. S., Bhatt, A., Nataraj, V., Rothschild, B. M., Spigelman, M., & Donoghue, H. D. (2015). Ancient mycobacterial lipids: Key reference biomarkers in charting the evolution of tuberculosis. *Tuberculosis*, *95*(S1), S133–S139. https://doi.org/10.1016/j.tube.2015.02.009

Mintern, J. D., & Villadangos, J. A. (2012). Autophagy and Mechanisms of Effective Immunity. *Frontiers in Immunology*, *3*. https://doi.org/10.3389/fimmu.2012.00060

Mishra, B. B., Moura-Alves, P., Sonawane, A., Hacohen, N., Griffiths, G., Moita, L. F., & Anes, E. (2010). Mycobacterium tuberculosis protein ESAT-6 is a potent activator of the NLRP3/ASC inflammasome. *Cellular Microbiology*, *12*(8), 1046–1063. https://doi.org/10.1111/j.1462-5822.2010.01450.x

Mok, S., Roycroft, E., Flanagan, P. R., Montgomery, L., Borroni, E., Rogers, T. R., & Fitzgibbon, M. M. (2021). Overcoming the challenges of pyrazinamide susceptibility testing in clinical mycobacterium tuberculosis isolates. *Antimicrobial Agents and Chemotherapy*, *65*(8). https://doi.org/10.1128/AAC.02617-20

Moon, S. M., Kim, S. Y., Chung, M. J., Lee, S. H., Shin, S. J., & Koh, W. J. (2015). Nontuberculous mycobacterial lung disease caused by mycobacterium shinjukuense: The first reported case in Korea. *Tuberculosis and Respiratory Diseases*, *78*(4), 416–418. https://doi.org/10.4046/trd.2015.78.4.416

Mottola, G. (2014). The complexity of Rab5 to Rab7 transition guarantees specificity of pathogen subversion mechanisms. *Frontiers in Cellular and Infection Microbiology*, *4*. https://doi.org/10.3389/fcimb.2014.00180

Moule, M. G., & Cirillo, J. D. (2020). Mycobacterium tuberculosis Dissemination Plays a Critical Role in Pathogenesis. *Frontiers in Cellular and Infection Microbiology*, *10*. https://doi.org/10.3389/fcimb.2020.00065

Mudde, S. E., Upton, A. M., Lenaerts, A., Bax, H. I., & De Steenwinkel, J. E. M. (2022). Delamanid or pretomanid? A Solomonic judgement! *Journal of Antimicrobial Chemotherapy*, *77*(4), 880–902. https://doi.org/10.1093/jac/dkab505

Mussi, V. O., Simão, T. L. B. V., Almeida, F. M., Machado, E., de Carvalho, L. D., Calixto, S. D., Sales, G. A. M., Carvalho, E. C. Q., Vasconcellos, S. E. G., Catanho, M., Suffys, P. N., & Lasunskaia, E. B. (2021). A Murine Model of Mycobacterium kansasii Infection Reproducing Necrotic Lung Pathology Reveals Considerable Heterogeneity in Virulence of Clinical Isolates. *Frontiers in Microbiology*, *12*. https://doi.org/10.3389/fmicb.2021.718477

Narasimhan, P., Wood, J., MacIntyre, C. R., & Mathai, D. (2013). Risk Factors for Tuberculosis. *Pulmonary Medicine*, *2013*, 1–11. https://doi.org/10.1155/2013/828939

Nataraj, V., Pang, P., Haslam, S. M., Veerapen, N., Minnikin, D. E., Dell, A., Besra, G. S., & Bhatt, A. (2015). MKAN27435 is required for the biosynthesis of higher subclasses of lipooligosaccharides in Mycobacterium kansasii. *PloS One*, *10*(3), e0122804. https://doi.org/10.1371/journal.pone.0122804

Nathan, C., & Cunningham-Bussel, A. (2013). Beyond oxidative stress: an immunologist's guide to reactive oxygen species. *Nature Reviews Immunology*, *13*(5), 349–361. https://doi.org/10.1038/nri3423

Nessar, R., Cambau, E., Reyrat, J. M., Murray, A., & Gicquel, B. (2012). Mycobacterium abscessus: A new antibiotic nightmare. *Journal of Antimicrobial Chemotherapy*, *67*(4), 810–818. https://doi.org/10.1093/jac/dkr578

Nessar, R., Reyrat, J. M., Murray, A., & Gicquel, B. (2011). Genetic analysis of new 16s rRNA mutations conferring aminoglycoside resistance in Mycobacterium abscessus. *Journal of Antimicrobial Chemotherapy*, *66*(8), 1719–1724. https://doi.org/10.1093/jac/dkr209

Newton-Foot, M., Warren, R. M., Sampson, S. L., van Helden, P. D., & Gey van Pittius, N. C. (2016). The plasmid-mediated evolution of the mycobacterial ESX (Type VII) secretion systems. *BMC Evolutionary Biology*, *16*, 62. https://doi.org/10.1186/s12862-016-0631-2

Neyrolles, O., Mintz, E., & Catty, P. (2013). Zinc and copper toxicity in host defense against pathogens: Mycobacterium tuberculosis as a model example of an emerging paradigm. *Frontiers in Cellular and Infection Microbiology*, *3*. https://doi.org/10.3389/fcimb.2013.00089

Ngabonziza, J. C. S., Loiseau, C., Marceau, M., Jouet, A., Menardo, F., Tzfadia, O., Antoine, R., Niyigena, E. B., Mulders, W., Fissette, K., Diels, M., Gaudin, C., Duthoy, S., Ssengooba, W.,

André, E., Kaswa, M. K., Habimana, Y. M., Brites, D., Affolabi, D., … Supply, P. (2020). A sister lineage of the Mycobacterium tuberculosis complex discovered in the African Great Lakes region. *Nature Communications*, *11*(1), 1–11. https://doi.org/10.1038/s41467-020-16626-6

Nguyen, J. A., & Yates, R. M. (2021). Better Together: Current Insights Into Phagosome-Lysosome Fusion. *Frontiers in Immunology*, *12*. https://doi.org/10.3389/fimmu.2021.636078

Niederweis, M., Wolschendorf, F., Mitra, A., & Neyrolles, O. (2015). Mycobacteria, metals, and the macrophage. *Immunological Reviews*, *264*(1), 249–263. https://doi.org/10.1111/imr.12265

Nieuwenhuizen, N. E., Kulkarni, P. S., Shaligram, U., Cotton, M. F., Rentsch, C. A., Eisele, B., Grode, L., & Kaufmann, S. H. E. (2017). The Recombinant Bacille Calmette–Guérin Vaccine VPM1002: Ready for Clinical Efficacy Testing. *Frontiers in Immunology*, *8*. https://doi.org/10.3389/fimmu.2017.01147

Nigou, J., Zelle-Rieser, C., Gilleron, M., Thurnher, M., & Puzo, G. (2001). Mannosylated Lipoarabinomannans Inhibit IL-12 Production by Human Dendritic Cells: Evidence for a Negative Signal Delivered Through the Mannose Receptor. *The Journal of Immunology*, *166*(12), 7477–7485. https://doi.org/10.4049/jimmunol.166.12.7477

Nishiuchi, Y., Iwamoto, T., & Maruyama, F. (2017). Infection sources of a common non-tuberculous mycobacterial pathogen, Mycobacterium avium complex. *Frontiers in Medicine*, *4*(MAR). https://doi.org/10.3389/fmed.2017.00027

Novotny, L., Dvorska, L., Lorencova, A., Beran, V., & Pavlik, I. (2004). Fish: a potential source of bacterial pathogens for human beings. In *Vet. Med.-Czech* (Vol. 49, Issue 9). https://doi.org/10.17221/5715

Nuermberger, E. L. (2017). Preclinical Efficacy Testing of New Drug Candidates. *Microbiology Spectrum*, *5*(3). https://doi.org/10.1128/microbiolspec.tbtb2-0034-2017

Obata, S., Zwolska, Z., Toyota, E., Kudo, K., Nakamura, A., Sawai, T., Kuratsuji, T., & Kirikae, T. (2006). Association of rpoB mutations with rifampicin resistance in Mycobacterium avium. *International Journal of Antimicrobial Agents*, *27*(1), 32–39. https://doi.org/10.1016/j.ijantimicag.2005.09.015

O'Brien, D. P., McDonald, A., Callan, P., Robson, M., Friedman, N. D., Hughes, A., Holten, I., Walton, A., & Athan, E. (2012). Successful outcomes with oral fluoroquinolones combined with rifampicin in the treatment of Mycobacterium ulcerans: an observational cohort study. *PLoS Neglected Tropical Diseases*, *6*(1), e1473. https://doi.org/10.1371/journal.pntd.0001473

Ojo, M. M., Peter, O. J., Goufo, E. F. D., & Nisar, K. S. (2023). A mathematical model for the co-dynamics of COVID-19 and tuberculosis. *Mathematics and Computers in Simulation*, *207*, 499–520. https://doi.org/10.1016/j.matcom.2023.01.014

Ok, V., Aubry, A., Morel, F., Bonnet, I., Robert, J., & Sougakoff, W. (2021). Rapid Molecular Diagnosis of Tuberculosis and Its Resistance to Rifampicin and Isoniazid with Automated MDR/MTB ELITe MGB® Assay. *Antibiotics*, *10*(7), 797. https://doi.org/10.3390/antibiotics10070797

Orgeur, M., Frigui, W., Pawlik, A., Clark, S., Williams, A., Ates, L. S., Ma, L., Bouchier, C., Parkhill, J., Brodin, P., & Brosch, R. (2021). Pathogenomic analyses of Mycobacterium microti, an ESX-1-deleted member of the Mycobacterium tuberculosis complex causing disease in various hosts. *Microbial Genomics*, *7*(2). https://doi.org/10.1099/mgen.0.000505

Oshima, K., Yokouchi, H., Minemura, H., Saito, J., Tanino, Y., & Munakata, M. (2015). Pulmonary infection caused by mycobacterium shinjukuense - Letter. *American Thoracic Society*, *12*(6), 958–959.

Pagán, A. J., & Ramakrishnan, L. (2015). Immunity and Immunopathology in the Tuberculous Granuloma. *Cold Spring Harbor Perspectives in Medicine*, *5*(9), a018499. https://doi.org/10.1101/cshperspect.a018499

Pai, M., Behr, M. A., Dowdy, D., Dheda, K., Divangahi, M., Boehme, C. C., Ginsberg, A., Swaminathan, S., Spigelman, M., Getahun, H., Menzies, D., & Raviglione, M. (2016). Tuberculosis. *Nature Reviews Disease Primers*, *2*. https://doi.org/10.1038/nrdp.2016.76

Pai, M., Denkinger, C. M., Kik, S. V., Rangaka, M. X., Zwerling, A., Oxlade, O., Metcalfe, J. Z., Cattamanchi, A., Dowdy, D. W., Dheda, K., & Banaei, N. (2014). Gamma Interferon Release Assays for Detection of Mycobacterium tuberculosis Infection. *Clinical Microbiology Reviews*, *27*(1), 3–20. https://doi.org/10.1128/CMR.00034-13

Pajuelo, D., Tak, U., Zhang, L., Danilchanka, O., Tischler, A. D., & Niederweis, M. (2021). Toxin secretion and trafficking by Mycobacterium tuberculosis. *Nature Communications*, *12*(1). https://doi.org/10.1038/s41467-021-26925-1

Pal, R., Bisht, M. K., & Mukhopadhyay, S. (2022). Secretory proteins of *Mycobacterium tuberculosis* and their roles in modulation of host immune responses: focus on therapeutic targets. *The FEBS Journal*, *289*(14), 4146–4171. https://doi.org/10.1111/febs.16369

Palomino, J. C., & Martin, A. (2014). Drug resistance mechanisms in Mycobacterium tuberculosis. *Antibiotics*, *3*(3), 317–340. https://doi.org/10.3390/antibiotics3030317

Pang, X., Samten, B., Cao, G., Wang, X., Tvinnereim, A. R., Chen, X. L., & Howard, S. T. (2013). MprAB regulates the espA operon in Mycobacterium tuberculosis and modulates ESX-1 function and host cytokine response. *Journal of Bacteriology*, *195*(1), 66–75. https://doi.org/10.1128/JB.01067-12

Pang, Y., Lu, J., Wang, Y., Song, Y., Wang, S., & Zhao, Y. (2013). Study of the rifampin monoresistance mechanism in mycobacterium tuberculosis. *Antimicrobial Agents and Chemotherapy*, *57*(2), 893–900. https://doi.org/10.1128/AAC.01024-12

Pasparakis, M., & Vandenabeele, P. (2015). Necroptosis and its role in inflammation. *Nature*, *517*(7534), 311–320. https://doi.org/10.1038/nature14191

Passemar, C., Arbués, A., Malaga, W., Mercier, I., Moreau, F., Lepourry, L., Neyrolles, O., Guilhot, C., & Astarie-Dequeker, C. (2014). Multiple deletions in the polyketide synthase gene repertoire of mycobacterium tuberculosis reveal functional overlap of cell envelope lipids in host-pathogen interactions. *Cellular Microbiology*, *16*(2), 195–213. https://doi.org/10.1111/cmi.12214

Patel, K., Butala, S., Khan, T., Suvarna, V., Sherje, A., & Dravyakar, B. (2018). Mycobacterial siderophore: A review on chemistry and biology of siderophore and its potential as a target for tuberculosis. *European Journal of Medicinal Chemistry*, *157*, 783–790. https://doi.org/10.1016/j.ejmech.2018.08.030

Pawar, A., Jha, P., Konwar, C., Chaudhry, U., Chopra, M., & Saluja, D. (2019). Ethambutol targets the glutamate racemase of Mycobacterium tuberculosis—an enzyme involved in peptidoglycan biosynthesis. *Applied Microbiology and Biotechnology*, *103*(2), 843–851. https://doi.org/10.1007/s00253-018-9518-z

Pawlik, A., Garnier, G., Orgeur, M., Tong, P., Lohan, A., Le Chevalier, F., Sapriel, G., Roux, A.-L., Conlon, K., Honoré, N., Dillies, M.-A., Ma, L., Bouchier, C., Coppée, J.-Y., Gaillard, J.-L., Gordon, S. V, Loftus, B., Brosch, R., & Herrmann, J. L. (2013). Identification and

characterization of the genetic changes responsible for the characteristic smooth-to-rough morphotype alterations of clinically persistent Mycobacterium abscessus. *Molecular Microbiology*, *90*(3), 612–629. https://doi.org/10.1111/mmi.12387

Pérez, E., Samper, S., Bordas, Y., Guilhot, C., Gicquel, B., & Martín, C. (2001). An essential role for phoP in Mycobacterium tuberculosis virelence. *Molecular Microbiology*, *41*(1), 179–187. https://doi.org/10.1046/j.1365-2958.2001.02500.x

Perrin, C., Athersuch, K., Elder, G., Martin, M., & Alsalhani, A. (2022). Recently developed drugs for the treatment of drug-resistant tuberculosis: a research and development case study. *BMJ Global Health*, *7*(4), e007490. https://doi.org/10.1136/bmjgh-2021-007490

Peterson, N. D., Rosen, B. C., Dillon, N. A., & Baughn, A. D. (2015). Uncoupling Environmental pH and Intrabacterial Acidification from Pyrazinamide Susceptibility in Mycobacterium tuberculosis. *Antimicrobial Agents and Chemotherapy*, *59*(12), 7320–7326. https://doi.org/10.1128/AAC.00967-15

Pethe, K., Bifani, P., Jang, J., Kang, S., Park, S., Ahn, S., Jiricek, J., Jung, J., Jeon, H. K., Cechetto, J., Christophe, T., Lee, H., Kempf, M., Jackson, M., Lenaerts, A. J., Pham, H., Jones, V., Seo, M. J., Kim, Y. M., … Kim, J. (2013). Discovery of Q203, a potent clinical candidate for the treatment of tuberculosis. *Nature Medicine*, *19*(9), 1157–1160. https://doi.org/10.1038/nm.3262

Petruccioli, E., Petrone, L., Chiacchio, T., Farroni, C., Cuzzi, G., Navarra, A., Vanini, V., Massafra, U., Lo Pizzo, M., Guggino, G., Caccamo, N., Cantini, F., Palmieri, F., & Goletti, D. (2021). Mycobacterium tuberculosis Immune Response in Patients With Immune-Mediated Inflammatory Disease. *Frontiers in Immunology*, *12*. https://doi.org/10.3389/fimmu.2021.716857

Picardeau, M., Prod'hom, G., Raskine, L., Lepennec, M. P., & Vincent, V. (1997). Genotypic Characterization of Five Subspecies of Mycobacterium kansasii. *Journal of Clinical Microbiology*, *35*(1), 25–32.

Poirier, V., & Av-Gay, Y. (2015). Intracellular Growth of Bacterial Pathogens: The Role of Secreted Effector Proteins in the Control of Phagocytosed Microorganisms. *Microbiology Spectrum*, *3*(6). https://doi.org/10.1128/microbiolspec.VMBF-0003-2014

Porvaznik, I., Solovic, I., & Mokry, J. (2016). *Non-Tuberculous Mycobacteria: Classification, Diagnosis, and Therapy* (I. R. Cohen, N. S. A. Lajtha, J. D. Lambris, & R. Paoletti, Eds.; Mieczyslaw Pokorski, Vol. 944). http://www.springer.com/series/13457

Prabowo, S. A., Painter, H., Zelmer, A., Smith, S. G., Seifert, K., Amat, M., Cardona, P.-J., & Fletcher, H. A. (2019). RUTI Vaccination Enhances Inhibition of Mycobacterial Growth ex vivo and Induces a Shift of Monocyte Phenotype in Mice. *Frontiers in Immunology*, *10*. https://doi.org/10.3389/fimmu.2019.00894

Prevots, D. R., Shaw, P. A., Strickland, D., Jackson, L. A., Raebel, M. A., Blosky, M. A., De Oca, R. M., Shea, Y. R., Seitz, A. E., Holland, S. M., & Olivier, K. N. (2010). Nontuberculous mycobacterial lung disease prevalence at four integrated health care delivery systems. *American Journal of Respiratory and Critical Care Medicine*, *182*(7), 970–976. https://doi.org/10.1164/rccm.201002-0310OC

Pym, A. S., Brodin, P., Brosch, R., Huerre, M., & Cole, S. T. (2002). Loss of RD1 contributed to the attenuation of the live tuberculosis vaccines Mycobacterium bovis BCG and Mycobacterium microti. *Molecular Microbiology*, *46*(3), 709–717. https://doi.org/10.1046/j.1365-2958.2002.03237.x

Pym, A. S., Saint-Joanis, B., & Cole, S. T. (2002). Effect of *katG* Mutations on the Virulence of *Mycobacterium tuberculosis* and the Implication for Transmission in Humans. *Infection and Immunity*, *70*(9), 4955–4960. https://doi.org/10.1128/IAI.70.9.4955-4960.2002

Quan, S., Venter, H., & Dabbs, E. R. (1997). Ribosylative inactivation of rifampin by Mycobacterium smegmatis is a principal contributor to its low susceptibility to this antibiotic. *Antimicrobial Agents and Chemotherapy*, *41*(11), 2456–2460. https://doi.org/10.1128/AAC.41.11.2456

Queval, C. J., Brosch, R., & Simeone, R. (2017). The Macrophage: A Disputed Fortress in the Battle against Mycobacterium tuberculosis. *Frontiers in Microbiology*, *8*. https://doi.org/10.3389/fmicb.2017.02284

Quigley, J., Hughitt, V. K., Velikovsky, C. A., Mariuzza, R. A., El-Sayed, N. M., & Briken, V. (2017). The cell wall lipid PDIM contributes to phagosomal escape and host cell exit of Mycobacterium tuberculosis. *MBio*, *8*(2). https://doi.org/10.1128/mBio.00148-17

Raghavan, S., Manzanillo, P., Chan, K., Dovey, C., & Cox, J. S. (2008). Secreted transcription factor controls Mycobacterium tuberculosis virulence. *Nature*, *454*(7205), 717–721. https://doi.org/10.1038/nature07219

Rahlwes, K. C., Dias, B. R. S., Campos, P. C., Alvarez-Arguedas, S., & Shiloh, M. U. (2023). Pathogenicity and virulence of *Mycobacterium tuberculosis*. *Virulence*, *14*(1). https://doi.org/10.1080/21505594.2022.2150449

Ramakrishnan, L. (2012). Revisiting the role of the granuloma in tuberculosis. *Nature Reviews Immunology*, *12*(5), 352–366. https://doi.org/10.1038/nri3211

Ramakrishnan, L. (2020). Mycobacterium tuberculosis pathogenicity viewed through the lens of molecular Koch's postulates. *Current Opinion in Microbiology*, *54*, 103–110. https://doi.org/10.1016/j.mib.2020.01.011

Ramakrishnan, L., Tran, H. T., Federspiel, N. A., & Falkow, S. (1997). A crtB homolog essential for photochromogenicity in Mycobacterium marinum: isolation, characterization, and gene disruption via homologous recombination. *Journal of Bacteriology*, *179*(18), 5862–5868. https://doi.org/10.1128/jb.179.18.5862-5868.1997

Ramos, B., Gordon, S. V., & Cunha, M. V. (2020). Revisiting the expression signature of pks15/1 unveils regulatory patterns controlling phenolphtiocerol and phenolglycolipid production in pathogenic mycobacteria. *PLoS ONE*, *15*(5). https://doi.org/10.1371/journal.pone.0229700

Rastogi, S., Ellinwood, S., Augenstreich, J., Mayer-Barber, K. D., & Briken, V. (2021). Mycobacterium tuberculosis inhibits the NLRP3 inflammasome activation via its phosphokinase PknF. *PLOS Pathogens*, *17*(7), e1009712. https://doi.org/10.1371/journal.ppat.1009712

Ratnatunga, C. N., Lutzky, V. P., Kupz, A., Doolan, D. L., Reid, D. W., Field, M., Bell, S. C., Thomson, R. M., & Miles, J. J. (2020). The Rise of Non-Tuberculosis Mycobacterial Lung Disease. *Frontiers in Immunology*, *11*. https://doi.org/10.3389/fimmu.2020.00303

Reingewertz, T. H., Meyer, T., McIntosh, F., Sullivan, J., Meir, M., Chang, Y. F., Behr, M. A., & Barkana, D. (2020). Differential sensitivity of mycobacteria to isoniazid is related to differences in katg-mediated enzymatic activation of the drug. *Antimicrobial Agents and Chemotherapy*, *64*(2). https://doi.org/10.1128/AAC.01899-19

Ren, H., Dover, L. G., Islam, S. T., Alexander, D. C., Chen, J. M., Besra, G. S., & Liu, J. (2007). Identification of the lipooligosaccharide biosynthetic gene cluster from Mycobacterium marinum. *Molecular Microbiology*, *63*(5), 1345–1359. https://doi.org/10.1111/j.1365-2958.2007.05603.x

Renshaw, P. S., Panagiotidou, P., Whelan, A., Gordon, S. V., Glyn Hewinson, R., Williamson, R. A., & Carr, M. D. (2002). Conclusive evidence that the major T-cell antigens of the Mycobacterium tuberculosis complex ESAT-6 and CFP-10 form a tight, 1:1 complex and characterization of the structural properties of ESAT-6, CFP-10, and the ESAT-6·CFP-10 complex. Implications for pathogenesis and virulence. *Journal of Biological Chemistry*, *277*(24), 21598–21603. https://doi.org/10.1074/jbc.M201625200

Restrepo, B. I. (2016). Diabetes and Tuberculosis. *Microbiology Spectrum*, *4*(6). https://doi.org/10.1128/microbiolspec.TNMI7-0023-2016

Reuter, A., Hughes, J., & Furin, J. (2019). Challenges and controversies in childhood tuberculosis. *The Lancet*, *394*(10202), 967–978. https://doi.org/10.1016/S0140-6736(19)32045-8

Ricketts, W. M., O'Shaughnessy, T. C., & Van Ingen, J. (2014). Human-to-human transmission of Mycobacterium kansasii or victims of a shared source? *European Respiratory Journal*, *44*(4), 1085–1087. https://doi.org/10.1183/09031936.00066614

Riehl, G., & Paltauf, R. (1886). Tuberculosis verrucosa cutis. Eine bisher noch nicht beschriebene Form yon Hauttuberculose. *Vierteljahrschritft Für Dermatologie (Wien)*, *13*, 19–49.

Ringshausen, F. C., Wagner, D., de Roux, A., Diel, R., Hohmann, D., Hickstein, L., Welte, T., & Rademacher, J. (2016). Prevalence of nontuberculous mycobacterial pulmonary disease, Germany, 2009-2014. *Emerging Infectious Diseases*, *22*(6), 1102–1105. https://doi.org/10.3201/eid2206.151642

Roca, F. J., Whitworth, L. J., Redmond, S., Jones, A. A., & Ramakrishnan, L. (2019). TNF Induces Pathogenic Programmed Macrophage Necrosis in Tuberculosis through a Mitochondrial-Lysosomal-Endoplasmic Reticulum Circuit. *Cell*, *178*(6), 1344-1361.e11. https://doi.org/10.1016/j.cell.2019.08.004

Rominski, A., Roditscheff, A., Selchow, P., Böttger, E. C., & Sander, P. (2017). Intrinsic rifamycin resistance of Mycobacterium abscessus is mediated by ADP-ribosyltransferase MAB_0591. *Journal of Antimicrobial Chemotherapy*, *72*(2), 376–384. https://doi.org/10.1093/jac/dkw466

Rostamian, M., Kooti, S., Abiri, R., Khazayel, S., Kadivarian, S., Borji, S., & Alvandi, A. (2023). Prevalence of Mycobacterium tuberculosis mutations associated with isoniazid and rifampicin resistance: A systematic review and meta-analysis. *Journal of Clinical Tuberculosis and Other Mycobacterial Diseases*, *32*. https://doi.org/10.1016/j.jctube.2023.100379

Rüger, K., Hampel, A., Billig, S., Rücker, N., Suerbaum, S., & Bange, F. C. (2014). Characterization of rough and smooth morphotypes of mycobacterium abscessus isolates from clinical specimens. *Journal of Clinical Microbiology*, *52*(1), 244–250. https://doi.org/10.1128/JCM.01249-13

Runyon, E. H. (1959). Anonymous Mycobacteria in Pulmonary Disease. *Medical Clinics of North America*, *43*, 273–290.

Russell, D. G. (2007). Who puts the tubercle in tuberculosis? *Nature Reviews Microbiology*, *5*(1), 39–47. https://doi.org/10.1038/nrmicro1538

Saad, M. M., Alshukairi, A. N., Qutub, M. O., Elkhizzi, N. A., Hilluru, H. M., & Omrani, A. S. (2015). Mycobacterium riyadhense infections. *Saudi Medical Journal*, *36*(5), 620–625. https://doi.org/10.15537/smj.2015.5.11226

Saito, H., Iwamoto, T., Ohkusu, K., Otsuka, Y., Akiyama, Y., Sato, S., Taguchi, O., Sueyasu, Y., Kawabe, Y., Fujimoto, H., Ezaki, T., & Butler, R. (2011). Mycobacterium shinjukuense sp.

nov., a slowly growing, non-chromogenic species isolated from human clinical specimens. *International Journal of Systematic and Evolutionary Microbiology*, *61*(8), 1927–1932. https://doi.org/10.1099/ijs.0.025478-0

Sanduzzi Zamparelli, S., Mormile, M., Sanduzzi Zamparelli, A., Guarino, A., Parrella, R., & Bocchino, M. (2022). Clinical impact of COVID-19 on tuberculosis. *Le Infezioni in Medicina*, *30*(4), 495–500. https://doi.org/10.53854/liim-3004-3

Sankey, N., Merrick, H., Singh, P., Rogers, J., Reddi, A., Hartson, S. D., & Mitra, A. (2023). Role of the Mycobacterium tuberculosis ESX-4 Secretion System in Heme Iron Utilization and Pore Formation by PPE Proteins. *MSphere*, *8*(2). https://doi.org/10.1128/msphere.00573-22

Sapriel, G., & Brosch, R. (2019). Shared Pathogenomic Patterns Characterize a New Phylotype, Revealing Transition toward Host-Adaptation Long before Speciation of Mycobacterium tuberculosis. *Genome Biology and Evolution*, *11*(8), 2420–2438. https://doi.org/10.1093/gbe/evz162

Sarathy, J., Blanc, L., Alvarez-Cabrera, N., O'Brien, P., Dias-Freedman, I., Mina, M., Zimmerman, M., Kaya, F., Liang, H. P. H., Prideaux, B., Dietzold, J., Salgame, P., Savic, R. M., Linderman, J., Kirschner, D., Pienaar, E., & Dartois, V. (2019). Fluoroquinolone efficacy against tuberculosis is driven by penetration into lesions and activity against resident bacterial populations. *Antimicrobial Agents and Chemotherapy*, *63*(5). https://doi.org/10.1128/AAC.02516-18

Sarathy, J. P., Gruber, G., & Dick, T. (2019). Re-Understanding the Mechanisms of Action of the Anti-Mycobacterial Drug Bedaquiline. *Antibiotics*, *8*(4), 261. https://doi.org/10.3390/antibiotics8040261

Sassetti, C. M., & Rubin, E. J. (2003). Genetic requirements for mycobacterial survival during infection. *Proceedings of the National Academy of Sciences*, *100*(22), 12989–12994. https://doi.org/10.1073/pnas.2134250100

Saunders, B. M., & Cooper, A. M. (2000). Restraining mycobacteria: Role of granulomas in mycobacterial infections. *Immunology & Cell Biology*, *78*(4), 334–341. https://doi.org/10.1046/j.1440-1711.2000.00933.x

Sayes, F., Pawlik, A., Frigui, W., Gröschel, M. I., Crommelynck, S., Fayolle, C., Cia, F., Bancroft, G. J., Bottai, D., Leclerc, C., Brosch, R., & Majlessi, L. (2016). CD4+ T Cells Recognizing PE/PPE Antigens Directly or via Cross Reactivity Are Protective against Pulmonary Mycobacterium tuberculosis Infection. *PLOS Pathogens*, *12*(7), e1005770. https://doi.org/10.1371/journal.ppat.1005770

Scorpio, A., & Zhang, Y. (1996). Mutation in pncA, a gene encoding pyrazinamidase/nicotinamidase, cause resistance to the anti tuberculous drug Pyrazinamide in tubercule bacillus. *Nature Medicine*, *2*, 662–667.

Seeliger, J. C., Holsclaw, C. M., Schelle, M. W., Botyanszki, Z., Gilmore, S. A., Tully, S. E., Niederweis, M., Cravatt, B. F., Leary, J. A., & Bertozzi, C. R. (2012). Elucidation and chemical modulation of sulfolipid-1 biosynthesis in Mycobacterium tuberculosis. *Journal of Biological Chemistry*, *287*(11), 7990–8000. https://doi.org/10.1074/jbc.M111.315473

Seemann, T. (2014). Prokka: rapid prokaryotic genome annotation. *Bioinformatics*, *30*(14), 2068–2069. https://doi.org/10.1093/bioinformatics/btu153

Serafini, A., Pisu, D., Palù, G., Rodriguez, G. M., & Manganelli, R. (2013). The ESX-3 Secretion System Is Necessary for Iron and Zinc Homeostasis in Mycobacterium tuberculosis. *PLoS ONE*, *8*(10). https://doi.org/10.1371/journal.pone.0078351

Shah, N. M., Davidson, J. A., Anderson, L. F., Lalor, M. K., Kim, J., Thomas, H. L., Lipman, M., & Abubakar, I. (2016). Pulmonary Mycobacterium avium-intracellulare is the main driver of the rise in non-tuberculous mycobacteria incidence in England, Wales and Northern Ireland, 2007-2012. *BMC Infectious Diseases*, *16*(1). https://doi.org/10.1186/s12879-016-1521-3

Sharma, S., & Upadhyay, V. (2020). Epidemiology, diagnosis & treatment of non-tuberculous mycobacterial diseases. *Indian Journal of Medical Research*, *152*(3), 185–226. https://doi.org/10.4103/ijmr.IJMR_902_20

Shepard, C. C. (1965). Temperature optimum of Mycobacterium leprae in mice. *Journal of Bacteriology*, *90*(5), 1271–1275. https://doi.org/10.1128/jb.90.5.1271-1275.1965

Shingadia, D. (2012). The Diagnosis of Tuberculosis. *Pediatric Infectious Disease Journal*, *31*(3), 302–305. https://doi.org/10.1097/INF.0b013e318249f26d

Shitikov, E., & Bespiatykh, D. (2023). A revised SNP-based barcoding scheme for typing Mycobacterium tuberculosis complex isolates . *MSphere*. https://doi.org/10.1128/msphere.00169-23

Siddalingaiah, N., Chawla, K., Nagaraja, S. B., & Hazra, D. (2023). Risk factors for the development of tuberculosis among the pediatric population: a systematic review and meta-analysis. *European Journal of Pediatrics*, *182*(7), 3007–3019. https://doi.org/10.1007/s00431-023-04988-0

Siegrist, M. S., Unnikrishnan, M., Mcconnell, M. J., Borowsky, M., Cheng, T.-Y., Siddiqi, N., Fortune, S. M., Branch Moody, D., & Rubin, E. J. (2009). Mycobacterial Esx-3 is required for mycobactin-mediated iron acquisition. *PNAS*, *106*(44), 18792–18797. www.pnas.orgcgidoi10.1073pnas.0900589106

Siegrist, M. S., Unnikrishnan, M., McConnell, M. J., Borowsky, M., Cheng, T.-Y., Siddiqi, N., Fortune, S. M., Moody, D. B., & Rubin, E. J. (2009). Mycobacterial Esx-3 is required for mycobactin-mediated iron acquisition. *Proceedings of the National Academy of Sciences of the United States of America*, *106*(44), 18792–18797. https://doi.org/10.1073/pnas.0900589106

Silva, D. R., Muñoz-Torrico, M., Duarte, R., Galvão, T., Bonini, E. H., Arbex, F. F., Arbex, M. A., Augusto, V. M., Rabahi, M. F., & Mello, F. C. de Q. (2018). Risk factors for tuberculosis: diabetes, smoking, alcohol use, and the use of other drugs. *Jornal Brasileiro de Pneumologia*, *44*(2), 145–152. https://doi.org/10.1590/s1806-37562017000000443

Silva, M. L., Cá, B., Osório, N. S., Rodrigues, P. N. S., Maceiras, A. R., & Saraiva, M. (2022). Tuberculosis caused by Mycobacterium africanum: Knowns and unknowns. *PLoS Pathogens*, *18*(5). https://doi.org/10.1371/journal.ppat.1010490

Simeone, R., Bobard, A., Lippmann, J., Bitter, W., Majlessi, L., Brosch, R., & Enninga, J. (2012). Phagosomal rupture by Mycobacterium tuberculosis results in toxicity and host cell death. *PLoS Pathogens*, *8*(2). https://doi.org/10.1371/journal.ppat.1002507

Simeone, R., Sayes, F., Lawarée, E., & Brosch, R. (2021). Breaching the phagosome, the case of the tuberculosis agent. *Cellular Microbiology*, *23*(7). https://doi.org/10.1111/cmi.13344

Simner, P. J., Hyle, E. P., Buckwalter, S. P., Branda, J. A., Brown-Elliott, B. A., Franklin, J., Toney, N. C., De Man, T. J. B., Wallace, R. J., Vasireddy, R., Gandhi, R. T., & Wengenack, N. L. (2014). Tenosynovitis caused by a novel nontuberculous mycobacterium species initially misidentified as a member of the Mycobacterium tuberculosis complex. *Journal of Clinical Microbiology*, *52*(12), 4414–4418. https://doi.org/10.1128/JCM.00967-14

Singh, B., Cocker, D., Ryan, H., & Sloan, D. J. (2019). Linezolid for drug-resistant pulmonary tuberculosis. *Cochrane Database of Systematic Reviews*. https://doi.org/10.1002/14651858.CD012836.pub2

Solans, L., Aguiló, N., Samper, S., Pawlik, A., Frigui, W., Martín, C., Brosch, R., & Gonzalo-Asensio, J. (2014). A specific polymorphism in Mycobacterium tuberculosis H37Rv causes differential ESAT-6 expression and identifies WhiB6 as a novel ESX-1 component. *Infection and Immunity*, *82*(8), 3446–3456. https://doi.org/10.1128/IAI.01824-14

Soldevilla, P., Vilaplana, C., & Cardona, P.-J. (2022). Mouse Models for Mycobacterium tuberculosis Pathogenesis: Show and Do Not Tell. *Pathogens*, *12*(1), 49. https://doi.org/10.3390/pathogens12010049

Sonnenkalb, L., Carter, J. J., Spitaleri, A., Iqbal, Z., Hunt, M., Malone, K. M., Utpatel, C., Cirillo, D. M., Rodrigues, C., Nilgiriwala, K. S., Fowler, P. W., Merker, M., Niemann, S., Barilar, I., Battaglia, S., Borroni, E., Brandao, A. P., Brankin, A., Cabibbe, A. M., … Zhu, B. (2023). Bedaquiline and clofazimine resistance in Mycobacterium tuberculosis: an in-vitro and in-silico data analysis. *The Lancet Microbe*, *4*(5), e358–e368. https://doi.org/10.1016/S2666-5247(23)00002-2

Sørensen, A. L., Nagai, S., Houen, G., Andersen, P., & Andersen, Å. B. (1995). Purification and Characterization of a Low-Molecular-Mass T-Cell Antigen Secreted by Mycobacterium tuberculosis. *Infection and Immunity*, *63*(5), 1710–1717.

Srivastava, S., Ernst, J. D., & Desvignes, L. (2014). Beyond macrophages: the diversity of mononuclear cells in tuberculosis. *Immunological Reviews*, *262*(1), 179–192. https://doi.org/10.1111/imr.12217

Stanley, S. A., Raghavan, S., Hwang, W. W., & Cox, J. S. (2003). Acute infection and macrophage subversion by Mycobacterium tuberculosis require a specialized secretion system. *PNAS*, *100*(22), 13001–13006. www.pnas.org

Stead, W. W., Eisenach, K. D., Cave, M. D., Beggs, M. L., Templeton, G. L., Thoen, C. O., & Bates, J. H. (1995). When did Mycobacterium tuberculosis infection first occur in the New World? An important question with public health implications. *American Journal of Respiratory and Critical Care Medicine*, *151*(4), 1267–1268. https://doi.org/10.1164/ajrccm/151.4.1267

Steigler, P., Chhiba, M., Francis, V., Keyser, A., Abrahams, D., Hanekom, W., Ntsekhe, M., & Scriba, T. J. (2022). T cell responses to Mycobacterium indicus pranii immunotherapy and adjunctive glucocorticoid therapy in tuberculous pericarditis. *Vaccine: X*, *11*, 100177. https://doi.org/10.1016/j.jvacx.2022.100177

Stephen, J., & Gluckman, J. (1995). Mycobacterium marinum. *Clinical Dermatology* , *13*, 273–276.

Stinear, T. P., Seemann, T., Harrison, P. F., Jenkin, G. A., Davies, J. K., Johnson, P. D. R., Abdellah, Z., Arrowsmith, C., Chillingworth, T., Churcher, C., Clarke, K., Cronin, A., Davis, P., Goodhead, I., Holroyd, N., Jagels, K., Lord, A., Moule, S., Mungall, K., … Cole, S. T. (2008). Insights from the complete genome sequence of Mycobacterium marinum on the evolution of Mycobacterium tuberculosis. *Genome Research*, *18*(5), 729–741. https://doi.org/10.1101/gr.075069.107

Sun, Q., Zhang, Q., Xiao, H., Cui, H., & Su, B. (2012). Significance of the frequency of CD4+CD25+CD127− T-cells in patients with pulmonary tuberculosis and diabetes mellitus. *Respirology*, *17*(5), 876–882. https://doi.org/10.1111/j.1440-1843.2012.02184.x

Supply, P., & Brosch, R. (2017). The biology and epidemiology of mycobacterium canettii. In *Advances in Experimental Medicine and Biology* (Vol. 1019, pp. 27–41). Springer New York LLC. https://doi.org/10.1007/978-3-319-64371-7_2

Supply, P., Marceau, M., Mangenot, S., & Roche, D. (2013). Genome analysis of smooth tubercle bacilli provides insights into ancestry and pathoadaptation of the etiologic agent of tuberculosis. *Nature Genetics*, *45*(2). https://doi.org/10.1038/ng.2517.Genome

Szulc-Kielbik, I., Pawelczyk, J., Kielbik, M., Kremer, L., Dziadek, J., & Klink, M. (2017). Severe inhibition of lipooligosaccharide synthesis induces TLR2-dependent elimination of Mycobacterium marinum from THP1-derived macrophages. *Microbial Cell Factories*, *16*(1). https://doi.org/10.1186/s12934-017-0829-z

Tahlan, K., Wilson, R., Kastrinsky, D. B., Arora, K., Nair, V., Fischer, E., Barnes, S. W., Walker, J. R., Alland, D., Barry, C. E., & Boshoff, H. I. (2012). SQ109 targets MmpL3, a membrane transporter of trehalose monomycolate involved in mycolic acid donation to the cell wall core of Mycobacterium tuberculosis. *Antimicrobial Agents and Chemotherapy*, *56*(4), 1797–1809. https://doi.org/10.1128/AAC.05708-11

Tait, D. R., Hatherill, M., Van Der Meeren, O., Ginsberg, A. M., Van Brakel, E., Salaun, B., Scriba, T. J., Akite, E. J., Ayles, H. M., Bollaerts, A., Demoitié, M.-A., Diacon, A., Evans, T. G., Gillard, P., Hellström, E., Innes, J. C., Lempicki, M., Malahleha, M., Martinson, N., … Roman, F. (2019). Final Analysis of a Trial of M72/AS01 $_E$ Vaccine to Prevent Tuberculosis. *New England Journal of Medicine*, *381*(25), 2429–2439. https://doi.org/10.1056/NEJMoa1909953

Tait, S. W. G., & Green, D. R. (2010). Mitochondria and cell death: outer membrane permeabilization and beyond. *Nature Reviews Molecular Cell Biology*, *11*(9), 621–632. https://doi.org/10.1038/nrm2952

Takeda, K., Ohshima, N., Nagai, H., Sato, R., Ando, T., Kusaka, K., Kawashima, M., Masuda, K., Matsui, H., Aono, A., Chikamatsu, K., Mitarai, S., & Ohta, K. (2016). Six cases of pulmonary Mycobacterium shinjukuense infection at a single hospital. *Internal Medicine*, *55*(7), 787–791. https://doi.org/10.2169/internalmedicine.55.5460

Taoka, T., Shinohara, T., Hatakeyama, N., Iwamura, S., Murase, Y., Mitarai, S., & Ogushi, F. (2020). Mycobacterium Shinjukuense Pulmonary Disease Progressed to Pleuritis after Iatrogenic Pneumothorax: A Case Report. *Journal of Clinical Tuberculosis and Other Mycobacterial Diseases*, *19*. https://doi.org/10.1016/j.jctube.2020.100160

Tekaia, F., Gordon, S. V, Garnier, T., Brosch, R., Barrell, B. G., & Cole, S. T. (1999). Analysis of the proteome of Mycobacterium tuberculosis in silico. *Tubercle and Lung Disease : The Official Journal of the International Union against Tuberculosis and Lung Disease*, *79*(6), 329–342. https://doi.org/10.1054/tuld.1999.0220

Telenti, A., Imboden, P., Marchesi, F., Lowrie, D., Cole, S., Colston, M. J., Matter, L., Schopper, H., & Bodmer, T. (1993). Detection of rifampicin-resistance mutations in Mycobacterium tuberculosis. *The Lancet*, *341*, 647–650.

Tientcheu, L. D., Koch, A., Ndengane, M., Andoseh, G., Kampmann, B., & Wilkinson, R. J. (2017). Immunological consequences of strain variation within the Mycobacterium tuberculosis complex. In *European Journal of Immunology* (Vol. 47, Issue 3, pp. 432–445). Wiley-VCH Verlag. https://doi.org/10.1002/eji.201646562

Tiwari, S., Casey, R., Goulding, C. W., Hingley-Wilson, S., & Jacobs, Jr., W. R. (2019). Infect and Inject: How Mycobacterium tuberculosis Exploits Its Major Virulence-Associated Type VII Secretion System, ESX-1 . *Microbiology Spectrum*, *7*(3). https://doi.org/10.1128/microbiolspec.bai-0024-2019

Tjelle, T. E., Løvdal, T., & Berg, T. (2000). Phagosome dynamics and function. *BioEssays*, *22*(3), 255–263. https://doi.org/10.1002/(SICI)1521-1878(200003)22:3<255::AID-BIES7>3.0.CO;2-R

Tobin, D. M., & Ramakrishnan, L. (2008). Comparative pathogenesis of Mycobacterium marinum and Mycobacterium tuberculosis. *Cellular Microbiology*, *10*(5), 1027–1039. https://doi.org/10.1111/j.1462-5822.2008.01133.x

Tornheim, J. A., & Dooley, K. E. (2018). Challenges of TB and HIV co-treatment. *Current Opinion in HIV and AIDS*, *13*(6), 486–491. https://doi.org/10.1097/COH.0000000000000495

Torrelles, J. B., Ellis, D., Osborne, T., Hoefer, A., Orme, I. M., Chatterjee, D., Brennan, P. J., & Cooper, A. M. (2002). Characterization of virulence, colony morphotype and the glycopeptidolipid of Mycobacterium avium strain 104. *Tuberculosis*, *82*(6), 293–300. https://doi.org/10.1054/TUBE.2002.0373

Torrelles, J. B., & Schlesinger, L. S. (2017). Integrating Lung Physiology, Immunology, and Tuberculosis. *Trends in Microbiology*, *25*(8), 688–697. https://doi.org/10.1016/j.tim.2017.03.007

Tortoli, E., Brown-Elliott, B. A., Chalmers, J. D., Cirillo, D. M., Daley, C. L., Emler, S., Floto, R. A., Garcia, M. J., Hoefsloot, W., Koh, W.-J., Lange, C., Loebinger, M., Maurer, F. P., Morimoto, K., Niemann, S., Richter, E., Turenne, C. Y., Vasireddy, R., Vasireddy, S., … van Ingen, J. (2019). Same meat, different gravy: ignore the new names of mycobacteria. *The European Respiratory Journal*, *54*(1). https://doi.org/10.1183/13993003.00795-2019

Tortoli, E., Fedrizzi, T., Meehan, C. J., Trovato, A., Grottola, A., Giacobazzi, E., Serpini, G. F., Tagliazucchi, S., Fabio, A., Bettua, C., Bertorelli, R., Frascaro, F., De Sanctis, V., Pecorari, M., Jousson, O., Segata, N., & Cirillo, D. M. (2017). The new phylogeny of the genus Mycobacterium: The old and the news. *Infection, Genetics and Evolution*, *56*(August), 19–25. https://doi.org/10.1016/j.meegid.2017.10.013

Tram, T. T. B., Nhung, H. N., Vijay, S., Hai, H. T., Thu, D. D. A., Ha, V. T. N., Dinh, T. D., Ashton, P. M., Hanh, N. T., Phu, N. H., Thwaites, G. E., & Thuong, N. T. T. (2018). Virulence of Mycobacterium tuberculosis Clinical Isolates Is Associated With Sputum Pre-treatment Bacterial Load, Lineage, Survival in Macrophages, and Cytokine Response. *Frontiers in Cellular and Infection Microbiology*, *8*. https://doi.org/10.3389/fcimb.2018.00417

Turenne, C., Chedore, P., Wolfe, J., Jamieson, F., Broukhanski, G., May, K., & Kabani, A. (2002). Myobacterium lacus sp. nov., a novel slowly growing, non-chromogenic clinical isolate. *International Journal of Systematic and Evolutionary Microbiology*, *52*(6), 2135–2140. https://doi.org/10.1099/ijs.0.02170-0

Uribe-Querol, E., & Rosales, C. (2017). Control of Phagocytosis by Microbial Pathogens. *Frontiers in Immunology*, *8*. https://doi.org/10.3389/fimmu.2017.01368

Vallenet, D., Calteau, A., Cruveiller, S., Gachet, M., Lajus, A., Josso, A., Mercier, J., Renaux, A., Rollin, J., Rouy, Z., Roche, D., Scarpelli, C., & Médigue, C. (2017). MicroScope in 2017: an expanding and evolving integrated resource for community expertise of microbial genomes. *Nucleic Acids Research*, *45*(D1), D517–D528. https://doi.org/10.1093/nar/gkw1101

van de Veerdonk, F. L., Netea, M. G., Dinarello, C. A., & Joosten, L. A. B. (2011). Inflammasome activation and IL-1β and IL-18 processing during infection. *Trends in Immunology*, *32*(3), 110–116. https://doi.org/10.1016/j.it.2011.01.003

van der Wel, N., Hava, D., Houben, D., Fluitsma, D., van Zon, M., Pierson, J., Brenner, M., & Peters, P. J. (2007). M. tuberculosis and M. leprae Translocate from the Phagolysosome

to the Cytosol in Myeloid Cells. *Cell*, *129*(7), 1287–1298. https://doi.org/10.1016/j.cell.2007.05.059

Van Der Woude, A. D., Sarkar, D., Bhatt, A., Sparrius, M., Raadsen, S. A., Boon, L., Geurtsen, J., Van Der Sar, A. M., Luirink, J., Houben, E. N. G., Besra, G. S., & Bitter, W. (2012). Unexpected link between lipooligosaccharide biosynthesis and surface protein release in Mycobacterium marinum. *Journal of Biological Chemistry*, *287*(24), 20417–20429. https://doi.org/10.1074/jbc.M111.336461

Van Ingen, J. (2013). Diagnosis of nontuberculous mycobacterial infections. *Seminars in Respiratory and Critical Care Medicine*, *34*(1), 103–109. https://doi.org/10.1055/s-0033-1333569

van Ingen, J., Al-Haijoj, S. A. M., Boeree, M., Al-Rabiah, F., Enaimi, M., de Zwaan, R., Tortoli, E., Dekhuijzen, R., & van Soolingen, D. (2009). Mycobacterium riyadhense sp. nov., a non-tuberculous species identified as Mycobacterium tuberculosis complex by a commercial line-probe assay. *International Journal of Systematic and Evolutionary Microbiology*, *59*(5), 1049–1053. https://doi.org/10.1099/ijs.0.005629-0

Van Ingen, J., Boeree, M. J., Van Soolingen, D., & Mouton, J. W. (2012). Resistance mechanisms and drug susceptibility testing of nontuberculous mycobacteria. *Drug Resistance Updates*, *15*(3), 149–161. https://doi.org/10.1016/j.drup.2012.04.001

van Ingen, J., Rahim, Z., Mulder, A., Boeree, M. J., Simeone, R., Brosch, R., & van Soolingen, D. (2012). Characterization of Mycobacterium orygis as M. tuberculosis complex subspecies. *Emerging Infectious Diseases*, *18*(4), 653–655. https://doi.org/10.3201/eid1804.110888

van Rijn, S. P., Zuur, M. A., Anthony, R., Wilffert, B., van Altena, R., Akkerman, O. W., de Lange, W. C. M., van der Werf, T. S., Kosterink, J. G. W., & Alffenaar, J.-W. C. (2019). Evaluation of Carbapenems for Treatment of Multi- and Extensively Drug-Resistant *Mycobacterium tuberculosis*. *Antimicrobial Agents and Chemotherapy*, *63*(2). https://doi.org/10.1128/AAC.01489-18

Vanino, E., Granozzi, B., Akkerman, O. W., Munoz-Torrico, M., Palmieri, F., Seaworth, B., Tiberi, S., & Tadolini, M. (2023). Update of drug-resistant tuberculosis treatment guidelines: A turning point. *International Journal of Infectious Diseases*, *130*, S12–S15. https://doi.org/10.1016/j.ijid.2023.03.013

Varghese, B., Enani, M. A., Althawadi, S., Johani, S., Fernandez, G. M., Al-Ghafli, H., & Al-Hajoj, S. (2017). *Mycobacterium riyadhense* in Saudi Arabia. *Emerging Infectious Diseases*, *23*(10), 1732–1734. https://doi.org/10.3201/eid2310.161430

Vaziri, F., & Brosch, R. (2019). ESX/Type VII Secretion Systems-An Important Way Out for Mycobacterial Proteins. *Microbiology Spectrum*, *4*. https://doi.org/10.1128/microbiolspec.PSIB

Villarreal-Ramos, B., Berg, S., Whelan, A., Holbert, S., Carreras, F., Salguero, F. J., Khatri, B. L., Malone, K., Rue-Albrecht, K., Shaughnessy, R., Smyth, A., Ameni, G., Aseffa, A., Sarradin, P., Winter, N., Vordermeier, M., & Gordon, S. V. (2018). Experimental infection of cattle with Mycobacterium tuberculosis isolates shows the attenuation of the human tubercle bacillus for cattle. *Scientific Reports*, *8*(1), 894. https://doi.org/10.1038/s41598-017-18575-5

Visca, D., Tiberi, S., Pontali, E., Spanevello, A., & Migliori, G. B. (2020). Tuberculosis in the time of COVID-19: quality of life and digital innovation. *European Respiratory Journal*, *56*(2), 2001998. https://doi.org/10.1183/13993003.01998-2020

VPM1002 Tuberculosis Vaccine. (2023, February 9). Precisionvaccinations. https://www.precisionvaccinations.com/vaccines/vpm1002-tuberculosis-vaccine#:~:text=”%2C%20commented%20Prof.-,Dr.,generation%20BCG%20vaccine%20moves%20forward.

Walters, S. B., Dubnau, E., Kolesnikova, I., Laval, F., Daffe, M., & Smith, I. (2006). The Mycobacterium tuberculosis PhoPR two-component system regulates genes essential for virulence and complex lipid biosynthesis. *Molecular Microbiology*, *60*(2), 312–330. https://doi.org/10.1111/j.1365-2958.2006.05102.x

Wang, J., McIntosh, F., Radomski, N., Dewar, K., Simeone, R., Enninga, J., Brosch, R., Rocha, E. P., Veyrier, F. J., & Behr, M. A. (2015). Insights on the emergence of Mycobacterium tuberculosis from the analysis of Mycobacterium kansasii. *Genome Biology and Evolution*, *7*(3), 856–870. https://doi.org/10.1093/gbe/evv035

Wang, Q., Boshoff, H. I. M., Harrison, J. R., Ray, P. C., Green, S. R., Wyatt, P. G., & Barry, C. E. (2020). PE/PPE proteins mediate nutrient transport across the outer membrane of Mycobacterium tuberculosis. *Science (New York, N.Y.)*, *367*(6482), 1147–1151. https://doi.org/10.1126/science.aav5912

Watanabe, K., Shinkai, M., Yamaguchi, N., Shinoda, M., Hara, Y., Ishigatsubo, Y., & Kaneko, T. (2013). Mycobacterium shinjukuense lung disease that was successfully treated with antituberculous drugs. *Internal Medicine*, *52*(23), 2653–2655. https://doi.org/10.2169/internalmedicine.52.1116

Watson, R. O., Bell, S. L., MacDuff, D. A., Kimmey, J. M., Diner, E. J., Olivas, J., Vance, R. E., Stallings, C. L., Virgin, H. W., & Cox, J. S. (2015). The Cytosolic Sensor cGAS Detects Mycobacterium tuberculosis DNA to Induce Type I Interferons and Activate Autophagy. *Cell Host & Microbe*, *17*(6), 811–819. https://doi.org/10.1016/j.chom.2015.05.004

Weiss, G., & Schaible, U. E. (2015). Macrophage defense mechanisms against intracellular bacteria. *Immunological Reviews*, *264*(1), 182–203. https://doi.org/10.1111/imr.12266

Whelan, A. O., Coad, M., Cockle, P. J., Hewinson, G., Vordermeier, M., & Gordon, S. V. (2010). Revisiting Host Preference in the Mycobacterium tuberculosis Complex: Experimental Infection Shows M. tuberculosis H37Rv to Be Avirulent in Cattle. *PLoS ONE*, *5*(1), e8527. https://doi.org/10.1371/journal.pone.0008527

WHO module 4. (2022). *WHO consolidated guidelines on tuberculosis Module 4: Drug-resistant tuberculosis treatment*.

Wink, D. A., Hines, H. B., Cheng, R. Y. S., Switzer, C. H., Flores-Santana, W., Vitek, M. P., Ridnour, L. A., & Colton, C. A. (2011). Nitric oxide and redox mechanisms in the immune response. *Journal of Leukocyte Biology*, *89*(6), 873–891. https://doi.org/10.1189/jlb.1010550

Woods, G. L., Wengenack, N. L., Lin, G., Brown-Elliot, B. A., Cirillo, D. M., Conville, P. S., Desmond, E. P., Killian, S. B., Pfelts, R., Richter, E., & Turnidge, J. D. (2011). CLSI M62 : performance standards for susceptibilitytesting of mycobacteria, nocardia spp., and other. In *Clinical and Laboratory Standard Institute* (Vol. 31, Issue 5). GOBI US LIBRARY SOLUTIONS. https://www.ncbi.nlm.nih.gov/books/NBK544374/

World Health Organization. (2011). *Mise en oeuvre rapide du test diagnostique Xpert MTB/RIF : guide technique et opérationnel : considérations pratiques*.

World Health Organization. (2020). *Global Tuberculosis Report 2020*.

World Health Organization. (2022). *Global Tuberculosis Report 2022*. http://apps.who.int/bookorders.

World Health Organization - Geneva. (2013). *The use of molecular line probe assay for the detection of resistance to second-line anti-tuberculous drugs*.

World Health Organization - Geneva. (2016). *The Use of Loop-Mediated Isothermal Amplification (TB-LAMP) for the Diagnosis of Pulmonary Tuberculosis: Policy Guidance*.

World Health Organization module 5. (2022). *WHO operational handbook on tuberculosis Module 5: Management of tuberculosis in children and adolescents*.

Wu, M. L., Aziz, D. B., Dartois, V., & Dick, T. (2018). NTM drug discovery: status, gaps and the way forward. *Drug Discovery Today*, *23*(8), 1502–1519. https://doi.org/10.1016/j.drudis.2018.04.001

Yamamoto, Y., Saito, H., Setogawa, T., & Tomioka1, H. (1991). Sex Differences in Host Resistance to Mycobacterium marinum Infection in Mice. *Infection and Immunity*, *59*(11), 4089–4096.

Young, D. B. (2003). Building a better tuberculosis vaccine. *Nature Medicine*, *9*(5), 503–504. https://doi.org/10.1038/nm868

Zhang, Y., Shi, W., Zhang, W., & Mitchison, D. (2013). Mechanisms of Pyrazinamide Action and Resistance. *Microbiology Spectrum*, *2*(4). https://doi.org/10.1128/microbiolspec.mgm2-0023-2013

Zhang, Y., & Yew, W. W. (2009). Mechanisms of drug resistance in Mycobacterium tuberculosis. *The International Journal of Tuberculosis and Lung Disease*, *13*(11), 1320–1330.

Zheng, H., Williams, J. T., Coulson, G. B., Haiderer, E. R., & Abramovitch, R. B. (2018). HC2091 Kills Mycobacterium tuberculosis by Targeting the MmpL3 Mycolic Acid Transporter. *Antimicrobial Agents and Chemotherapy*, *62*(7). https://doi.org/10.1128/AAC.02459-17

ANNEXES

Annex 1: First pages of the article and the review related to the thesis

Annex 2: Picture of resazurin assay results

Plate layout:

µg/mL											Range (% OD)	
RIF	4	2	1	0.5	0.25	0.125	0.0625	0.0313	0.0156	0.0078	100	100
	4	2	1	0.5	0.25	0.125	0.0625	0.0313	0.0156	0.0078	90	90
INH	32	16	8	4	2	1	0.5	0.25	0.125	0.0625	75	75
	32	16	8	4	2	1	0.5	0.25	0.125	0.0625	50	50
ETH	60	30	15	7.5	3.75	1.875	0.9375	0.4688	0.2344	0.1172	10	10
	60	30	15	7.5	3.75	1.875	0.9375	0.4688	0.2344	0.1172	5	5
BDQ	0.2	0.1	0.05	0.025	0.0125	0.00625	0.00313	0.00156	0.00078	0.00039	2	2
	0.2	0.1	0.05	0.025	0.0125	0.00625	0.00313	0.00156	0.00078	0.00039	0	0

M. decipiens

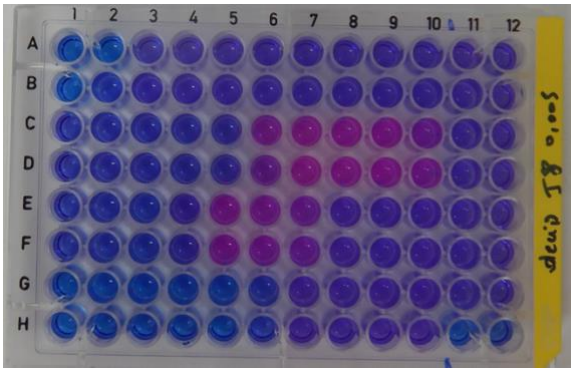

M. lacus

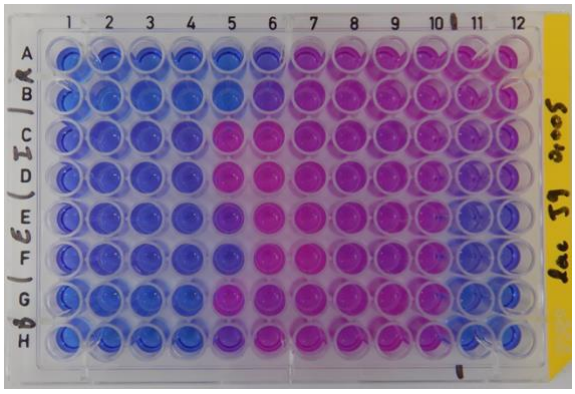

M. riyadhense

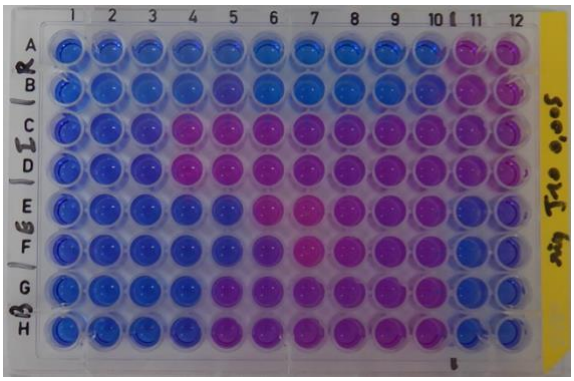

M. shinjukuense

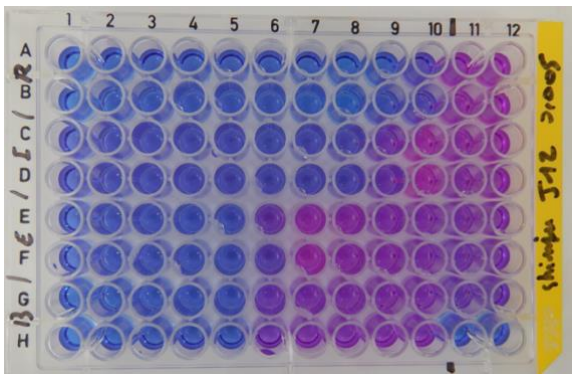

M. kansasii

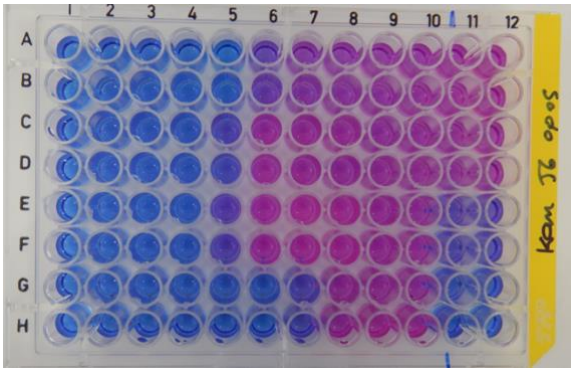

Mtb H37Rv

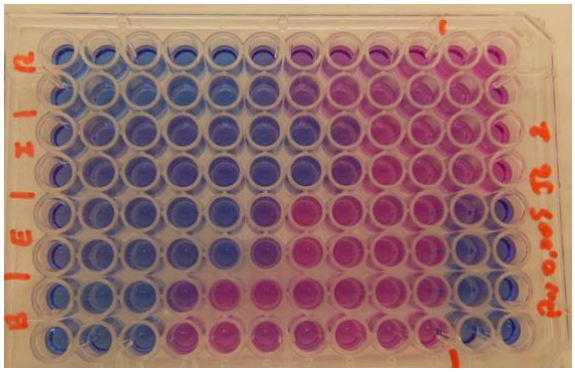

Annex 3: Comparison of ESX systems of *M. lacus*, *M. riyadhense*, and *M. shinjukuense* with *M. kansasii* and *Mtb*

ESX-1

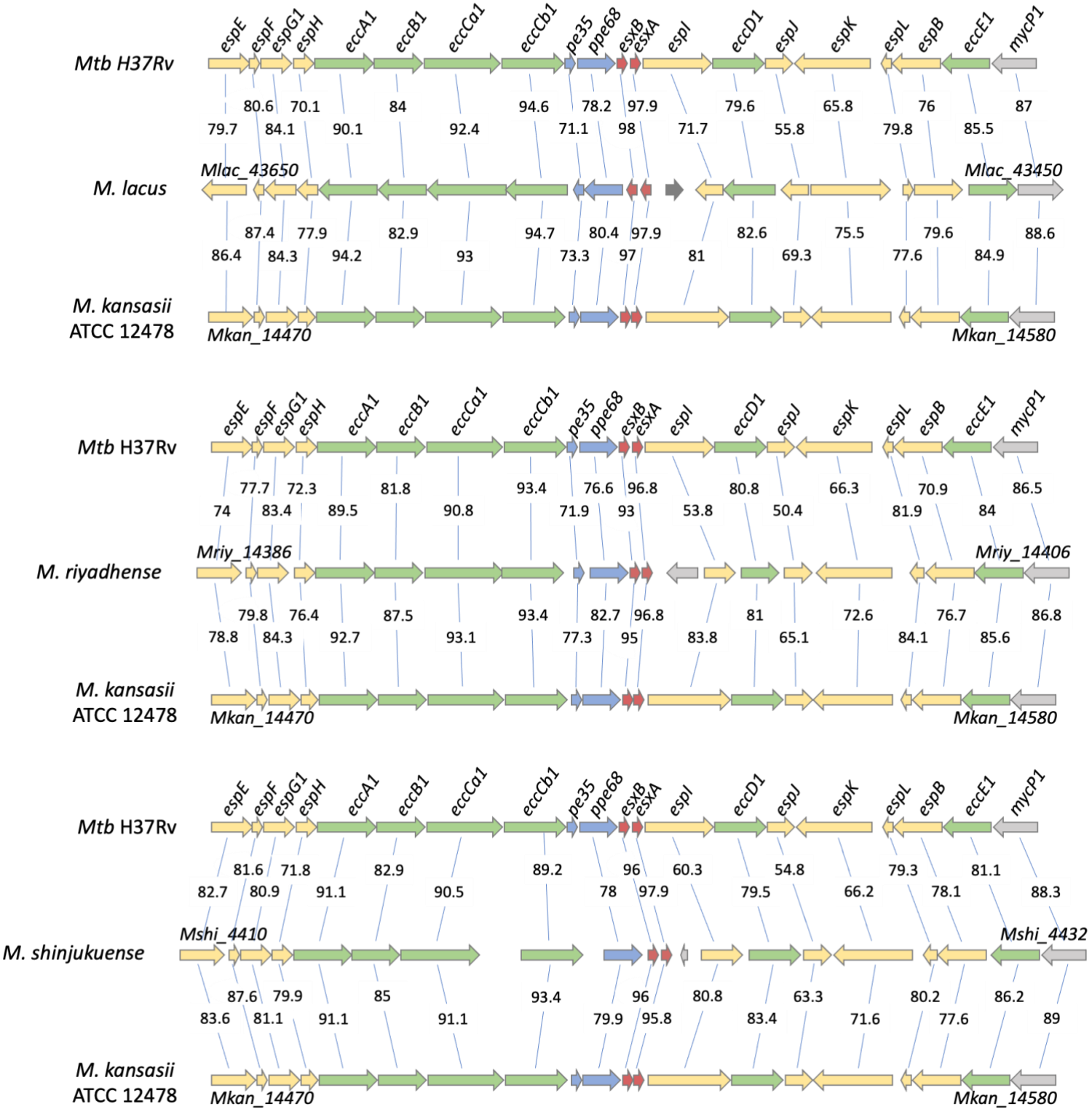

ESX-2

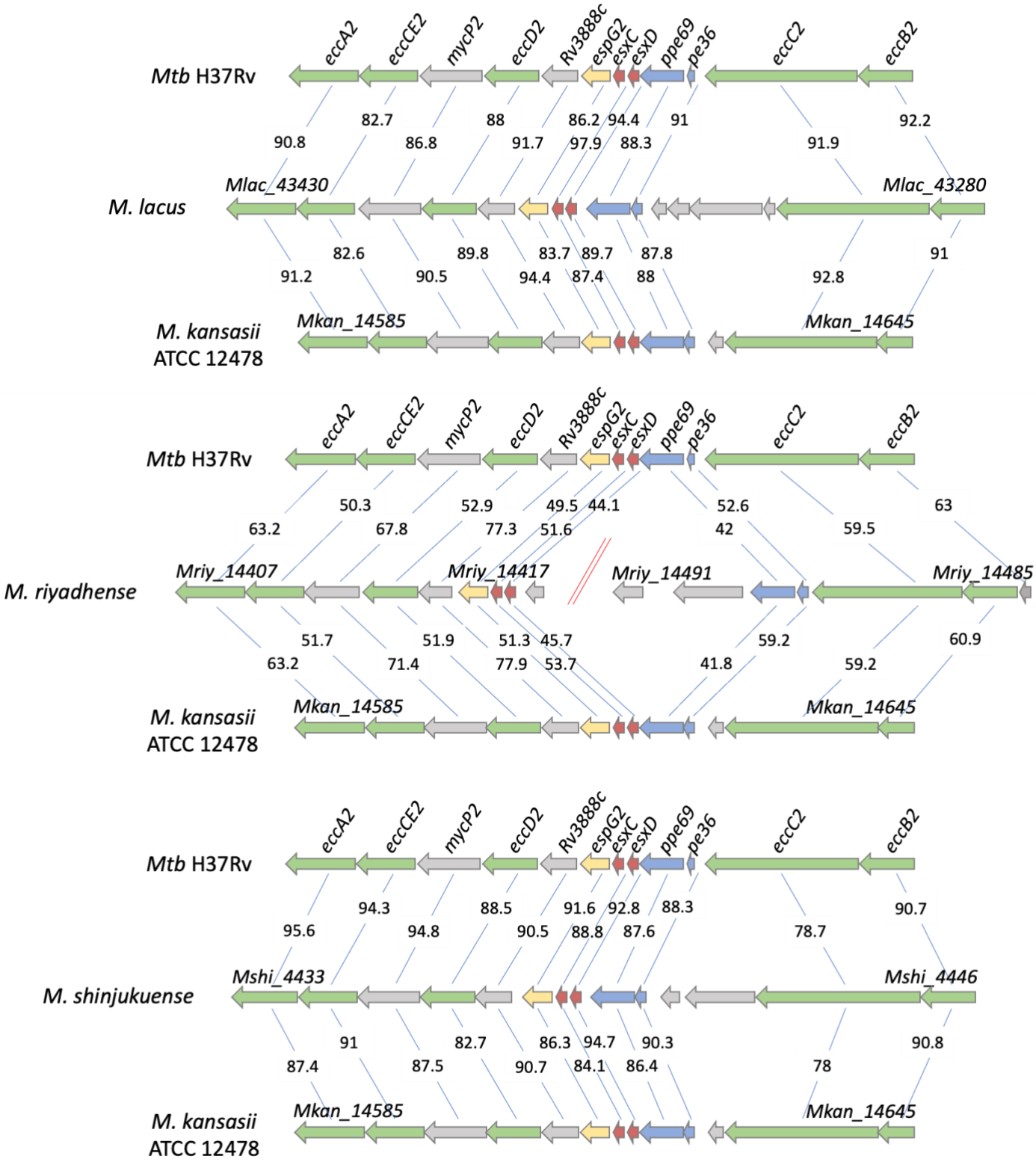
Mtb H37Rv
eccA2
eccCE2
mycP2
eccD2
Rv3888c
espG2
esxC
esxD
ppe69
pe36
eccC2
eccB2
82.7
88
86.2
94.4
91
92.2
90.8
86.8
91.7
97.9
88.3
91.9
M. lacus
Mlac_43430
Mlac_43280
82.6
89.8
83.7
89.7
87.8
91
91.2
90.5
94.4
87.4
88
92.8
M. kansasii
ATCC 12478
Mkan_14585
Mkan_14645
Mtb H37Rv
50.3
52.9
49.5
44.1
52.6
63
63.2
67.8
77.3
51.6
42
59.5
M. riyadhense
Mriy_14407
Mriy_14417
Mriy_14491
Mriy_14485
51.7
51.9
51.3
45.7
59.2
60.9
63.2
71.4
77.9
53.7
41.8
59.2
M. kansasii
ATCC 12478
Mkan_14585
Mkan_14645
Mtb H37Rv
94.3
88.5
91.6
92.8
88.3
90.7
95.6
94.8
90.5
88.8
87.6
78.7
M. shinjukuense
Mshi_4433
Mshi_4446
91
82.7
86.3
94.7
90.3
90.8
87.4
87.5
90.7
84.1
86.4
78
M. kansasii
ATCC 12478
Mkan_14585
Mkan_14645

ESX-3

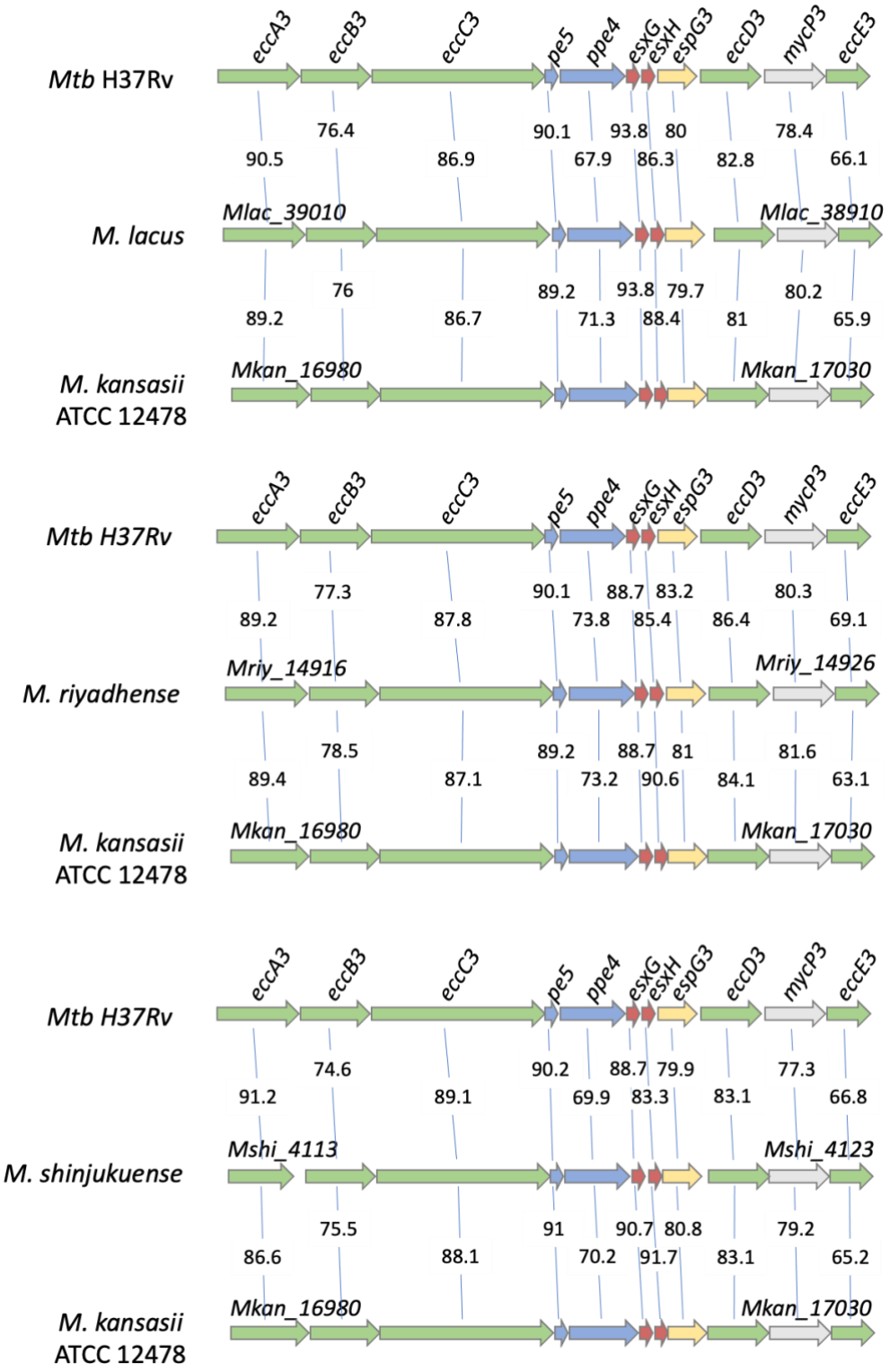
Mtb H37Rv
eccA3
eccB3
eccC3
pe5
ppe4
esxG
esxH
espG3
eccD3
mycP3
eccE3
76.4
90.1
93.8
80
78.4
90.5
86.9
67.9
86.3
82.8
66.1
M. lacus
Mlac_39010
Mlac_38910
76
89.2
93.8
79.7
80.2
89.2
86.7
71.3
88.4
81
65.9
M. kansasii ATCC 12478
Mkan_16980
Mkan_17030
Mtb H37Rv
77.3
90.1
88.7
83.2
80.3
89.2
87.8
73.8
85.4
86.4
69.1
M. riyadhense
Mriy_14916
Mriy_14926
78.5
89.2
88.7
81
81.6
89.4
87.1
73.2
90.6
84.1
63.1
M. kansasii ATCC 12478
Mkan_16980
Mkan_17030
Mtb H37Rv
74.6
90.2
88.7
79.9
77.3
91.2
89.1
69.9
83.3
83.1
66.8
M. shinjukuense
Mshi_4113
Mshi_4123
75.5
91
90.7
80.8
79.2
86.6
88.1
70.2
91.7
83.1
65.2
M. kansasii ATCC 12478
Mkan_16980
Mkan_17030

ESX-4

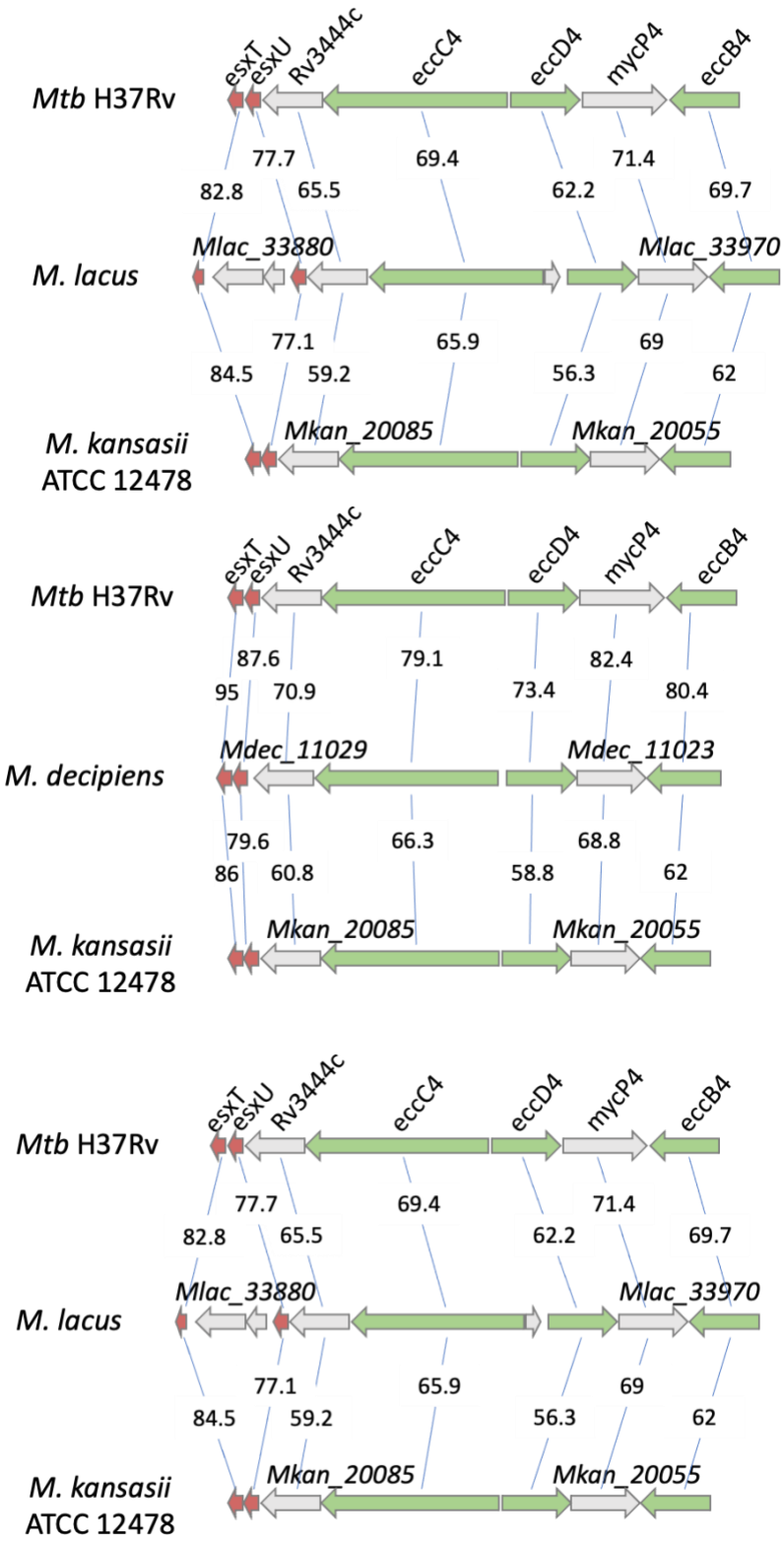
Mtb H37Rv
esxT
esxU
Rv3444c
eccC4
eccD4
mycP4
eccB4
77.7
69.4
71.4
82.8
65.5
62.2
69.7
M. lacus
Mlac_33880
Mlac_33970
77.1
65.9
69
84.5
59.2
56.3
62
M. kansasii
ATCC 12478
Mkan_20085
Mkan_20055
Mtb H37Rv
esxT
esxU
Rv3444c
eccC4
eccD4
mycP4
eccB4
87.6
79.1
82.4
95
70.9
73.4
80.4
M. decipiens
Mdec_11029
Mdec_11023
79.6
66.3
68.8
86
60.8
58.8
62
M. kansasii
ATCC 12478
Mkan_20085
Mkan_20055
Mtb H37Rv
esxT
esxU
Rv3444c
eccC4
eccD4
mycP4
eccB4
77.7
69.4
71.4
82.8
65.5
62.2
69.7
M. lacus
Mlac_33880
Mlac_33970
77.1
65.9
69
84.5
59.2
56.3
62
M. kansasii
ATCC 12478
Mkan_20085
Mkan_20055

ESX-5

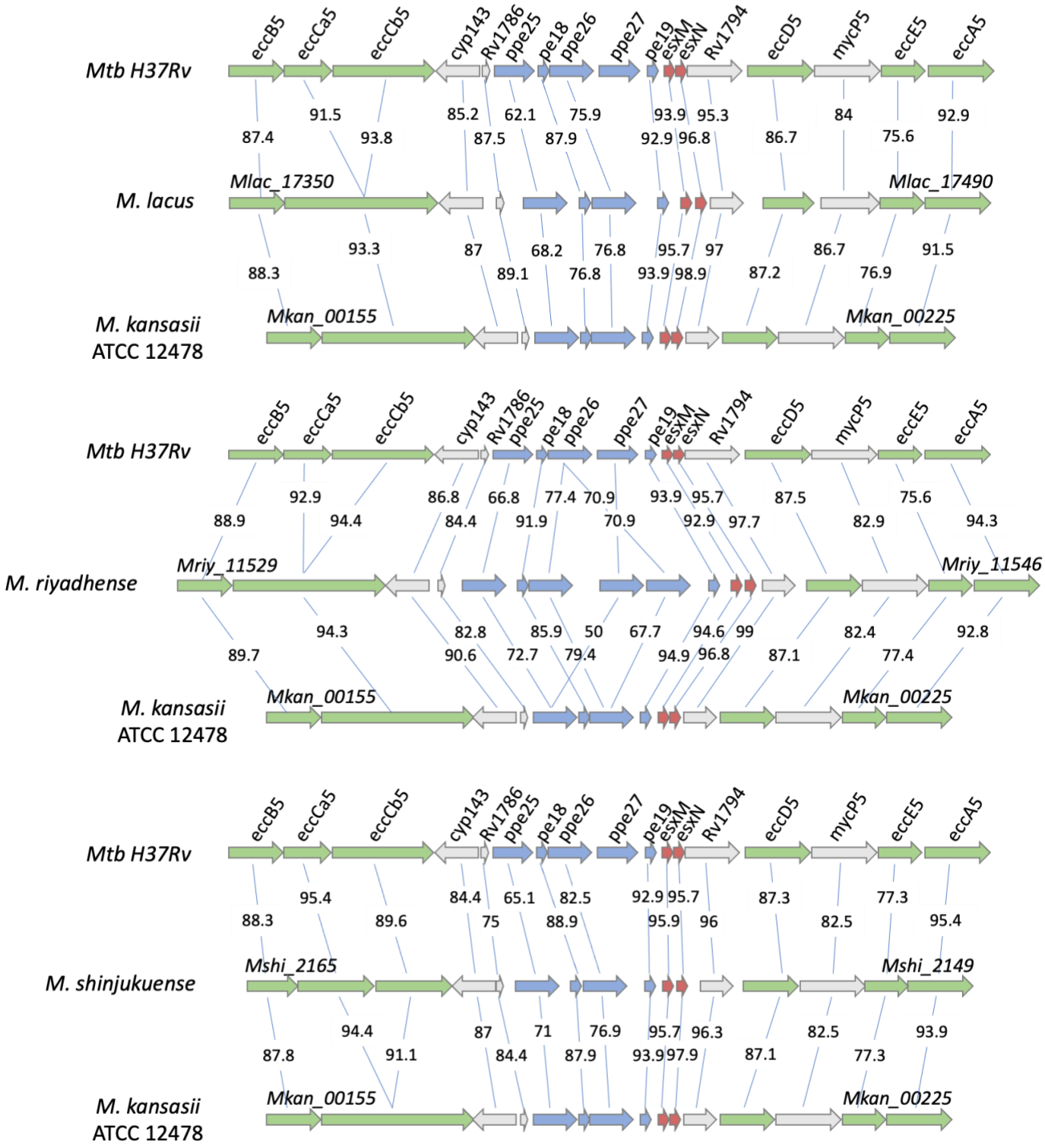
Mtb H37Rv
eccB5
eccCa5
eccCb5
cyp143
Rv1786
ppe25
pe18
ppe26
ppe27
pe19
esxM
esxN
Rv1794
eccD5
mycP5
eccE5
eccA5
91.5
85.2
62.1
75.9
93.9
95.3
84
92.9
87.4
93.8
87.5
87.9
92.9
96.8
86.7
75.6
M. lacus
Mlac_17350
Mlac_17490
93.3
87
68.2
76.8
95.7
97
86.7
91.5
88.3
89.1
76.8
93.9
98.9
87.2
76.9
M. kansasii
ATCC 12478
Mkan_00155
Mkan_00225
Mtb H37Rv
eccB5
eccCa5
eccCb5
cyp143
Rv1786
ppe25
pe18
ppe26
ppe27
pe19
esxM
esxN
Rv1794
eccD5
mycP5
eccE5
eccA5
92.9
86.8
66.8
77.4
70.9
93.9
95.7
87.5
75.6
88.9
94.4
84.4
91.9
70.9
92.9
97.7
82.9
94.3
M. riyadhense
Mriy_11529
Mriy_11546
94.3
82.8
85.9
50
67.7
94.6
99
82.4
92.8
89.7
90.6
72.7
79.4
94.9
96.8
87.1
77.4
M. kansasii
ATCC 12478
Mkan_00155
Mkan_00225
Mtb H37Rv
eccB5
eccCa5
eccCb5
cyp143
Rv1786
ppe25
pe18
ppe26
ppe27
pe19
esxM
esxN
Rv1794
eccD5
mycP5
eccE5
eccA5
95.4
84.4
65.1
82.5
92.9
95.7
87.3
77.3
88.3
89.6
75
88.9
95.9
96
82.5
95.4
M. shinjukuense
Mshi_2165
Mshi_2149
94.4
87
71
76.9
95.7
96.3
82.5
93.9
87.8
91.1
84.4
87.9
93.9
97.9
87.1
77.3
M. kansasii
ATCC 12478
Mkan_00155
Mkan_00225

Annex 4: Résumé substantiel en français

Le genre *Mycobacterium* appartient à l'embranchement des *Actinobacteria* et comprend un grand nombre d'espèces connues sous le nom de mycobactéries. Ce genre peut être divisé en deux groupes en fonction de la vitesse de croissance (rapide ou lente) des différentes espèces. Si la plupart des espèces sont des bactéries environnementales et inoffensives, certaines espèces du genre *Mycobacterium* sont des agents pathogènes opportunistes ou obligatoires chez l'homme et/ou l'animal (Forbes et al., 2018). Le genre *Mycobacterium* peut également être divisé en trois catégories : les mycobactéries responsables de la tuberculose, qui appartiennent principalement au complexe de *Mycobacterium tuberculosis*, les mycobactéries responsables de la lèpre (*Mycobacterium leprae*) et les mycobactéries non tuberculeuses (MNT) classées comme des agents pathogènes potentiellement opportunistes ou des mycobactéries non pathogènes (Meehan et al., 2021). En général, les espèces opportunistes ou pathogènes appartiennent aux mycobactéries à croissance lente, à quelques exceptions près, comme *Mycobacterium abscessus* (Bachmann et al., 2020), qui est devenu ces dernières années un pathogène majeur pour les patients atteints de mucoviscidose.

Le complexe de *Mycobacterium tuberculosis* regroupe des espèces pathogènes génétiquement proches (>99% d'identité de séquence génomique) et responsables de la tuberculose chez l'homme et/ou l'animal (Gagneux, 2018). Les membres de ce complexe auraient évolués de manière clonale à partir d'un ancêtre commun, dont *Mycobacterium canettii*, une mycobactérie présumée responsable de la tuberculose dans l'environnement, pourrait être le représentant le plus proche (Supply & Brosch, 2017). *Mycobacterium tuberculosis* (*Mtb*) et *Mycobacterium africanum* sont les espèces du complexe de *Mtb* adaptées à l'homme, tandis que *Mycobacterium bovis* représente probablement le membre le plus connu du complexe adapté à l'animal (Gagneux, 2018).

Au cours de son évolution, des modifications du génome ont permis à *Mtb*, l'agent étiologique de la tuberculose humaine, de s'adapter à la vie intracellulaire au dépit de la vie environnementale des MNT. Ces évolutions, caractérisées par la perte des gènes nécessaire à la vie environnementale et l'acquisition ou l'adaptation de nombreux facteurs de virulence,

ont fait de ce pathogène la principale cause de mortalité humaine dû à un seul agent pathogène.

Malgré les nombreuses études réalisées sur ce pathogène, de nombreuses étapes de son évolution restent encore mal comprises, comme l'acquisition de certains facteurs de virulence qui sont spécifiques aux espèces du complexe de *Mtb* et que l'on ne retrouve chez aucune autre espèce du genre *Mycobacterium*, bien que cette comparaison dépende aussi largement des espèces utilisées pour ces analyses. De nombreuses hypothèses s'appuient sur le transfert horizontal de gène, qui aurait permis à l'ancêtre des bactéries responsables de la tuberculose et/ou du complexe de *Mtb* d'acquérir de telles particularités. D'autres modifications génomiques ont également été notées et auraient eu lieu au cours de l'évolution du complexe de *Mtb*, notamment une réduction de la taille du génome, et la perte de certains gènes centraux par rapport à d'autres mycobactéries (Bachmann et al., 2020 ; Sapriel & Brosch, 2019 ; J. Wang et al., 2015).

Mtb étant un organisme hautement pathogène, un laboratoire de classe 3 est nécessaire pour sa manipulation. Pour faciliter la recherche, les MNT sont souvent utilisées comme modèles d'étude pour étudier certains mécanismes communs partagés avec *Mtb*, ou au contraire sont utilisés pour distinguer *Mtb* d'autres mycobactéries. Deux MNT opportunistes à croissance lente sont souvent utilisées comme modèles : *Mycobacterium marinum* et *Mycobacterium kansasii*, longtemps considérées comme les espèces les plus proches de *Mtb* et de son ancêtre (Berg & Ramakrishnan, 2012 ; J. Wang et al., 2015). Mais même si ces deux espèces partagent de nombreuses caractéristiques communes avec *Mtb*, certaines étapes de l'évolution de ce pathogène ne sont pas retrouvées chez ces deux espèces, ce qui rend parfois caduc la précision des modèles et les connaissances acquises pour les questions liées à *Mtb* (Sapriel & Brosch, 2019).

Une étude récente de G. Sapriel et R. Brosch a montré que quatre MNT isolées chez des patients dans les années 2000 partagent plus de traits évolutifs avec *Mtb* que les deux comparateurs précédemment utilisés. Ces espèces, nommées *Mycobacterium decipiens*, *Mycobacterium lacus*, *Mycobacterium riyadhense* et *Mycobacterium shinjukuense*, ont été suggérées comme partageant un ancêtre commun avec les membres du complexe de *Mtb*, sur la base d'une analyse qui a révélé que ces espèces partageaient certaines caractéristiques

évolutives avec les membres du complexe de *Mtb*, précédemment considérées comme uniques (Sapriel & Brosch, 2019).

Mon projet de thèse avait pour but de caractériser ces quatre espèces afin d'établir de nouvelles connaissances dans l'évolution de *Mtb* et d'étudier la possibilité d'en utiliser une ou plusieurs d'entre elles comme modèles de *Mtb*, étant des organismes de classe de biosécurité 1 ou 2.

Pour cela, différents objectifs avaient été définit. Le premier objectif consistait en la caractérisation phénotypique des quatre espèces. Ensuite, nous avons déterminé la capacité de multiplication intracellulaire des espèces dans différents modèles. Afin d'approfondir les résultats précédents et après avoir séquencé leur génome, nous avons comparé différentes régions génomiques afin de déterminer les caractéristiques partagées des quatre espèces avec *Mtb*. Finalement, grâce à nos résultats, nous avons pu émettre des hypothèses quant à l'utilisation de certaines de ces espèces comme modèle d'étude de *Mtb*.

La caractérisation phénotypique de ces quatre espèces nous a permis de déterminer que *M. decipiens* avait une température optimale comprise entre 32 et 35°C, et non 37°C comme les autres espèces de cette étude et les différents contrôles (*M. kansasii*, *Mtb*). Cela nous a donc amené à penser que certaines caractéristiques du génome de *M. decipiens* étaient partagées avec *M. marinum*, deuxième espèce couramment utilisée comme modèle d'étude de *Mtb*, qui a une température de croissance optimale comprise entre 30 et 32°C (Aubry et al., 2017 ; Hashish et al., 2018). Ces résultats nous ont permis d'optimiser la croissance des espèces afin d'avoir les meilleures cultures possibles pour la suite des expériences. Nous avons pu également démontrer la sensibilité à trois des antituberculeux de première ligne (rifampicine, isoniazide, et éthambutol) ainsi qu'à un antituberculeux de troisième ligne (bédaquiline). Alors que *M. shinjukuense* montre une sensibilité aux quatre antituberculeux testés, une résistance est observée pour l'isoniazide et l'éthambutol chez *M. lacus* et *M. riyadhense*. *M. decipiens* quant à lui semble résister aux trois antituberculeux de première lignes testés. Il est possible que les espèces aient développé des résistances naturelles à certaines molécules comme d'autres espèces de mycobactéries (Reingewertz et al., 2020). Ces résultats nécessitent

cependant une confirmation car il a été montré que certaines molécules peuvent avoir un effet atténué lors des expérience *in vitro* (Brown-Elliott & Woods, 2019).

Afin d'étudier la possibilité d'utiliser une de ces espèces comme modèle d'étude, nous avons comparé leur capacité d'infection dans des modèles *in vitro* et *in vivo*. *M. decipiens* a été capable de se multiplier dans des macrophages dérivés de cellules THP-1 à sa température optimale (35°C) mais cette capacité a été atténuée à 37°C. *M. lacus* et *M. shinjukuense* ont quant à elles montrées un état assimilé à de la persistance, bien que des études complémentaires doivent être réalisées afin de confirmer leur capacité de persistance. Pour finir, *M. riyadhense* a montré des capacités de multiplication intéressantes et étonnantes dans le modèle cellulaire comme dans les modèles murins. En effet, nos résultats ont montré que cette bactérie est capable de se répliquer après infections par voie aérosol dans des modèles murins. Il a même été montré qu'à une dose d'infection utilisée normalement pour les MNT, considérées comme moins virulente que *Mtb*, la bactérie entrainait de graves symptômes chez les souris pouvant conduire à leur mort en quelques semaines, et qu'à une faible dose d'infection normalement utilisée pour *Mtb*, la bactérie était capable de causer une infection mais semble pouvoir être contrôlée par l'hôte après la mise en place du système immunitaire adaptatif.

L'étude réalisée par G. Sapriel et R. Brosch en 2019 a montré que ces souches partageaient plus de caractéristiques avec *Mtb* que ne pouvaient le faire les deux espèces comparateurs *M. kansasii* et *M. marinum*. Lors de cette étude, *M. decipiens* a été décrit comme étant l'espèces la plus proche de *Mtb* au niveau génomique comparée aux trois autres espèces et aux deux comparateurs, avec par exemple un plus fort pourcentage d'identité nucléotidique moyenne, ou encore des facteurs de virulence communs avec *Mtb* jusqu'alors considérés unique chez le pathogène. Mais les trois autres espèces partagent également des caractéristiques communes à *Mtb* qui ne sont pas retrouvés dans les autres espèces. Par exemple, en analysant les génomes des quatre espèces lors des comparaisons génomiques, nous avons pu constater que la réduction du génome de *Mtb* considérée comme spécifique au pathogène était finalement partagé par *M. shinjukuense,* tandis que les trois autres espèces montrent des génomes de taille intermédiaire entre *M. marinum* et *Mtb*.

Afin d'approfondir les résultats des capacités de réplication des espèces observés, nous nous sommes concentrés sur différents facteurs de virulences connus chez *Mtb*.

Tout d'abord, nous avons étudié la sécrétion de la protéine ESAT-6 (6 kDa early secretory antigenic target) qui est l'un des facteurs de virulence le plus connu de *Mtb*. ESAT-6 est produite et sécrétée par le locus ESX-1 du génome mycobactérien qui appartient aux systèmes de sécrétion de types VII (Brodin et al., 2004). Son rôle principal lors d'une infection à *Mtb* est d'induire la perforation de la membrane du phagosome, entrainant la rupture de celle-ci et permettant à la bactérie d'accéder au cytosol du macrophage entrainant la nécrose cellulaire (Majlessi & Brosch, 2015 ; Simeone et al., 2012, 2021). Cette protéine est produite et sécrétée sous forme de complexe avec sa protéine chaperonne nommée CFP-10 (10-kDA culture filtrate protein) (De Jonge et al., 2007 ; Renshaw et al., 2002).

Une analyse par Western Blot nous a permis de déterminer que les quatre espèces étaient capable de produire les deux protéines, mais que seule *M. decipiens* était capable de les sécréter dans des conditions de culture *in vitro*. Les résultats ont également montré que *M. lacus* semble capable de sécréter la protéine CFP-10 seule. Cependant, nous n'avons pas trouvé de sécrétion d'ESAT-6 chez *M. riyadhense* malgré sa capacité de multiplication trouvée lors des différentes infections. La sécrétion de ESAT-6 par *M. decipiens* peut s'expliquer par la présence du cluster *espACD* dans son génome en plus de la région principale de ESX-1, qui est l'un des composants essentiels à la sécrétion de cette protéine chez *Mtb* et qui n'est pas retrouvé dans le génome des trois autres espèces. En revanche, la sécrétion de CFP-10 sans la présence du cluster *espACD* chez *M. lacus* était inattendue, bien qu'une étude ait récemment montré que cela était aussi possible chez certains mutant de *Mtb* qui ont une fonctionnalité du cluster *espACD* réduite, et que CFP-10 pouvait être retrouvé dans le milieu extracellulaire même si l'opéron *espACD* n'était pas fonctionnel (Aguilo et al., 2017).

Pour poursuivre la comparaison des facteurs de virulence entre les quatre espèces et *Mtb*, nous nous sommes concentrés sur la production de certains lipides démontrés comme étant impliqués dans la virulence lors d'infection à *Mtb*. Les lipides phthiocéroles dimycocérosates (PDIM) et les glycolipides phénoliques (PGL), sont produits et transportés par des enzymes synthétisées par deux locus situés dans la même région génomique. Bien que la composition du locus des PDIMs soit conservée au sein des quatre espèces et de *Mtb*, les quatre MNT montrent des profils lipidiques différents, qui pourraient être dues à un faible pourcentage

d'identité d'acides aminées aux protéines orthologues de *Mtb*. En revanche, le locus des PGLs montre des diversités de composition des gènes entre les espèces. En effet, certains gènes sont absents de *M. decipiens*, *M. lacus*, *M. shinjukuense*, et du comparateur *M. kansasii* alors que le locus n'est pas retrouvé chez *M. riyadhense*. Chez *Mtb*, un défaut de production ou de transport des PGLs n'empêche pas l'infection par la bactérie mais atténue néanmoins sa virulence (Cambier et al., 2017). Cependant, chez le pathogène, une altération des PDIMs entraine une plus forte atténuation de la virulence, d'autant qu'un défaut dans le locus des PDIMs peut avoir un impact sur le locus des PGLs situé en aval (Constant et al., 2002 ; Ramos et al., 2020). Les différences de ces deux loci sont plus importantes pour *M. riyadhense* que les trois autres espèces comparées à *Mtb* mais malgré ces différences, *M. riyadhense* est l'espèce la plus virulente des quatre étudiées dans ce projet.

Pour finir, plusieurs études ont montré que la morphologie pouvait influencer la virulence de la bactérie. Des études sur *M. abscessus*, *M. kansasii*, et *M. canettii* ont toutes montré qu'un phénotype rugueux entrainait une plus forte virulence qu'un phénotype lisse (Torrelles et al., 2002 ; Boritsch et al., 2016 ; Belisle & Brennan, 1989). Chez les mycobactéries à croissance lente, le morphotype est en partie dû aux lipides oligosaccharides (LOS) et aux nombres de copies de polyketide synthase (*pks5*) et de son gène associé (*pap*) que contient le locus. Généralement, les bactéries à morphologie lisse contenant un locus LOS possèdent un gène *pap* entre deux copies de *pks5* alors que, chez *Mtb* qui a un phénotype rugueux, une seule copie de *pks5* est trouvée dans le locus LOS (Boritsch et al., 2016). Grâce à l'optimisation de la croissance des espèces, nous avons pu remarquer que des colonies rugueuses sont observées chez *M. decipiens*, *M. riyadhense*, et *M. shinjukuense* lors que *M. lacus* arbore des colonies lisses comme *M. marinum* et *M. kansasii*. La composition génomique de ce locus chez les quatre espèces n'est pas celui attendu quant à l'observation de leur morphologie. *M. decipiens* à un locus pouvant être assimilé à celui de *M. canettii* qui a un morphotype lisse. Nous supposons donc qu'un ou plusieurs gènes de *pks5* ou des gènes voisins ne sont pas fonctionnel entrainant la morphologie rugueuse. *M. lacus* et *M. shinjukuense* ont une composition du locus particulière car plus de deux copies tronquées de *pks5* sont retrouvées dans leur locus. Pour finir, *M. riyadhense* à la particularité d'arborer plusieurs phénotypes après infection et contient deux copies de *pks5* dans son locus. Malgré ses observations, les profils lipidiques des LOS semblent différents de ceux retrouvés chez *Mtb*, *M. canettii*, ou

M. kansasii. Des études complémentaires sont donc nécessaires pour expliquer la morphologie de ces espèces qui peuvent dépendre de différents lipides produits par les bactéries.

En regroupant les différents résultats obtenus au cours de ce projet de thèse, nous pouvons conclure que les quatre MNT ont pu, au travers de leur étude, montrer que certaines d'entre elles partageaient plus de similitudes avec *Mtb* que les deux espèces de comparaison *M. kansasii* et *M. marinum*. Cependant, malgré les pourcentages plus élevés d'identité au niveau des acides aminées des protéines entre *Mtb* et *M. decipiens* par rapport aux trois autres espèces, *M. riyadhense* s'est avérée être la plus virulente. Il est possible que cette différence soit due à la température de croissance de *M. decipiens*, qui a montré une forte diminution de la capacité de croissance intracellulaire à la température optimale de croissance de *Mtb*. Bien que d'autres études soient nécessaires pour valider nos hypothèses, ces résultats nous amènent à penser que *M. decipiens*, étant génomiquement plus proche de *Mtb*, pourrait être utilisée comme modèle d'étude *in vitro* afin d'être à sa température de croissance, pour éclaircir des mécanismes de sécrétion ou des résistances à certains antibiotiques, tandis que si *M. riyadhense* présente un profil similaire à *Mtb* dans les infections pulmonaires, cette espèce pourrait être utile pour une utilisation dans les modèles murins, car la bactérie présente une caractéristique intéressante en ce qui concerne la dose d'infection et est classée comme organisme de classe 1. Enfin, *M. lacus* et *M. shinjukuense* pourraient représenter des modelés intéressants pour l'étude de certaines étapes dans l'évolution des mycobactéries pathogènes, avec par exemple la réduction du génome trouvée chez *M. shinjukuense*, ou la capacité de *M. lacus* à sécréter CFP-10, et dont l'étude de l'insertion de certains opérons comme *espACD* pourrait conduire à de nouvelles hypothèses sur les étapes impliquées dans l'acquisition de facteurs de virulence chez *Mtb*. Avec les sensibilités variées à des médicaments antituberculeux testées dans ce projet, les quatre espèces représentes également des modèles intéressants qui peuvent être appliqués dans des conditions de biosécurité de niveau un ou deux pour l'étude des nouvelles molécules antituberculeux qui sont en développent dans des différents projets de collaboration.

LISTE DES ÉLÉMENTS SOUS DROITS

Figure 1: Estimated TB incidence in 2021, for countries with at least 100,000 incident cases. Picture from (World Health Organization, 2022).

Figure 2: Infection cycle of *Mtb*. Picture from (Chandra et al., 2022).

Figure 5: Composition of the mycobacterial cell envelope. Image adapted from (Le Chevalier et al., 2014).

Figure 6: Phylogenetic tree of the genus *Mycobacterium*. Picture from (Tortoli et al., 2017).

Figure 7: Phylogenetic tree of mycobacterial species based on more than 100 universally conserved bacterial genes and their associated proteins. Picture from (Sapriel & Brosch, 2019).

Figure 8: Secretion systems present in *Mtb* genome. Picture from (Pal et al., 2022).

Figure 9: Genetic organization of the ESX systems from T7SS in *Mtb* H37Rv. Picture from (Bitter et al., 2009).

Figure 10: Structural cryo-electron microscopy representation of an ESX system inner-membrane complex (ESX-5) from the T7SS of *Mtb*. Picture from (Bunduc et al., 2021).

Figure 11: Representation of the regulation of ESAT-6 and CFP-10 secretion. Picture from (Ates & Brosch, 2017).

Annex 1: First pages of the article and the review related to the thesis.